THE UNIVERSITY OF QUEENSLAND

AUSTRALIA

Development of Nanoparticle based Vaccine Delivery Systems

Karishma Trilok Mody

B.Sc M.Sc

A thesis submitted for the degree of Doctor of Philosophy at

The University of Queensland 2015

Queensland Alliance for Agriculture and Food Innovation

Abstract

Development of subunit vaccine formulation requires a careful selection of potent antigen, efficient adjuvant and route of delivery. The desirable physicochemical characteristics of the mesoporous silica nanoparticles (MSNs) such as ease of synthesis, excellent *in vivo* biocompatibility and good thermal and chemical stability, make them optimal nanocarriers for various biomolecules (Mody *et al.* Nanoscale, 2013). Freeze-drying process can be used to further improve both th e short and long-term stability of protein-loaded nanovaccine components (Mody *et al.* Drug Deliv. Lett., 2012). Bovine Viral Diarrhoea Virus-1 (BVDV-1) is one of the most serious pathogens, which causes tremendous economic loss to the cattle industry worldwide, meriting the development of improved subunit vaccines. E2 is the structural envelope glycoprotein of BVDV-1 and is a major immunogenic determinant, making it an ideal candidate for the development of subunit vaccines. The current research project investigated range of silica nanoparticles with different physico-chemical characteristics for the development of 'non freeze-dried' (wet or non-FD) and 'freeze-dried' (FD) vaccine delivery systems using model protein Ovalbumin (OVA) and BVDV-1 *Escherichia coli*-expressed optimised E2 (oE2) protein. The nanoparticles repertoire included amino functionalised mesoporous silica nanoparticles (AM-41), amino functionalised hollow mesoporous silica nanoparticles (HMSAs) and novel silica vesicles (SV).

The capacity of AM-41 sized 90 nm to act as self-adjuvants and nanocarriers was first investigated for model protein OVA as non-FD as well as FD [after freeze-drying with trehalose (5%) and PEG8000 (1%)] nanovaccine formulations. Administration of the non-FD and reconstituted FD OVA-41 (after storage for 2 months at ambient temperature) nanovaccine induced both humoral as well as cell-mediated immune responses after four immunisations of 10 µg OVA/150 µg AM-41 (Mody *et al.* Int. J Pharm, 2014). Low protein adsorption capacity of AM-41 (72 µg OVA/mg AM-41) was a major limitation of this study. Therefore, HMSAs, (particle size 120 nm, pores on the wall of entrance sized 2 nm) were investigated for developing recombinant BVDV-1 E2 nanovaccine (60-80 µg oE2 /mg HMSA). The immunogenicity of the oE2/HMSA nanovaccine before and after a freeze-drying with trehalose (5%) and glycine (1%) was evaluated in a sheep trial. The non-FD and FD oE2/HMSA generated oE2 specific antibody and cell-mediated immune responses after three subcutaneous injections with 500 µg oE2 adsorbed to 6.2 mg HMSA. Importantly, it was found that the long-term cell-mediated immune responses were detectable up to five months after immunisation (Manuscript submitted to PLoS ONE).

In order to further improve the oE2 adsorption and immunogenicity of the nanovaccine as compared to conventional adjuvant Quil-A, novel silica vesicles termed SV-140 (diameter 50 nm, wall thickness 6 nm, perforated by pores of entrance size 16 nm and total pore volume of 0.934 cm^3g^{-1}) were evaluated. The SV-140 significantly improved the loading capacity (~250 μg/mg) and controlled release of oE2 protein. The *in vivo* functionality of the developed vaccine delivery system was validated in mice immunisation trials comparing oE2 plus Quil-A (50 μg of oE2 plus 10 μg of Quil-A) to the oE2/SV-140 (50 μg of oE2 adsorbed to 250 μg of SV-140). Compared to the oE2 plus Quil-A, which generated BVDV-1 specific antibody responses at a titre of 10^4, the oE2/SV-140 group induced a 10 times higher oE2 specific antibody response. In addition, the cell-mediated response, which is essential to recognise and eliminate the invading pathogens, was also found to be higher [1954-2628 spot forming units (SFU)/million cells] in mice immunised with oE2/SV-140 compared to oE2 plus Quil-A (512-1369 SFU/million cells) (Mody *et al.* Biomaterials, 2014).

The ability of oE2/SV-140 and a FD oE2/SV-140 formulation (excipients trehalose (5%) and glycine (0.1%) used to freeze-dry), to generate long-term immune response was investigated after only two subcutaneous injections in mice. The oE2 (100 μg)/SV-140 (500 μg) and FD oE2 (100 μg)/SV-140 (500 μg) nanovaccines generated oE2-specific antibody responses for up to six months post the final second immunisation in mice. Significantly, the cell-mediated responses were consistently high in all the four mice immunised with oE2/SV-140 (1500 SFU/million cells) at the six month time point. The FD oE2/SV-140 also generated strong cell-mediated responses (340-1500 SFU/million cells) at the six month time point. Histopathology studies on the site of injection and different organs of mice immunised with 500 μg SV-140 nanovaccine showed no morphological changes. This showed that the oE2/SV-140 can elicit long-term balanced immune responses for at least six months both as non-FD and FD nanoformulation with SVs acting as excellent self adjuvants and nanocarriers (Manuscript submitted to PLoS ONE). The advancement made in this project addresses key features of: reduction in vaccine dosage, adjuvants, long-term balanced immune response and elimination of cold chain storage towards vaccine delivery.

Declaration by author

This thesis is composed of my original work, and contains no material previously published or written by another person except where due reference has been made in the text. I have clearly stated the contribution by others to jointly-authored works that I have included in my thesis.

I have clearly stated the contribution of others to my thesis as a whole, including statistical assistance, survey design, data analysis, significant technical procedures, professional editorial advice, and any other original research work used or reported in my thesis. The content of my thesis is the result of work I have carried out since the commencement of my research higher degree candidature and does not include a substantial part of work that has been submitted to qualify for the award of any other degree or diploma in any university or other tertiary institution. I have clearly stated which parts of my thesis, if any, have been submitted to qualify for another award.

I acknowledge that an electronic copy of my thesis must be lodged with the University Library and, subject to the policy and procedures of The University of Queensland, the thesis be made available for research and study in accordance with the Copyright Act 1968 unless a period of embargo has been approved by the Dean of the Graduate School.

I acknowledge that copyright of all material contained in my thesis resides with the copyright holder(s) of that material. Where appropriate I have obtained copyright permission from the copyright holder to reproduce material in this thesis.

Publications during candidature

Peer-reviewed publications

- Mody KT, Mahony D, Zhang J, Cavallaro AS, Zhang B, Popat A, Mahony TJ, Yu C, Mitter N. Silica vesicles as nanocarriers and adjuvants for generating both antibody and T-cell mediated immune resposes to Bovine Viral Diarrhoea Virus E2 protein. Biomaterials. 2014;35:9972-83.
- Mody KT, Mahony D, Cavallaro AS, Stahr F, Qiao SZ, Mahony TJ, Mitter N. Freeze-drying of ovalbumin loaded mesoporous silica nanoparticle vaccine formulation increases antigen stability under ambient conditions. Int J Pharm. 2014.
- Mody KT, Popat A, Mahony D, Cavallaro AS, Yu C, Mitter N. Mesoporous silica nanoparticles as antigen carriers and adjuvants for vaccine delivery. Nanoscale. 2013:5167-79.
- Mody K, Mahony D, Mahony TJ, Mitter N. Freeze-drying of protein loaded nanoparticles for vaccine delivery. Drug Deliv Lett. 2012;2:83-91.

Manuscripts submitted for publication

- Mody KT, Mahony D, Cavallaro AS, Zhang J, Mahony TJ, Yu C, Mitter N. Silica vesicle nanovaccine formulations stimulate long-term immune responses to the Bovine Viral Diarrhoea Virus E2 protein. Manuscript submitted to PLoS ONE.
- Mahony D, Mody KT, Cavallaro AS, Hu Q, Mahony T, Qiao SZ, Mitter N. Immunisation of sheep with Bovine Viral Diarrhoea Virus, E2 Protein using a Freeze-dried Hollow Silica Mesoporous Nanoparticle Formulation. Manuscript submitted to PLoS ONE.

Publications related to thesis

- Mahony D, Cavallaro AS, Mody KT, Xiong L, Mahony TJ, Qiao SZ, Mitter N. In vivo delivery of bovine viral diahorrea virus, E2 protein using hollow mesoporous silica nanoparticles. Nanoscale. 2014;6:6617-26.
- Cavallaro A, Mahony D, Mody K, Mahony T, Mitter N. Lots of Bovine Viral Diarrhoea Virus E2 protein – A Subunit Vaccine. 1st ed: iConcept Press.; 2013.

Conference proceedings

Poster (presenting author's name in bold)

- **Mody, K.,** Mahony, D., Cavallaro., Mahony, T., Yu, C., Mitter, N. **"**The Next Generation Nanovaccines using silica vesicles." 3rd International Conference on BioNano Innovation (ICBNI). 6-10 July 2014, Brisbane, Australia.

- **Mody, K.,** Mahony, D., Cavallaro., Mahony, T., Yu, C., Mitter, N. "Single Dose and Shelf-Stable - The Next Generation Nanovaccines." International Conference on Nanoscience and Nanotechnology. 2-6 February 2014, Adelaide Convention Centre, Adelaide, Australia
- **Mody, K.,** Mahony, D., Cavallaro, A., Stahr, F., Qiao, S., Mahony, T., Mitter, N. "Freeze-drying of protein loaded silica nanoparticles for vaccine delivery." 1st International Conference on BioNano Innovation (ICBNI). 19-20 July 2012, Brisbane Convention Centre, Brisbane, Australia.

Publications included in this thesis

Mody KT, Popat A, Mahony D, Cavallaro AS, Yu C, Mitter N. Mesoporous silica nanoparticles as antigen carriers and adjuvants for vaccine delivery. Nanoscale. 2013:5167-79 - incorporated as Chapter 2.

Contributor	Statement of contribution
Karishma Mody (Candidate)	Review of literature (100%) Wrote the paper (100%) Edited the paper (20%)
Amir Popat	Edited the paper (15%)
Donna Mahony (Co-supervisor)	Edited the paper (10%)
Antonino Cavallaro	Edited the paper (10%)
Chengzhong Yu (Co-supervisor)	Edited the paper (15%)
Neena Mitter (Principal Advisor)	Edited the paper (30%)

Mody K, Mahony D, Mahony TJ, Mitter N. Freeze-drying of protein loaded nanoparticles for vaccine delivery. Drug Deliv Lett. 2012;2:83-91 - incorporated as Chapter 3.

Contributor	Statement of contribution
Karishma Mody (Candidate)	Review of literature (100%) Wrote the paper (100%) Edited the paper (30%)
Donna Mahony (Co-supervisor)	Edited the paper (20%)
Timothy Mahony (Co-supervisor)	Edited the paper (20%)
Neena Mitter (Principal Advisor)	Edited the paper (30%)

Mody KT, Mahony D, Cavallaro AS, Stahr F, Qiao SZ, Mahony TJ, Mitter N. Freeze-drying of ovalbumin loaded mesoporous silica nanoparticle vaccine formulation increases antigen stability under ambient conditions. Int J Pharm. 2014 - incorporated as Chapter 4.

Contributor	Statement of contribution
Karishma Mody (Candidate)	Concept design (60%) Experiments and Statistical analysis (80%) Wrote the paper (100%) Edited the paper (10%)
Donna Mahony (Co-supervisor)	Concept design (20%) Experiments and Statistical analysis (20%) Edited the paper (20%)
Antonino Cavallaro	Technical assistance (20%) Edited the paper (10%)
Francis Stahr	Synthesis and characterisation of nanoparticles (100%)
Shizhang Qiao	Edited the paper (10%)
Timothy Mahony (Co-supervisor)	Edited the paper (20%)
Neena Mitter (Principal Advisor)	Concept design (20%) Edited the paper (30%)

Mahony D, Mody KT, Cavallaro AS, Hu Q, Mahony T, Qiao SZ, Mitter N. Immunisation of sheep with Bovine Viral Diarrhoea Virus, E2 Protein using a Freeze-dried Hollow Silica Mesoporous Nanoparticle Formulation. Manuscript submitted to PLoS ONE - included as Chapter 5.

Contributor	Statement of contribution
Donna Mahony (Co-supervisor)	Concept design (40%) Experiments and Statistical analysis (40%) Wrote the paper (100%) Edited the paper (10%)
Karishma Mody (Candidate)	Concept design (30%) Experiments and Statistical analysis (60%) Edited the paper (20%)
Antonino Cavallaro	Technical assistance (20%) Edited the paper (10%)
Quihong Hu	Synthesis and characterisation of silica nanoparticles (100%)
Timothy Mahony (Co-supervisor)	Edited the paper (20%)

Shi Zhang Qiao	Edited the paper (10%)
Neena Mitter (Principal Advisor)	Concept design (30%) Edited the paper (30%)

Mody KT, Mahony D, Zhang J, Cavallaro AS, Zhang B, Popat A, Mahony TJ, Yu C, Mitter N. Silica vesicles as nanocarriers and adjuvants for generating both antibody and T-cell mediated immune resposes to Bovine Viral Diarrhoea Virus E2 protein. Biomaterials. 2014;35:9972-83 - incorporated as Chapter 6.

Contributor	Statement of contribution
Karishma Mody (Candidate)	Concept design (60%) Experiments and Statistical analysis (100%) Wrote the paper (90%) Edited the paper (10%)
Donna Mahony (Co-supervisor)	Concept design (10%) Technical assistance (10%) Edited the paper (10%)
Jun Zhang	Synthesis and characterisation of silica materials (100%) Wrote the paper (10%)
Antonino Cavallaro	Technical assistance (10%) Edited the paper (10%)
Bing Zhang	Technical assistance (10%) Edited the paper (5%)
Amir Popat	Edited the paper (10%)
Timothy Mahony (Co-supervisor)	Edited the paper (10%)
Chengzhong Yu (Co-supervisor)	Edited the paper (15%)
Neena Mitter (Principal Advisor)	Concept design (30%) Edited the paper (30%)

Mody KT, Mahony D, Cavallaro AS, Zhang J, Mahony TJ, Yu C, Mitter N. Silica vesicle nanovaccine formulations stimulate long-term immune responses to the Bovine Viral Diarrhoea Virus E2 protein. Manuscript submitted to PLoS ONE - incorporated as Chapter 7.

Contributor	Statement of contribution
Karishma Mody (Candidate)	Concept design (50%) Experiments and Statistical analysis (100%) Wrote the paper (100%) Edited the paper (20%)
Donna Mahony (Co-supervisor)	Concept design (10%) Technical assistance (10%) Edited the paper (10%)
Antonino Cavallaro	Technical assistance (5%) Edited the paper (10%)
Jun Zhang	Synthesis and characterisation of the silica materials and edited the paper (100%)
Bing Zhang	Technical assistance (5%)
Timothy Mahony (Co-supervisor)	Edited the paper (20%)
Chengzhong Yu (Co-supervisor)	Edited the paper (10%)
Neena Mitter (Principal Advisor)	Concept design (40%) Edited the paper (30%)

Contributions by others to the thesis

List the significant and substantial inputs made by others to the research, work and writing represented and/or reported in the thesis. These could include significant contributions to: the conception and design of the project; non-routine technical work; analysis and interpretation of research data; drafting significant parts of the work or critically revising it so as to contribute to the interpretation. If no one contributed significantly then state "No contributions by others."

Statement of parts of the thesis submitted to qualify for the award of another degree

None

Acknowledgements

I would like to acknowledge my sincere gratitude to those who helped me keep my sanity intact by providing advice, support, encouragement and assistance throughout the duration of my PhD.

I would like to express my deep gratitude to my principal supervisor A/Prof. Neena Mitter. When we first met, I was a fresh graduate exploring a potential career in research. Thankyou for believing in me and giving me this opportunity in the first place. Your mentorship played an important role in shaping me into the researcher and person I am today and made my dreams and aspirations a reality. Personally, I would like to thankyou for offering me this fantastic PhD project. I am deeply appreciative of everything you have done for me!

To my co-supervisor Dr Donna Mahony, thankyou for the invaluable advice, time, efforts and the long hours you put into mentoring me throughout my candidature. I have learnt many valuable lessons from your mentorship starting from performing experiments to recording data systematically and of course to be organised. Personally, I would like to thank you for your friendship!

Thankyou to my co-supervisor A/Prof. Timothy Mahony for many man-hours of manuscript editing. I have learnt a lot from your mentorship and feel my writing has improved from your inputs.

To my co-supervisor Prof. Chengzhong (Michael) Yu, thankyou for providing technical expertise and valuable suggestions. I have been very fortunate as a researcher to learn the nanomaterial know-how from you.

I would like to thank Antonino (Tony) Cavallaro for being my go to person in the laboratory and for assistance, technical support and friendship. We have done many long, hard hours together however your company made the hours seem shorter and stress-free. Thank you to Amir Popat and Jun Zhang for your valuable contributions to the research carried out by me. Madeleine (Maddy) Gleeson, thankyou for helping me with your excellent proof reading skills and for being my 3MT practice audience over and again. I also wish to acknowledge my friends and co-workers who are/were part of the Ritchie Facility, Karl Robinson, Robyn Hall, Bing Zhang, Elizabeth Worrall, Roger Mitchell, Christopher O'Brien, Myrna Constantin, Alice Hayward, Ann Parisi,

Megan Vance, Jenny Gravel, Marg Commins, Sandy Jarrett, Anshu Raghuwanshi and Adam Gunjilac. I am thankful for your patience, guidance, assistance and friendship. I also am grateful that you were there to listen and provide support when I needed it.

For financial support, I sincerely acknowledge Queensland Alliance for Agriculture and Food Innovation (QAAFI) and UQ Graduate School for the UQ Research Scholarship. To the UQ Graduate School for the travel award which gave me the opportunity to learn and enhance my technical skills at the Washington State University (WSU), Pullman, Washington. Thank you to Prof. Wendy Brown, Prof. Hanu Pappu, Dr. Joshua Turse and Ms Shelley Whidbee at WSU for providing assistance and looking after me during my visit to WSU.

To my family: I would like to thank my parents Mr Trilok Pothiwala and Mrs Kumudini Pothiwala for your unconditional love, patience and encouragement. Thankyou for all the sacrifices you made for me along the way and for giving me strength to reach for the stars and chase my dreams. I could only achieve this because of your ongoing support. I would like to thank my in laws Mr Hemant Mody and Mrs Asha Mody for supporting my academic endeavour. I could completely focus on completing my research throughout and after my pregnancy largely because of your help. To my little brother Ronak, sister in law Nabam and my darling niece Aricia thankyou for your kindness and for always being there for me! I feel incredibly lucky to have you as my family!

My dearest husband Chirag, I could not have achieved this without your unwavering love, patience, guidance and support. Thankyou for being my pillar of strength throughout these years, I promise this is the last of my studies! Your silly science jokes (Poor farmer John!) and hugs made this journey a tad bit easy. My dearest son Aaryan (Ari) I love you so much! You are the best thing that happened to us! Your distracting cuteness didn't go well with thesis writing and even though managing everything wasn't easy I wouldn't have it any other way. I am extremely proud of you!

Thankyou!

Keywords

antigen, adjuvant, bvdv, freeze-drying, immune responses, nanocarriers, silica nanoparticles, vaccine delivery systems

Australian and New Zealand Standard Research Classifications (ANZSRC)

ANZSRC code: 070705, Veterinary Immunology, 50%
ANZSRC code: 100703, Nanobiotechnology, 50%

Fields of Research (FoR) Classification

FoR code: 0707, Veterinary Sciences, 50%
FoR code: 1007, Nanotechnology, 50%

TABLE OF CONTENTS

LIST OF FIGURES

LIST OF TABLES

ABBREVIATIONS

AFM	Atomic force microscopy
AIBN	Australian Institute for Bioengineering and Nanotechnology
Alum	Aluminium-based mineral salts
$Al(OH)_3$	Aluminium hydroxide
AM-41	Amino functionalised MCM-41 nanoparticles
APC	Antigen Presenting Cells
BET	Barrett-Emmett-Teller
BJH	Barrett-Joyner-Halenda
BRD	Bovine Respiratory Disease
BSA	Bovine Serum Albumin
BVDV	*Bovine Viral Diarrhoea Virus*
CAN	Carbonic anhydrase
C dots	Cornell dots
CTAB	Cetyltrimethyl ammonium bromide
CTLs	Cytotoxic T lymphocytes
CTA	Cholest-5-en-3-ol (3 beta)(trimethylammonio) acetate
DC	Dendritic cells
DDAB	Dioctadecyl dimethyl ammonium bromide
DLS	Dynamic light scattering
DMEM	Dulbecco's Modified Eagle Medium
DPPC	Dipalmitoyl phosphatidyl choline
DSC	Differential scanning calorimetry
DS	Dextran sulfate
ELISA	Enzyme-linked Immunosorbent Assay
ELISPOT	Enzyme-linked Immunosorbent Spot
FACS	Fluorescence activated cell sorting
FBS	Foetal Bovine Serum
FCA	Freund's Complete Adjuvant
FD	Freeze-dried
FDA	The Food and Drug Administration
FDU	Fudan University
HAS	Human serum albumin
HMSA	Amino functionalised hollow mesoporous silica nanoparticles

HMSCs	Hollow Mesoporous Silica Capsules
LYZ	Lysozyme
IBN-*n*	Institute for Bioengineering and Nanotechnology
IFA	Incomplete Freund adjuvant
IFN-γ	Interferon-gamma
IHC	Immunohistochemistry
IRIV	Immunopotentiating reconstituted influenza virosomes
i.m.	Intramuscular
KV	Killed Virus
MDBK	Madin-Darby bovine kidney
M-cells	Microfold cells
MCM-41	Mobil Composition of Matter No.41
MLV	Modified-live vaccine
MPLA	Monophosphoryl lipid A
MSN	Mesoporous Silica Nanoparticles
Mϕ	Macrophage
OVA	Ovalbumin
OVA-41	OVA loaded AM-41
oE2	optimised E2
PAGE	Polyacryalamide gel electrophoresis
PBMC	Peripheral blood mononucleocyte cell
PCV2	Procine circovirus type-2
PEI	Polyethylenimine
PEG	Polyethylene glycol
PLA	Poly(D,L-lactic acid)
PLG	Poly(lactide-co-glycolide)
PVA	Polyvinyl alcohol
Quil-A	*Quillaja saponira*
RES	Reticuloendothelial system
ROS	Reactive oxygen species
SBA	Santa Barbara Amorphous
s.c.	Subcutaneous
SEM	Scanning electron microscopy
SFU	Spot Forming Units

SLS	Sodium lauryl sulfate
SRB	Sulforhodamibe B
SSS	Solid Silica Spheres
SV	Silica Vesicles
TEOS	Tetraethylorthosilicate
T_c	Collapse temperature
T_p	Product temperature
TEM	Transmission electron microscope
Th1	T-helper type 1
Th2	T-helper type 2
TPP	Tripolyphosphate
XRD	X-ray diffraction
XPS	X-ray photoelectron spectra
rHBsAg	Hepatitis B surface antigen
γ-PGA	Poly(gamma-glutamic acid)

1.

Introduction

1.1 Aim

The aim of this research was to develop efficient vaccine delivery systems using a variety of novel silica nanoparticles as adjuvants and nanocarriers for the delivery of model protein Ovalbumin (OVA) and real virus protein *Bovine Viral Diarrhoea Virus-1* (BVDV-1) E2. The following types of silica materials, amino functionalised MCM-41 (Mobil Composition of Matter No. 41) termed as AM-41, amino functionalised hollow mesoporous silica nanoparticles (HMSA) and the novel silica vesicles (SV) were investigated to develop nanovaccine formulations. Development of successful

nanoparticle based vaccine delivery systems requires a thorough understanding of adjuvants and their use in vaccine formulations, to produce a safe, stable and immunogenic product.

Silica nanoparticles have desirable characteristics such as high surface area, large entrance size, tunable pore size, and large pore volume, which make them ideal candidates for adsorption of proteins/antigens. Protein was first adsorbed onto silica nanoparticles to develop nanovaccine and subsequently the release kinetics of protein was investigated. Following the cellular uptake and cytotoxicity analyses the efficacy of the developed nanovaccine formulation was verified in animal models. The specific objectives of the project were to:

1. Test a variety of silica nanoparticles for developing vaccine delivery systems.
2. Optimise the adsorption of protein and the desorption kinetics of protein loaded silica nanoparticles.
3. Investigate the cellular uptake and cytotoxicity of the silica nanoparticles/protein loaded silica nanoparticles.
4. Optimise the freeze-drying process for the nanovaccine formulations.
5. Analyse the physico-chemical characteristics of the 'wet' (non-freeze-dried) and 'freeze-dried' (FD) nanovaccine formulations.
6. Test the biological functionality of the developed 'non-FD' and 'FD' vaccine delivery systems in animal trials

1.2 Background

Bovine Viral Diarrhoea Virus-1 (BVDV-1), a bovine pestivirus, is a viral infection of cattle well recognised as a significant disease in both beef and dairy herds in Australia and many countries around the world. Genetically classified in the virus family *Flaviviridae* which includes diseases such as hepatitis C, yellow fever and dengue in the genus *Pestivirus* [1] BVDV species have been classified into type-1 and type-2 viruses and recently a new group has been classified as BVDV-3. [2, 3] BVDV-1 infection in cattle has been highly investigated in several countries due to its clinical and economical importance. A major concern regarding pestiviruses is not only limited to the substantial economic losses incurred but also to the fact that these viruses are not host specific signifying that they can easily spread amongst livestock such as sheep and pigs. It has been well established that sheep and goats can carry and be infected with BVDV-1 and then be able to pass the virus back to cattle. [4] BVDV-1 has also been found in bison and water buffaloes. [5]

BVDV-1 is a major contributor to the bovine respiratory disease (BRD) complex, which also causes tremendous economic loss to the cattle industry. An economic analysis in 2009 has shown that yearly losses due to BVDV could reach approximately US$88 per animal. [6] BVDV-1 is of high economic importance to the Australian cattle industry as over 80% of all feedlots having some exposure to the virus. It has been reported that in Queensland the cattle/beef industry is estimated at $3.5 billion each year, [7] economic losses from BVDV-1 through loss of cattle and productivity is estimated at $60 million each year. [8]

Infections of BVDV-1 can occur either via persistent infected (PI) or acutely infected animals. Transmission of BVDV-1 occurs when uninfected animals come in contact with the body fluid discharges from infected cattle. The virus is mainly transmitted through PI animals as they continuously shed large amounts of virus in the environment and are an important source of virus transmission within and between herds. [9, 10] A persistent infection can develop if the foetus is infected with the virus in the first trimester or up to the first 125 days of gestation an abortion or stillbirth may occur resulting in reduced productivity. [11] If a developing foetus survives to the end of pregnancy, the calf may be PI infected and may be born with severe birth defects, be developmentally delayed or appear normal. PI calves spread BVDV-1 to the other cattle as they constantly shed the virus throughout their life. In acute infection, even though the virus is excreted in lower amounts the virus is shed for two to three weeks by animals. The virus generally is incubated for 3-4 days and then circulated in the blood for a further 7-10 days, any secretion of body fluids may result in easy transmission of virus. [12] BVDV-1 infected cattle have a reduced immune response thus making them more susceptible to other diseases like pneumonia, mastitis, BRD and diarrhoea. Immunosupression caused by BVDV-1 infection can lead to a secondary infection, which mainly is the major cause of death in BVDV-1 infected cattle. [13, 14]

Killed Virus (KV) and modified-live vaccines (MLV) can be used to protect cattle from BVDV-1 infection. However, both of these types of vaccines can have certain drawbacks, MLV vaccines may be deactivated beyond certain temperatures or by some chemicals and revert to virulence while KV vaccines require more antigen per dose compared to the MLV and are more expensive.[15]

Current Vaccines: To date, only one BVDV vaccine has been approved for use in Australia known as Pestigard® produced by Zoetis. The vaccine needs to be administered as two doses, 6-8 weeks apart with annual booster injections required thereafter, it has a shelf-life of one month when refrigerated. Vaccination can reduce BVDV diseases; therefore, many countries in the European Union (EU) have developed an eradication program to assist in the fight and control of the disease

with the use of vaccines. [16] BVDV vaccine Bovilis BVD by Merck available in the UK too requires an annual booster dose and has a shelf-life of 18 months and needs to be stored at +2°C to +8°C, however, once the vaccine bottle is opened the shelf-life is reduced to 10 h. [17]

The economic impact BVDV-1 pathogen underpins the merits of the development of improved subunit vaccines. The BVDV-1 genome is a 12.3 kb single stranded RNA molecule containing a single open reading frame that is translated into a single polyprotein, which is processed into individual viral proteins by viral and cellular proteases. [18] E2 is the major structural glycoprotein of BVDV-1 and is the most immunogenic determinant of BVDV-1 virion. [13, 19-22] E2 when used in immunisation studies induces neutralizing antibodies, which are required to fight BVDV-1 infection. [2, 23-25] This makes E2 protein an excellent candidate for the development of subunit vaccines.

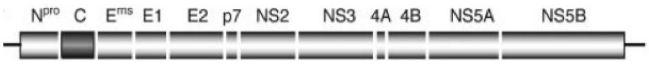

Fig 1.1. BVDV genome with the individual protein labelled. [26]

The major role of veterinary vaccines is to improve the health and welfare of the animals and increase production of livestock in cost-effective manner. Veterinary vaccines comprise of either whole pathogens, protein subunit vaccines, genetically engineered organisms or chimeras, vectored antigen formulations or naked DNA injections. [27] Vaccines are designed to mimic the immune responses associated with an active infection whilst avoiding the undesirable effects of disease. [28] Administration of a priming dose of the subunit vaccine followed by two or three booster doses facilitates immunogenicity, which occurs with repeated or sustained exposure to the same antigen. [29] Protein antigens can get degraded by proteases limiting their bioavailability and reducing their immunogenicity. Hence, vaccines utilise adjuvants to improve the immunogenicity by providing pro-inflammatory signals and prolonging the persistence of vaccine antigens. [30]

Adjuvants are often added to the subunit vaccine formulations in order to generate strong antigen specific immune responses. Unfortunately, the currently available adjuvants may induce undesirable side effects and may not generate long-term balanced humoral and cell-mediated immune responses, which limits their use in clinical studies. [31-33] To find an optimal antigen carrier and an optimal adjuvant are the most challenging aspects in the development of subunit

vaccines. As premature release and degradation of an antigen before uptake and activation of DC, in addition to generation of both humoral and cell-mediated responses have acted as a limiting factor in development of subunit vaccines comprising of protein antigens.

Veterinary vaccines comprise of approximately 23% of the global market and this sector has been growing consistently due to the new technological innovations. [27] Recent, advancements include development of nanoparticle based veterinary vaccine delivery systems, as continuous presentation of antigens by nanoparticles could be the crucial factor in inducing long-term immune responses. The sustained release of the antigen from the nanoparticles creates a 'depot effect' and enhances the immunogenicity of the adjuvants by producing prolonged immunological response. [34] Nanoparticles such as the polymeric [35], nucleoprotein [36] have been investigated to develop bovine veterinary vaccines and hydroxyapatite nanoparticles have been researched for development of diagnostic tests for cattle infected with *Mycobacterium bovis* [37].

Silica nanoparticles can be the new generation of adjuvants and delivery vehicles for protein antigens. Currently, they are used in diverse number of applications including enzyme adsorption and immobilisation [38], cell imaging and labelling. [39] Structurally, silica nanoparticles can exist as three dimensional solid spheres or can be porous with pore diameters in the microporous (< 2 nm), mesoporous (2-50 nm) and macroporous range (> 50nm). They can be structurally modified to be in different shapes such as rods and have chirality. [40] Since the discovery of the M41S family of mesoporous materials in 1992, a number of different mesoporous silica nanoparticles have been invented, which include MCM-*n* [41], SBA-*n* (Santa Barbara Amorphous) [42], IBN-*n* (Institute for Bioengineering and Nanotechnology) [43] and FDU-*n* (Fudan University). [44] Different organic functional groups such as amino ($-NH_2$), thiol (-SH), vinyl ($-CH=CH_2$) and phenyl ($-C_6H_5$) can be incorporated into or onto the walls of the silica particles. [45] The advantage of functionalisation of silica depends on the type of application. For example, amino functionalised have been explored in areas such as adsorption [46], catalysis [47] and enzyme immobilisation [48] with very promising results.

Protein antigens can either bind on the surface or internal pores of the silica nanoparticles. The sites at which the proteins bind to the nanoparticles greatly depend on the type and properties of the target proteins and pore structure, as well as available pore surface area of the nanoparticles. [49, 50] The forces that bind the proteins to the nanoparticles are the electrostatic protein-

surface interactions, hydrogen bonding and weak van der Waals interactions. [51] It is interpreted that if the protein is larger than the pore size of the nanoparticle, the protein will only adsorb onto the surface of the material and not utilise the high surface area provided by the pores. [52] In addition, other factors like functionalisation of the nanoparticles and pH of the protein can also affect the adsorption capacity. The pH at which the protein has an overall neutral charge is known as the relative isoelectric point (pI). Above the pI, the protein has a negative charge and below the pI it has a positive charge. [52] The highest amount of adsorption is observed when adsorption is carried out at the pI point of the protein. [53] However, the pH at which maximum loading can be achieved does not necessarily indicate that the activity of the protein is at its highest. Therefore, during adsorption it is important to select the pH as well as the buffer solution, which helps preserve the biological activity of the protein.

Mesoporous silica nanoparticles (MSNs) are considered highly advantageous for adsorption of proteins due to their large pore size, which allows adsorption of proteins into the particles and protects the protein molecules from degradation. [54] MSNs can act as both the nanocarriers as well as adjuvanting components to enhance vaccine efficacy. [55-59] A comprehensive review study on MSNs and adsorption of different proteins on MSNs to develop vaccine delivery systems has been included in Chapter 2.

Freeze-drying is a technique which can be used to further enhance the stability of nanovaccine formulations. [60] By freeze-drying unstable biomolecules such as proteins and peptides their chemical properties can be preserved for longer periods of time. [61-63] Freeze-drying of proteins offers the advantages such as prolonged shelf-life, improved storage and ease of shipping to the end user. [60, 64] These are all important issues in developing countries where maintenance of cold chain storage can be problematic. [65] Moreover, freeze-drying strategies are extensively used to facilitate the stability of nanoparticle-based vaccine formulations and enhance the antigen immunogenicity. [56, 60] While nanoparticle technologies can improve overall stability of some vaccines the degree of improvement can be dependent on the specific formulation under evaluation. A detailed review about freeze-drying process and advantages associated to freeze-drying nanovaccine formulations are included in Chapter 3.

Recently, there have been increasing reports focusing on development of nanoparticle based vaccine delivery systems using silica nanoparticles with a particular focus on BVDV-1. [31, 55-57,

66] In our laboratory, generation of soluble and endotoxin-free BVDV-1 E2 protein using an *E. coli* expression system has been well established. [66, 67] Reports from Mitter laboratory has demonstrated that model protein OVA delivered by AM-41 [68] and oE2 delivered by amino functionalised hollow mesoporous silica nanoparticles (HMSAs) [55] generated immune responses in animal studies. Though, OVA adsorbed AM-41 and oE2 adsorbed HMSAs induced detectable antibody and cell mediated responses, a major limitation was the low protein adsorption efficiency of 60-80 μg protein/mg particles. Therefore, in order to improve the antigen adsorption and facilitate sustained release of the antigen, 'novel' SV were evaluated as the 'new-generation' vaccine adjuvants and delivery systems. These 50 nm SV were designed specifically with thin shell wall and large entrance size for improving the BVDV-1 E2 adsorption.

1.3 Significance of project

The advancement made in this vaccine delivery system project is highly significant, as this research work identifies the use of protein loaded silica nanoparticles towards the development of a new platform technology for safer and more effective subunit vaccines. To demonstrate that silica nanoparticles can efficiently deliver a virus antigen and act as strong adjuvants we chose the BVDV E2 protein due to the global economic significance associated with the disease throughout the world. The silica nanoparticles used in the current study included AM-41, HMSAs and SV for the delivery of model protein OVA and with a viral antigen E2.

The ability of the developed nanovaccine formulations to generate humoral and cell-mediated responses in animal trials was compared to immunisation of antigen together with the traditional adjuvant *Quillaja saponira* Molina tree saponins (Quil-A). The OVA protein adsorbed on amino functionalised MCM-41 (AM-41) (72 μg OVA/mg AM-41) was freeze-dried with 5% trehalose and 1% PEG8000 as excipients, the ability of the developed freeze-dried vaccine formulation was tested in an animal trial. The non-FD and the FD 10 μg OVA adsorbed to 150 μg AM-41 nanovaccine generated OVA-specific antibody and cell-mediated immune responses lower than the traditional adjuvant Quil-A (50 μg OVA plus 10 μg Quil-A) after four immunisations. [56] However, the work on the freeze-dried OVA adsorbed AM-41 provided the proof-of-concept in small animal (mice) trials that freeze-dried nanovaccine formulations were able to elicit both humoral and cell-mediated immune responses.

Moving forward, the amino functionalised hollow mesoporous silica nanoparticles (HMSAs) with small pore entrance size 2 to 3.5 nm were investigated for BVDV E2 adsorption [55], only 60-80 μg oE2 adsorbed to per mg of HMSA. The efficacy of the non-FD and FD oE2/HMSA nanovaccine was tested in sheep after three immunisations. The level of the antibody responses to both the non-FD and FD 500 μg oE2 adsorbed to 6.2 mg HMSA nanoformulations were similar to those obtained for oE2 plus Quil-A, which provided a proof-of-concept that the E2 nanoformulations were immunogenic in a large animal and freeze-drying did not affect the immunogenicity of the nanoformulation. Importantly, it was found that the long-term cell-mediated immune responses were detectable up to five months after immunisation. The cell-mediated immune responses were consistently high in all sheep immunised with the freeze-dried oE2/HMSA nanovaccine formulation (>2200 spot forming units (SFU)/million cells) compared to the non-FD nanovaccine formulation (213-500 SFU/million cells) (Manuscript submitted to PLoS ONE). However, to further improve the BVDV E2 adsorption efficiency and immunogenicity of the nanovaccine, different types of novel SV were investigated.

Silica vesicles were rationally designed using a two-step synthesis process and have a uniform size of 50 nm. In the first step the vesicular structure was formed and in the second step the entrance size (5.7 nm to 16 nm) of the vesicle was controlled by tuning the temperature. The hydrophobic modified SV have shown to be exceptional nanocarriers for cellular delivery applications of therapeutical biomolecules like Ribonuclease A. [69] The four SV (SV-140, SV-140-A, SV-100 and SV-100-A) investigated in this study have controllable entrance size in the range of 5.7-16 nm and total pore volume in the range of (0.49-1.24 cm^3/g). They also have a thin porous shell wall with a thickness of ~6 nm, the large entrance size of all the four SV resulted in higher oE2 protein adsorption (~250 μg/mg SV) and slow release of the antigen. Based on the results from the *in vitro* studies the SV-140 was selected for *in vivo* investigation. [57] Mice were immunised with oE2 plus Quil-A (50 μg of oE2 plus 10 μg of Quil-A) or oE2/SV-140 (50 μg of oE2 adsorbed to 250 μg of SV-140) or oE2/SV-140 together with 10 μg of Quil-A. The animals in the oE2/SV-140 group generated oE2 specific antibody response at a titre of 10^5 compared to oE2 plus Quil-A group that generated antibody response at a titre of 10^4. In addition, the oE2/SV-140 group also induced higher cell-mediated response (1954-2628 SFU/million cells) compared to oE2 plus Quil-A (512-1369 SFU/million cells).

The ability of SV-140 as nanocarrier and adjuvant was further investigated in a long-term immunisation study and it was also used to develop a freeze-dried vaccine. Mice were immunised

with two subcutaneous injections of the non-FD and FD oE2 (100 μg)/SV-140 (500 μg) nanovaccine formulations. The non-FD as well as the FD oE2/SV-140 nanovaccines elicited total anti-oE2 IgG responses for at least six months post vaccination. The cell-mediated responses were found to be consistently higher with the oE2/SV-140 compared to all the treatment groups at the six-month time point. The FD oE2/SV-140 induced cell-mediated responses comparable to oE2 plus Quil-A at the six-month time point. This work for the first time demonstrated that vaccination with non-FD and FD oE2 /SV-140 elicited balanced T-helper type-1 (Th1) and T-helper type-2 (Th2) responses for up to 6 months post the final second immunisation (Manuscript submitted to PLoS ONE). The most promising results for efficient adsorption, sustained release and *in vivo* delivery of BVDV E2 antigen were obtained with SV-140. The capacity of SV to induce robust balanced humoral and cell-mediated immune responses is a huge advantage over traditional adjuvant such as Quil-A, which often induces only one arm of the immune response. This extensive research work will provide a platform to develop advanced veterinary vaccines using silica nanoparticles.

1.4 Structure of the thesis

The thesis consists of eight chapters. Chapters 2-7 are collection of journal papers that have been published or submitted as manuscripts for journal publications.

Chapter 1: Introduces the background along with the scope of this research work.

Chapter 2: Mesoporous Silica Nanoparticles as Antigen Carriers and Adjuvants for Vaccine Delivery **(Published in *Nanoscale 2013, 10, 5167-5179*)**.

Chapter 3: Freeze-drying of Protein loaded Nanoparticles for Vaccine Delivery **(Published in *Drug Delivery Letters 2012, 2, 83-91*)**.

Chapter 4: Freeze-drying of Ovalbumin loaded Mesoporous Silica Nanoparticle Vaccine Formulation Increases Antigen Stability under Ambient Conditions **(Published in *International Journal of Pharmaceutics 2014, 465, 325-332*)**.

Chapter 5: Immunisation of sheep with Bovine Viral Diarrhoea Virus, E2 protein using a Freeze-dried Hollow Silica Mesoporous Nanoparticle Formulation **(Manuscript submitted to PLoS ONE, K Mody as co-author)**.

Chapter 6: Silica Vesicles as Nanocarriers and Adjuvants for generating both Antibody and T-cell mediated Immune Responses to Bovine Viral Diarrhoea Virus E2 protein **(Published in *Biomaterials 2014, 35, 9972-9983*)**.

Chapter 7: Silica Vesicle Nanovaccine Formulations Stimulate Long-term Immune Responses to the *Bovine Viral Diarrhoea Virus* E2 protein **(Manuscript submitted to PLoS ONE)**.

Chapter 8: Conclusions and Recommendations.

1.5 References

1. Sako K, Aoyama H, Sato S, Hashimoto Y, Baba M (2008) γ-Carboline derivatives with anti-bovine viral diarrhea virus (BVDV) activity. Bioorganic & Medicinal Chemistry 16: 3780-3790.
2. Snider M, Garg R, Brownlie R, van den Hurk JV, Hurk SvDL-vd (2014) The bovine viral diarrhea virus E2 protein formulated with a novel adjuvant induces strong, balanced immune responses and provides protection from viral challenge in cattle. Vaccine 32: 6758-6764.
3. Liu L, Xia H, Wahlberg N, Belak S, Baule C (2009) Phylogeny, classification and evolutionary insights into pestiviruses. Virology 385: 351-357.
4. Sako K, Aoyama H, Sato S, Hashimoto Y, Baba M (2008) Carboline derivatives with anti-bovine viral diarrhea virus (BVDV) activity. Bioorganic and Medicinal Chemistry 16: 3780-3790.
5. Craig MI, Venzano A, Konig G, Morris WE, Jimenez L, et al. (2008) Detection of bovine viral diarrhoea virus (BVDV) nucleic acid and antigen in different organs of water buffaloes (Bubalus bubalis). Res Vet Sci 85: 194-196.
6. Hessman BE, Fulton RW, Sjeklocha DB, Murphy TA, Ridpath JF, et al. (2009) Evaluation of economic effects and the health and performance of the general cattle population after exposure to cattle persistently infected with bovine viral diarrhea virus in a starter feedlot. American Journal of Veterinary Research 70: 73-85.
7. AgForce (2007) Billion dollar beef industry goes under the spotlight at special future forum. Brisbane.
8. Meat-Livestock-Australia (2007) Pestivirus – a serious threat to productivity.
9. Hans H (1999) Epidemiological features and economical importance of bovine virus diarrhoea virus (BVDV) infections. Veterinary Microbiology 64: 89-107.
10. Corbett EM, Grooms DL, Bolin SR, Bartlett B, Grotelueschen DM (2011) Use of sentinel serology in a Bovine viral diarrhea virus eradication program. Journal of Veterinary Diagnostic Investigation 23: 511-515.
11. Divers TJ, Peek SF (2008) Rebuhn's Diseases of Dairy Cattle. St Louis,USA: Saunders Elsevier.
12. McGowan M, Kirkland P, Howard R, Morton J, Younis P, et al. (2008) Guidelines for hte investigation and control of BVDV (bovine viral diarrhea virus of bovine pestivirus) in beef and dairy herds and feedlots.
13. Nelson G, Marconi P, Periolo O, La Torre J, Alvarez MaA (2012) Immunocompetent truncated E2 glycoprotein of bovine viral diarrhea virus (BVDV) expressed in Nicotiana tabacum

plants: A candidate antigen for new generation of veterinary vaccines. Vaccine 30: 4499-4504.

14. Houe H (1999) Epidemiological features and economical importance of bovine virus diarrhoea virus (BVDV) infections. Veterinary Microbiology 64: 89-107.
15. Veterinary Services (December 2007) Bovine Viral Diarrhea Virus, Centers for Epidemiology and Animal health, editor. Safeguarding American Agriculture. Colorado: United States Department of Agriculture.
16. Alvarez M, Bielsa JM, Santos L, Makoschey B (2007) Compatibility of a live infectious bovine rhinotraheitis (IBR) marker vaccine and an inactivated bovine viral diarrhoea virus (BVDV) vaccine. Vaccine 25: 6613-6617.
17. Bovilis BVD. [cited 16.04.12]. Merck.
18. Donis RO, Corapi W, Dubovi EJ (1988) Neutralizing monoclonal antibodies to bovine viral diarrhoea virus bind to the 56K to 58K glycoprotein. Journal of General Virology 69 (Pt 1): 77-86.
19. Patterson R, Nerren J, Kogut M, Court P, Villarreal-Ramos B, et al. (2012) Yeast-surface expressed BVDV E2 protein induces a Th1/Th2 response in naive T cells. Developmental & Comparative Immunology 37: 107-114.
20. Pecora A, Aguirreburualde MS, Aguirreburualde A, Leunda MR, Odeon A, et al. (2012) Safety and efficacy of an E2 glycoprotein subunit vaccine produced in mammalian cells to prevent experimental infection with bovine viral diarrhoea virus in cattle. Veterinary Research Communications.
21. Ciulli S, Galletti E, Battilani M, Galligioni V, Prosperi S (2009) Analysis of variability and antigenic peptide prediction of E2 BVDV glycoprotein in a mucosal-disease affected animal. Veterinary Research Communications 33 Suppl 1: 125-127.
22. Bolin SR, Ridpath JF (1996) Glycoprotein E2 of bovine viral diarrhea virus expressed in insect cells provides calves limited protection from systemic infection and disease. Archives of Virology 141: 1463-1477.
23. Bruschke CJ, Moormann RJ, van Oirschot JT, van Rijn PA (1997) A subunit vaccine based on glycoprotein E2 of bovine virus diarrhea virus induces fetal protection in sheep against homologous challenge. Vaccine 15: 1940-1945.
24. Chimeno Zoth S, Leunda MR, Odeon A, Taboga O (2007) Recombinant E2 glycoprotein of bovine viral diarrhea virus induces a solid humoral neutralizing immune response but fails to confer total protection in cattle. Brazilian Journal of Medical and Biological Research 40: 813-818.

25. Aguirreburualde MSP, Gomez MC, Ostachuk A, Wolman F, Albanesi G, et al. (2013) Efficacy of a BVDV subunit vaccine produced in alfalfa transgenic plants. Veterinary Immunology and Immunopathology 151: 315-324.
26. Murray CL, Marcotrigiano J, Rice CM (2008) Bovine viral diarrhea virus core is an intrinsically disordered protein that binds RNA. Journal of Virology 82: 1294-1304.
27. Meeusen ENT, Walker J, Peters A, Pastoret P-P, Jungersen G (2007) Current Status of Veterinary Vaccines. Clinical Microbiology Reviews 20: 489-510.
28. Ulery BD, Kumar D, Ramer-Tait AE, Metzger DW, Wannemuehler MJ, et al. (2011) Design of a protective single-dose intranasal nanoparticle-based vaccine platform for respiratory infectious diseases. PLoS One 6: e17642.
29. Lambert PH, Liu M, Siegrist CA (2005) Can successful vaccines teach us how to induce efficient protective immune responses? Natural Medicines 11: S54-62.
30. Zepp F (2010) Principles of vaccine design-Lessons from nature. Vaccine 28 Suppl 3: C14-24.
31. Mody KT, Popat A, Mahony D, Cavallaro AS, Yu C, et al. (2013) Mesoporous silica nanoparticles as antigen carriers and adjuvants for vaccine delivery. Nanoscale: 5167-5179.
32. Foged C (2011) Subunit vaccines of the future: the need for safe, customized and optimized particulate delivery systems. Ther Deliv 2: 1057-1077.
33. Sun H-X, Xie Y, Ye Y-P (2009) Advances in saponin-based adjuvants. Vaccine 27: 1787-1796.
34. Ochoa J, Irache JM, Tamayo I, Walz A Protective immunity of biodegradable nanoparticle-based vaccine against an experimental challenge with Salmonella Enteritidis in mice.
35. Shephard MJ, Todd D, Adair BM, Po ALW, Mackie DP, et al. (2003) Immunogenicity of bovine parainfluenza type 3 virus proteins encapsulated in nanoparticle vaccines, following intranasal administration to mice. Research in Veterinary Science 74: 187-190.
36. Riffault S, Meyer G, Deplanche M, Dubuquoy C, Durand G, et al. (2010) A new subunit vaccine based on nucleoprotein nanoparticles confers partial clinical and virological protection in calves against bovine respiratory syncytial virus. Vaccine 28: 3722-3734.
37. Saleem IY, Vordermeier M, Barralet JE, Coombes AGA Improving peptide-based assays to differentiate between vaccination and Mycobacterium bovis infection in cattle using nanoparticle carriers for adsorbed antigens.
38. Vamvakaki V, Chaniotakis NA (2007) Immobilization of enzymes into nanocavities for the improvement of biosensor stability. Biosens Bioelectron 22: 2650-2655.
39. Wu SH, Lin YS, Hung Y, Chou YH, Hsu YH, et al. (2008) Multifunctional mesoporous silica nanoparticles for intracellular labeling and animal magnetic resonance imaging studies. Chembiochem 9: 53-57.

40. Che S, Liu Z, Ohsuna T, Sakamoto K, Terasaki O, et al. (2004) Synthesis and characterization of chiral mesoporous silica. Nature 429: 281-284.

41. Hou Q, Margolese D, Stucky GD (1996) Surfactant control ofphases in the synthesis of mesoporous silica-based materials. Chemistry of Materials 8: 1147-1160.

42. Vinu A, Hossain KZ, Ariga K (2005) Recent advances in functionalization of mesoporous silica. Journal of Nanoscience and Nanotechnology 5: 347-371.

43. Han Y, Ying JY (2004) Generalized fluorocarbon-surfactant-mediated synthesis of nanoparticles with various mesoporous structures. Angew Chem Int Ed Engl 44: 288-292.

44. Kruk M, Hui CM (2008) Synthesis and characterization of large-pore FDU-12 silica. Microporous and Mesoporous Materials 114: 64-73.

45. Wei Q, Nie ZR, Hao YL, Liu L, Chen ZX, et al. (2006) Effect of synthesis conditions on the mesoscopical order of mesoporous silica SBA-15 functionalized by amino groups. Journal of Sol-Gel Science and Technology 39: 103-109.

46. Hicks JC, Drese JH, Fauth DJ, Gray ML, Qi G, et al. (2008) Designing adsorbents for CO_2 capture from flue gas-hyperbranched aminosilicas capable of capturing CO_2 reversibly. Journal of the American Chemical Society 130: 2902-2903.

47. Park SE, Sujandi (2008) Green approaches via nanocatalysts with nanoporous materials: Functionalisation of mesoporous materials forsingle site catalysis. Current Applied Physics 8: 664-668.

48. Shah P, Sridevi N, Prabhune A, Ramaswamy VD-S (2008) Structural features of Penicillin acylase adsorption on APTES functionalized SBA-15. Microporous and Mesoporous Materials 116: 157-165.

49. Chen Y, Wang YJ, Yang LM, Luo GS (2008) Micrometer-sized monodispersed silica spheres with advanced adsorption properties. AIChE Journal 54: 298-309.

50. Chesko J, Kazzaz J, Ugozzoli M, O'Hagan DT, Singh M (2005) An investigation of the factors controlling the adsorption of protein antigens to anionic PLG microparticles. Journal of Pharmaceutical Sciences 94: 2510-2519.

51. Yiu HHP, Wright PA (2005) Enzymes supported on ordered mesoporous solids: a special case of an inorganic-organic hybrid. Journal of materials chemistry 15: 3690-3700.

52. Hudson S, Cooney J, Magner E (2008) Proteins in Mesoporous Silicates. Angew Chem Int Ed Engl 47: 8582-8594.

53. Yiu H, Wright P (2005) Enzymes supported on ordered mesoporous solids: a special case of an inorganic-organic hybrid. Journal of Materials Chemistry 15: 3690-3700.

54. Slowing II, Trewyn BG, Lin VSY (2007) Mesoporous Silica Nanoparticles for Intracellular Delivery of Membrane-Impermeable Proteins. Journal of the American Chemical Society 129: 8845-8849.

55. Mahony D, Cavallaro AS, Mody KT, Xiong L, Mahony TJ, et al. (2014) In vivo delivery of bovine viral diahorrea virus, E2 protein using hollow mesoporous silica nanoparticles. Nanoscale 6: 6617-6626.

56. Mody KT, Mahony D, Cavallaro AS, Stahr F, Qiao SZ, et al. (2014) Freeze-drying of ovalbumin loaded mesoporous silica nanoparticle vaccine formulation increases antigen stability under ambient conditions. International Journal of Pharmaceutics 465: 325-332.

57. Mody KT, Mahony D, Zhang J, Cavallaro AS, Zhang B, et al. (2014) Silica vesicles as nanocarriers and adjuvants for generating both antibody and T-cell mediated immune resposes to Bovine Viral Diarrhoea Virus E2 protein. Biomaterials 35: 9972-9983.

58. Panyam J, Labhasetwar V (2003) Biodegradable nanoparticles for drug and gene delivery to cells and tissue. Adv Drug Deliv Rev 55: 329-347.

59. Koping-Hoggard M, Sanchez A, Alonso MJ (2005) Nanoparticles as carriers for nasal vaccine delivery. Expert Rev Vaccines 4: 185-196.

60. Abdelwahed W, Degobert G, Stainmesse S, Fessi H (2006) Freeze-drying of nanoparticles: formulation, process and storage considerations. Adv Drug Deliv Rev 58: 1688-1713.

61. Tang X, Pikal MJ (2004) Design of freeze-drying processes for pharmaceuticals: practical advice. Pharm Res 21: 191-200.

62. Anhorn MG, Mahler HC, Langer K (2008) Freeze drying of human serum albumin (HSA) nanoparticles with different excipients. Int J Pharm 363: 162-169.

63. Vandana M, Sahoo SK (2009) Optimization of physicochemical parameters influencing the fabrication of protein-loaded chitosan nanoparticles. Nanomedicine (Lond) 4: 773-785.

64. Mody K, Mahony D, Mahony TJ, Mitter N (2012) Freeze-drying of protein loaded nanoparticles for vaccine delivery. Drug Deliv Lett 2: 83-91.

65. Roy I, Gupta MN (2004) Freeze-drying of proteins: some emerging concerns. Biotechnology and applied biochemistry 39: 165-177.

66. Cavallaro A, Mahony D, Mody K, Mahony T, Mitter N (2013) Lots of Bovine Viral Diarrhoea Virus E2 protein – A Subunit Vaccine.; Ltd iP, editor: iConcept Press.

67. Cavallaro AS, Mahony D, Commins M, Mahony TJ, Mitter N (2011) Endotoxin-free purification for the isolation of Bovine Viral Diarrhoea Virus E2 protein from insoluble inclusion body aggregates. Microb Cell Fact 10: 57.

68. Mahony D, Cavallaro AS, Stahr F, Mahony TJ, Qiao SZ, et al. (2013) Mesoporous Silica Nanoparticles Act as a Self-Adjuvant for Ovalbumin Model Antigen in Mice. Small 9: 3138-3146.

69. Zhang J, Karmakar S, Yu M, Mitter N, Zou J, et al. (2014) Synthesis of silica vesicles with controlled entrance size for high loading, sustained release, and cellular delivery of therapeutical proteins. Small 10: 5068-5076.

2.

Literature Review

Mesoporous Silica Nanoparticles as Antigen Carriers and Adjuvants for Vaccine Delivery

---

The aim of Chapter 2 is to understand the fundamentals of silica nanoparticle based vaccine delivery systems. In this literature review, different aspects of mesoporous silica nanoparticles (MSNs) based nanovaccine delivery systems like MSNs as antigen carriers, MSNs as adjuvants in vaccine formulation and biocompatibility and biodistribution of MSNs were discussed in depth.

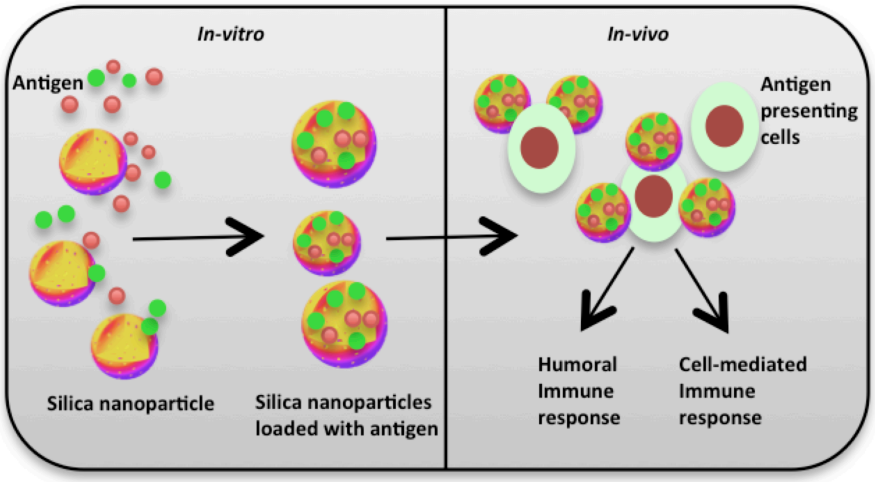

Fig 2.1. Schematic representation showing the development of silica nanoparticles based vaccine delivery systems. **Chapter 2 is as published in *Nanoscale 2013, 10, 5167-5179***

2.1 Introduction

Development of efficient and potent vaccines still remains as one of the most effective strategies for preventing diseases. [1] Traditional vaccines comprise of attenuated pathogens (live vaccines) or inactivated pathogens, which can elicit a strong immune response. But, traditional vaccines are generally difficult to deploy, may have side effects like inflammation at the site of vaccination, require multiple doses for effective immunisation [2, 3] and are often expensive. On the other hand, subunit vaccines comprise of highly purified recombinant antigens such as proteins and peptides, these vaccines are more stable and have better safety profiles compared to the conventional vaccines. [4] However, subunit vaccines can have poor immunogenicity and are often unable to cross intestinal mucosal tissues due to degradation by metabolic enzymes. [5-9] To improve the immunogenicity of subunit vaccines, adjuvants are often added to the formulation.

Adjuvants can be defined as compounds that are added to the vaccine formulations in order to enhance the activation of the dendritic cells (DC) and generate robust immune responses. [10] Adjuvants can be classified in two categories, depending on whether they have an immunostimulatory effect on the antigen presenting cells (APCs) or function as delivery systems initiating antigen uptake. [11] However, very few adjuvants have been approved for animal as well as human use as they can be highly toxic and induce undesirable severe side effects, limiting their use in clinical studies. [12] Adjuvants approved for use in human vaccines include, aluminium-based mineral salts (Alum), MF59® (oil-in-water emulsion), virus like

particles (VLPs), MPL® (a glycolipid), immunopotentiating reconstituted influenza virosomes (IRIV) and cholera toxin. [13] Two of the most challenging aspects in the development of novel vaccines are finding the optimal antigen carrier and optimal adjuvant combination.

In the past few years application of nanotechnology has undergone a rapid development holding promise to provide a new generation of improved vaccines. Nanoparticles are molecular materials that range between 1–1000 nm to which drugs or biologically active material can be entrapped or encapsulated, adsorbed or attached. [14] When an antigen is associated with nanoparticles, a stronger immune response is generated compared to the soluble antigen alone.[15] Nanoparticles due to their unique chemical, physical and biological properties are considered efficient delivery vectors to deliver drugs, proteins, peptides and nucleic acids. Several particle-based vaccine delivery systems such as polymeric [14, 16-21], lipid-based [22, 23] and chitosan [24] nanoparticles have been investigated. Though, polymeric and liposomal nanoparticles have been designed to achieve controlled drug release, release of antigenic proteins and induce immune responses very effectively, [21, 23] these nanoparticles are structurally unstable and are prone to hydrolysis in the harsh gastric environment. In most cases the entrapped molecules in the matrices of polymer or inorganic particles would leak out within a few hours due to diffusion or degradation of the polymer matrix. This premature release and degradation of the drug or antigens during intestinal transit presents a major challenge in vaccine development. Mesoporous silica nanoparticles (MSNs)[25-28] are being investigated as the likely candidates to overcome instability and leakage issues associated with other nanoparticles.

Since the discovery of MCM-41 type MSNs in 1992 by Mobil scientists, [29] significant efforts have been devoted to establish a clinical potential of these particles in the biomedical field. [30] In addition many research studies have focussed on synthesis, biocompatibility and biodistribution of MSNs. [15, 31-45] Various studies have shown that MSNs are excellent vehicles for gene and drug delivery because of their ease of synthesis, surface functionalisation, excellent *in vivo* biocompatibility as well as good thermal and chemical stability. [40, 46, 47] Additionally, MSNs are capable of controlling the release of drugs or proteins depending on their size, shape and surface modification. [15, 35] These properties of MSNs make them very attractive vehicles for targeted delivery and release of biomolecules such as nucleic acids, enzymes, proteins and peptides. [20, 25, 32, 33, 48-51] *In vitro* studies using HeLa cells demonstrated that MSN could successfully deliver the membrane-impermeable protein

cytochrome c. [49, 52, 53] Advancements on different types of drugs and enzymes immobilised on to MSNs have already been exhaustively reviewed by Popat *et al.*[25]. Despite rapid developments made on biomedical applications of MSNs, there is very limited literature citing the use of MSNs as vaccine adjuvants or as antigen delivery carriers. [28, 51, 54] Hence, it is important to provide a concise and critical review of the latest advances in the field of vaccine delivery using MSNs. This review will give us an overview on different types of proteins/antigens that have been delivered using MSNs and also discuss key factors affecting the loading and release of antigens to/from MSNs. Additionally, the cytotoxicity of MSNs, an important aspect in clinical applications will be addressed. Lastly, we will focus on some of the challenges faced by researchers in this field; provide some outlook and concluding remarks.

2.2 MSNs as antigen carriers

Examples of different proteins loaded on to MSNs for a variety of applications are summarised in Table 2.1. Surface modified MSNs have been investigated as efficient protein delivery systems. [45, 55-57] Aminosilane functionalised ordered silica materials (SBA-15) have been used to study the adsorption and release kinetics of different proteins including bovine serum albumin (BSA), lysozyme and myoglobin. [42, 58] Recently, studies have been focusing on the use of hollow mesoporous silica nanoparticles (HMSNs) for the delivery of proteins due to their desirable characteristics such as the high loading capacity. Functionalised and unmodified cell membrane-permeable hollow mesoporous silica capsules (HMSCs) have been used for intracellular delivery of BSA and goat IgG. [43]

In our laboratory, we have developed nanoparticle-based vaccine delivery systems using model protein ovalbumin (OVA) and the viral antigen E2 from Bovine Viral Diarrhoea Virus (BVDV) and amino functionalised MSNs and HMSNs type materials. We observed that the optimal protein and nanoparticle combination needs to be developed empirically as the adsorption and desorption kinetics is dependant on various factors such as functionalisation of nanoparticles and zeta potential of proteins and nanoparticles. HMSNs can significantly improve the protein loading capacity. Different parameters including synthesis, functionalisation, adsorption and release studies of the mesoporous silica used for protein delivery and vaccine development are discussed below.

In the literature various techniques for the synthesis of MSNs have been discussed. The first reports on the synthesis of MSNs with uniform pore size and ordered pore structure using surfactant and structure-directing agents were published in 1992. [59, 60] The deep understanding of the sol-gel chemistry and availability of the different types of surfactants have made possible to produce MSNs with varied structures. Until now most of the research has focused on using MCM-41, MCM-48 and SBA-15 type MSNs for delivery applications. One of the major drawbacks of these conventional MSNs is their limited pore size (2-10 nm), which restricts their use in adsorption of large molecules such as proteins and DNA. Recently, several reviewers have discussed in depth the synthesis of various types of MSNs, [30, 61, 62] thus in this review we will only focus on recent advances in synthesis of MSNs especially in the area of vaccine delivery.

Table 2.1. Summary of different types of proteins loaded onto the mesoporous silica nanoparticles

Material	Modification	Protein	Ref.
Hollow Mesoporous silica nanoparticles	Unmodified	PC2 GST-ORF2-E2	[26]
Hollow Mesoporous silica capsules	Carboxy, Amino, 5-aminofluorescein (AFL)	BSA (bovine serum albumin), Goat IgG	[43]
MSN	2-(methoxy [polyethyleneoxy]propyl)	BSA	[45]
MSN	CD4	HIV-gp120	[55]
MSN	Citraconic amide	Cytochrome C	[56]
MSN	Aminopropyl	Insulin	[57]
SBA-15	Unmodified	BSA	[51]
SBA-15	Unmodified	BSA	[28]
SBA-15	Aminosilane	Lysozyme	[42]
SBA-15	Aminosilane	Myoglobin	[42]
SBA-15	Aminosilane	Myoglobin	[58]
SBA-15	Aminosilane	BSA	[58]
SBA-15	Aminosilane	Lysozyme	[58]
SBA-15	Amine	BSA	[71]
SBA-15	Unmodified	Bacterial recombinant protein *Int1β*	[54]
SBA-15	Unmodified	Snake venom proteins (20 proteins from 84-7 kDa)	[54]
MCM-41	Unmodified	Cytochrome C	[49]
MCM-41	PEGylated	BSA	[86]
FDU-12	Unmodified	BSA	[87]
FDU-12	Amine	BSA	[88]
FDU-12	Amine, Mercapto, Vinyl, Phenyl	BSA	[89]

Typically, a base-catalysed sol-gel process has been used to produce silica nanoparticles with suitable particle properties. [63] The Stöber method has been applied to produce monodispersed solid silica nanoparticles ranging between 20-2000 nm in size, by using the ammonia-catalysed hydrolysis of tetraethylorthosilicate (TEOS) in a water-alcohol solution. [64] Later, Cai *et al.*[65],[66] reported factors affecting morphology control and particle size of MCM-41. They synthesised particles with a variety of shapes and sizes using alkaline conditions. Subsequently, Zhao *et al.*[67] reported the synthesis of SBA-15 particles with highly ordered, 2-D hexagonal (space group p6mm) silica-block copolymer mesophases in acidic media with a particle size of approximately 1 μm. Although, MCM-41 and SBA-15 are amongst the most widely discussed family of MSNs in the biomedical field, their use in some specific applications such as protein adsorption and separation is limited due to its pore size and structure.

Current studies have focused on the synthesis of new types of MSNs with specific structures (large pores, small particle size) and controlled release properties like hollow and rattle-type nanomaterials, the methods to fabricate hollow and rattle-type particles has been recently reviewed. [68] The synthesis of hollow structures can be classified into four groups, conventional hard templating, sacrificial templating, soft templating and template-free techniques. Extension of hard templating method to the sacrificial templating is known to be the most promising as it does not require additional surface functionalisation and readily forms a shell by chemical reaction. [68] These hollow/rattle type MSNs consist of an interstitial hollow space and a mesoporous shell with low density and high specific area. The high loading capacity of these particles makes them ideal as the next-generation of nanomaterials for vaccine delivery. [68]

HMSNs have been synthesised using a sol-gel/emulsion method with modifications to adsorb antigens; [69] in addition, HMSCs with novel capsular morphology have been synthesised using the cetyltrimethyl ammonium bromide (CTAB) micellar assembly in cholesterol emulsion. [43] Synthesising materials with large pore (~30 nm to 50 nm), small particle size (50 nm to 200 nm) and tunable surface properties will allow sufficient space for proteins and peptides to adsorb and release the payload at the desired site, and hence remains the area of intense focus.

One of the most useful features of MSNs is its flexible physical and chemical properties through which adsorption and release of biomolecules can be tuned. [70] Functionalisation is one of the most widely used strategies to alter release of biomolecules from MSNs. To achieve

higher endocytosis MSNs that have been functionalised with positively charged functional groups (e.g. amino, triethanolamine, polyethylenimine, etc) have been investigated. Varieties of functional groups have been used to achieve adjustable stimuli responsive delivery systems such as pH,[71-78] time,[79] enzyme,[80-82] thermal and light. [73, 83] The pH responsive functionalisation is most widely used in cancer targeting utilising the distinct pH difference between intra and extracellular environment. Functionalisation is also vital for gene therapy as silica nanoparticles from a negative to a positive charge allowing the binding nucleic acids, which are also negatively charged. Additionally, functionalisation can also protect peptides and siRNA from degradation, ensuring their effectiveness as therapeutic delivery agents. Hence, efforts has been devoted to prepare positively charged MSNs to adsorb and protect DNA, siRNA and proteins for gene therapy. [47]

In the pioneer work, Kneuer *et al.*[83] employed solid silica spheres (SSS) and modified them with primary amino groups to form complexes with negatively charged DNA. The concept of co-delivery of drug/gene therapy became feasible by delivering the specific siRNA to inactivate the gene responsible for a particular disease, followed by the release of an active moiety to achieve high efficiency. MSNs have emerged as one of the most promising components for co-delivery of drugs and genes in the last decade. Traditionally, MSNs loaded with drugs have been functionalised with positively charged polymer to form complexes with proteins and peptides. [84, 85]

Functionalisation of porous silica with a positive charge is also used to adsorb and separate a variety of protein-based antigens (Table 2.1). Song *et al.*[71] showed amino functionalised SBA-15 particles adsorb more BSA than bare silica due to strong interaction between negatively charged protein and amine. Post-synthesis grafting method was used to functionalise inner and outer surfaces of MSNs, which resulted in higher protein adsorption (~ 23%), compared to bare silica. The release of BSA from functionalised particles was low compared to the unfunctionalised counterparts, which is consistent with other studies. [45, 58] Interestingly, this phenomenon is protein dependent as *Kim et al.*[42] demonstrated a faster release of lysozyme and myoglobin from the amino functionalised material compared to the unmodified particles. Although, BSA successfully adsorbed onto amine modified SBA-15, spherical MSNs showed about ~50% of BSA adsorption due to high surface area and small particle size. [28] The protein adsorption efficiency could be further increased if these MSNs are functionalised with amino groups. Release of proteins from functionalised MSNs is a challenge and materials

with better adsorption and release kinetics are required in order to utilise MSNs as functional nanovaccine carrier. Many studies have been conducted on adsorption and release of DNA and siRNA using positively charged molecules. This strategy is less utilised when it comes to adsorption and release of proteins and peptides especially to induce immune response.

The encapsulation of antigenic proteins onto a silica nanoparticle carrier system mainly takes place through adsorption and/or encapsulation (Fig 2.2). To determine the level of protein adsorption, protein-adsorbed samples are centrifuged and the unbound protein remaining in the supernatant is measured and compared to the pre-adsorption concentration using a colorimetric protein assay or by measuring the absorbance of the Soret band of the protein. The potential of ordered mesoporous silica as a vaccine adjuvant was first observed by Mercuri *et al.*[54], using SBA-15 as a carrier and adjuvant for bacterial recombinant protein *Int1β.* They demonstrated an increased immune response in mice. However, there was no evidence of *in vitro* release of the protein from the silica carriers.

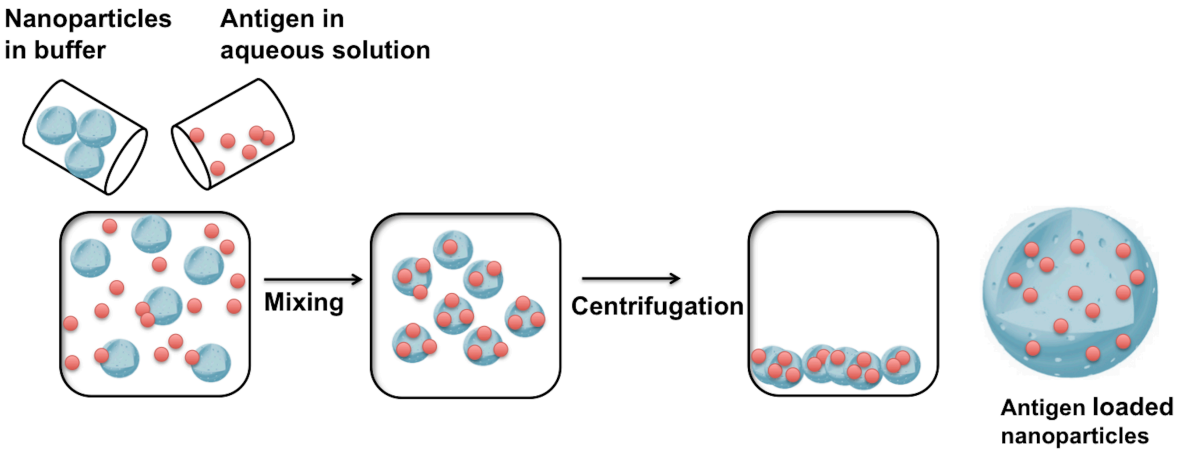

Fig 2.2. Schematic representation of preparation of antigen loaded nanoparticles by adsorption method.

Many researchers have studied the adsorption and release of proteins such as BSA, cytochrome c, lysozymes, and other antigens onto MSNs (listed in Table 2.1). Hartono *et al.*[89] demonstrated that the adsorption of BSA was significantly dependent on the type of functional group when using the large pore FDU-12. Amino functionalised and vinyl functionalised FDU-12 particles showed the highest adsorption capacities of 132.6 and 50 mg/g respectively. Although protein adsorption was dependent on the pore entrance and cavity size, amino functionalised FDU-12 particles adsorbed BSA due to electrostatic interaction, while vinyl

functionalised particles relied on hydrophobic interaction for protein adsorption. However, in most cases the protein was used as a model drug but not as an antigen for gene therapy or immunotherapy. The adsorption and release kinetics of Type 2 ORF2 protein from porcine circovirus adsorbing to HMSN particles, suggests adsorption takes place in a two-step process with the capacity of 150 μg protein/mg HMSN. In vitro release behaviour of this protein was very fast in first 12 hr followed by a slow release for about a week confirming a weak interaction between protein and HMSNs. [26] Additionally, lymphocytes proliferation and IFN-γ responses showed encouraging results.

Silica architecture also affects adsorption and release of large antigens such as proteins and peptides. BSA was shown to bind highest to the 430 nm S1 particle with an eye combed pore structure, compared to S2 (130nm) and SBA-15 (1-2μm). [28] S1 bound BSA also resulted in the highest antibody titres *in vivo*, which is in line with earlier studies. [88, 90] While these results are encouraging, more work needs to be done in designing nanocarriers for vaccine delivery. For instance, higher protein loading capacity will reduce the systemic concentration of silica nanoparticles whilst maintaining a high antigen dose. Elicitation of an immune response is heavily dependent on how the antigen is presented or released. It is also dependant on its uptake by M-cells (microfold cells) and APCs. M-cells are involved in transport of particles from gut lumen to immune cells across epithelial barrier in order to generate mucosal immunity. Thus, precise control over release of the antigen is necessary in order to achieve target specificity. Novel nanomaterials with high protein loading and immune cell specific release are sought after in order to achieve clinically acceptable formulation based on MSNs.

2.3 MSNs as Adjuvants in vaccine formulation

Adjuvants are often added to vaccine formulations to obtain a desired level of immunogenicity against the antigens and they can be classified based on their component sources, mechanisms and physicochemical properties. Adjuvants act as immunostimulants by directly acting on the immune system or as delivery vehicles carrying antigens to the immune system. [13] Adjuvants must be suitably formulated for stability and maximum effect. The advantages of adjuvants include: 1) they increase the total antibody titre, 2) decrease the number of doses required to achieve complete immunisation, 3) enhance immune response, and 4) potentiate cell-mediated immunity, mucosal immunity and provide cross-protection. [91]

In general terms, immunity is divided into two major categories: innate and acquired immunity. Innate immunity is the first line of defence; however when a foreign organism is not removed by innate immunity acquired immunity produces antigen specific B-cells and T-cells to prevent reinfection with the same organism. Furthermore, acquired immunity is divided into two separate arms of defence, B-cell mediated or humoral immunity and T-cell mediated or cellular immunity. [92] There are two subsets of T-lymphocyte cells. CD4+ T helper cells and CD8+ cytotoxic T cells. The T-cell receptors on the surface of T-cells regulate the cells and eliminate antigen to mount an effective immune response. [93] CD4+ T cells differentiate into T-helper type 1 (Th1) cells and T-helper type 2 (Th2) cells. Th1 cells drive the immune response towards a cell-mediated immune response and Th2 cells promote a humoral or allergic response (Fig 2.3). [94] Adjuvants on their own have limited or no efficacy, nonetheless strong adjuvant activity in a formulation is often correlated with increased toxicity and adverse side effects. Therefore, both adjuvant components and formulation specifications e.g. resuspension medium, particle size, and charge are crucial for enhancing vaccine potency. [13]

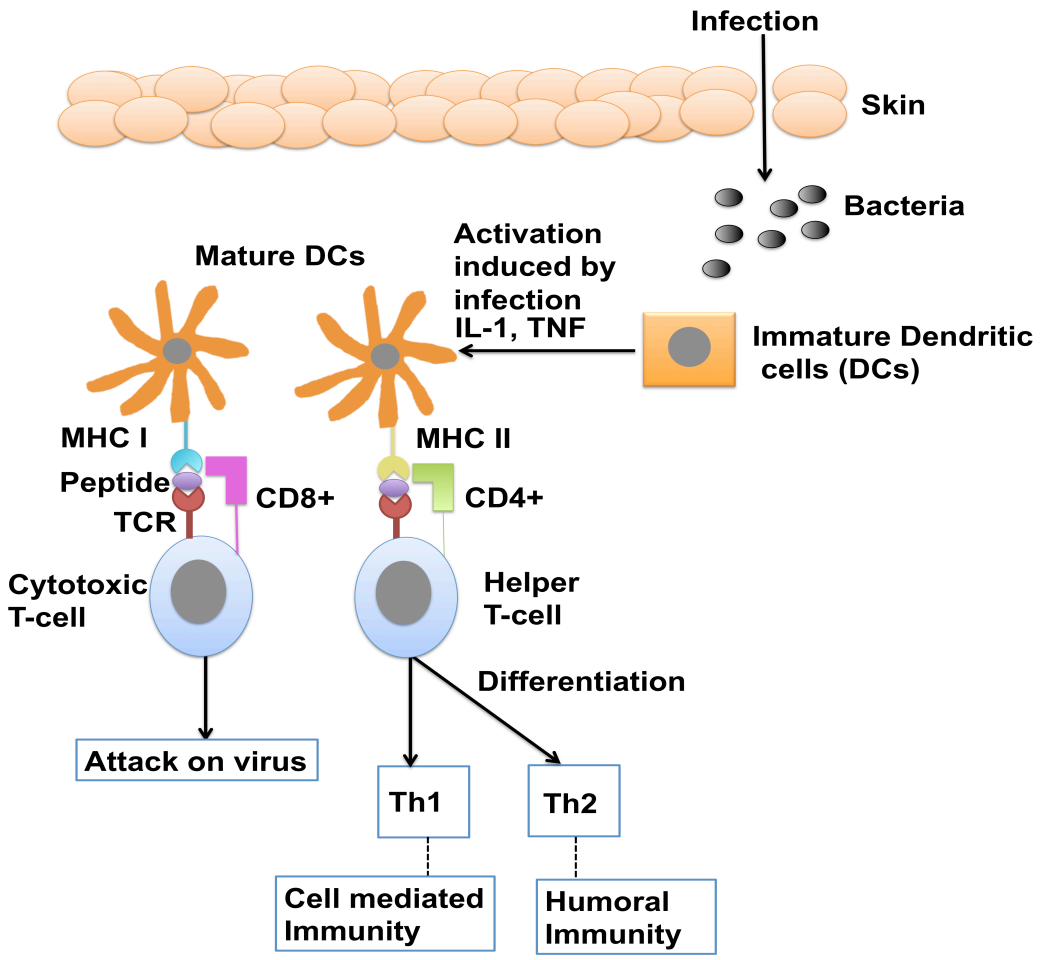

Fig 2.3. Schematic representation of induction of T-cell mediated immune response.

Quil-A, an extract from the bark of *Quillaja saponaria* and its purified saponin QS-21 is the most common adjuvant used in mice trials. The saponin-based adjuvants stimulate Th1 immune response and production of cytotoxic T-lymphocytes against antigens, making them ideal for use in subunit vaccines for infectious diseases and cancer immunotherapy. [95-97] However, disadvantages like pain at the site of injection, severe local reactions and toxicity profile of these adjuvants make them unsuitable for human use. [13, 98] Freund's complete adjuvant (FCA) and immune-stimulating complexes induce both humoral and cellular immune responses, making FCA as one of the most effective adjuvant. Nevertheless, FCA is known to induce high toxicity and severe reactions, limiting its use in humans. [99]

Alum-type adjuvants are widely used in human and veterinary vaccines. The Food and Drug Administration (FDA) of the United States have only approved aluminium salts as adjuvant for human use. [100] Alum based adjuvants induce strong antibody responses and directly activate DCs. Adsorption of antigens to aluminium compounds can help retain the antigen at the injection site at a higher concentration, therefore providing a sufficient uptake time for DCs. However, drawbacks associated with these adjuvants is that they are not effective for all antigens and often induce local reactions at the site of injection and generally fail to induce CD8+ T-cell immunity. [101] Reed *et al.*[13] have comprehensively covered different types of immune responses triggered by a variety of delivery systems and have given an overview on different types of adjuvants that are being used in the development of human vaccine formulations in pre-clinical and clinical trials. [13]

Most of the conventional vaccines produce either a Th1 or Th2 mediated response (Table 2.2), hence there is a need for a robust, non-toxic and effective adjuvant that can induce the co-production of immune responses with minimal or no side effects. [102, 103] Silica nanoparticles may provide us with a solution as they have the potential to act as adjuvants in vaccine delivery (Table 2.3).

Table 2.2. Different types of immune responses elicited by nanocarriers or delivery systems.

Carriers or delivery systems	**Th1 response**	**Th2 response**	**Cross priming**	**B-cell response**
Aluminium salts (Alum)		✓	-	✓
Saponins (Quil-A)	✓		-	✓
Incomplete Freund's adjuvant and Complete Freund's adjuvant	-	✓	-	✓
ISCOMs	✓	✓	✓	✓
Liposomes	✓		✓	✓
Emulsions (MF59®)	✓	-	-	✓
Silica nanoparticles (SBA-15, HMSNs [hollow mesoporous silica nanoparticles])	✓	✓		✓
Polymeric microparticles, PLA (polylactic acid), PLG (poly[lactide-co-glycolide])	✓	✓		✓
Chitosan nanoparticles	✓	✓		✓

As an alternative to currently available adjuvants, new approaches in vaccine development have been antigen encapsulation, surface-immobilisation or protein adsorption onto nanoparticles. The potential of any biomaterial to act as an adjuvant is determined by the degree of DC maturation induced (Fig 2.4).

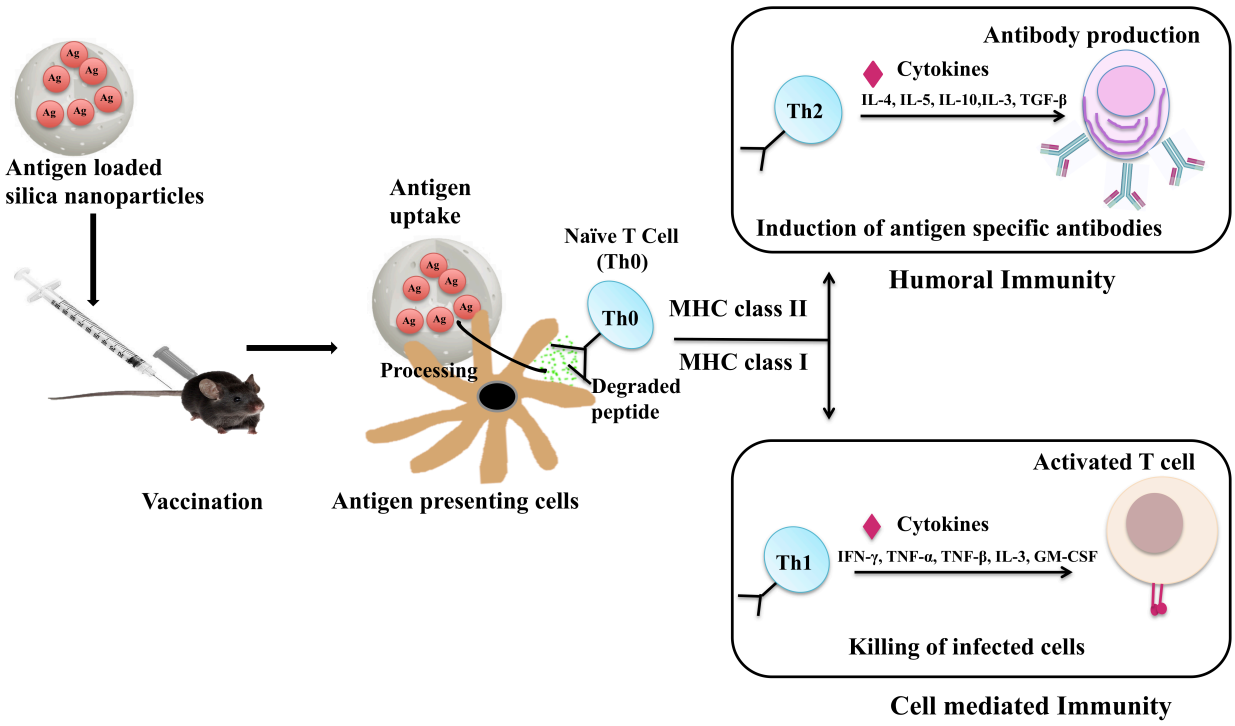

Fig 2.4. Schematic representation of initiation of immune responses by silica nanoparticle-based vaccine.

Table 2.3. Summary of different sized silica particles showing the systemic adjuvant effect.

Particle type	Size	Antigen	Route	Result	Ref.
HMSN	200 nm	PC2 GST-ORF2-E2	i.m.	Protein loaded nanoparticles induced a higher humoral and cellular immune response compared to protein alone	[26]
S1 S2 SBA-15	430 nm 130 nm 1-2 µm	BSA	i.m. / oral	IgG and IgA titers obtained with protein loaded silica nanoparticles were in the order of S1 > S2 > SBA-15.	[28]
SBA-15	10–12 nm	BSA	i.m. / oral	Induced coproduction of both IgG2 and IgG1 isotypes.	[51]
SBA-15		Recombinant protein *Int1β* and snake venom proteins	s.c.	SBA-15 showed better adjuvant property than alum	[54]

The maturation of DC is associated with increased expression of several cell surface markers, including the co-stimulatory molecules: CD40, CD80, CD83, CD86, MHC class I and II. DC maturation can be induced by inflammatory cytokines like tumour necrosis factor-alpha (TNF-α) or inflammatory factors like lipopolysaccharide and bacterial DNA. The DC maturation process is highly important for the initiation of immune response. [104, 105]

Moghimi *et al.*[106] have demonstrated that by attaching a polyethylene glycol (PEG) or any other type of polymer to nanoparticles a hydrophilic environment can be created which protects the nanoparticles from non-specific recognition. Antigen loaded nanocarriers have shown promising potential in cancer therapy due to their capacity of being actively taken up by the APCs and eliciting antigen-specific immune responses. [107] Few studies have focused on the use of biodegradable nanoparticles as adjuvants for vaccine delivery. [95, 108]

Gennari *et al.*[109] conducted an *in vivo* study to compare the effect of silica injection on antibody responsiveness to selection antigens in H and L mice of four selections. They reported that administration of amorphous silica particles had a weakening effect on macrophage (Mϕ) cell activity and its treatment constantly improved antibody response. They administered silica intravenously or locally in one hind footpad at 6 h or 24 h before immunisation by the same route. Mϕ have a weak APCs capacity but are known to initiate innate or acquired immune response as they compete with B-lymphocytes and DCs, which have a powerful APC function, necessary to initiate an efficient immune response. [54]

Silica nanoparticles might provide a solution to tackle the issues associated with conventional adjuvants and improve the overall safety profile of the vaccine formulations. However, whether or not MSNs act as adjuvants and induce an immune response greatly depends on the factors including architecture of the particle and protein, binding capacity of the particles, protein conformation, concentration and surface charge of the nanoparticles and proteins, and uptake of protein loaded nanoparticles by M-cells and APCs as well as their release profile.

The first report on the use of porous silica nanoparticles as an adjuvant was described in 2006 using ordered mesoporous silica SBA-15 particles. [51, 54] To explore the efficiency of SBA-15 as antigen carrier Mercuri *et al.*[54] used bacterial recombinant protein *Int1β* (16.5 kDa) and 20 snake (*Micrurus ibiboboca*) venom proteins. Mice were immunised by a 200 µL subcutaneous injection (s.c.) dose containing *Int1β* (10 µg) encapsulated in 100 µg SBA-15 or

100 μg aluminium hydroxide [$Al(OH)_3$], the booster dose for *Int1β* consisted of the same concentration. The *Micrurus* venom (2 μg) was administered with SBA-15 (20 μg) or with incomplete Freund adjuvant (IFA). The authors compared the efficacy of the protein loaded SBA-15 particles to that of protein plus traditional adjuvant using antibody responder mouse lines high (H) and low (L). The antibody titres of IgG1 and IgG2a were determined using the sera samples and the SBA-15 was found to have a better adjuvant property than $Al(OH)_3$ and was found to be as effective as IFA in maintaining the antibody levels for 30 days during the primary response. After the second immunisation with *Int1β* protein the animals were challenged with *Int1β* (10 μg) in $Al(OH)_3$. Mice primed with SBA-15 containing *Int1β* gave better antibody titres of 8.5 $\log_2$ compared to the mice immunised with protein plus traditional adjuvant $Al(OH)_3$ which only gave an antibody titre of 5.2 $\log_2$. This study established the potential of SBA-15 nanoparticles to induce a memory response.

The ability of SBA-15, as an adjuvant, to carry, protect and deliver entrapped antigens and to elicit an immune response was further analysed by Carvalho *et al.*[51] using BSA. They compared the adjuvant effect of BSA adsorbed to SBA-15 or $Al(OH)_3$ or emulsified in IFA. H and L antibody responsive (Selection III and IVA) mice were vaccinated with a 50 μL dose via intramuscular (i.m.) injection or a 200 μL dose was given orally comprising of 10 μg of BSA adsorbed to SBA-15 or $Al(OH)_3$ or BSA emulsified in IFA via i.m. In the Selection IVA mice, the antibody response difference in the responder H and L lines is mainly due to antigen catabolism of Mϕ and other APC, and in the Selection III mice, the difference is due to the basic genetic modifications of B-lymphocytes. [110-112] Both H and L lines for Selection IVA and III elicited comparable serum specific IgG antibody titres when immunised through i.m. and oral route with BSA in SBA-15. However, the levels of anti-BSA IgG in the L_{IVA} mice immunised with BSA in $Al(OH)_3$ were 16 fold lower than the H_{IVA} after the initial immunisation and 4 fold lower after the second immunisation. In comparison the Selection III mice had 4 fold lower anti-BSA IgG titres after the initial immunisation and the difference increase to 256 fold after the booster dose. Both SBA-15 and IFA elicited comparable antibody titres. Administration of BSA in SBA-15 or emulsified on the IFA, corrected the antibody responsiveness of the low responder mice and eliminated the phenotypic differences between the H-L responders in both Selections III and IVA. The protein encapsulated/adsorbed SBA-15 nanoparticles induced an antibody response comparable to that of the traditional adjuvant IFA in mice. Furthermore, the administration of SBA-15 did not induce any local tissue damage or granulomas formation. [51]

An earlier report has shown that the administration of colloidal silica greatly increased antibody responsiveness in L_{IVA} but not in L_{III}, additionally the effect of silica was found to be absent in H_{III} and H_{IVA}.[109] Wang *et al.*[28] investigated three kinds of silica nanoparticles (S1, S2 and SBA-15) with different sizes (430 nm, 130 nm and 1–2 μm) and pore characteristics for adsorption of BSA and to develop vaccine delivery systems. They compared the immune responses obtained by BSA loaded onto silica with BSA emulsified in FCA. Mice were administered a 200 μL dose by intragastric gavage and 100 μL dose via i.m. injection with the doses consisting of 10 μg of BSA. The oral immunisation with BSA alone did not produce any IgG antibodies, but the mice vaccinated with BSA loaded on silica nanoparticles produced significant amount of BSA-specific IgG antibody response (S1 > S2 > SBA-15) in the plasma. However the IgG titre of BSA plus S1 nanoparticles was lower than the BSA antigen emulsified in FCA. The mucosal immune response was assessed using the intestinal and oral secretions and negligible amount IgA response was obtained following (i.m.) vaccination with BSA plus FCA and oral BSA, whilst oral immunisation with protein loaded silica nanoparticles resulted in a higher IgA immune response, with S1 showing the highest titre, followed by S2 and SBA-15. It was found that the immune response elicited was significantly dependant on the uptake and release profile of the antigen and the structure of silica. Slowing down the release rate of proteins from 47% (SBA-15) to less than 8% (S1) enhanced the antibody titre. All the three nanoparticles had different release rates, the justification by the authors is that it might be due to the different pore sizes; large pores improve the interaction of antigen with the nanoparticles and lead to their slow release. Increase in the particle size can reduce the release of BSA, which in turn would allow a longer interaction between antigen and the immune system. [28]

The hollow structured MSNs (HMSNs) have been used as an antigen delivery vehicle for Porcine circovirus type-2 (PCV2) ORF2 protein. The mice were immunised intramuscularly with a 100 μg dose (0.7 mg HMSNs loaded with 100 μg of protein) or GST-ORF2-E protein alone or empty HMSNs. The humoral antibody titres of mice injected with GST-ORF2-E protein alone increased in the 2^{nd} week and reduced dramatically in the 3^{rd} week post-immunisation. However, the antibody titres of the mice administered HMSNs loaded with GST-ORF2-E protein increased continuously for three weeks post-immunisation. Similarly, HMSNs loaded GST-ORF2-E protein gave a higher T-lymphocyte mediated immune response compared to the mice immunised with GST-ORF2-E protein alone. The percentage of CD4+ and CD8+ cells in mice immunised with HMSN/GST-ORF2-E was found to be higher than the mice immunised with HMSNs particles only and GST-ORF2-E protein at the 4^{th} and the 6^{th} week.

The authors have highlighted that HMSNs as vaccine carriers can improve both humoral and cell mediated immune responses and induce persistent immune response. [26]

Slowing *et al.*[52] explained that the slow release of antigens from silica nanoparticles can be due to the highly stable and rigid framework of the porous silica, which might form a barrier to prevent the degradation of the antigen in the stomach and digestive tract. In our laboratory, we successfully loaded model antigen OVA and the viral antigen E2 from Bovine Viral Diarrhoea Virus onto mesoporous silica nanoparticles and conducted *in vivo* mice studies. Immunisation with OVA loaded onto amino fuctionalised MSNs induced both Th1 and Th2 immune responses (Mahony *et al*., in press). Immunisation with E2 viral protein loaded onto amino functionalised HMSN induced both antibody and cell mediated immune responses (personal communication).

The research reviewed above, highlights the exciting progress that has been achieved in the area of vaccine delivery using silica nanoparticles in the last decade. In addition, the FDA recently approved the use of ultrasmall multimodal silica nanoparticles termed Cornell dots (C dots) in the first-in-human clinical trial for diagnostics of advanced melanoma. [113, 114]

Indeed, MSNs have a bright future as adjuvants for vaccine delivery. Nonetheless, *in vivo* biodistribution and biocompatibility of these novel nanocarriers is still a topic of intense research and demands long-term *in vitro* and *in vivo* trials in future as discussed in the following section.

2.4 Biocompatibility and Biodistribution of MSNs

For *in vivo* biomedical applications it is highly important that nanoparticles perform their desired function and do not cause any histopathological lesions or abnormalities. Even though, silica is considered non-toxic in low doses, having been used in the pharmaceutical industry as an excipient for decades, the long-term effect of MSNs *in vivo* needs to be assessed. The biocompatibility of MSNs depends on the particle size, morphology, structure, surface properties and the dosage. At lower concentrations MSNs are found to be non-toxic in a variety of cell lines but at higher concentrations they can have inhibiting effect on cells. [36, 115, 116] *In vitro* interactions of MSNs with various cell lines like HeLa cells,[57, 117] 3T3 endothelial cells,[118] human mesenchymal stem cells,[119] and human colon carcinoma[120] have been investigated. The compatibility of nanoparticles is directly related to their biotranslocation. [30]

In this section we discuss the cytotoxicity and *in vivo* toxicity effect of MSNs, their distribution when injected in small animals like mice and their route of excretion from the immune system. The surface area of the particles is positively correlated with the toxicity of nanoparticles. Small sized nanoparticles with large surface areas and abundant silanol groups have the ability to generate reactive oxygen species (ROS), which play a role in the ability of nanoparticles to cause injury. [121]

Eom *et al.*[122] studied the relationship between physico-chemical properties and toxicity of silica nanoparticles and their ability to activate transcription factors and the signal transduction pathway. They further demonstrated that MSNs (MCM-41 and SBA-15) can inhibit cellular and mitochondrial respiration causing oxidative stress. [122, 123] Recently, it was found that the pore architecture of silica nanoparticles too greatly influences their biocompatibility. *In vitro* and *in vivo* studies on spherical 100 nm MSNs exhibited less cytotoxicity (time and dose dependant), reduced inflammatory response, and contact hypersensitivity than the colloidal solid counterparts. [124]

Toxic effects of silica nanoparticles on the immune system are mainly due to the interference with signalling pathways involved in immune response activation. MSNs elicit lower expression of pro-inflammatory cytokines, such as TNF-α, interleukin (IL)-1β and IL-6 in Mϕ. The lower activation of mitogen-activated protein kinases, nuclear factor-κB, and caspase 3 by MSNs are responsible for reduced inflammatory response and apoptosis. Similarly, porous MSNs induce less cytotoxicity compared to the non-porous counterparts,[124, 125] 35 nm and 70 nm non-porous silica nanoparticles when administered intravenously to mice can cause pregnancy complications. [126] Lin *et al.*[127] demonstrated that MSNs have low haemolytic activity compared to the non-porous counterparts and the pore stability of MSNs determined the hemolytic activity. Modifying the silanol surface with PEG coating can eliminate haemolytic activity. Porous silica was found to be less toxic than the non-porous silica due to the larger surface area while the 'cell-contactable surface area', the area available for proteins and other biomolecules to interact with the porous silica is lower. [125] In addition, the porosity of silica nanoparticles determines the cellular uptake of MSNs by cells.

Using human monocyte derived dendritic cells, Vallhov *et al.*[128] reported that the particle size and concentration of MSNs affected the viability, uptake and immune regulatory markers

of the cells. Smaller particles (270 nm) with lower concentrations had a lesser affect on the cells

compared to large sized particles (2.5 μm) at higher concentrations; encouraging the use of small sized MSNs for vaccine delivery. [128] Lu *et al.*[129] demonstrated 50 nm MSN particles showed the maximum cellular uptake by HeLa cells, which was about two times greater than the uptake of 30 nm particles. Cellular uptake of 110 nm, 280 nm and 170 nm MSNs was observed to be proportionally lower. In addition, the authors established that the excretion properties of MSNs was also size dependent. Different sized (80, 120, 200 & 360 nm) spherical and PEGylated MSNs were administered intravenously into mice to study biodistribution and excretion of the particles. [31] The results indicated that after immunisation, MSNs were mainly distributed in liver and spleen, with a minority in the lungs and a small amount in the kidney and heart. Significantly, neither MSNs nor PEG MSNs caused *in vivo* tissue toxicity. The biodistributed percentage of both MSNs and the PEG-MSNs in the liver and spleen increased with the increase in the particle size for 30 min after injection, however, the PEG-MSNs with 360 nm diameter were found to be an exception as they were not captured by spleen within 30 min of injection. This indicates that mostly the organs can easily capture both MSNs and PEG-MSNs with larger particle size. In addition, the excretion from urine significantly increased with the increase in particle size, importantly smaller sized particles had longer blood circulation lifetime. [31]

Polymers like PEG are known to improve the circulation time of particles by delaying opsonisation and reducing the excretion rate.[130] The *in vivo* biodegradation and excretion rate of the degraded products is highly dependant on particle size. Research studies using 45 nm MSNs found that the particles largely accumulated in liver, kidney and urinary bladder a few hours after intravenous injection and were excreted through the renal route. [131] In another study it was found that approximately 95% of MSNs (100-130 nm) were excreted in urine and faeces. [36] Burns *et al.*[132] found smaller sized silica nanoparticles (3.3 nm and 6.0 nm) had a longer blood circulation time and the particles were excreted via renal filtration.

It is clear from the above-mentioned studies that majority of the particles are excreted from the immune system via the renal route. Sergent *et al.*[133] studied the toxic effect of core-dye doped silica nanoparticles (25 nm and 100 nm) to track nanoparticles using confocal and video microscopy in human epithelial intestinal HT-29 cells. They used the sulforhodamine B (SRB) test, which measures the global metabolism activity based on Skehan protocol [134] as well as conventional approaches like flow cytometry and γ-H2Ax foci. In addition they performed real-

time monitoring of cell proliferation to measure the physico-chemical characteristics of the

nanoparticles. Both SiO_2-25 nm and SiO_2-100 nm induced limited cytotoxic effect on the cells after 24 h exposure (at concentrations ranging from 10 to 150 μg mL^{-1}) However, an inverse dose-dependant relationship was observed with the 100 nm nanoparticles, increasing the dose of SiO_2-100 nm particles lower the cytotoxic effect on the cells compared to the SiO_2-25 nm particles.

Similarly, Passagne *et al.*[135] demonstrated toxicity of silica nanoparticles on human HK-2 and porcine LLC-PK1 renal proximal tubular cells to be time (24 h, 48 h, 72 h) and size (20 nm and 100 nm) dependant. The 100 nm particles were found to be less toxic than the 20 nm particles, and when observed using an transmission electron microscope (TEM) the 20 nm particles were localised in vesicles. [135] Hudson *et al.*[34] reported a detailed study on the cytotoxicity and biocompatibility of mesoporous silicates (MCM-41, SBA-15 and mesocellular foam) with different sizes and pore diameters on *in vitro* mammalian cells and *in vivo* mouse models. They found that administration of 30 mg mesoporous silicates was found to be toxic when administered intraperitoneally or intravenously, but not subcutaneously.

SBA-15 particles have a smaller surface area and poor porosity compared to MCM-41. Tao *et al.*[123] found that positively charged amino functionalised SBA-15 and MCM-41 particles did not cause significant cell death in human T-cell lymphoma (Jurkat) cells, as the positively charged quaternary amines prevent cellular injury from mesoporous nanoparticles. They confirmed this by conducting an endocytosis study using bright field microscopy and cell imaging with TEM, and observed that the unmodified MSNs got internalised but not the amino functionalised MSNs. However, the SK-N-SH cells were found to be more resistant to both unmodified and functionalised nanoparticles. Only at a high dose of 200 μg/mL amino functionalised MSNs induced a noticeable cell death. Unmodified MSNs have a negative zeta potential and rapidly associate with serum opsonin after entering the blood stream and are cleared by Mϕ in the reticuloendothelial system (RES). The authors concluded that structures, dose-dependency as well as surface functionalisation of silica nanoparticles (MCM-41, SBA-15 and solid-cored spheres) can have cytotoxic effects on Jurkat and human neuroblastoma cells. [123]

Surface modification plays an important role in changing the surface properties of MSNs, hence improving the biocompatibility and *in vivo* circulation time of the particles. Although,

PEGylation can decrease the endocytosis of mesoporous silica nanoparticles,[123, 136] a recent study has suggested that the PEGylated nanoparticles can induce production of specific anti-PEG IgM, which is responsible for accelerated blood clearance of nanoparticles after repeated injection. [137] At higher concentrations the mesoporous silicates induce toxicity, although toxicity can be reduced by addition of a functional group. [123] Even though, our understanding on biocompatibility and biodistribution of MSNs and their interaction with the immune system has improved significantly, the adjuvant effect of MSNs still requires deeper investigation and understanding before its use in a clinical setting.

2.5 Conclusion and Future Outlook

In conclusion, we have reviewed the potential of MSNs as antigen carriers and their ability to act as adjuvants in vaccine delivery. MSNs can be easily synthesised with controlled size, shape and structure, making them highly attractive as delivery vehicles. Nonetheless, the application of MSNs in vaccine delivery is a relatively new area and has not been studied in great details. There exist unsolved questions and challenges that need to be addressed before their practical use in clinical applications.

Designed synthesis of new MSNs with optimised structures and functions is of ultimate importance for generating highly efficient adjuvants. Ideally, MSNs as adjuvants should be prepared using simple, reproducible, economical and scalable methods. It will be of great advantage to synthesise MSNs with low toxicity, large loading capacity, and controlled antigen release profiles. A comprehensive understanding on the impact of structural parameters of MSNs, such as morphology, size, and surface functional groups, on the antigen adsorption and release performance, may provide useful guide for the rational choice of suitable MSNs.
Apart from the interaction between antigen and MSNs, the cellular interaction of MSNs as well as antigen loaded MSNs should be studied in more details. Although the influence of a few parameters (e.g. the particle size) on cellular uptake has been studied, the interplay of various structural parameters of MSNs, interactions of antigen-MSNs and MSNs-cells has received little attention, which may significantly impact on the *in vivo* release profiles of antigen and the effective dosage, hence the eventual generation of immune response. Moreover, the in vivo immune response is an outcome of a sequence of complicated biological events, including the interaction of antigens and MSNs as the adjuvants with various types of immune cells (e.g., macrophage or phagocytic cells). Variation in one parameter such as the antigen or MSNs may change the overall response. It is suggested that future studies should focus on the entire

immune system, which includes antigen-MSNs-various immune cells as an integrated system. Systematic studies in the regard may provide genuine and comprehensive information towards a highly efficient vaccine formulation.

The factors like nanoparticles architecture, antigen type, antigen loading/encapsulation, dose administered, and immunisation route can influence the adjuvant properties of silica nanoparticles. To test the immune response of a formulation, a pre-clinical model is crucial which provides more information compared to cell studies. It is important to select a reliable and reproducible biological model and conduct biocompatibility and immune response studies at the cell biology, molecular biological and immunochemistry levels. In this regard, material scientists, biologists and immunologists are expected to work closely and bring in complementary expertise from various fields in order to have a deep understanding on the fundamental interaction mechanisms in a complex bionano system. Multidisciplinary and collaborative research will provide a concrete platform to bring MSNs as promising adjuvants for vaccine delivery in practical applications. The capacity of MSNs to induce both humoral and cell-mediated immune responses is advantageous over traditional adjuvants, which often induces only one arm of the immune response, taking us one step closer towards developing effective and safe vaccines.

2.6 Acknowledgements

The support scholarship from the University of Queensland and Queensland Alliance of Agriculture and Food Innovation is gratefully acknowledged. The authors thank Dr. Surajit Karmakar for his critical reading of the manuscript.

2.7 References

1. Kar UK, Jiang J, Champion CI, Salehi S, Srivastava M, et al. (2012) Vault Nanocapsules as Adjuvants Favor Cell-Mediated over Antibody-Mediated Immune Responses following Immunization of Mice. PLoS One 7: e38553.
2. Zhou F (2010) Perforin: more than just a pore-forming protein. International Reviews of Immunology 29: 56-76.
3. Fritsche PJ, Helbling A, Ballmer-Weber BK (2010) Vaccine hypersensitivity--update and overview. Swiss Medical Weekly 140: 238-246.
4. Skwarczynski. M, Toth. I (2011) Peptide-Based Subunit Nanovaccines. Curr Drug Deliv 8: 282-289.
5. Koping-Hoggard M, Sanchez A, Alonso MJ (2005) Nanoparticles as carriers for nasal vaccine delivery. Expert Rev Vaccines 4: 185-196.
6. de la Fuente M, Csaba N, Garcia-Fuentes M, Alonso MJ (2008) Nanoparticles as protein and gene carriers to mucosal surfaces. Nanomedicine (Lond) 3: 845-857.
7. Lee HJ (2002) Protein drug oral delivery: the recent progress. Archives of pharmacal research 25: 572-584.
8. Mody K, Mahony D, Mahony TJ, Mitter N (2012) Freeze-drying of protein loaded nanoparticles for vaccine delivery. Drug Deliv Lett 2: 83-91.
9. Kammer AR, Amacker M, Rasi S, Westerfeld N, Gremion C, et al. (2007) A new and versatile virosomal antigen delivery system to induce cellular and humoral immune responses. Vaccine 25: 7065-7074.
10. Foged C (2011) Subunit vaccines of the future: the need for safe, customized and optimized particulate delivery systems. Ther Deliv 2: 1057-1077.
11. Singh M, Chakrapani A, O'Hagan D (2007) Nanoparticles and microparticles as vaccine-delivery systems. Expert Review of Vaccines 6: 797-808.
12. Sun H-X, Xie Y, Ye Y-P (2009) Advances in saponin-based adjuvants. Vaccine 27: 1787-1796.
13. Reed SG, Bertholet S, Coler RN, Friede M (2009) New horizons in adjuvants for vaccine development. Trends in Immunology 30: 23-32.
14. Kreuter J (1996) Nanoparticles and microparticles for drug and vaccine delivery. Journal of Anatomy 189 (Pt 3): 503-505.
15. Vallet-Regi M, Ramila A, del Real RP, Perez-Pariente J (2001) A New Property of MCM-41:, A Drug Delivery System. Chem Mater 13: 308-311.

16. Florindo HF, Pandit S, Goncalves LMD, Alpar HO, Almeida AJ (2010) Surface modified polymeric nanoparticles for immunisation against equine strangles. International Journal of Pharmaceutics 390: 25-31.
17. Tobío M, Gref R, Sánchez A, Langer R, Alonso MJ (1998) Stealth PLA-PEG Nanoparticles as Protein Carriers for Nasal Administration. Pharmaceutical Research 15: 270-275.
18. Jung T, Kamm W, Breitenbach A, Hungerer KD, Hundt E, et al. (2001) Tetanus toxoid loaded nanoparticles from sulfobutylated poly(vinyl alcohol)-graft-poly(lactide-co-glycolide): evaluation of antibody response after oral and nasal application in mice. Pharm Res 18: 352-360.
19. Puri A, Blumenthal R (2011) Polymeric lipid assemblies as novel theranostic tools. Accounts of Chemical Research 44: 1071-1079.
20. Wendorf J, Singh M, Chesko J, Kazzaz J, Soewanan E, et al. (2006) A practical approach to the use of nanoparticles for vaccine delivery. J Pharm Sci 95: 2738-2750.
21. Kumari A, Yadav SK, Yadav SC (2010) Biodegradable polymeric nanoparticles based drug delivery systems. Colloids Surf, B 75: 1-18.
22. Peer D (2012) Immunotoxicity derived from manipulating leukocytes with lipid-based nanoparticles. Advanced Drug Delivery Reviews.
23. Adlakha-Hutcheon G, Bally MB, Shew CR, Madden TD (1999) Controlled destabilization of a liposomal drug delivery system enhances mitoxantrone antitumor activity. Nature Biotechnology 17: 775-779.
24. Zhang W, Yin Z, Liu N, Yang T, Wang J, et al. (2010) DNA-chitosan nanoparticles improve DNA vaccine-elicited immunity against Newcastle disease virus through shuttling chicken interleukin-2 gene. J Microencapsul 27: 693-702.
25. Popat A, Hartono SB, Stahr F, Liu J, Qiao SZ, et al. (2011) Mesoporous silica nanoparticles for bioadsorption, enzyme immobilisation, and delivery carriers. Nanoscale 3: 2801-2818.
26. Guo HC, Feng XM, Sun SQ, Wei YQ, Sun DH, et al. (2012) Immunization of mice by Hollow Mesoporous Silica Nanoparticles as carriers of Porcine Circovirus Type 2 ORF2 Protein. Virology Journal 9: 108.
27. Guo H, Hao R, Qian H, Sun S, Sun D, et al. (2012) Upconversion nanoparticles modified with aminosilanes as carriers of DNA vaccine for foot-and-mouth disease. Applied Microbiology and Biotechnology 95: 1253-1263.
28. Wang T, Jiang H, Zhao Q, Wang S, Zou M, et al. (2012) Enhanced mucosal and systemic immune responses obtained by porous silica nanoparticles used as an oral vaccine adjuvant:

Effect of silica architecture on immunological properties. International Journal of Pharmaceutics 436: 351-358.

29. C.T. Kresge, M.E. Leonowicz, W.J. Roth, J.C. Vartuli, Beck JS (1992) Ordered mesoporous molecular sieves synthesized by a liquid-crystal template mechanism. Nature 359: 710-712.
30. Tang F, Li L, Chen D (2012) Mesoporous Silica Nanoparticles: Synthesis, Biocompatibility and Drug Delivery. Advanced Materials 24: 1504-1534.
31. He Q, Zhang Z, Gao F, Li Y, Shi J (2011) In vivo Biodistribution and Urinary Excretion of Mesoporous Silica Nanoparticles: Effects of Particle Size and PEGylation. Small 7: 271-280.
32. He Q, Shi J (2011) Mesoporous silica nanoparticle based nano drug delivery systems: synthesis, controlled drug release and delivery, pharmacokinetics and biocompatibility. Journal of Materials Chemistry 21: 5845-5855.
33. Hudson S, Cooney J, Magner E (2008) Proteins in Mesoporous Silicates. Angew Chem Int Ed 47: 8582-8594.
34. Hudson SP, Padera RF, Langer R, Kohane DS (2008) The biocompatibility of mesoporous silicates. Biomaterials 29: 4045-4055.
35. Manzano M, Aina V, Arean CO, Balas F, Cauda V, et al. (2008) Studies on MCM-41 mesoporous silica for drug delivery: Effect of particle morphology and amine functionalization. Chemical Engineering Journal 137: 30-37.
36. Lu J, Liong M, Li Z, Zink JI, Tamanoi F (2010) Biocompatibility, Biodistribution, and Drug-Delivery Efficiency of Mesoporous Silica Nanoparticles for Cancer Therapy in Animals. Small 6: 1794-1805.
37. Sameti M, Bohr G, Ravi Kumar MN, Kneuer C, Bakowsky U, et al. (2003) Stabilisation by freeze-drying of cationically modified silica nanoparticles for gene delivery. Int J Pharm 266: 51-60.
38. Di Pasqua AJ, Sharma KK, Shi Y-L, Toms BB, Ouellette W, et al. (2008) Cytotoxicity of mesoporous silica nanomaterials. Journal of Inorganic Biochemistry 102: 1416-1423.
39. Gary-Bobo M, Hocine O, Brevet D, Maynadier M, Raehm L, et al. (2012) Cancer therapy improvement with mesoporous silica nanoparticles combining targeting, drug delivery and PDT. International Journal of Pharmaceutics 423: 509-515.
40. Giri S, Trewyn BG, Stellmaker MP, Lin VSY (2005) Stimuli-Responsive Controlled-Release Delivery System Based on Mesoporous Silica Nanorods Capped with Magnetic Nanoparticles. Angew Chem Int Ed 44: 5038-5044.

41. Han Y-J, Stucky GD, Butler A (1999) Mesoporous Silicate Sequestration and Release of Proteins. Journal of the American Chemical Society 121: 9897-9898.

42. Kim SI, Pham TT, Lee JW, Roh SH (2010) Releasing properties of proteins on SBA-15 spherical nanoparticles functionalized with aminosilanes. Journal of Nanoscience and Nanotechnology 10: 3467-3472.

43. Lim JS, Lee K, Choi JN, Hwang YK, Yun MY, et al. (2012) Intracellular protein delivery by hollow mesoporous silica capsules with a large surface hole. Nanotechnology 23: 085101.

44. Meng H, Liong M, Xia T, Li Z, Ji Z, et al. (2010) Engineered design of mesoporous silica nanoparticles to deliver doxorubicin and P-glycoprotein siRNA to overcome drug resistance in a cancer cell line. ACS Nano 4: 4539-4550.

45. Sharif F, Porta F, Meijer AH, Kros A, Richardson MK (2012) Mesoporous silica nanoparticles as a compound delivery system in zebrafish embryos. International Journal of Nanomedicine 7: 1875-1890.

46. Trewyn BG, Nieweg JA, Zhao Y, Lin VSY (2008) Biocompatible mesoporous silica nanoparticles with different morphologies for animal cell membrane penetration. Chemical Engineering Journal 137: 23-29.

47. Niu Y, Popat A, Yu M, Karmakar S, Gu W, et al. (2012) Recent advances in the rational design of silica-based nanoparticles for gene therapy. Therapeutic Delivery 3: 1217-1237.

48. Vivero-Escoto JL, Slowing, II, Trewyn BG, Lin VS (2010) Mesoporous silica nanoparticles for intracellular controlled drug delivery. Small 6: 1952-1967.

49. Slowing II, Trewyn BG, Lin VSY (2007) Mesoporous Silica Nanoparticles for Intracellular Delivery of Membrane-Impermeable Proteins. Journal of the American Chemical Society 129: 8845-8849.

50. H.H.P. Yiu, P.A. Wright, Botting NP (2001) Enzyme immobilisation using SBA-15 mesoporous molecular sieves with functionalised surfaces. J Mol Catal B: Enzym 15: 81-92.

51. Carvalho LV, Ruiz Rde C, Scaramuzzi K, Marengo EB, Matos JR, et al. (2010) Immunological parameters related to the adjuvant effect of the ordered mesoporous silica SBA-15. Vaccine 28: 7829-7836.

52. Slowing, II, Vivero-Escoto JL, Wu CW, Lin VS (2008) Mesoporous silica nanoparticles as controlled release drug delivery and gene transfection carriers. Adv Drug Deliv Rev 60: 1278-1288.

53. Slowing II, Trewyn BG, Giri S, Lin VSY (2007) Mesoporous Silica Nanoparticles for Drug Delivery and Biosensing Applications. Advanced Functional Materials 17: 1225-1236.

54. Mercuri LP, Carvalho LV, Lima FA, Quayle C, Fantini MC, et al. (2006) Ordered mesoporous silica SBA-15: a new effective adjuvant to induce antibody response. Small (Weinheim an der Bergstrasse, Germany) 2: 254-256.

55. Cheng K, El-Boubbou K, Landry CC (2012) Binding of HIV-1 gp120 glycoprotein to silica nanoparticles modified with CD4 glycoprotein and CD4 peptide fragments. ACS Applied Materials and Interfaces 4: 235-243.

56. Park HS, Kim CW, Lee HJ, Choi JH, Lee SG, et al. (2010) A mesoporous silica nanoparticle with charge-convertible pore walls for efficient intracellular protein delivery. Nanotechnology 21: 225101.

57. Zhao Y, Trewyn BG, Slowing, II, Lin VS (2009) Mesoporous silica nanoparticle-based double drug delivery system for glucose-responsive controlled release of insulin and cyclic AMP. Journal of the American Chemical Society 131: 8398-8400.

58. Lee JW, Tra PT, Kim SI, Roh SH (2008) Adsorption properties of proteins on SBA-15 nanoparticles functionalized with aminosilanes. Journal of Nanoscience and Nanotechnology 8: 5152-5157.

59. T. Yanagisawa T, Shimizu, K.Kuroda, C.Kato (1990) The Preparation of Alkyltriinethylaininonium–Kaneinite Complexes and Their Conversion to Microporous Materials. *Bull Chem Soc Jpn* 63: 988-992.

60. Kresge CT, Leonowicz ME, Roth WJ, Vartuli JC, Beck JS (1992) Ordered mesoporous molecular sieves synthesized by a liquid-crystal template mechanism. Nature 359: 710-712.

61. Wan Y, Zhao (2007) On the Controllable Soft-Templating Approach to Mesoporous Silicates. Chemical Reviews 107: 2821-2860.

62. Hoffmann F, Cornelius M, Morell J, Fröba M (2006) Silica-Based Mesoporous Organic–Inorganic Hybrid Materials. Angew Chem Int Ed 45: 3216-3251.

63. Li Z, Barnes JC, Bosoy A, Stoddart JF, Zink JI (2012) Mesoporous silica nanoparticles in biomedical applications. Chemical Society Reviews 41: 2590-2605.

64. W. Stober, A. Fink, Bohn E (1968) Controlled Growth of Manodisperse Silica Spheres in the Micron Size Range. J Colloid Interface Sci 26: 62-69.

65. Cai Q, Luo Z-S, Pang W-Q, Fan Y-W, Chen X-H, et al. (2001) Dilute Solution Routes to Various Controllable Morphologies of MCM-41 Silica with a Basic Medium,Ä†. Chemistry of Materials 13: 258-263.

66. CaiQ , Cui F Z , Chen X H, Zhang Y, S LZ Nanosphere of Ordered Silica MCM-41 Hydrothermally Synthesized with Low Surfactant Concentration. Chem Lett 9: 1044-1045(2000).

67. Zhao D, Feng J, Huo Q, Melosh N, Fredrickson GH, et al. (1998) Triblock copolymer syntheses of mesoporous silica with periodic 50 to 300 angstrom pores. Science 279: 548-552.

68. X. W. Lou, L. A. Archer, Z. C. Yang (2008) Hollow Micro-/Nanostructures: Synthesis and Applications. Adv Mater 20: 3987-4019.

69. Guo H, Qian H, Sun S, Sun D, Yin H, et al. (2011) Hollow mesoporous silica nanoparticles for intracellular delivery of fluorescent dye. Chemistry Central Journal 5: 1.

70. Popat A, Liu J, Hu Q, Kennedy M, Peters B, et al. (2012) Adsorption and release of biocides with mesoporous silica nanoparticles. Nanoscale 4: 970-975.

71. Song SW, Hidajat K, Kawi S (2007) pH-Controllable drug release using hydrogel encapsulated mesoporous silica. Chemical Communications: 4396-4398.

72. Angelos S, Khashab NM, Yang Y-W, Trabolsi A, Khatib HA, et al. (2009) pH Clock-Operated Mechanized Nanoparticles. Journal of the American Chemical Society 131: 12912-12914.

73. Aznar E, Marcos MD, Martinez-Manez R, Sancenon F, Soto J, et al. (2009) pH- and Photo-Switched Release of Guest Molecules from Mesoporous Silica Supports. Journal of the American Chemical Society 131: 6833-6843.

74. DeMuth P, Hurley M, Wu C, Galanie S, Zachariah MR, et al. (2011) Mesoscale porous silica as drug delivery vehicles: Synthesis, characterization, and pH-sensitive release profiles. Microporous and Mesoporous Materials 141: 128-134.

75. Ma Y, Zhou L, Zheng H, Xing L, Li C, et al. (2011) pH-responsive mitoxantrone (MX) delivery using mesoporous silica nanoparticles (MSN). Journal of Materials Chemistry 21: 9483-9486.

76. Muhammad F, Guo M, Qi W, Sun F, Wang A, et al. (2011) pH-Triggered Controlled Drug Release from Mesoporous Silica Nanoparticles via Intracelluar Dissolution of ZnO Nanolids. Journal of the American Chemical Society 133: 8778-8781.

77. Popat A, Liu J, Lu GQM, Qiao SZ (2012) A pH-responsive drug delivery system based on chitosan coated mesoporous silica nanoparticles Journal of Materials Chemistry 22: 11173-11178.

78. Xu Y, Qu F, Wang Y, Lin H, Wu X, et al. (2011) Construction of a novel pH-sensitive drug release system from mesoporous silica tablets coated with Eudragit. Solid State Sciences 13: 641-646.

79. S. Angelos, N.M. Khashab, Y.-W. Yang, A. Trabolsi, H.A. Khatib, et al. (2009) pH Clock-operated Mechanized nanoparticles. Journal of the American Chemical Society 131: 12912-12914.

80. Coll C, Mondragón L, Martínez-Máñez R, Sancenón F, Marcos MD, et al. (2011) Enzyme-Mediated Controlled Release Systems by Anchoring Peptide Sequences on Mesoporous Silica Supports. Angew Chem Int Ed 50: 2138-2140.

81. Bernardos A, Aznar E, Marcos MD, Martínez-Máñez R, Sancenón F, et al. (2009) Enzyme-Responsive Controlled Release Using Mesoporous Silica Supports Capped with Lactose. Angew Chem Int Ed 48: 5884-5887.

82. Zhu Y, Meng W, Gao H, Hanagata N (2011) Hollow Mesoporous Silica/Poly(l-lysine) Particles for Codelivery of Drug and Gene with Enzyme-Triggered Release Property. J Phys Chem C 115: 13630-13636.

83. Kneuer C, Sameti M, Bakowsky U, Schiestel T, Schirra H, et al. (2000) A Nonviral DNA Delivery System Based on Surface Modified Silica-Nanoparticles Can Efficiently Transfect Cells in Vitro. Bioconjugate Chemistry 11: 926-932.

84. Xia T, Kovochich M, Liong M, Meng H, Kabehie S, et al. (2009) Polyethyleneimine Coating Enhances the Cellular Uptake of Mesoporous Silica Nanoparticles and Allows Safe Delivery of siRNA and DNA Constructs. ACS Nano 3: 3273-3286.

85. Kim M-H, Na H-K, Kim Y-K, Ryoo S-R, Cho HS, et al. (2011) Facile Synthesis of Monodispersed Mesoporous Silica Nanoparticles with Ultralarge Pores and Their Application in Gene Delivery. ACS Nano 5: 3568-3576.

86. Yague C, Moros M, Grazu V, Arruebo M, Santamaria J (2008) Synthesis and stealthing study of bare and PEGylated silica micro- and nanoparticles as potential drug-delivery vectors. Chemical Engineering Journal 137: 45-53.

87. Itoh T, Ishii R, Matsuura S-i, Mizuguchi J, Hamakawa S, et al. (2010) Enhancement in thermal stability and resistance to denaturants of lipase encapsulated in mesoporous silica with alkyltrimethylammonium (CTAB). Colloids Surf, B 75: 478-482.

88. Budi Hartono S, Qiao SZ, Jack K, Ladewig BP, Hao Z, et al. (2009) Improving adsorbent properties of cage-like ordered amine functionalized mesoporous silica with very large pores for bioadsorption. Langmuir 25: 6413-6424.

89. S. B. Hartono, S.Z. Qiao, J. Liu, K. Jack, B.P. Ladewig, et al. (2010) Fuctionalised Mesoporous silica with very large pores for Cellulase Immobilization Journal of Physical Chemistry 114: 8353-8362.

90. Hartono SB, Gu W, Kleitz F, Liu J, He L, et al. (2012) Poly-L-lysine functionalized large pore cubic mesostructured silica nanoparticles as biocompatible carriers for gene delivery. ACS Nano 6: 2104-2117.

91. Cornelia L. Dekker, Lance Gordon, Klein J (2008) Dose Optimization Strategies for Vaccines: The Role of Adjuvants and New Technologies US Department of Health and Human Services. 1-21 p.

92. R. Coico, Sunshine G (2009) Immunology - A Short Course. N.J: Hoboken.

93. Dhur A, Galan P, Preziosi P, Hercberg S (1991) Lymphocyte subpopulations in the thymus, lymph nodes and spleen of iron-deficient and rehabilitated mice. Journal of Nutrition 121: 1418-1424.

94. Constant SL, Bottomly K (1997) Induction of Th1 and Th2 CD4+ T cell responses: the alternative approaches. Annual Review of Immunology 15: 297-322.

95. Wen ZS, Xu YL, Zou XT, Xu ZR (2011) Chitosan nanoparticles act as an adjuvant to promote both Th1 and Th2 immune responses induced by ovalbumin in mice. Mar Drugs 9: 1038-1055.

96. Kensil CR, Kammer R (1998) QS-21: a water-soluble triterpene glycoside adjuvant. Expert Opinion on Investigational Drugs 7: 1475-1482.

97. Skene CD, Sutton P (2006) Saponin-adjuvanted particulate vaccines for clinical use. Methods 40: 53-59.

98. Chwalek M, Lalun N, Bobichon H, Ple K, Voutquenne-Nazabadioko L (2006) Structure-acitivity relationships of some hederagenin diglycosides: Haemolysis, cytotoxicity and apoptosis induction. Biochim Biophys Acta 1760: 1418-1427.

99. Freund J, Casals J, Hosmer E (1937) Sensitization and antibody formation after injection of tubercle bacili and paraffin oil. Proc Soc Exp Biol Med 37: 509-513.

100. Mbow ML, De Gregorio E, Valiante NM, Rappuoli R (2010) New adjuvants for human vaccines. Current Opinion in Immunology 22: 411-416.

101. HogenEsch H (2002) Mechanisms of stimulation of the immune response by aluminum adjuvants. Vaccine 20, Supplement 3: S34-S39.

102. Bomford R, Stapleton M, Winsor S, McKnight A, Andronova T (1992) The control of the antibody isotype response to recombinant human immunodeficiency virus gp120 antigen by adjuvants. AIDS Research and Human Retroviruses 8: 1765-1771.

103. Comoy EE, Capron A, Thyphronitis G (1997) In vivo induction of type 1 and 2 immune responses against protein antigens. International Immunology 9: 523-531.

104. Babensee JE (2008) Interaction of dendritic cells with biomaterials. Seminars in Immunology 20: 101-108.

105. Black M, Trent A, Tirrell M, Olive C (2010) Advances in the design and delivery of peptide subunit vaccines with a focus on toll-like receptor agonists. Expert Review of Vaccines 9: 157-173.

106. Moghimi SM (2002) Chemical camouflage of nanospheres with a poorly reactive surface: towards development of stealth and target-specific nanocarriers. Biochim Biophys Acta 1590: 131-139.

107. Krishnamachari Y, Geary S, Lemke C, Salem A (2011) Nanoparticle Delivery Systems in Cancer Vaccines. Pharmaceutical Research 28: 215-236.

108. Akagi T, Baba M, Akashi M (2011) Biodegradable Nanoparticles as Vaccine Adjuvants and Delivery Systems: Regulation of Immune Responses by Nanoparticle-Based Vaccine. In: Kunugi S, Yamaoka T, editors. Polymers in Nanomedicine: Springer Berlin Heidelberg. pp. 31-64.

109. Gennari M, Bouthillier Y, Ibanez OM, Ferreira VC, Mevel JC, et al. (1987) Effect of silica on the genetic regulation of antibody responsiveness. Annales de l Institut Pasteur Immunologie 138: 359-370.

110. Cabrera WH, Ibanez OM, Oliveira SL, Sant'Anna OA, Siqueira M, et al. (1982) Evidence for distinct polygenic regulation of antibody responses to some unrelated antigens in lines of mice selected for high or low antibody responses to somatic antigen of Salmonella. Immunogenetics 16: 583-592.

111. Biozzi G, Mouton D, Stiffel C, Bouthillier Y (1984) A major role of the macrophage in quantitative genetic regulation of immunoresponsiveness and antiinfectious immunity. Advances in Immunology 36: 189-234.

112. Biozzi G, Mouton D, Sant'Anna OA, Passos HC, Gennari M, et al. (1979) Genetics of immunoresponsiveness to natural antigens in the mouse. Current Topics in Microbiology and Immunology 85: 31-98.

113. Friedman R (2011) Nano Dot Technology Enters Clinical Trials. Journal of the National Cancer Institute 103: 1428-1429.

114. Benezra M, Penate-Medina O, Zanzonico PB, Schaer D, Ow H, et al. (2011) Multimodal silica nanoparticles are effective cancer-targeted probes in a model of human melanoma. Journal of Clinical Investigation 121: 2768-2780.

115. Slowing I, Trewyn BG, Lin VSY (2006) Effect of Surface Functionalization of MCM-41-Type Mesoporous Silica Nanoparticles on the Endocytosis by Human Cancer Cells. Journal of the American Chemical Society 128: 14792-14793.

116. Lu J, Liong M, Zink JI, Tamanoi F (2007) Mesoporous Silica Nanoparticles as a Delivery System for Hydrophobic Anticancer Drugs. Small 3: 1341-1346.

117. Fisichella M, Dabboue H, Bhattacharyya S, Saboungi M-L, Salvetat J-P, et al. (2009) Mesoporous silica nanoparticles enhance MTT formazan exocytosis in HeLa cells and astrocytes. Toxicology In Vitro 23: 697-703.

118. Thomas MJK, Slipper I, Walunj A, Jain A, Favretto ME, et al. (2010) Inclusion of poorly soluble drugs in highly ordered mesoporous silica nanoparticles. International Journal of Pharmaceutics 387: 272-277.

119. Huang D-M, Chung T-H, Hung Y, Lu F, Wu S-H, et al. (2008) Internalization of mesoporous silica nanoparticles induces transient but not sufficient osteogenic signals in human mesenchymal stem cells. Toxicology and Applied Pharmacology 231: 208-215.

120. Heikkila T, Santos HlA, Kumar N, Murzin DY, Salonen J, et al. (2010) Cytotoxicity study of ordered mesoporous silica MCM-41 and SBA-15 microparticles on Caco-2 cells. European Journal of Pharmaceutics and Biopharmaceutics 74: 483-494.

121. Nel A, Xia T, Madler L, Li N (2006) Toxic Potential of Materials at the Nanolevel. Science 311: 622-627.

122. Eom H-J, Choi J (2009) Oxidative stress of silica nanoparticles in human bronchial epithelial cell, Beas-2B. Toxicology In Vitro 23: 1326-1332.

123. Tao Z, Toms BB, Goodisman J, Asefa T (2009) Mesoporosity and Functional Group Dependent Endocytosis and Cytotoxicity of Silica Nanomaterials. Chemical Research in Toxicology 22: 1869-1880.

124. Lee S, Yun H-S, Kim S-H (2011) The comparative effects of mesoporous silica nanoparticles and colloidal silica on inflammation and apoptosis. Biomaterials 32: 9434-9443.

125. Maurer-Jones MA, Lin Y-S, Haynes CL (2010) Functional Assessment of Metal Oxide Nanoparticle Toxicity in Immune Cells. ACS Nano 4: 3363-3373.

126. Yamashita K, Yoshioka Y, Higashisaka K, Mimura K, Morishita Y, et al. (2011) Silica and titanium dioxide nanoparticles cause pregnancy complications in mice. Nature Nanotechnology 6: 321-328.

127. Lin Y-S, Haynes CL (2010) Impacts of Mesoporous Silica Nanoparticle Size, Pore Ordering, and Pore Integrity on Hemolytic Activity. Journal of the American Chemical Society 132: 4834-4842.

128. Vallhov H, Gabrielsson S, Stromme M, Scheynius A, Garcia-Bennett AE (2007) Mesoporous silica particles induce size dependent effects on human dendritic cells. Nano letters 7: 3576-3582.

129. Lu F, Wu S-H, Hung Y, Mou C-Y (2009) Size Effect on Cell Uptake in Well-Suspended, Uniform Mesoporous Silica Nanoparticles. Small 5: 1408-1413.

130. Veronese FM, Pasut G (2005) PEGylation, successful approach to drug delivery. Drug Discovery Today 10: 1451-1458.

131. He X, Nie H, Wang K, Tan W, Wu X, et al. (2008) In Vivo Study of Biodistribution and Urinary Excretion of Surface-Modified Silica Nanoparticles. Analytical Chemistry 80: 9597-9603.

132. Burns AA, Vider J, Ow H, Herz E, Penate-Medina O, et al. (2008) Fluorescent Silica Nanoparticles with Efficient Urinary Excretion for Nanomedicine. Nano Letters 9: 442-448.

133. Sergent J-A, Paget V, Chevillard S (2012) Toxicity and Genotoxicity of Nano-SiO2 on Human Epithelial Intestinal HT-29 Cell Line. Annals of Occupational Hygiene 56: 622-630.

134. Skehan P, Storeng R, Scudiero D, Monks A, McMahon J, et al. (1990) New colorimetric cytotoxicity assay for anticancer-drug screening. Journal of the National Cancer Institute 82: 1107-1112.

135. Passagne I, Morille M, Rousset M, Pujalte I, L'Azou B (2012) Implication of oxidative stress in size-dependent toxicity of silica nanoparticles in kidney cells. Toxicology 299: 112-124.

136. He Q, Zhang J, Shi J, Zhu Z, Zhang L, et al. (2010) The effect of PEGylation of mesoporous silica nanoparticles on nonspecific binding of serum proteins and cellular responses. Biomaterials 31: 1085-1092.

137. Ishida T, Ichihara M, Wang X, Yamamoto K, Kimura J, et al. (2006) Injection of PEGylated liposomes in rats elicits PEG-specific IgM, which is responsible for rapid elimination of a second dose of PEGylated liposomes. Journal of Controlled Release 112: 15-25.

3.

Literature Review

Freeze-drying of Protein loaded Nanoparticles for Vaccine Delivery

---

In Chapter 3, the basics of the freeze-drying process and its impact on development of nanoparticle based vaccine delivery systems was investigated. This literature review discusses different steps of freeze-drying process, role of excipients, freeze-drying of protein loaded nanoparticles and assessment of the physico-chemical characteristics of the formulation after freeze-drying. **Chapter 3 is published in *Drug Delivery Letters 2012, 2, 83-91.***

3.1 Introduction

Vaccination is considered as one of the greatest achievements in the field of science. [1] Most of the vaccines currently available in the market comprise of biomolecules, protein, antigens and nucleic acids and they have drawbacks such as instability and limited efficacy associated to them. Biomolecules like proteins and peptides when delivered as oral vaccines can fail to cross biological barriers due to metabolic enzymes and impermeable mucosal tissues in the intestine and hence fail to reach the target sites. [2-4] In addition, some conventional vaccines have issues such as manufacturing difficulties and storage instability and this encourages development of safe, stable and effective vaccines.

Nanoparticles can be used as delivery vehicles to deliver drugs, proteins, peptides and nucleic acids as they have desirable chemical, physical and biological properties. The nanoparticles can act as both the delivery vehicles and adjuvants, [2, 5] in addition strong immune responses can be induced when an antigen is associated to nanoparticles. [6-8] Development of novel delivery systems for peptide and protein vaccines has the potential to be useful in clinical medicine and research; by providing antigen protection and thereby improving the pharmacokinetics of easily degradable peptides and proteins, which often have short half-life *in vivo*. [4, 9, 10] Adsorbing proteins (antigens) to nanoparticles can enhance the shelf-life of the vaccine. [11] While nanoparticle technologies can improve overall stability of some vaccines the degree of improvement can be dependent on the specific formulation under evaluation. To further enhance stability of nanovaccines formulations freeze-drying techniques can be used.

The freeze-drying process also known as lyophilisation; removes water from a frozen sample and has been used to preserve unstable molecules for long periods of time by maintaining the chemical properties of substances like proteins, peptides and other complex synthetic organic molecules. [12-14] Freeze-drying proteins offer the advantages of prolonged shelf-life, improved storage and ease of shipping to the end user all of which are important issues in developing countries where maintenance of cold chain storage can be problematic. [15] In addition, freeze-drying strategies are extensively used to facilitate the stability of nanoparticle-based vaccine formulations and thereby the long-term antigen immunogenicity as well as ensuring formulation sterility. [16] Abdelwahed *et al.* [16] have reviewed freeze-dried nanoparticle formulations with different encapsulated drugs. Zillies *et al*. [17] have briefly discussed examples of different nanoparticle formulations that have been successfully freeze-dried and reported in the literature. However, very limited information is

available about successful freeze-drying of protein-loaded nanoparticles for vaccine delivery applications.

The focus of this paper is to provide an overview on different parameters of the freeze-drying process that may have an impact on the potency of nanoparticle-protein formulations. Description of the freeze-drying process, importance of using cryoprotectants and lyoprotectants towards the development of new protein-based nanovaccines and assessment of physico-chemical characteristics on the freeze-dried samples has been reviewed.

3.2 Freeze-drying Process

During the freeze-drying procedure the solvent is removed from the frozen solution by sublimation and desorption under reduced pressure. [18] The freeze-drying process is divided into three steps, freezing (solidification), primary drying (ice sublimation), and secondary drying (desorption of unfrozen water). [16]

3.2.1 Freezing

The initial freezing step of the nanoparticle suspension can be performed rapidly in liquid nitrogen or by slowly freezing of the samples (-20°C or -80°C). Slow freezing can increase the protein damage in systems prone to phase separation [19] and liquid nitrogen freezing is more suitable for freezing smaller volumes. [12]

3.2.2 Primary drying

Primary drying is the longest step of the freeze-drying cycle and it has a significant impact on the final product outcome. [20] Determining the optimal drying parameters for the primary drying step can require extensive experimental studies. During the primary drying step the shelf temperature is increased, and the heat in the chamber is removed by ice sublimation. Properties of the proteins and excipients are used determine the collapse temperature of the formulation (T_c). This is the temperature at which the freeze-dried product collapses during the freeze-drying process and loses its structural integrity. [12, 21] The primary drying step is used to optimise the product temperature (T_p) [12] and the T_p depends on various factors such as type of freeze-dryer, shelf temperature, chamber pressure, the container system, heat transfer, type of vials, the volume of sample to be freeze-dried and product resistance. [22] Since the primary drying step depends on the various factors mentioned above it is difficult to optimise the freeze-drying process for the nanoparticle

formulation even when the T_c of the formulation and the glass transition temperature (T_g') are known. [12] The target product temperature, collapse temperature of the formulation, chamber pressure, shelf temperature, and target product temperature of the protein formulation, need to be considered to design an optimised primary drying step and have been reviewed by Roy *et al.*[15], Tang *et al.* [12] and Abdelwahed *et al*.[16].

3.2.3 Secondary drying

This is the last stage of freeze-drying process during which water that did not freeze is removed, and this stage usually lasts only a few hours. For the desorption of the water to occur the secondary drying is always performed at higher temperature relative to the temperature used for the primary drying. [12] The preferred amount of residual moisture content in the final product controls the length of the secondary drying cycle. The main objective of the secondary drying stage is to get a stable product with residual moisture content of less than 1% [16]; freeze-drying process can only be developed empirically and is assessed by testing the physico-chemical characteristics of the resulting freeze-dried products.

3.3 Role of Excipients

Freeze-drying process involves two denaturing conditions: freezing and drying. The addition of excipients can protect protein-loaded nanoparticles from freezing and drying stresses. [14, 15, 23-25] The excipients used to protect from the freezing stress are known as cryoprotectants while the lyoprotectants are known to minimise the effects caused by the drying stress. [26] Various studies have revealed that during the freeze-drying process, protein solutes start to freeze; pure water is separated as ice and may cause proteins to undergo physical stress leading to protein denaturation, unfolding and aggregation. [27] By using cryo/lyo protectants during the drying process water that is normally hydrogen-bonded to the surface of proteins is replaced by the cryo/lyo protectants to protect the protein conformation and structural integrity. [28]

Many sugars like glucose, sucrose, mannitol, and trehalose have been used as protein stabilisers. The widely used cryoprotectants include sugars/polyols, polymers, amino acids, proteins itself and surfactants; these cryoprotectants can also be used as lyoprotectants except for non-aqueous solvents like PEG and glycerol, as they reduce the loss of protein activity during freezing. [26] Moreover, the commonly used excipients are classified as bulking agents, buffering agents, or solubilising agents. Examples of the bulking agents are mannitol, lactose, sucrose, and trehalose,

amino acids like arginine, glycine, and histidine and polymers like dextran and polyethylene glycol (PEG). Bulking agents are added to aid the formation of bulk and provide adequate structure to the freeze-dried cake. Buffering agents like hydrochloric acid and sodium hydroxide control the pH of the freeze-dried product thereby avoiding degradation of the vaccine during processing, storage and reconstitution. Examples of solubilising agents include surfactants, co-solvents and complexing agents like ethylenediamine tetra acetic acid (EDTA). If the freeze-dried cake demonstrates poor wetting characteristics the solubilising agents can be added at low concentrations to assist reconstitution. [29]

Sugars in combination with non-aqueous solvents can be used to preserve the characteristics and maintain stability of both the protein as well as nanoparticles during lyophilisation. [13, 14, 30] For example, Carpenter *et al.* [31] and Prestrelski *et al.* [32] described a two-component excipient system in which PEG acted as the cryoprotectant and glucose at low concentration acted the lyoprotectant. They determined that until the native form of protein was protected during freeze-drying with the help of excipients complete recovery of active protein on reconstitution could be difficult. Different excipients may stabilise the proteins in different ways depending on the target proteins. [31, 32] Amphiphilic excipients like PEG when dispersed into sugar-matrices act as good stabilisers for freeze-drying proteins. [33] PEG has a high molecular weight [34] and increases the collapse temperature of the product resulting in higher drying temperature and enhances product stabilisation probably by creating steric interference. [16, 24] For example, high-molecular weight PEG like 8000 and 10000 have negative preferential interactions with the human serum albumin protein stabilising the native form of the protein. [35]

Surfactants are usually present in the original nanoparticle formulation post-synthesis so very few studies have focused on the use of surfactants as excipients to preserve the nanoparticle integrity during freeze-drying. [34] Poly(lactide-co-glycolide) (PLG) nanoparticles lyophilised with 100% and 131% (w/w) polyvinyl alcohol (PVA) as an excipient, once resuspended retained their initial size, however, lowering the PVA concentration between 10% to 66% (w/w) led to particle aggregation. As the Food and Drug administration (FDA) rarely allows surfactants in injectable drugs, the 100% (w/w) amount of PVA required for complete particle resuspension might not be feasible for vaccine formulations. [36] According to the research carried out by Quintanar-Guerrero *et al.* [37] the best cryoprotectants were sugars for freeze-drying poly(D,L-lactic acid) (PLA) nanoparticles. This study suggested that the size of PLA nanoparticles increased significantly post-

lyophilisation, however when glucose units were added to the formulation the nanoparticle size did not change significantly. [37]

Freeze-drying nanoparticle-based delivery systems with excipients protect the nanoparticles from freeze-drying stress resulting in a stable end product. The level of product stabilisation can also be dependant upon the concentration and type of excipients used; when bovine serum albumin (BSA)-loaded chitosan nanoparticles were freeze-dried with different concentrations of PEG 2000, 6000, 8000 and 10,000, it resulted in inconsistent sized nanoparticles which were difficult to resuspend. However, the particle size was maintained when sucrose was used as lyoprotectant in the BSA-chitosan nanoformulation. [14] The hepatitis B surface antigen (rHBsAg)-loaded chitosan-based nanoparticles containing 2.5% glucose as an excipient readily resuspended in water and also preserved the structural entity of the antigen and the physico-chemical characteristics of the chitosan nanoparticles for at least 3 months storage at 4^{o}C. [38]

Sameti *et al.* [39] investigated the freeze-drying process for silica nanoparticles and DNA formulations. They reported that the physical properties of the freeze-dried nanoparticles were preserved post lyophilisation depending on whether the lyoprotectants interacted with the nanoparticle surface prior to lyophilisation. The addition of sugars helped inhibit permanent particle aggregation and preserve the DNA-binding activity of the particles. Addition of either 5% (w/v) trehalose or 10% (w/v) glycerol helped preserve the DNA binding activity of the cationic silica nanoparticles. Freeze-drying of the silica nanoformulation resulted in a stable final product suitable for nanoscaled drug delivery system. [39]

Addition of excipients can also influence the zeta-potential of the nanoformulations. Zeta potential studies on the polyethylenimine (PEI)-dextran sulfate (DS) nanoparticles showed that modification in the ratio of polymers or difference in the pH of PEI solution did not change the zeta-potential (+26 mV) of the nanoparticles significantly, however, the zeta potential of the nanoparticles increased when the amount of zinc sulfate was decreased. [40] The zeta-potential of cationically modified silica nanoparticles before and after lyophilisation showed that at pH 3.0 the nanoparticles had a surface charge of +46 mV but at pH 10 it decreased to -37 mV. At pH 4.0, the zeta-potential of the nanoparticles did not change significantly upon addition of lyoprotectants (5%) - trehalose, glucose, mannitol, sorbitol, acetic or glycerol. However when these lyoprotectant were added to nanoparticle formulation at higher concentrations (up to 20%) the positive zeta-potential decreased significantly with the exception of acetic acid. [39] de Chasteigner *et al.* [41] discovered that the

addition of 10% sucrose as an excipient to itraconazole loaded poly(ε-capro-lactone) nanospheres during the freeze-drying process significantly decreased the negative surface charge of the nanosphere formulation from -40.9 to -20.4 mV. The interaction between the OH groups of the cryoprotectants and the wall of the nanospheres might have resulted in surface modification of the nanospheres. [41]

Presence of excipient in the nanoformulation during lyophilisation can also affect the nanoparticle size. The size of ovalbumin (OVA) encapsulated poly(gamma-glutamic acid) (γ-PGA) nanoparticles before and after freeze-drying was measured in PBS by dynamic light scattering (DLS). [42] The samples freeze-dried with 1% glucose formed aggregations above 1 μm compared to the samples freeze-dried with 2.5% glucose, which did not form any large aggregations and nanoparticle size was also preserved. DLS was also used to study insulin-loaded PEI-DS nanoparticles with and without zinc sulphate as a stabiliser. [40] Freeze-dried nanoformulation without zinc sulfate showed two fold increase in the mean particle size compared to the samples before lyophilisation. Zinc sulfate maintained the particle size before and after lyophilisation, presumably through electrostatic interactions that increase the stability of the nanoparticles.
Work in our laboratory is in progress on optimising the freeze-drying process for mesoporous silica nanoparticles (MSN) using OVA as a model protein. The OVA-loaded MCM-41 silica nanoparticles were freeze-dried in the presence of the excipients trehalose and PEG 8000. Addition of these excipients prevented particle aggregation as assessed by TEM analyses (manuscript in preparation).

3.4 Adsorption of protein on nanoparticles

Development of successful protein-based vaccines depends on a close understanding of their biological characteristics, chemical, physical stability and their safety profile. [43] The use of nanoparticles as delivery systems can improve protein and peptide stability, enhance protection and facilitate presentation of antigen to the immune system. [40, 44] Protein/antigens on adsorption onto the nanoparticles, can either adsorb on the surface or internal pores of the nanoparticles; site at which the proteins bind to the nanoparticles greatly depend on the type and properties of the target proteins and nanoparticles (Fig 3.1). The electrostatic protein-surface interactions, hydrogen bonding and weak van der Waals forces adsorb protein to nanoparticles. The pore surface area determines the protein binding capacity. The surface area of the nanoparticles can be easily adjusted by modifying the concentration of the nanoparticles in the aqueous phase. [45]

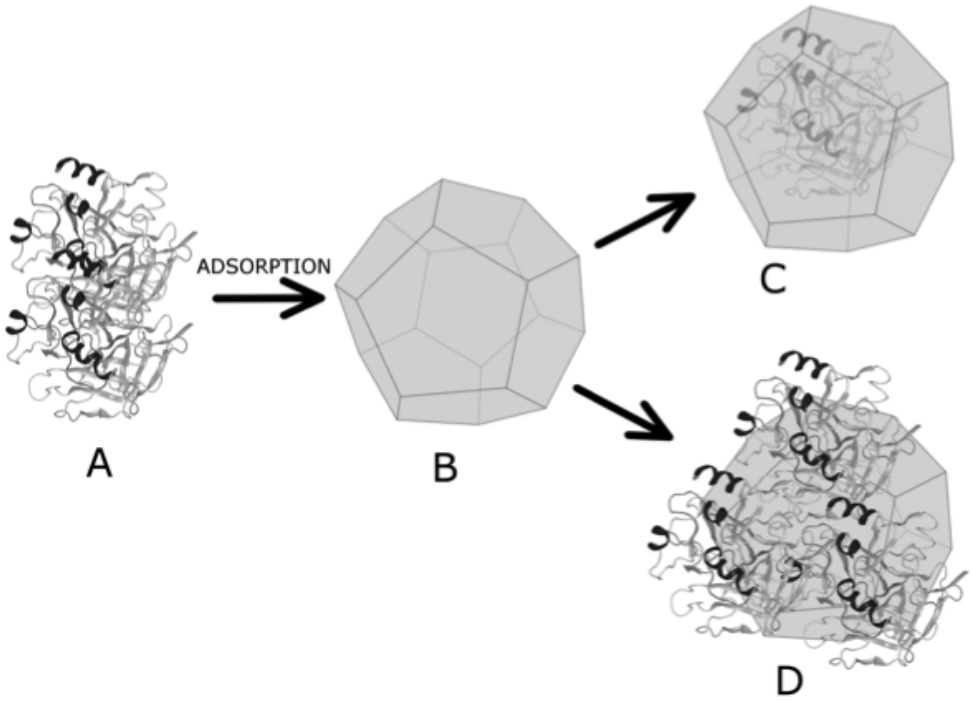

Fig 3.1. Protein-based nanovaccine: **(A)** Protein **(B)** Nanoparticle **(C)** Internalised protein **(D)** Protein on the surface of the nanoparticles.

Nguyen *et al.* [46] reported adsorption kinetics of BSA protein to SBA-15 silica nanoparticles. On adsorption the BSA protein could not penetrate into the conventional SBA-15 because the pore size of the nanoparticles is very small compared to the size of protein. Therefore, most of the protein was adsorbed on the external surface of the nanoparticles or at the mouth of the pore; however, adsorption of protein on the inside of the particles can be obtained by increasing the pore size of the SBA-15 particles. This shows that the pore size also plays an important role in determining the protein binding capacity. Park *et al.* [47] described the use of MSN for protein delivery. They designed MSN functionalized with citraconic amide with terminal carboxyl group to deliver model protein horse heart Cyt C. They demonstrated that modifying the functionalisation of nanoparticles from positive to negative facilitated the release of proteins. Their *in vitro* studies showed that MSN could act as an efficient intracellular delivery vehicle for many membrane-impermeable therapeutic proteins. Chesko *et al*. adsorbed different proteins like BSA, OVA, carbonic anhydrase (CAN), lysozyme (LYZ), lactic acid dehydrogenase, and an HIV envelope glycoprotein to PLG microparticles. They found similar results that protein adsorption and release from the PLG microparticles occurs through a combination of electrostatic and van der Waals interactions taking place at the polymer-solution interface. [45]

Skwarczynski and Toth have reviewed that nanoparticle-based vaccine delivery systems can improve synthetic peptides immunogenicity as vaccines. [11] Biodegradable and biocompatible polyesters such as derivatives of chitosan and chitosan nanoparticles have promising future as protein carriers, since the polymers are non-toxic and are biodegradable. [48] Biodegradable polymeric PLGA nanoparticles have been extensively studied and used for delivery of proteins and peptides as they are stable in biological fluids and can protect the encapsulated antigen. Polymeric nanoparticles when administered intravenously can be easily recognised by the body's immune systems. [49, 50] Moon *et al.* [51] demonstrated that when malaria antigen VMP001 was combined with PLGA nanoparticles along with monophosphoryl lipid A (MPLA) as adjuvant a better antigen-specific response was elicited with significantly higher antibody titers *in* vivo, while the vaccines composed of soluble protein mixed with adjuvant MPLA showed less response. [51] The use of adjuvants is usually necessary with PLGA based vaccine delivery systems to produce enhanced immune response.

Biodegradable γ-PGA nanoparticles have also been excellent delivery vehicles for different proteins and peptides. [52, 53] Matsuo *et al.* reported that OVA entrapped γ-PGA nanoparticles when injected subcutaneously into mice produced strong immune responses by inhibiting the growth of OVA-transfected tumors, compared to mice vaccinated with OVA and Freund's complete adjuvant. [54] They further investigated the antitumor efficacy and immune responses in mice vaccinated with OVA/γ-PGA nanoparticles via the nasal cavity. They found that immune responses to cytotoxic T lymphocytes (CTLs) and interferon-γ-secreting cells specific for OVA in the spleen and lymph nodes were produced whether the vaccination was administered via subcutaneously or intranasal route. These nanoparticles have a promising future in development of non-invasive vaccines. [55] Nanoparticles are used to create and develop mucosal vaccines because of their adjuvanting properties. Mucosal vaccines offer great potential as they can be administered via oral and intranasal delivery routes. Administration of mucosal vaccines does not require trained personnel, in addition it avoids the use of needles and helps with overall pateint acceptability. [56] Nanovaccines can be delivered through oral or nasal route, allowing development of pain-free vaccine delivery technology. [57]

Nanotechnology has paved way for development of novel diagnostic and therapeutic applications. The advantages associated with polymeric nanoparticles and nanobeads has been found to be useful in developing protein and peptide based nanovaccines as reviewed by Nandedkar. [58] Conventional subunit vaccine formulations need multiple immunisations to elicit immune response.

[59] However, encapsulating antigen on to the nanoparticles can protect the proteins from degradation and enhance target delivery of the proteins. Protein loaded nanoparticle-based vaccine delivery system improve the presentation of proteins immunogens when incorporated into nanoparticles as they are protected against enzymatic degradation and are presented to the immune system more effectively inducing a good immune response without the need of a traditional adjuvant. [11]

3.5 Freeze-dried nanoformulations

As with most traditional subunit vaccines, nanovaccines also have stability issues that need to be addressed to facilitate their use in vaccine formulations. The increasing development of therapeutic protein based nanovaccines has highlighted issues such as proteins stability, elimination of cold-chain storage and efficacious vaccine delivery to avoid adverse immunogenic side effects. Freeze-drying process (Fig 3.2) can lead to shelf stable vaccines. Freeze-drying of nanoparticle formulations can enhance the physical and chemical stability of the nanoparticles, by removing water from these systems [20], and also improve the optimal efficacy and thermostability range of the final vaccine. [38]

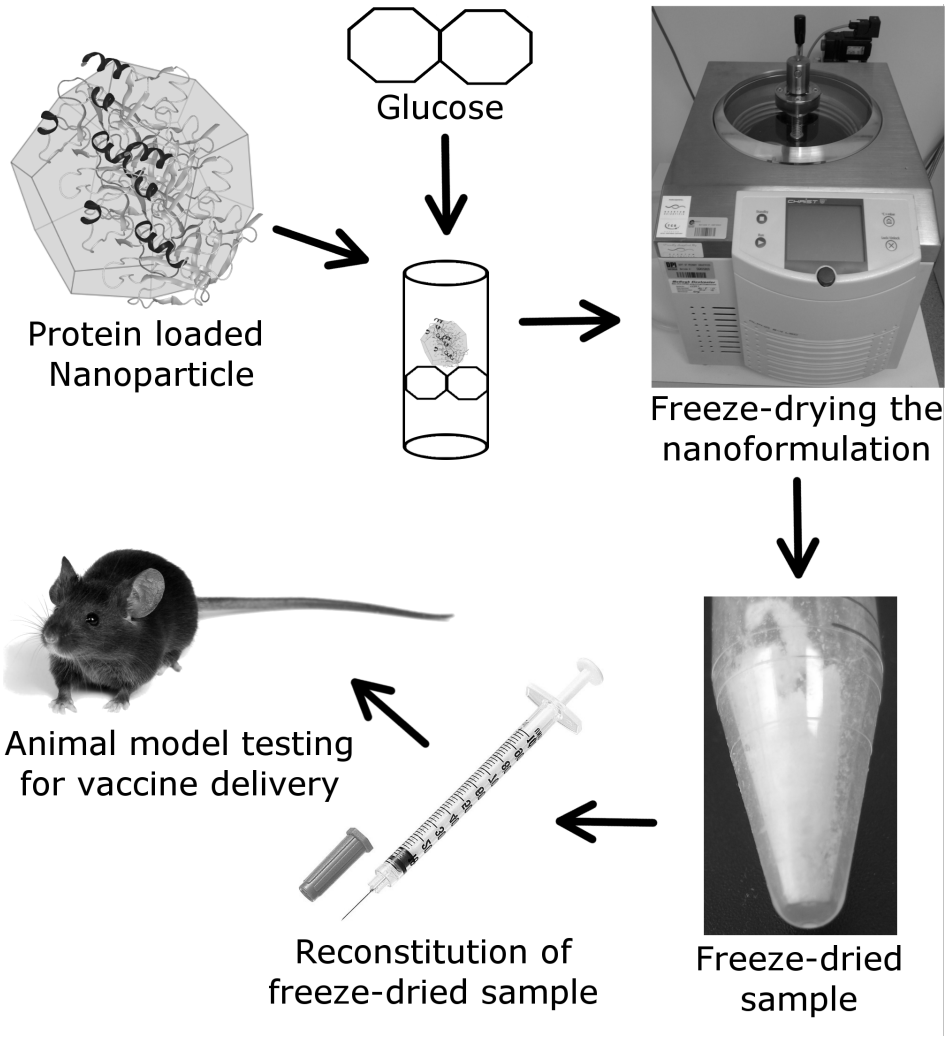

Fig 3.2. Schematic representation of the overall freeze-drying process.

Immunization studies on freeze-dried Gantrez® AN nanoparticles encapsulated with OVA showed that the nanoparticles acted as an excellent adjuvants when orally administrated in mice as they helped enhance the Th1 and Th2 immune responses. [60] Manosroi *et al.* [61] conducted studies using human insulin loaded onto liposomal formulations like DPPC (dipalmitoyl phosphatidyl choline) mixed with cholesterol and CTA [cholest-5-en-3-ol (3 beta)(trimethylammonio) acetate] or DDAB (dioctadecyl dimethyl ammonium bromide). Insulin bound to freeze-dried liposomes showed enhanced stability when stored at different temperatures for 4 months compared to the samples stored in aqueous solution. [61]

Long-term stability studies conducted on freeze-dried human serum albumin (HSA) nanoparticles showed that 3% trehalose protected the particles from aggregation. Furthermore, freeze-dried HSA samples stored for 13 weeks between 2-8°C showed no increase in the residual water content. [13] Genetically engineered hydrophobin fusion protein when coupled with two cellulose domains

facilitated drug (itraconazole) nanoparticle binding to nanofibrillar cellulose. These drug nanoparticles were freeze-dried with D±trehalose (1:1.25 protein:D±trehalose ratio) as an excipient, and were immobilised in nanofibrillar cellulose matrix. The matrix provided protection to the nanoparticle morphology during processing and storage. Differential scanning calorimetry (DSC) studies revealed that trehalose formed an amorphous matrix which prevented dehydration of proteins and protected the formulation from aggregation and induced controlled release of the drug. [62] Storage temperature and length impacts the long-term stability of the nanoparticles. These factors may cause reduction in particle size and eventually lead to degradation of particles. For example, no major changes were observed in tripolyphosphate (TPP) chitosan nanoparticles stored between 4 and 25°C for 12 months, but at 40°C the chitosan nanoparticles degraded within 6 months of storage. [63] It is likely that hydrolysis during storage affected the polymer chains resulting in decrease in particle size and subsequent degradation. Stability of these nanoparticles could be improved with the freeze-drying technique in the presence of different excipients.

Vandana and Sahoo [14] found sucrose was the most effective excipient in maintaining the size and surface charge of the chitosan nanoparticles after freeze-drying using the model protein BSA. Optimisation of different parameters like particle size, encapsulation efficiency and *in vitro* release led to improved encapsulation and controlled release of the BSA protein. [14] Freeze-drying rHBsAg loaded chitosan-based nanoparticles preserved the characteristics of the antigen for up to 3 months of storage at 4°C. Addition of 2.5% glucose to the nanoformulation helped preserve the physico-chemical properties of the nanoparticle. The ability of these lyophilised nanoparticles to induce an immune response was confirmed by an animal immunisation trial indicating that chitosan-based nanoparticles are a promising adjuvant candidate with the capacity to enhance and prolong the immune response of the rHBsAg after *in vivo* administration. [38]

Freeze-drying oligonucleotide-loaded gelatin nanoparticles in the presence of the excipients trehalose, sucrose and mannitol produced a highly concentrated formulation that retained its biological *in vivo* activity after 4 weeks of storage at 40°C. [17] Akagi *et al.* [42] developed a biodegradable γ-PGA nanoparticle with a hydrophilic segment, an inner hydrophobic core and carboxyl functional groups at the side chains, allowing hydrophobic drugs to be easily entrapped within the core via hydrophobic interactions. The model protein OVA was immobilised onto the γ-PGA nanoparticles by an amide bond between the carboxyl group on the surface of the nanoparticles and the amide group of OVA. Both untreated and freeze-dried OVA encapsulated nanoparticles released less than 5% of the loaded OVA. This proved that the OVA-encapsulated

γ-PGA nanoparticles were highly suitable for the freeze-drying process. The freeze-dried OVA encapsulated γ-PGA nanoparticles with 1, 2.5, and 5% glucose showed less particle aggregation compared to particles without cryoprotectants. [42]

Tiyaboonchai *et al.* [40] developed a freeze-dried nanoparticle delivery system for insulin using the polymers PEI and DS. The system achieved a high level of insulin entrapment and preserved its secondary structure and biological activity with no degradation of insulin in the reported potency studies. The presence of zinc sulfate in the formulation stabilised the nanoparticles and prolonged the release of protein over a 4 h period. In addition, the results proved that when the freeze-dried nanoparticle formulation was stored for 6 months in a desiccator at 2-8°C, the insulin nanoformulation revealed similar potency and purity as the initial freeze-dried preparation. [40]

Protein encapsulated/adsorbed to silica nanoparticles have been used for the successful delivery of proteins due to their great capability for the entrapment of antigenic proteins. [36, 64] Carvalho *et al.* [64] reported that the mesoporous SBA-15 silica acted as an adjuvant in *in vivo* studies. [64] Uptake studies using HeLa cells demonstrated that MSN could successfully deliver the membrane-impermeable protein cytochrome C *in vitro*. [65-67] Collectively these studies demonstrated that silica nanoparticles have an encouraging future in delivery of proteins, peptides and other antigens, this has been reviewed in more detail in [68].

In our laboratory, we have been investigating the usefulness of MCM-41 mesoporous silica nanoparticles for the *in vivo* delivery of OVA antigen. OVA showed significant degradation when stored at room temperature, however, freeze-dried MCM-41 bound OVA showed no degradation for up to two months when stored under similar conditions, as analysed by polyacrylamide gel electrophoresis. Our research showed that freeze-dried OVA encapsulated MCM-41 nanoparticles released less than 5% OVA, this was comparable to the results obtained for freeze-dried OVA encapsulated γ-PGA nanoparticles. [42] The freeze-dried OVA nanoformulation showed complete reconstitution within 30 seconds upon the addition of injectable saline. The ability to completely resuspend a vaccine is important to obtain a stable vaccine that can be safely administered. Mice immunised with the freeze-dried OVA nanoparticles vaccine resulted in enhanced antibody and cell-mediated responses compared to the equivalent dose of unprocessed OVA bound nanoparticles (manuscript in preparation). There is very limited information available on stability of freeze-dried protein-based or protein-loaded nanoparticle systems. Few examples of freeze-dried protein/nanoparticle delivery systems have been summarised in Table 3.1.

Table 3.1. Comparison of freeze-dried protein/nanoparticles systems using different excipients and freeze-drying conditions

Nanoparticles	Protein	Excipients	Freeze-drying process	References
Poly (gamma-glutamic acid)(γ-PGA)	Ovalbumin	1, 2.5, 5% Glucose	Freezing-Liquid nitrogen 10min Freeze-dried for 24 h	[42]
Polyethylenimine (PEI) and Dextran Sulfate (DS)	Insulin	5%(w/v) Mannitol Zinc sulfate	Freezing (-46°C) Primary drying 1.695 mbar* for 24 h	[40]
Itraconazole nanoparticles	Hydrophobin fusion protein	Cryo/lyoprotectants with D±Trehalose 1:1.25 (drug: excipient) ratio	Primary drying 0.133mbar* - 40°C 3 h -30°C 17 h Secondary drying 0.133 mbar* -25°C to 40°C, 5°C step each for 1h	[62]
Chitosan nanoparticles	Bovine serum albumin	2000-10,000 PEG, sucrose, mannitol, mannose, glucose in concentration of 20 mg/ml	Freezing (-80°C) Lyophilisation at 0.05 mbar -48°C, 48 h	[14]
Chitosan nanoparticles	Hepatitis B surface antigen (rHBsAg)	0,1,2.5, and 5% glucose	Freezing (-80°C) Primary drying 35°C 40 h under high vacuum Secondary drying 8h gradually increasing the temperature to +20°C	[38]
Human serum albumin (HSA)	With and without	1, 2 and 3% (w/v) trehalose, sucrose	Freezing 0.08mbar, shelf	[13]

* The pressure units have been converted from mTorr to mbar for ease of comparison.

3.6 Assessment of physico-chemical characteristics of the nanoformulation after freeze-drying

After lyophilisation, high-resolution microscopic techniques like transmission electron microscopy (TEM), scanning electron microscopy (SEM), and atomic force microscopy (AFM) can be used to observe the architecture of the nanoparticles. The final freeze-dried cake should appear voluminous and snow-like; TEM images can provide information about the preservation status of the nanoparticles. For example, after negative staining of freeze-dried rHBsAg loaded chitosan-based nanoparticles TEM images showed that the nanoparticles maintained their spherical shape and were homogenously scattered. [38] A similar finding was found for freeze-dried cationically modified silica nanoparticle formulation. [39] The samples freeze-dried with 5% trehalose showed a matrix separating individual nanoparticles; additionally the trehalose formed a coat that over the nanoparticle surface.

For the freeze-dried nanoformulation to be injectable and efficient it is important that on reconstitution the protein is stable and the nanoparticles do not form aggregation as well as have uniform structure and size. Reconstitution of freeze-dried nanoparticles is achieved by the addition of water at a volume equal to the assimilated volume during the freeze-drying process. Reconstitution usually occurs rapidly but may require mechanical agitation (shaking, gentle vortexing) or sonication. [16] The type and concentration of excipients used during lyophilisation can also potentially impact upon reconstitution of the freeze-dried samples. Cationically modified silica nanoparticles rehydrated readily by inverting the tube 10 times when freeze-dried using trehalose, but required vortexing when freeze-dried using higher concentrations of trehalose and 15 min sonication was required when freeze-dried with lyoprotectants like glucose, acetic acid and mannitol. [39]

Naproxen (an anti-inflammatory drug) nanoparticles when freeze-dried with 10 wt% sucrose resulted in aggregation, however, freeze-drying of the samples with 25 or 40 wt% PEG as a cryoprotectant maintained the particle size and the final freeze-dried product resuspended easily. [23] The ciprofloxacin HCl-loaded PLGA nanoparticles were freeze-dried in the presence of different cryoprotectants such as 5.0% (w/v) mannitol, trehalose or glucose, and 5.0% (w/v) or 15.0% (w/v) dextran. Samples containing glucose did not reconstitute easily presumably because after freezing the nanoparticle formulation formed a sticky freeze-dried cake. In addition, the samples freeze-dried with dextran aggregated on reconstitution. [69]

Surfactant-free PLGA nanoparticles when lyophilised with 2.0% (w/v) sucrose, trehalose and lactose, reconstituted completely into aqueous solution without significantly affecting the particle size, whereas with 1.0% (w/v) mannitol the particles precipitated. Furthermore, the authors showed that testosterone-encapsulated PLGA nanoparticles reconstituted with 2.0% (w/v) sucrose, trehalose and lactose. [70] SEM was used to observe the freeze-dried PCL nanospheres containing silicon dioxide (SiO_2) and it was observed the nanospheres readily dispersed and formed lower sized nanostructures of about 80 nm onto the microparticle surface. The samples freeze-dried without SiO_2, formed an agglomerate of nanoparticles with diameters between 150 nm and 200 nm, which were similar to those characterised in the original suspension. [71] These results demonstrate that reconstitution of freeze-dried nanoformulation greatly depend on the type of excipients used during lyophilisation.

The Karl Fischer titration technique can be used to analyse the residual moisture content of the freeze-dried samples. This method has been used to determine the residual moisture content of freeze-dried doxorubicin-loaded human serum albumin (HSA) nanoparticles. All the freeze-dried samples irrespective of the excipients used had a residual water content of about 3% (w/v). Furthermore, no increase in the residual water content was observed when the samples were stored for 13 weeks at 2-8°C, however samples stored at 25°C/60% relative humidity and 40°C/75% relative humidity showed a 5% increase in water content, which may be due to the moisture coming from the stoppers. [13] As discussed before residual moisture content is important in the final vaccine as it influences the structural and thermal properties of freeze-dried proteins and nanoparticles. [16]

3.7 Conclusion

This review shows that development of freeze-dried nanovaccine delivery systems is an emerging area with the capacity to facilitate important advancements in this field. We have highlighted that it is critically important to characterise and establish the optimal freeze-drying conditions for each nanovaccine formulation during the development phase, as each vaccine formulation may behave differently. Freeze-drying of protein-loaded nanoparticles can not only help preserve the chemical and physical integrity of nanoparticle structures but it can also facilitate the maintenance of the immunogenicity of the biological vaccine components. The application of freeze-drying process to nanoparticle based vaccine platforms can be easily applied to vaccine manufacturing in cost effective manner if considered early in the vaccine development pipeline. Moreover the successful

development of a freeze-drying procedure is critical, as it facilitates the elimination of cold storage chains and enhancement of shelf-life under environmental conditions which are key considerations in long-term stability and wide spread nanovaccine adoption. This area of work is highly significant with the potential to pave way for the next generation of vaccine delivery technologies.

3.8 Acknowledgements

This work was funded by the Queensland Government through the Department of Employment, Economic Development and Innovation Reinvestment Fund. The authors thank Antonino Cavallaro for helpful discussions and for his critical reading of the manuscript.

3.9 References

1. Friede M, Aguado MT (2005) Need for new vaccine formulations and potential of particulate antigen and DNA delivery systems. Adv Drug Deliv Rev 57: 325-331.
2. Koping-Hoggard M, Sanchez A, Alonso MJ (2005) Nanoparticles as carriers for nasal vaccine delivery. Expert Rev Vaccines 4: 185-196.
3. de la Fuente M, Csaba N, Garcia-Fuentes M, Alonso MJ (2008) Nanoparticles as protein and gene carriers to mucosal surfaces. Nanomedicine (Lond) 3: 845-857.
4. Lee HJ (2002) Protein drug oral delivery: the recent progress. Archives of pharmacal research 25: 572-584.
5. Panyam J, Labhasetwar V (2003) Biodegradable nanoparticles for drug and gene delivery to cells and tissue. Adv Drug Deliv Rev 55: 329-347.
6. Jung T, Kamm W, Breitenbach A, Hungerer KD, Hundt E, et al. (2001) Tetanus toxoid loaded nanoparticles from sulfobutylated poly(vinyl alcohol)-graft-poly(lactide-co-glycolide): evaluation of antibody response after oral and nasal application in mice. Pharm Res 18: 352-360.
7. Singh M, Briones M, Ott G, O'Hagan D (2000) Cationic microparticles: A potent delivery system for DNA vaccines. Proc Natl Acad Sci U S A 97: 811-816.
8. Gemeinhart RA, Luo D, Saltzman WM (2005) Cellular fate of a modular DNA delivery system mediated by silica nanoparticles. Biotechnol Prog 21: 532-537.
9. Parveen S, Misra R, Sahoo S (2011) Nanoparticles: a boon to drug delivery, therapeutics, diagnostics and imaging. Nanomedicine: Nanotechnology, Biology and Medicine 8: 147-166.
10. Parveen S, Sahoo SK (2006) Nanomedicine: Clinical Applications of Polyethylene Glycol Conjugated Proteins and Drugs. Clinical Pharmacokinetics 45: 965-988.
11. Skwarczynski. M, Toth. I (2011) Peptide-Based Subunit Nanovaccines. Curr Drug Deliv 8: 282-289.
12. Tang X, Pikal MJ (2004) Design of freeze-drying processes for pharmaceuticals: practical advice. Pharm Res 21: 191-200.
13. Anhorn MG, Mahler HC, Langer K (2008) Freeze drying of human serum albumin (HSA) nanoparticles with different excipients. Int J Pharm 363: 162-169.
14. Vandana M, Sahoo SK (2009) Optimization of physicochemical parameters influencing the fabrication of protein-loaded chitosan nanoparticles. Nanomedicine (Lond) 4: 773-785.

15. Roy I, Gupta MN (2004) Freeze-drying of proteins: some emerging concerns. Biotechnology and applied biochemistry 39: 165-177.
16. Abdelwahed W, Degobert G, Stainmesse S, Fessi H (2006) Freeze-drying of nanoparticles: formulation, process and storage considerations. Adv Drug Deliv Rev 58: 1688-1713.
17. Zillies JC, Zwiorek K, Hoffmann F, Vollmar A, Anchordoquy TJ, et al. (2008) Formulation development of freeze-dried oligonucleotide-loaded gelatin nanoparticles. Eur J Pharm Biopharm 70: 514-521.
18. Edinara Adelaide Boss RMF, Eduardo Coselli Vasco de Toledo (2004) Freeze drying process: real time model and optimization. Chemical Engineering and Processing.
19. Heller MC, Carpenter JF, Randolph TW (1999) Protein formulation and lyophilization cycle design: prevention of damage due to freeze-concentration induced phase separation. Biotechnol Bioeng 63: 166-174.
20. Franks F (1998) Freeze-drying of bioproducts: putting principles into practice. Eur J Pharm Biopharm 45: 221-229.
21. Mackenzie AP (1966) Basic principles of freeze-drying for pharmaceuticals. Bull Parenter Drug Assoc 20: 101-130.
22. Pikal MJ (1985) Use of laboratory data in freeze drying process design: heat and mass transfer coefficients and the computer simulation of freeze drying. J Parenter Sci Technol 39: 115-139.
23. Lee MK, Kim MY, Kim S, Lee J (2009) Cryoprotectants for freeze drying of drug nano-suspensions: effect of freezing rate. J Pharm Sci 98: 4808-4817.
24. Wei W (1999) Instability, stabilization, and formulation of liquid protein pharmaceuticals. International Journal of Pharmaceutics 185: 129-188.
25. Wang B, Tchessalov S, Warne NW, Pikal MJ (2009) Impact of sucrose level on storage stability of proteins in freeze-dried solids: I. correlation of protein–sugar interaction with native structure preservation. Journal of Pharmaceutical Sciences 98: 3131-3144.
26. Wei W (2000) Lyophilization and development of solid protein pharmaceuticals. International Journal of Pharmaceutics 203: 1-60.
27. Carpenter JF, Kendrick BS, Chang BS, Manning MC, Randolph TW (1999) Inhibition of stress-induced aggregation of protein therapeutics. Methods Enzymol 309: 236-255.
28. Nail SL, Jiang S, Chongprasert S, Knopp SA (2002) Fundamentals of freeze-drying. Pharm Biotechnol 14: 281-360.
29. Baheti A, Kumar L, Bansal AK (2010) Excipients used in lyophilization of small molecules. J Excipients and Food Chem 1.

30. Cui Z, Hsu CH, Mumper RJ (2003) Physical characterization and macrophage cell uptake of mannan-coated nanoparticles. Drug Dev Ind Pharm 29: 689-700.
31. Carpenter JF, Prestrelski SJ, Arakawa T (1993) Separation of freezing- and drying-induced denaturation of lyophilized proteins using stress-specific stabilization. I. Enzyme activity and calorimetric studies. Arch Biochem Biophys 303: 456-464.
32. Prestrelski SJ, Arakawa T, Carpenter JF (1993) Separation of Freezing- and Drying-Induced Denaturation of Lyophilized Proteins Using Stress-Specific Stabilization: II. Structural Studies Using Infrared Spectroscopy. Archives of Biochemistry and Biophysics 303: 465-473.
33. Izutsu K, Yoshioka S, Kojima S (1995) Increased stabilizing effects of amphiphilic excipients on freeze-drying of lactate dehydrogenase (LDH) by dispersion into sugar matrices. Pharm Res 12: 838-843.
34. Layre AM, Couvreur P, Richard J, Requier D, Eddine Ghermani N, et al. (2006) Freeze-drying of composite core-shell nanoparticles. Drug Dev Ind Pharm 32: 839-846.
35. Farruggia B, Garcia G, D'Angelo C, Pico G (1997) Destabilization of human serum albumin by polyethylene glycols studied by thermodynamical equilibrium and kinetic approaches. Int J Biol Macromol 20: 43-51.
36. Wendorf J, Singh M, Chesko J, Kazzaz J, Soewanan E, et al. (2006) A practical approach to the use of nanoparticles for vaccine delivery. J Pharm Sci 95: 2738-2750.
37. Quintanar-Guerrero D, Ganem-Quintanar A, Allemann E, Fessi H, Doelker E (1998) Influence of the stabilizer coating layer on the purification and freeze-drying of poly(D,L-lactic acid) nanoparticles prepared by an emulsion-diffusion technique. J Microencapsul 15: 107-119.
38. Prego C, Paolicelli P, Diaz B, Vicente S, Sanchez A, et al. (2010) Chitosan-based nanoparticles for improving immunization against hepatitis B infection. Vaccine 28: 2607-2614.
39. Sameti M, Bohr G, Ravi Kumar MN, Kneuer C, Bakowsky U, et al. (2003) Stabilisation by freeze-drying of cationically modified silica nanoparticles for gene delivery. Int J Pharm 266: 51-60.
40. Tiyaboonchai W, Woiszwillo J, Sims RC, Middaugh CR (2003) Insulin containing polyethylenimine-dextran sulfate nanoparticles. Int J Pharm 255: 139-151.
41. de Chasteigner S, Cavé G, Fessi H, Devissaguet J-P, Puisieux F (1996) Freeze-drying of itraconazole-loaded nanosphere suspensions: a feasibility study. Drug Development Research 38: 116-124.

42. Akagi T, Kaneko T, Kida T, Akashi M (2005) Preparation and characterization of biodegradable nanoparticles based on poly(gamma-glutamic acid) with l-phenylalanine as a protein carrier. J Control Release 108: 226-236.

43. Frokjaer S, Otzen DE (2005) Protein drug stability: a formulation challenge. Nature Reviews Drug Discovery 4: 298-306.

44. Csaba N, Garcia-Fuentes M, Alonso MJ (2009) Nanoparticles for nasal vaccination. Advanced Drug Delivery Reviews 61: 140-157.

45. Chesko J, Kazzaz J, Ugozzoli M, O'Hagan DT, Singh M (2005) An investigation of the factors controlling the adsorption of protein antigens to anionic PLG microparticles. Journal of Pharmaceutical Sciences 94: 2510-2519.

46. Nguyen TPB, Lee J-W, Shim WG, Moon H (2008) Synthesis of functionalized SBA-15 with ordered large pore size and its adsorption properties of BSA. Microporous and Mesoporous Materials 110: 560-569.

47. Park HS, Kim CW, Lee HJ, Choi JH, Lee SG, et al. (2010) A mesoporous silica nanoparticle with charge-convertible pore walls for efficient intracellular protein delivery. Nanotechnology 21: 225101.

48. Agnihotri SA, Mallikarjuna NN, Aminabhavi TM (2004) Recent advances on chitosan-based micro- and nanoparticles in drug delivery. Journal of Controlled Release 100: 5-28.

49. Mundargi RC, Babu VR, Rangaswamy V, Patel P, Aminabhavi TM (2008) Nano/micro technologies for delivering macromolecular therapeutics using poly(d,l-lactide-co-glycolide) and its derivatives. Journal of Controlled Release 125: 193-209.

50. Bhavsar MD, Amiji MM (2007) Polymeric nano- and microparticle technologies for oral gene delivery. Expert Opinion on Drug Delivery 4: 197-213.

51. Moon JJ, Suh H, Polhemus ME, Ockenhouse CF, Yadava A, et al. (2012) Antigen-Displaying Lipid-Enveloped PLGA Nanoparticles as Delivery Agents for a Plasmodium vivax Malaria Vaccine. PLoS One 7: e31472.

52. Uto T, Wang X, Sato K, Haraguchi M, Akagi T, et al. (2007) Targeting of antigen to dendritic cells with poly(gamma-glutamic acid) nanoparticles induces antigen-specific humoral and cellular immunity. Journal of Immunology 178: 2979-2986.

53. Uto T, Akagi T, Hamasaki T, Akashi M, Baba M (2009) Modulation of innate and adaptive immunity by biodegradable nanoparticles. Immunology Letters 125: 46-52.

54. Yoshikawa T, Okada N, Oda A, Matsuo K, Matsuo K, et al. (2008) Nanoparticles built by self-assembly of amphiphilic Œ≥-PGA can deliver antigens to antigen-presenting cells with high

efficiency: A new tumor-vaccine carrier for eliciting effector T cells. Vaccine 26: 1303-1313.

55. Matsuo K, Koizumi H, Akashi M, Nakagawa S, Fujita T, et al. (2011) Intranasal immunization with poly(γ-glutamic acid) nanoparticles entrapping antigenic proteins can induce potent tumor immunity. Journal of Controlled Release 152: 310-316.

56. Chadwick S, Kriegel C, Amiji M (2010) Nanotechnology solutions for mucosal immunization. Advanced Drug Delivery Reviews 62: 394-407.

57. Mark K (2006) Engineering of needle-free physical methods to target epidermal cells for DNA vaccination. Vaccine 24: 4651-4656.

58. Nandedkar TD (2009) Nanovaccines: recent developments in vaccination. Journal of biosciences 34: 995-1003.

59. Malik DK, Baboota S, Ahuja A, Hasan S, Ali J (2007) Recent advances in protein and peptide drug delivery systems. Current drug delivery 4: 141-151.

60. Gomez S, Gamazo C, Roman BS, Ferrer M, Sanz ML, et al. (2007) Gantrez AN nanoparticles as an adjuvant for oral immunotherapy with allergens. Vaccine 25: 5263-5271.

61. Manosroi A, Khositsuntiwong N, Komno C, Manosroi W, Werner RG, et al. (2011) Chemical Stability and Cytotoxicity of Human Insulin Loaded in Cationic DPPC/CTA/DDAB Liposomes. Journal of Biomedical Nanotechnology 7: 308-316.

62. Valo H, Kovalainen M, Laaksonen P, Hakkinen M, Auriola S, et al. (2011) Immobilization of protein-coated drug nanoparticles in nanofibrillar cellulose matrice-Enhanced stability and release. Journal of Controlled Release 156: 390-397.

63. Morris GA, Castile J, Smith A, Adams GG, Harding SE (2011) The effect of prolonged storage at different temperatures on the particle size distribution of tripolyphosphate (TPP) ‚Äì chitosan nanoparticles. Carbohydrate Polymers 84: 1430-1434.

64. Carvalho LV, Ruiz Rde C, Scaramuzzi K, Marengo EB, Matos JR, et al. (2010) Immunological parameters related to the adjuvant effect of the ordered mesoporous silica SBA-15. Vaccine 28: 7829-7836.

65. Slowing, II, Vivero-Escoto JL, Wu CW, Lin VS (2008) Mesoporous silica nanoparticles as controlled release drug delivery and gene transfection carriers. Adv Drug Deliv Rev 60: 1278-1288.

66. Slowing II, Trewyn BG, Giri S, Lin VSY (2007) Mesoporous Silica Nanoparticles for Drug Delivery and Biosensing Applications. Advanced Functional Materials 17: 1225-1236.

67. Slowing II, Trewyn BG, Lin VSY (2007) Mesoporous Silica Nanoparticles for Intracellular Delivery of Membrane-Impermeable Proteins. Journal of the American Chemical Society 129: 8845-8849.

68. Mishra B, Patel BB, Tiwari S (2010) Colloidal nanocarriers: a review on formulation technology, types and applications toward targeted drug delivery. Nanomedicine 6: 9-24.

69. Bozdag S, Dillen K, Vandervoort J, Ludwig A (2005) The effect of freeze-drying with different cryoprotectants and gamma-irradiation sterilization on the characteristics of ciprofloxacin HCl-loaded poly(D,L-lactide-glycolide) nanoparticles. J Pharm Pharmacol 57: 699-707.

70. Jeong YI, Shim YH, Kim C, Lim GT, Choi KC, et al. (2005) Effect of cryoprotectants on the reconstitution of surfactant-free nanoparticles of poly(DL-lactide-co-glycolide). J Microencapsul 22: 593-601.

71. Schaffazick SR, Pohlmann AR, Dalla-Costa T, Guterres SS (2003) Freeze-drying polymeric colloidal suspensions: nanocapsules, nanospheres and nanodispersion. A comparative study. Eur J Pharm Biopharm 56: 501-505.

4.

Freeze-drying of Ovalbumin loaded Mesoporous Silica Nanoparticle Vaccine Formulation Increases Antigen Stability under Ambient Conditions

---

In this chapter the *in vitro* and *in vivo* capacity of freeze-dried Ovalbumin (OVA) loaded amino functionalised mesoporous silica nanoparticles (AM-41) was determined. The ability of OVA loaded AM-41 (OVA/AM-41) vaccine formulation was first investigated by Mahony *et al.* [1] in a small animal study. The results obtained from that study provided the proof-of-concept that silica nanoparticles could act as excellent adjuvants and nanocarriers. However, OVA has a short shelf-life at room temperature, hence, to improve the shelf-life of the nanovaccine formulation by eliminating cold chain storage, I developed the freeze-drying process for OVA/AM-41

(termed as OVA-41). The optimal excipient formulation for freeze-drying of OVA bound AM-41 was determined to be 5% trehalose and 1% PEG8000. This formulation preserved both the OVA protein integrity and AM-41 particle structure. To investigate the efficacy of the freeze-dried formulation Dr. Donna Mahony and I successfully ran a mice trial and found that the developed freeze-dried OVA/AM-41 nanovaccine generated both Th1 and Th2 immune responses (Fig 4.1).

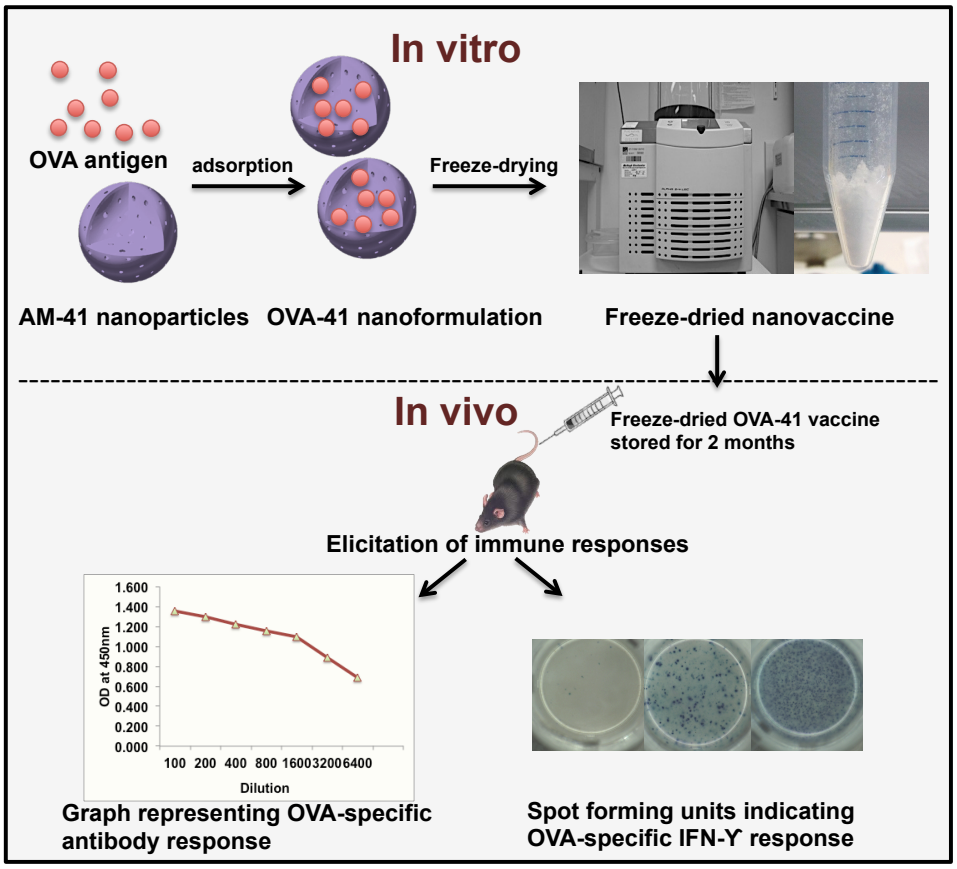

Fig 4.1. Schematic diagram showing the development of OVA/AM-41 vaccine delivery system. **Chapter 6 is published in *International Journal of Pharmaceutics 2014, 465, 325-332***

4.1 Introduction

The role of vaccines is to elicit protective immunity against infectious agents, while improvements have been made with the development of protein and peptide based subunit vaccine formulations, many challenges still remain. Key challenges include the complexities associated with physical and chemical stability of the vaccine antigen components. [2-6] Freeze-drying and novel delivery systems can address the issue of instability of conventional and subunit vaccines.

Mesoporous silica nanoparticles (MSNs) have emerged as excellent carriers for delivery of biologically active molecules such as drugs, genes, therapeutic proteins and enzymes. The ease of MSMs synthesis and characteristics such as porous structure, large surface area, flexible surface chemistry and *in vivo* biocompatibility all contribute the utility of this carrier system. [7-10] The efficiency of ordered silica nanoparticles (SBA-15) and MSNs as adjuvants and protein carriers have already been explored in mice immunisation studies. [9, 11-13] Silica nanoparticles have emerged as a new approach to address the limitations of current technologies such as high toxicity, severe side effects, and inflammation at the site of injection associated with conventional adjuvants and improves the overall safety profile of the vaccine formulations. [14]

The current investigation focused on the development of a freeze-dried MSN based vaccine delivery system. The freeze-drying process can preserve unstable molecules such as proteins and nanoparticles [15, 16] by removing water from the frozen sample by sublimation and desorption under specific vacuum pressure and temperature conditions. However, the freeze-drying process can damage biological molecules leading to loss of activity, therefore, excipients such as sugars, surfactants, amino acids and polymers are added to the formulation to protect and enhance the overall stability of proteins. [5, 17] The excipients used to protect from the freezing stress are known as cryoprotectants, whereas the ones protecting from drying stress are known as lyoprotectants. [18]

The physico-chemical property of freeze-dried human serum albumin nanoparticles was retained by addition of 3% trehalose. [19] It has been established that physical characteristics of freeze-dried polymeric nanoparticles such as poly(lactide-co-glycolide), poly(gamma-glutamic acid) and poly(D,L-lactic acid) have been preserved by the addition of excipients. [20-22] However, since the discovery of Mobile Crystalline Materials No. 41 (MCM-41) type MSNs in 1992 by Mobil scientists [23], no information has been reported on the freeze-drying of protein loaded MCM-41 type MSNs or the capacity of these formulations to elicit immunogenicity following reconstitution.

Here we report the successful freeze-drying of amino functionalised MCM-41 nanoparticles (AM-41) following the loading of the model antigen Ovalbumin (OVA). The OVA loaded AM-41 nanoparticles are termed as OVA-41. The OVA antigen was chosen for this study as we have observed degradation of OVA when stored at ambient temperature for periods as short as 16 h. We investigated the impact of the freeze-drying process and the effect of excipients trehalose and PEG8000 on the stability of OVA. The freeze-dried samples were stored at ambient temperature for

two months, following which the immunogenicity of the formulation was tested in mice. We have demonstrated the capacity of the freeze-dried OVA-41 nanoformulation to induce humoral and cell-mediated immune responses.

4.2 Materials and Methods

4.2.1 Materials

OVA Grade III, D-(+)-trehalose dihydrate, PEG8000, Bovine Serum Albumin (BSA) and PBS-T [PBS (1x), Tween-20 (0.1%)] were all obtained from Sigma-Aldrich (St. Louis, USA). PBS (137 mM NaCl 2.7mM KCl 10mM Phosphate buffer pH 7.2) was obtained from Amresco (Solon, USA). Dulbecco's Modified Eagle Medium (DMEM), antibiotic/antimycotic (containing penicillin G sodium, streptomycin sulphate, Fungizone) and Foetal Bovine Serum (FBS) were obtained from Life Technologies (Carlsbad, USA). ELISPOT^{PLUS} kit for the detection of the mouse Interferon (IFN)-γ by splenocytes was obtained from MabTech (Sweden).

4.2.2 Preparation of mesoporous silicate nanoparticles

The nanoparticles used in this investigation were unfunctionalised and amino functionalised MCM-41. The nanoparticles were prepared by co-condensation method as described previously. [11] To ensure maximum availability of the external surface area of the nanoparticles, the nanoparticle suspension was prepared in PBS. Nanoparticles (100 mg) and PBS (10 mL) were combined and ultrasonicated in a glass vial for 1 min at room temperature (RT) using probe (Hielscher UP100H, Teltow, Germany) set at 80% amplitude.

4.2.3 Trypan blue staining for in vitro cytotoxicity assay

Madin-Darby bovine kidney (MDBK) cells (ATCC) were seeded at 80-90% confluency onto glass coverslips in a 24 well plate and allowed to adhere overnight at 37°C, 5% CO_2. To investigate the effect of nanoparticle concentration on the cells a dilution range (0.5 mg/mL, 0.1 mg/mL and 0.01 mg/mL) of MCM-41 and AM-41 particles in Earle's Minimum Essential Media (containing 5% FBS) were prepared and gently added drop wise to the adherent cells. The cells and nanoparticles were incubated at 37°C, 5% CO_2 for 20 h. Media was carefully removed and the wells were gently washed three times with PBS to remove the nanoparticles. To determine the cell viability 0.2% trypan blue stain (Life Technologies) was added for 2 minutes. Trypan blue stain was carefully removed and the wells were washed once with PBS. Cells were fixed in 4% paraformaldehyde (PFA) pH 7.4 for 15 minutes, and then washed three times with PBS.

Coverslips were mounted with 5 µl of MOWIOL (Sigma). Cell viability was determined by imaging on a Zeiss HAL100 microscope under bright field.

4.2.4 OVA loaded AM-41 nanoparticles

Loading reaction consisted of 20 mg of AM-41 particles and OVA at 0.8 mg/mL in a 5 mL final volume of PBS at pH 7.0 as previously described (Mahony et al. 2013). This particle-protein slurry was placed in a shaker at 25°C for 240 min. A 200 µl sample of the particle-protein slurry was removed and centrifuged 16.2 *g* for 5 min. The amount of unbound OVA protein remaining in the supernatant was assessed by Biorad DC kit protein assay and visualised on SDS-PAGE gels.

4.2.5 Freeze-drying process

Following OVA loading, the sample was centrifuged at 16.2 *g* for 1 min and the supernatant was removed. The protein-nanoparticle (OVA-41) (4 mg OVA: 20 mg AM-41) pellet was freeze dried with different combinations of excipients: 1) OVA-41 alone, 2) OVA-41 + 20% trehalose, 3) OVA-41 + 1% PEG8000, 4) OVA-41 + 5% trehalose + 1% PEG8000. The final formulation was obtained by mixing the excipients to the nanoparticle-protein pellet at fixed concentration to make up the final volume to 1 mL. Samples were frozen in liquid nitrogen then placed in a Christ freeze-dryer (Model LPC-32, Martin Christ, Osterode AM Harz, Germany) at 24°C, 0.1 mbar for 17 h. Freeze-dried samples were stored in a vacuum desiccator at ambient temperature (23-27°C).

4.2.6 Desorption studies on the freeze-dried samples

Following 3 days of storage at ambient temperature, the freeze-dried samples were resuspended in 200 µL of PBS and centrifuged for 5 min at 16.2 *g* to remove the supernatant. Vaccinations were prepared by suspending the freeze-dried samples in 500 µL of saline. Hence, the nanoparticle pellet obtained was resuspended in 500 µL of pre-warmed PBS and incubated at 37°C for 120 min on a shaker at 200 rpm. The samples were centrifuged as above and the supernatant was assessed for desorbed protein by electrophoresis on SDS-PAGE gels.

4.2.7 Polyacryalamide gel electrophoresis (PAGE)

To prepare the particulate and the supernatant samples, particle slurry (20 µL) was taken and centrifuged at 16.2 *g* for 5 min. The supernatant and nanoparticle samples were resuspended in SRB (SDS Reducing Buffer consisting of 62.5 mM Tris-HCl (pH 6.8), 117 mM DTT, 10 % Glycerol, 2 % SDS, 0.02 % Bromophenol blue), incubated at 85 °C for 2 min then subjected to electrophoresis on 10 % Tris-Glycine gels (Invitrogen). The gels were visualised by staining in 50% methanol, 10%

acetic acid, 0.25% Coomassie Blue R250 for 30 minutes, followed by destaining in 30% methanol, 10% acetic acid with three 30 min washes.

4.2.8 Reconstitution, zeta-potential and transmission electron microscope (TEM) of lyophilised samples

Samples were reconstituted in 1 mL sterile PBS. The zeta-potential was measured on a Nanosizer Nano ZS analyser (Malvern Instruments, Worcestershire, UK) in PBS. The physical characteristics of the freeze-dried nanoparticles were observed using transmission electron microscopy (TEM) before and after freeze-drying.

4.2.9 Mouse immunisation studies

Animals – C57BL/6J mice were purchased from and housed in the Biological Resource Facility, The University of Queensland, Brisbane, Australia under specific pathogen-free conditions. Eight week old female mice were housed in HEPA-filtered cages with 4 animals per group in an environmentally controlled area with a cycle of 12 h of light and 12 h of darkness. Food and water were given *ad libitum*. All the animals were closely monitored throughout the study. All procedures involving animals were approved by the The University of Queensland Animal Ethics Committee.
Immunisation – Blood samples were collected by retro-orbital bleeds using heparin coated hematocrit tubes (Hirschmann Laborgeräte, Heilbronn, Germany).

Pre-immunisation blood samples collected prior to the first immunisation were referred to as the preimmune (PI) samples. OVA-41 reactions were prepared aseptically as described in the methods section 'OVA loaded AM-41 nanoparticles'. Quil-A (Superfos Biosector, Vedback, Denmark) was resuspended at 2 mg/ml in sterile injectable water (Pfizer**,** Brooklyn, USA). The 'wet test group' comprised of freshly prepared OVA-41 nanoformulation. The five groups used in the trial were: a positive control group (50 µg OVA+10 µg Quil-A), 'wet' and freeze-dried test groups (10 µg OVA, 150 µg AM-41), negative control groups comprising of (freeze-dried AM-41, 150 µg) and unimmunised group. The freeze-dried groups were stored at ambient temperature for 2 months prior to injection. The doses were prepared in 0.9% saline (Pfizer) and 100 µL was administered into the tail base by four subcutaneous injections using a sterile 27 gauge needle (Terumo, Tokyo, Japan). Four injections were administered at 2 week intervals and mice were sacrificed 14 days after the final immunisation.

4.2.10 Enzyme-Linked ImmunoSorbent Assay (ELISA)

ELISA was used to detect the OVA-specific antibody. Microtitre plates (96 well, Nunc, Maxisorb, Roskilde, Denmark) were coated overnight with OVA antigen (2 ng/µL, 50 µL) in PBS at 4 °C. To remove the coating solution, the plates were once washed with PBS-T. The plate was then blocked with 5% BSA and skim milk (5%, Fonterra, Auckland, New Zealand) in PBS (200 µL) for 1 h with gentle shaking at RT. To remove the block the plates were washed with PBS-T three times. The mouse sera samples were diluted in PBS (50 µL) from 1:100 to 1:6400, each dilution was added to the wells and the plate was incubated for 2 h at RT. To detect the mouse antibodies HRP conjugated polyclonal sheep anti-mouse IgG antibody (Chemicon Australia, Melbourne, VIC, Australia) diluted to 1:1000 in PBS was added to each well and incubated for 1 h at RT with gentle shaking. Plates were washed with PBS-T three times. To each well 100 µL of TMB substrate (Sigma-Aldrich) was added and the plate was incubated for 15 min at RT. To stop the chromogenic reaction 100 µL of 1N HCl was added to all the wells. At the end of the experiment the plates were read at 450nm on a Labsystems Multiskan RC plate scanner.

4.2.11 IFN-γ ELISPOT assays

After the final immunisation spleens from the mouse were aseptically removed following euthanasia and placed into ice cold DMEM media (5 mL) supplemented with 10% FBS, Hepes (20 mM, pH 7.3), sodium pyruvate (1 M), Glutamax (1 M), penicillin G (100 units/mL), streptomycin (100 µg/mL), Fungizone (0.25 µg/mL). The spleen samples were then gently disrupted and using a syringe plunger passed through a nylon mesh (100 µm, Becton Dickinson, Franklin Lakes, NJ). The splenocytes were washed with 5 ml of DMEM and centrifuged at 800 *g* for 5 min at 4 °C and then resuspended in lysis buffer (NH_4Cl (0.15 M), $KHCO_3$ (10 mM), Na_2-EDTA (0.1 mM), 1 mL) for 5 min at RT. The wash steps were repeated twice with DMEM (9 mL and 5 mL) each time. Cell pellets obtained at the end were resuspended in DMEM (2 mL) and the cell numbers were calculated by staining with trypan blue (0.2%). Cells from each mouse were seeded in triplicate at 1.0 – 1.5 x 10^5 cells/well into Polyvinylidene fluoride (PVDF) ELISPOT plates. In the presence or absence of synthetic OVA peptide (1 mg/mL, SIINFEKL, Auspep, Parkville, VIC, Australia) or the polyclonal activator concavalin A (Con A, 1 mg/mL, Sigma Aldrich) as a positive control the cells were were incubated in complete DMEM medium at 37 °C and 5% CO_2 for 40 h. IFN-γ ELISPOT (Mabtech) assay was performed following manufacturer's guide. The ELISPOT plates were read on an ELISPOT reader (Autoimmun Diagnostika, Strassburg, Germany).

4.2.12 Statistical Analysis

The unpaired two-tailed Student's *t*-test (Microsoft excel) was used for statistical comparisons of the number of spot forming units (SFU)/million cells for all the individual animals by as determined by the ELISPOT assay.

4.3 Results

4.3.1 Characteristics of MSN

The physical properties and atomic percentages of the MCM-41 and AM-41 nanoparticles were determined using TEM analysis, low angle powder X-ray diffraction (XRD), nitrogen adsorption isotherm and X-ray photoelectron spectra (XPS) analysis as described by Mahony et al. (2013). The pore size and diameter of the particles were calculated by Barrett-Emmett-Teller (BET) and Barrett-Joyner-Halenda (BJH) methodologies respectively. The measured and calculated properties of the particles are summarised in Table 4.1.

Table 4.1. Physical characteristics of MCM-41 and AM-41

Material	MCM-41	AM-41
Particle size (nm)	90	90
BET surface area ($m^2 g^{-1}$)	956.2	854.4
BJH Pore Diameter (nm)	3.6	3.7
Pore volume ($cm^3 g^{-1}$)	1.01	0.79
Atomic% as determined by XPS		
Si	24.79	22.12
O	65.58	60.15
C	9.63	14.55
N	0	3.17

4.3.2 In vitro cytotoxicity of MSN

The cytotoxicity of the MCM-41 and AM-41 nanoparticles was determined by trypan blue dye exclusion staining of MDBK cells treated with varying concentrations of nanoparticles. Dead cells exhibited a blue colour due to the uptake of the dye via permeabilised cell membranes whereas viable cells remain intact and do not take up the stain. Both MCM-41 and AM-41 nanoparticles had toxic effects at 0.5 mg/mL on the MDBK cells (Fig 4.2 c and f) after 20 h incubation. However, at

0.1 mg/mL concentration only the MCM-41 were slightly toxic (Fig 4.2 b). Cells exposed to MCM-41 at a lower concentration of 0.01 mg/mL (Fig 4.2 a) did not exhibit any overt signs of toxicity and appeared similar the control cells (Fig 4.2 g). The AM-41 particles on the other hand did not show any toxic effect on cell viability at either 0.01 mg/mL or 0.1 mg/mL (Fig 4.2 d and e). Based on these semi-quantitative cytotoxicity results all further experimental investigations were carried out using OVA-41.

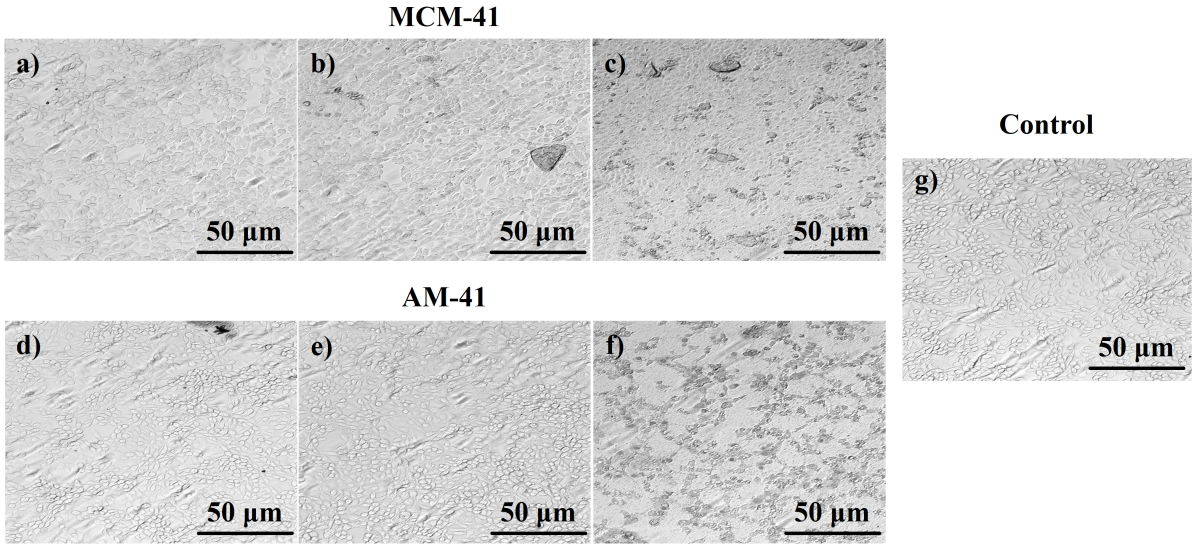

Fig 4.2. Cytotoxicity studies of nanoparticles using trypan blue Staining (0.2%) of MDBK cells; **(a)** 0.5 mg/mL MCM-41; **(b)** 0.1 mg/mL MCM-41; **(c)** 0.01 mg/mL MCM-41; **(d)** 0.5 mg/mL AM-41; **(e)** 0.1 mg/mL AM-41; **(f)** 0.01 mg/mL AM-41; **(g)** MDBK cells alone without nanoparticles.

4.3.3 Effect of excipients on in vitro stability of OVA -41 nanoparticles

The OVA protein was loaded onto the AM-41 nanoparticles at a concentration of 72 µg per mg of AM-41 particles as determined by protein assay. The loading isotherm reaction of protein to nanoparticle ratio was determined as 1:5; at this ratio complete binding of the OVA protein to the AM-41 nanoparticles was obtained as determined by SDS-PAGE analysis (Mahony et al., 2013). Excipients were added to OVA-41 nanoformulation and subjected to rapid freezing in liquid nitrogen and subsequently freeze-dried.

The physical appearance of the freeze-dried samples was assessed and recorded at the end of the process. The sample freeze-dried with 20% trehalose formed a flaky crystal-like structure on top of the freeze-dried cake (Fig 4.3 a, i). The formulation freeze-dried with 1% PEG8000 alone resulted in a dry white powder with an estimated shrinkage of 50% (Fig 4.3 a, ii). Lyophilisation with 5% trehalose and 1% PEG8000 resulted in a freeze-dried cake that did not collapse, maintained its structural integrity and appeared voluminous and snow-like without any shrinkage (Fig 4.3 a, iii).

The freeze-dried samples were reconstituted in PBS; the samples containing 5% trehalose and 1% PEG8000 and 1% PEG8000 alone dissolved readily within 30 seconds, but the sample containing 20% trehalose required additional measures such as gentle vortexing to facilitate solubilisation.

The stability of OVA contained in the freeze-dried OVA-41 was determined using SDS-PAGE analysis. The molecular weight of OVA is 45 kDa, seen as a doublet on PAGE (Fig 4.3 b. lane 1). Complete degradation of OVA protein was observed, when it was in the solution at the concentration of 0.8 mg/mL after 16 h of incubation at ambient temperature (Fig 4.3 b lane 2). OVA in the OVA-41 formulation remained stable when freeze-dried in the presence of the excipients (Fig 4.3 c lanes 3, 4 and 5), however, degradation of OVA occurred when it was freeze-dried without excipients (Fig 4.3 c lane 2). Distortion in the electrophoretic profile of OVA protein was observed in the samples containing PEG8000 as an excipient (Fig 4.3 c, lane 4 and 5).

To determine if the integrity of the OVA protein and its association with the AM-41 particles after the freeze-drying process, desorption studies were performed on reconstituted freeze-dried OVA-41 samples after storage for 3 days. Gel analysis on the supernatant showed no release of OVA (Fig 4.3 d lanes 1, 2 and 3). The protein remained associated to the nanoparticles post freeze-drying, storage and reconstitution (Fig 4.3 d lanes 4, 5 and 6). Furthermore, after desorption, the migration rate of the freeze-dried samples containing 1% PEG8000 was restored (Fig 4.3 c compare lanes 4, 5 to Fig 4.3 d lanes 5 and 6).

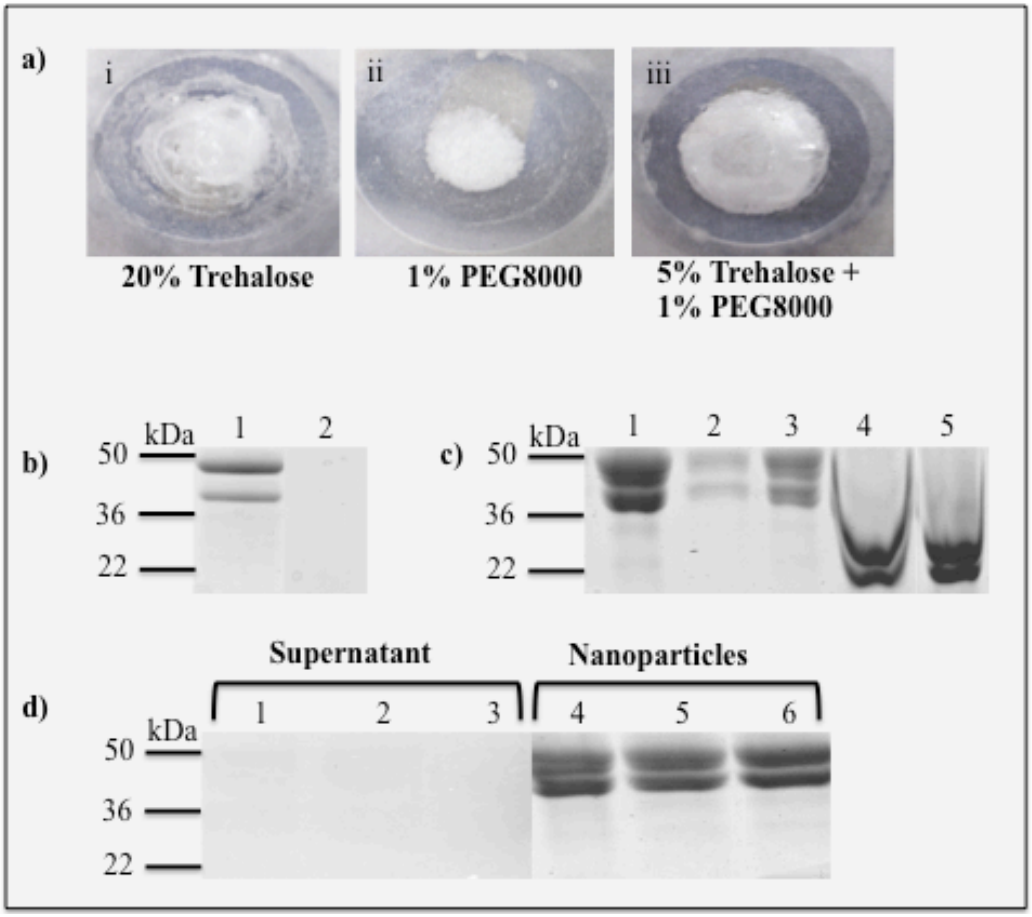

Fig 4.3. (a) Appearance of the freeze-dried OVA-41 formulation in the presence of different excipients, i: Freeze-dried OVA-41 with 20% Trehalose; ii: Freeze-dried OVA-41 with 1% PEG8000; and iii: Freeze-dried OVA-41 with 5% trehalose and 1% PEG8000. **(b)** Evaluation of OVA protein after 16 h storage by SDS-PAGE, lane 1: OVA protein at 4°C; lane 2: Degraded OVA protein at ambient temperature. **(c)** Evaluation of Freeze-dried OVA-41 nanoformulations, lane 1: 'wet' OVA-41; lane 2: Freeze-dried OVA-41 without excipients; lane 3: Freeze-dried OVA-41 with 20% trehalose; lane 4: Freeze-dried OVA-41 with 1% PEG8000; lane 5: Freeze-dried OVA-41 with 5% trehalose and 1% PEG8000. **(d)** Desorption studies of the freeze-dried OVA-41. Lanes 1-3: Supernatants; lane 1: Freeze-dried OVA-41 with 20% trehalose; lane 2: Freeze-dried OVA-41 with 1% PEG8000; lane 3: Freeze-dried OVA-41 with 5% trehalose and 1% PEG8000. Lanes 4-6: Nanoparticles; lane 4: Freeze-dried OVA-41 with 20% trehalose; lane 5: Freeze-dried OVA-41 with 1% PEG8000; lane 6: Freeze-dried OVA-41 with 5% trehalose and 1% PEG8000.

Zeta potential measurement for OVA-41 before and after the addition of 5% trehalose and 1% PEG8000 was also determined. The 'wet' OVA-41 formulation had a charge of +13.9 mV whereas the addition of excipients changed the zeta potential to -1 mV. The final zeta potential of the freeze-dried particles after 2 months of storage was found to be -3.34 mV at pH 7.0.

As observed by TEM, nanoparticles were found to be homogenously distributed and maintained their spherical shape and size following freeze-drying (Fig 4.4). The net-like structure formed over the surface of the nanoparticles might have been due to the presence of trehalose in the formulation.

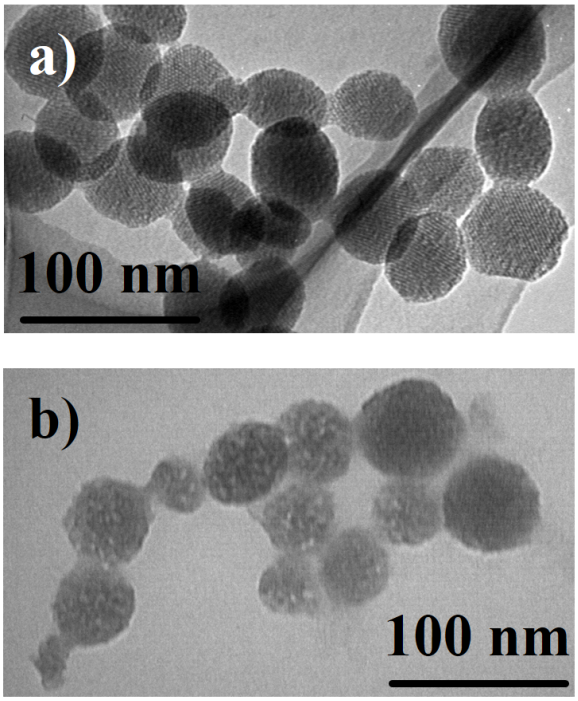

Fig 4.4. Morphology of AM-41 nanoparticles visualized by transmission electron microscope (TEM), **(a)** AM-41 particles before lyophilisation **(b)** OVA-41 particles after lyophilisation matrix formation in the presence of 5% trehalose and 1% PEG8000.

4.3.4 In vivo responses to 'wet' and freeze-dried OVA-41

The IgG responses of the immunised mice were analysed by anti-OVA-specific ELISA assays after four subcutaneous injections. The antibody responses to immunisation of mice with the 'wet' and the freeze-dried OVA-41 formulation were compared. The ELISA results (Fig 4.5) from the terminal bleeds suggest that the positive control group (50 µg OVA+10 µg Quil-A) showed an excellent antibody titre up to a dilution of 1:6400 with an average OD_{450nm} of 0.8 (Fig 4.5 a). Though the mice injected with freeze-dried OVA-41 and 'wet' OVA-41 (10 µg OVA/150 µg nanoparticles) showed a lower response compared to the positive control, both groups were similar in their antibody response up to the 1:6400 dilution (Fig 4.5 b and c). Even though, the positive control group induced excellent antibody response, variation in the response between the four animals was observed. However, the four mice receiving freeze-dried OVA-41 showed less mouse to mouse variation (Fig 4.5 b). The negative control group receiving freeze-dried AM-41 nanoparticles with excipients showed no specific antibody response to OVA protein (Fig 4.5 d), which was similar to the unimmunised mice group. In addition, administration of freeze-dried

OVA-41 had no visible toxic effects on the mice, as the mice remained in the normal weight range throughout the trial period (data not shown).

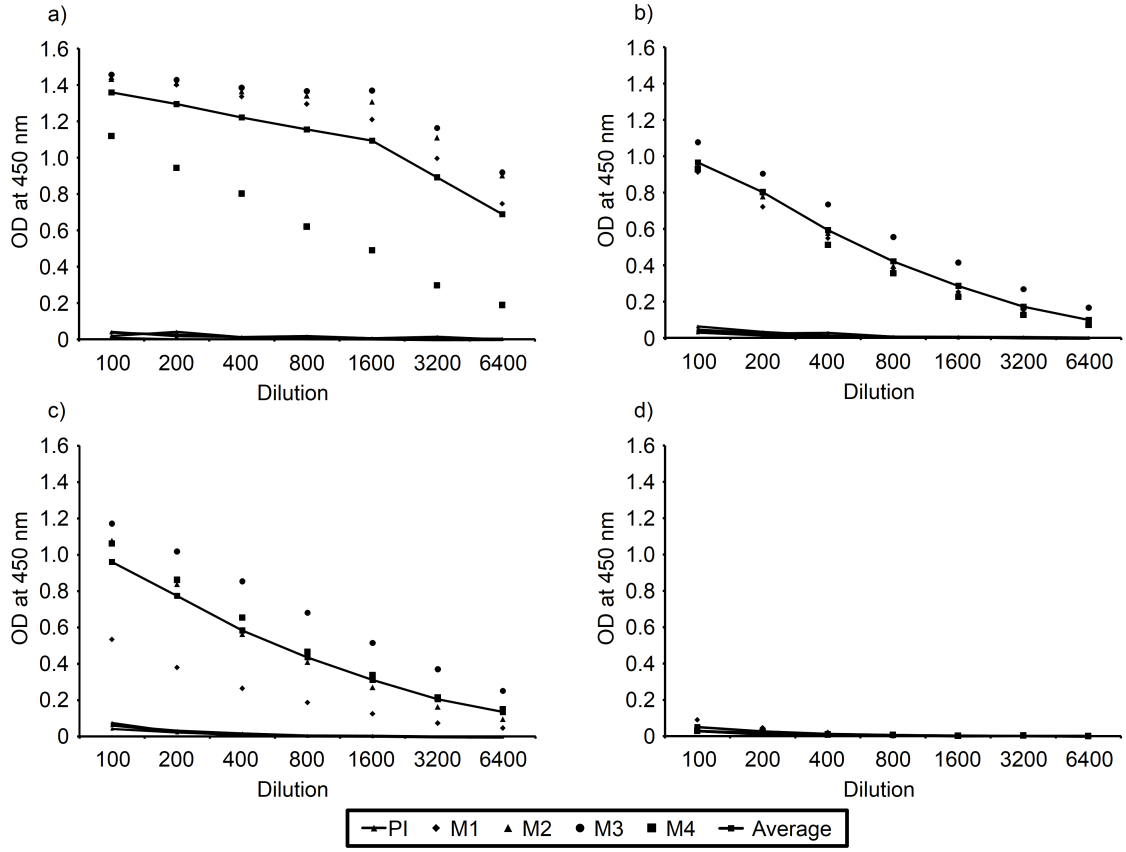

Fig 4.5. ELISA data of terminal sera bleeds of all 4 individual mice in each group. M1 to M4 are the individual mice in each group. All the mice were administered 100 µL dose at 2 week intervals to the tail base with **a)** OVA (50 µg) plus Quil-A (10 µg), **b)** 'wet' OVA (10 µg) loaded AM-41 (150 µg) nanoparticles, **c)** Freeze-dried OVA (10 µg) loaded AM-41 (150 µg) nanoparticles **d)** Freeze-dried AM-41 (150 µg). Sera of individual animals were diluted from 1:100 to 1:6400.

The cell-mediated response of mice immunised with the OVA-41 formulation was investigated using ELISPOT assay. To determine the Th1 cell-mediated immune response, two weeks after the final immunisation spleens from sacrificed mice were collected and harvested to obtain splenocyte cell populations. Splenocytes were used to determine T-cell IFN-γ response to OVA peptide. The mice from the positive control group, OVA plus Quil-A, showed high cell-mediated immune responses to OVA epitope. The 'wet' and the freeze-dried OVA-41 groups showed similar IFN-γ response. The result from the ELISPOT assay indicates that the freeze-dried OVA-41 did not have an adverse effect on the IFN-γ detected responses. Even though, the mice in the freeze-dried AM-41 and the unimmunised negative control groups produced some background IFN-γ response, the

response was not specific to the OVA antigen, as the response elicited with no antigen and OVA antigen looked similar (Fig 4.6).

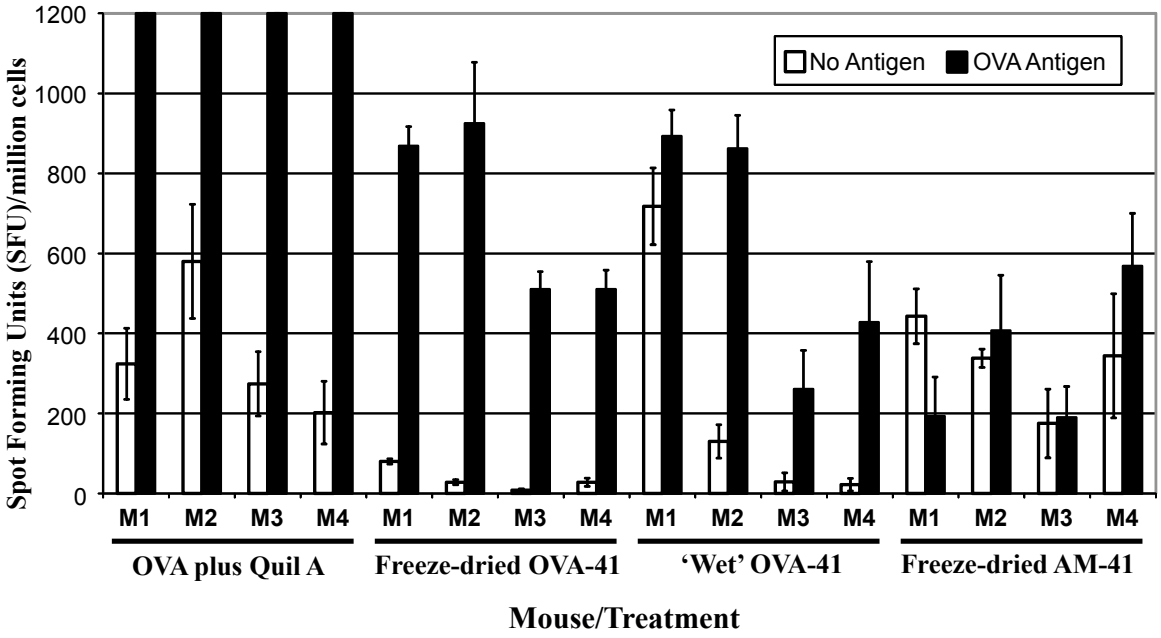

Fig 4.6. Detection of antigen specific IFN-γ secretion by ELISPOT assay of murine splenocytes from immunised mice. M1 to M4 are the individual mice in each group. The black bars in the figure indicate the spot forming units (SFU) producing IFN-γ in response to the OVA peptide, SIINFEKL (1 μg/mL).

4.4 Discussion

In this proof-of-concept study, we have developed a freeze-dried nanoparticle-based delivery system, to demonstrate the ability of MSNs as adjuvants and the improved stability of the vaccine formulation. This study confirms a previous study which demonstrated the nanoparticles can act as immune-potentiators in the absence of conventional adjuvants, such as Quil-A, in vaccine formulations (Mahony et al., 2013). The results of the study presented in this report extend these findings by demonstrating the combination of nanoparticle delivery and freeze-drying provides the basis for a highly effective vaccine delivery strategy. Freeze-drying process has proved an effective strategy for enhancing the stability of the vaccines. [24] Freeze-dried vaccines offers several advantages such as prolonged shelf-life, improved storage and ease of shipping to the end user.[25]

Nanoparticle based delivery systems can increase the delivery of the proteins to antigen presenting cells and act as nanocarriers as well as adjuvants in nanoparticle based vaccine formulations. [2, 26] Availability of different liquid crystal mesophases and surfactant assemblies makes the synthesis of

MSNs with controlled size, shape and structure easy [27], these characteristics of MSNs makes them highly attractive as delivery vehicles for proteins.

Guo et al. (2012) highlighted the capacity of hollow mesoporous silica nanoparticles (HMSNs) as antigen delivery vehicles for porcine circovirus type-2 ORF2 protein, as the HMSN/protein complex was able to elicit immune response in mice. The slow release of antigens from silica nanoparticles could be due to the highly stable and rigid framework of the porous silica forming a barrier to prevent the degradation of the antigen in the stomach and digestive tract as demonstrated by Slowing et al., (2008). The present study not only confirmed the promising nature of these materials for use in vaccines but also extended it by utilizing OVA loaded AM-41 nanoparticles in the freeze-dried formulations to elicit *in vivo* immune response after storage at ambient temperature.

The first step in the current investigation was to select the MSN with minimal cytotoxicity. Previous *in vitro* studies on cytotoxicity of the amorphous silica nanoparticles have shown that although they are believed to be non-toxic and are used in several biomedical applications, cytotoxicity is dependent on the concentration and size of the particles. [28, 29] Di Pasqua et al. (2008) using human neuroblastoma cells demonstrated that amino functionalised MCM-41 and solid sphere silica nanoparticles were less toxic compared to the pure MCM-41. The results of the current study also support the functionalisation of nanomaterials as a way of reducing *in vitro* cytotoxicity of nanomaterials (Fig 4.2). Future elucidation of the mechanisms of this phenomenon could be useful in understanding and documenting the *in vivo* safety of these novel nanomaterial based vaccination studies. In addition, previous research has shown that some cellular damage *in vivo* can be beneficial for generating strong immune responses. [30] However, a balance needs to be attained to ensure that over stimulation of the immune system does not negate the positive effects of vaccination.

It is critical to characterise and establish the optimal freeze-drying process for each nanovaccine formulation. The biological activity of DNA loaded on to cationic silica nanoparticles was restored when freeze-dried with either 5% trehalose or 10% glycerol as excipient. [31] While freeze-drying of the hepatitis B surface antigen adsorbed to chitosan-based nanoparticles with 2.5% glucose helped preserve the characteristics of the antigen for up to 3 months of storage at 4°C. [32]

In the current study, the combination of 5% trehalose and 1% PEG8000 as excipient was found to be the most suitable for freeze-drying OVA-41 formulations. The PEG8000 it is postulated to have

acted as the cryoprotectant and trehalose as the lyoprotectant. In this two-component excipient system the PEG protects from freezing stress while sugar protects from drying stress. [33, 34] The OVA-41 freeze-dried with 5% trehalose and 1% PEG8000 in combination, resulted in rapid reconstitution of the freeze-dried sample within 30 seconds. *In vitro* desorption studies on the freeze-dried OVA-41 stored at ambient temperature for three days showed that protein once bound did not easily dissociate from the particles (Fig 4.3 d).

Previously in our lab desorption studies have been conducted at different time points ranging from 5 min to overnight on OVA-41. However, protein only desorbed during the first 5 to 30 min, and no desorption was observed at later time points (Mahony et al., 2013). Even though, the OVA protein did not desorb *in vitro* in PBS at pH 7.0, when the reconstituted freeze-dried formulation was injected in the mice it elicited both humoral and cell-mediated immune responses, indicating that the protein may desorb from the nanoparticles *in vivo*. An alternative hypothesis would be that degradation of the nanoparticles *in vivo* results in additional and/or sustained release of OVA leading to immune stimulation. Further experimentation is required to fully elucidate the mode of action of these findings.

The aberrant migration rate of OVA-41 in Fig 4.3 c lanes 4 and 5 may have been caused by PEG8000 in the freeze-dried samples distorting the electrical flow within the gel. [35] Addition of excipients often changes the zeta-potential of the nanoformulations, the positive zeta potential measurements of cationic silica decreased significantly when lyoprotectants like trehalose, glucose, mannitol sorbitol and glycerol were added at a higher concentration (up to 20%) at pH 4.0. [31] Difference in the zeta potential measurements of the OVA-41 particles was observed before and after the addition of excipients at pH 7.0.

The potential of nanoformulations to induce antigen specific immune responses depends on various factors such as the architecture of the particle and protein, particle binding capacity, the uptake of the particle protein complex by antigen presenting cells and the release profile of the protein from the particle. [14] In the current study the OVA-41 formulation was stored for two months prior to reconstitution and immunisation of mice. We administered the vaccine subcutaneously as our hypothesis was that the nanovaccine would get adsorbed more slowly from the site of injection creating a depot effect and potentiating immune response. Following immunisation no local adverse reactions at the injection site were evident. In addition, administration of the stored freeze-dried

OVA-41 had no detectable toxic effects on the mice, as the mice remained in the normal weight range throughout the trial period.

Mahony et al., (2013) conducted histopathology studies of heart, lung, liver, spleen, kidney, lymph nodes (local and peripheral) and the injection site area (including skin and under- lying tissue) of mice injected with OVA loaded AM-41, no morphological changes could be detected between all organs derived from animals in the unimmunized control group compared to the treatment groups receiving the nanovaccine for the duration of the study. While these observations are qualitative in nature they do support the *in vivo* safety of MSN materials, as previously reported by Mahony et al. (2013).

For comparative purposes a treatment group was immunised with OVA plus Quil-A, a conventional immunopotentiating adjuvant with the capacity to induce both cell mediated and humoral immunity *in vivo*. [36, 37] We used Quil-A in our study, as it is one of the most widely used adjuvant in mice immunisation studies. [38, 39] The positive control group were immunised with 50 μg OVA plus 10 μg Quil-A to ensure that the mice had a robust and measurable immune responses to OVA. As expected strong immune responses were detected in this treatment group (Fig 4.5a). A possible limitation of the AM-41 particles was the amount of OVA that could be loaded to the material, as it was limited to 72 μg of protein per mg of nanoparticles. To reduce the likelihood of adverse effects in mice receiving OVA-41 formulations, a maximum of 150 μg of nanoparticles per injection was used, which limited the OVA to 10 μg per dose. As a result of this limitation, mice immunised with the 'wet' and freeze-dried nanoformulations received almost five times less of OVA protein compared to the positive control group (50 μg of OVA per dose). Despite this dramatic reduction in dose, strong antibody and cell-mediated response were detected in the mice immunised with OVA-41 formulations. These results indicated that the AM-41 nanoparticles have the capacity to stimulate strong immune responses with reduced levels of antigen. Further experimentation needs to be conducted to test higher concentration of antigen by improving the loading capacity of the nanoparticles.

4.5 Conclusion

We have presented a successful strategy for the freeze-drying of OVA loaded AM-41 nanoparticles utilising 5% trehalose and 1% PEG8000 as excipients. The freeze-dried formulation increased the ambient stability of this model antigen for at least two months. Once reconstituted and injected

subcutaneously into mice the freeze-dried OVA-41 elicited humoral and cell mediated responses. These findings demonstrate the potential effectiveness of freeze-dried AM-41 nanoparticles as carriers for improving the stability of vaccines.

4.6 Acknowledgements

This work was funded by the Queensland Government through its Department of Employment, Economic Development and Innovation Reinvestment Fund. The authors thank Dr. Qiuhong Hu for performing the TEM studies, Prof Rajiv Khanna and Dr Corey Smith for the use of the ELISPOT reader system at The Queensland Institute of Medical Research.

4.7 References

1. Mahony D, Cavallaro AS, Stahr F, Mahony TJ, Qiao SZ, et al. (2013) Mesoporous Silica Nanoparticles Act as a Self-Adjuvant for Ovalbumin Model Antigen in Mice. Small 9: 3138-3146.
2. Koping-Hoggard M, Sanchez A, Alonso MJ (2005) Nanoparticles as carriers for nasal vaccine delivery. Expert Rev Vaccines 4: 185-196.
3. de la Fuente M, Csaba N, Garcia-Fuentes M, Alonso MJ (2008) Nanoparticles as protein and gene carriers to mucosal surfaces. Nanomedicine (Lond) 3: 845-857.
4. Lee HJ (2002) Protein drug oral delivery: the recent progress. Archives of pharmacal research 25: 572-584.
5. Mody K, Mahony D, Mahony TJ, Mitter N (2012) Freeze-drying of protein loaded nanoparticles for vaccine delivery. Drug Deliv Lett 2: 83-91.
6. Kammer AR, Amacker M, Rasi S, Westerfeld N, Gremion C, et al. (2007) A new and versatile virosomal antigen delivery system to induce cellular and humoral immune responses. Vaccine 25: 7065-7074.
7. Giri S, Trewyn BG, Stellmaker MP, Lin VSY (2005) Stimuli-Responsive Controlled-Release Delivery System Based on Mesoporous Silica Nanorods Capped with Magnetic Nanoparticles. Angew Chem Int Ed 44: 5038-5044.
8. Trewyn BG, Nieweg JA, Zhao Y, Lin VSY (2008) Biocompatible mesoporous silica nanoparticles with different morphologies for animal cell membrane penetration. Chemical Engineering Journal 137: 23-29.
9. Carvalho LV, Ruiz Rde C, Scaramuzzi K, Marengo EB, Matos JR, et al. (2010) Immunological parameters related to the adjuvant effect of the ordered mesoporous silica SBA-15. Vaccine 28: 7829-7836.
10. Wendorf J, Singh M, Chesko J, Kazzaz J, Soewanan E, et al. (2006) A practical approach to the use of nanoparticles for vaccine delivery. J Pharm Sci 95: 2738-2750.
11. Mercuri LP, Carvalho LV, Lima FA, Quayle C, Fantini MC, et al. (2006) Ordered mesoporous silica SBA-15: a new effective adjuvant to induce antibody response. Small (Weinheim an der Bergstrasse, Germany) 2: 254-256.
12. Guo HC, Feng XM, Sun SQ, Wei YQ, Sun DH, et al. (2012) Immunization of mice by Hollow Mesoporous Silica Nanoparticles as carriers of Porcine Circovirus Type 2 ORF2 Protein. Virology Journal 9: 108.

13. Mody KT, Popat A, Mahony D, Cavallaro AS, Yu C, et al. (2013) Mesoporous silica nanoparticles as antigen carriers and adjuvants for vaccine delivery. Nanoscale: 5167-5179.
14. Abdelwahed W, Degobert G, Stainmesse S, Fessi H (2006) Freeze-drying of nanoparticles: formulation, process and storage considerations. Adv Drug Deliv Rev 58: 1688-1713.
15. Hsu CC, Nguyen HM, Yeung DA, Brooks DA, Koe GS, et al. (1995) Surface denaturation at solid-void interface--a possible pathway by which opalescent particulates form during the storage of lyophilized tissue-type plasminogen activator at high temperatures. Pharm Res 12: 69-77.
16. Baheti A, Kumar L, Bansal AK (2010) Excipients used in lyophilization of small molecules. J Excipients and Food Chem 1.
17. Wei W (2000) Lyophilization and development of solid protein pharmaceuticals. International Journal of Pharmaceutics 203: 1-60.
18. Anhorn MG, Mahler HC, Langer K (2008) Freeze drying of human serum albumin (HSA) nanoparticles with different excipients. Int J Pharm 363: 162-169.
19. Layre AM, Couvreur P, Richard J, Requier D, Eddine Ghermani N, et al. (2006) Freeze-drying of composite core-shell nanoparticles. Drug Dev Ind Pharm 32: 839-846.
20. Morris GA, Castile J, Smith A, Adams GG, Harding SE (2011) The effect of prolonged storage at different temperatures on the particle size distribution of tripolyphosphate (TPP) - chitosan nanoparticles. Carbohydrate Polymers 84: 1430-1434.
21. Quintanar-Guerrero D, Ganem-Quintanar A, Allemann E, Fessi H, Doelker E (1998) Influence of the stabilizer coating layer on the purification and freeze-drying of poly(D,L-lactic acid) nanoparticles prepared by an emulsion-diffusion technique. J Microencapsul 15: 107-119.
22. Kresge CT, Leonowicz ME, Roth WJ, Vartuli JC, Beck JS (1992) Ordered mesoporous molecular sieves synthesized by a liquid-crystal template mechanism. Nature 359: 710-712.
23. Adams GD (2003) Lyophilization of Vaccines. In: Robinson A, Hudson MJ, Cranage MP, editors. Vaccine Protocols. Totowa, NJ: Humana Press. pp. 223-243.
24. Etzl EE, Winter G, Engert J (2013) Toward intradermal vaccination: preparation of powder formulations by collapse freeze-drying. Pharmaceutical Development and Technology 0: 1-10.
25. Panyam J, Labhasetwar V (2003) Biodegradable nanoparticles for drug and gene delivery to cells and tissue. Adv Drug Deliv Rev 55: 329-347.
26. Wu S-H, Mou C-Y, Lin H-P (2013) Synthesis of mesoporous silica nanoparticles. Chemical Society Reviews 42: 3862-3875.

27. Uboldi C, Giudetti G, Broggi F, Gilliland D, Ponti J, et al. (2012) Amorphous silica nanoparticles do not induce cytotoxicity, cell transformation or genotoxicity in Balb/3T3 mouse fibroblasts. Mutat Res 745: 11-20.
28. Lin W, Huang Y-w, Zhou X-D, Ma Y (2006) In vitro toxicity of silica nanoparticles in human lung cancer cells. Toxicology and Applied Pharmacology 217: 252-259.
29. Tsang C, Babiuk S, van Drunen Littel-van den Hurk S, Babiuk LA, Griebel P (2006) A single DNA immunization in combination with electroporation prolongs the primary immune response and maintains immune memory for six months. Vaccine 25: 5485-5494.
30. Sameti M, Bohr G, Ravi Kumar MN, Kneuer C, Bakowsky U, et al. (2003) Stabilisation by freeze-drying of cationically modified silica nanoparticles for gene delivery. Int J Pharm 266: 51-60.
31. Prego C, Paolicelli P, Diaz B, Vicente S, Sanchez A, et al. (2010) Chitosan-based nanoparticles for improving immunization against hepatitis B infection. Vaccine 28: 2607-2614.
32. Carpenter JF, Prestrelski SJ, Arakawa T (1993) Separation of freezing- and drying-induced denaturation of lyophilized proteins using stress-specific stabilization. I. Enzyme activity and calorimetric studies. Arch Biochem Biophys 303: 456-464.
33. Prestrelski SJ, Arakawa T, Carpenter JF (1993) Separation of Freezing- and Drying-Induced Denaturation of Lyophilized Proteins Using Stress-Specific Stabilization: II. Structural Studies Using Infrared Spectroscopy. Archives of Biochemistry and Biophysics 303: 465-473.
34. Zheng CY, Ma G, Su Z (2007) Native PAGE eliminates the problem of PEG–SDS interaction in SDS-PAGE and provides an alternative to HPLC in characterization of protein PEGylation. Electrophoresis 28: 2801-2807.
35. Gordon S, Teichmann E, Young K, Finnie K, Rades T, et al. (2010) In vitro and in vivo investigation of thermosensitive chitosan hydrogels containing silica nanoparticles for vaccine delivery. European Journal of Pharmaceutical Sciences 41: 360-368.
36. Gordon S, Young K, Wilson R, Rizwan S, Kemp R, et al. (2011) Chitosan hydrogels containing liposomes and cubosomes as particulate sustained release vaccine delivery systems. Journal of Liposome Research.
37. Ahmed FK, Clark BE, Burton DR, Pantophlet R (2012) An engineered mutant of HIV-1 gp120 formulated with adjuvant Quil A promotes elicitation of antibody responses overlapping the CD4-binding site. Vaccine 30: 922-930.
38. Sun H-X, Xie Y, Ye Y-P (2009) Advances in saponin-based adjuvants. Vaccine 27: 1787-1796.

5.

Immunisation of sheep with Bovine Viral Diarrhoea Virus, E2 protein using a Freeze-dried Hollow Silica Mesoporous Nanoparticle Formulation

---

The capacity of amino functionalised hollow type mesoporous silica nanoparticles (HMSA) loaded with BVDV-1 *Escherichia coli*-expressed optimised E2 (oE2) protein to induce immunogenicity before and after freeze-drying was investigated in this chapter. oE2/HMSA nanovaccine, which was freeze-dried using trehalose and 1% glycine as excipients, was tested *in vivo* by Dr. Donna Mahony

and myself to determine the vaccines capacity to induced both antibody and cell-mediated immune responses in sheep. In addition, the integrity of E2 protein was preserved in the FD nanovaccine even after 14 months of storage at ambient temperature. This study was the first to demonstrate that silica nanoparticles can act as an efficient antigen carriers and adjuvants in a production animal. The following manuscript is submitted to PLoS ONE.

5.1 Introduction

BVDV-1 infection occurs in the target species of cattle and sheep herds worldwide and therefore remains of economic importance. BVDVs are a group of positive sense, single-stranded RNA viruses classified in the *Pestivirus* genus within the Flaviviradae family. [1] The BVDV-1 genome is transcribed as a single, large (~12.3 kb) open reading frame which is translated into a single polyprotein, and processed into individual viral proteins by viral and cellular proteases. [2]
Currently there is no commercially available recombinant subunit vaccine for BVDV-1, only modified live or inactivated vaccines. The E2 membrane glycoprotein has been shown to be the major immunogenic protein of BVDV-1 [2] and is the viral antigen that is efficiently recognised by the immune system. [3] Therefore E2 has been the focus as a potential candidate for the development of a subunit BVDV-1 vaccine in a number of studies. [4-8]

Subunit vaccines often require the addition of an adjuvant which potentiates the immune response to the protein antigen in the vaccinated host. The role of mesoporous silica nanoparticles (MSNs) as an antigen carrier and adjuvant has been recently been reviewed. [9,10] MSNs are proving to be a valuable alternative to conventional adjuvants such as aluminium hydroxide (or alum) which can have adverse effects at the injection site when administered subcutaneously or intradermally. [11] Various types of silica nanoparticles have been used to deliver antigens in immunisation studies that have induced both humoral and cell-mediated immune responses. [12-16]. Injection of MSNs showed no local reactions at the injection site both at a gross and histopathological level and they are well tolerated in the mammalian system. [16-18]

Recently we have demonstrated that E2 delivered by amino functionalised hollow mesoporous silica nanoparticles generated balanced immune responses in mice with both antibody and cell-mediated immunity.[17] Here, we expand on our previous work by developing a freeze-dried process for E2 adsorbed hollow type MSN with surface amino functionalisation (HMSA) and compare the immunogenicity of the non-freeze dried and freeze-dried nanoformulations in sheep.

To the best of our knowledge this is the first time that silica based nanoparticles have been used in a large animal model. Immunisation of sheep with the E2 nanovaccine did not show any adverse effects on animal health and produced both humoral and cell-mediated immune responses. Importantly, the long-term cell-mediated immune responses were detectable up to five months after immunisation and were higher in the sheep immunised with the freeze-dried E2 nanovaccine formulation.

5.2 Material and Methods

5.2.1 Preparation of amino functionalised hollow mesoporous silica nanoparticles (HMSA)

The nanoparticles used in this study were hollow mesoporous silica nanoparticles with amino groups added to the particle surface. The synthesis method of the HMSA nanoparticles used in this study has been described previously. [17] To obtain a monodisperse suspension, nanoparticles (100 mg) were dispersed in PBS (10 mL) and ultrasonicated in a glass vial for 1 min at ambient temperature (25°C) using a 5mm probe sonicator (Hielscher UP100H, Teltow, Germany) at 60% amplitude.

5.2.2 Adsorption of oE2 to HMSA for freeze-drying

An *Escherchia coli* codon-optimised, truncated version of E2 (which lacks the membrane binding domain of native BVDV E2) was expressed, purified, endotoxin-treated and then solubilised as described previously for oE2 protein. [19]

Suspensions of HMSA (10 mg/mL in 50 mM Tris (pH7.0), 0.2% Igepal CA630, (Sigma Aldrich, St. Louis, USA) were prepared as described above. Adsorption of oE2 protein on HMSA were performed at 25°C using 200 μg of oE2 and 2 mg HMSA (10 mg/ mL) in 50 mM Tris, 0.2% Igepal CA630 buffer (pH7.0) at 200 rpm for 22 h. A 200 μL sample of the particle-protein slurry was removed and centrifuged (16.2 g, 1 min). The amount of oE2 protein remaining in the adsorption supernatants were visualised by gel electrophoresis and quantified using a microtitre plate format protein assay kit (Biorad DC kit, Hercules, USA) following the manufacturer's instructions.

5.2.3 Freeze-drying process

Following oE2 adsorption to the HMSA particles, the samples were centrifuged at 4500 *g* for 5 min and the supernatants were removed. Different combinations and concentrations of excipients were added to the oE2/HMSA pellets prior to freeze-drying and the final volume adjusted to 1 mL. Samples were frozen in liquid nitrogen then placed in a freeze-dryer (Martin Christ Model LPC-32,

Osterode AM Harz, Germany) at 24°C, 0.11 mbar for 20 hr for the primary drying step. The secondary drying step was at 24°C, 0.01 mbar for 2 hr. Freeze-dried samples were stored in a vacuum desiccator at ambient temperature.

5.2.4 Reconstitution and transmission electron microscope (TEM) of lyophilised samples

Samples were reconstituted in 1 mL sterile PBS. The physical characteristics of the freeze-dried nanoparticles were observed using transmission electron microscopy (TEM) before and after freeze-drying.

5.2.5 SDS-PAGE Electrophoresis

SDS-PAGE analysis was performed using XCell *SureLock*® Mini-Cell precast system (Invitrogen, Carlsbad, USA) with NuPAGE 10% BIS-Tris gels according to manufacturer instructions. Size estimations were determined against SeeBlue® Plus2 (Invitrogen) pre-stained molecular weight standards. The resolved proteins were visualised by staining in 50% methanol, 10% acetic acid, 0.25% Coomassie Blue R250 for 30 min, followed by destaining in 30% methanol, 10% acetic acid for 10 min three times.

5.2.6 Screening of sheep to determine BVDV status

Forty sheep were purchased from Mungindi on the border between Queensland and New South Wales, Australia. All the procedures involving the animals were approved by The Department of Agriculture, Fisheries and Forestry Animal Ethics Committee. Ethics approval number SA 2011/05/358. The sheep were housed in 3 x 3 m pens with 4 animals per pen (in accordance with the Animal Ethics guidelines) for the first 3 months of the study and then the sheep were put out to pasture for the remaining 4 months of the study.

Since BVDV-1 is endemic in many sheep herds it was essential to screen the animals to determine whether they were currently infected or had been previously infected with BVDV-1 to determine their suitability for inclusion in the study.

The sheep (n = 40) were screened for BVDV-1 infection status using quantitative real time PCR as described previously. [20] The sheep were also screened for the presence of BVDV IgG antibodies using an E2-specific ELISA (described below). Sera samples from the sheep were diluted from 1:100 to 1:6400 for the ELISA assays. The ELISA results showed that 23 out of the 40 had an absorbance reading of less than 0.1 at 690 nm (data not shown) at 10^2 dilution of the sera samples.

This showed there was a no response to E2 and therefore these animals were designated BVDV negative. The other 17 animals had a range of absorbance readings from >0.1 to 0.4 at 10^2 dilution of the sera samples. For the immunisation trial 16 animals with no E2 ELISA response were randomly assigned into 4 groups (4 sheep per group).
The sheep were closely monitored throughout the study and weighed routinely to monitor changes in health. All the animals remained in good health for the duration of the 7 month study with no visible deleterious health effects. The average weight range of the sheep at start of trial was 37 kg and at the end of the trial was 49 kg.

5.2.7 Immunisation of sheep

Four animals were allocated into each of the four treatment groups (Table 5.1). oE2 protein adsorption to HMSA was performed within 24 hr of animal immunisation.

Injection doses of the E2 nanovaccine were prepared by isotherm adsorption reactions. 80 µg oE2 binds per mg to The oE2/HMSA adsorption reactions were prepared aseptically using 500 µg oE2 protein and 6.2 mg HMSA (10 mg/mL) in sterile 50 mM Tris, 0.2% Igepal CA630 buffer (pH 7.0) in a total volume of 5 mL at 25 °C, 200 rpm for 22 hr. Following adsorption the particles were centrifuged at 4500 *g* for 5 mins and the supernatant was removed.

Freeze-dried oE2/HMSA nanoformulation included 5% trehalose and 1% glycine. Samples were frozen in liquid nitrogen then freeze-dried as described above. Freeze-dried samples were stored in a vacuum desiccator at ambient temperature (25^oC) before use.

Quil-A (2 mg/mL, Superfos Biosector, Vedback, Denmark) was resuspended in sterile injectable water (Pfizer). The doses were resuspended in 1 mL injectable saline (0.9%) and administered by subcutaneous injection at the base of the ear using a sterile 23 gauge needle. Three injections were administered at three week intervals. The injection doses (Table 5.1) administered were oE2 plus Quil-A (500 µg oE2 and 1 mg Quil-A), non-freeze-dried oE2-HMSA (500 µg/6.2 mg HMSA), freeze-dried oE2-HMSA (500 µg/6.2 mg HMSA) and HMSA (6.2 mg).

Pre-immune (PI) blood samples were collected prior to immunisation and subsequent samples were collected at two-week intervals following each injection and then at monthly intervals for 5 months after the final injection. Blood samples were collected via jugular vein collection using 20 gauge needle into lithium-heparin vacutainer tubes (Becton Dickinson, New Jersey, USA).

Table 5.1. The immunisation groups in the sheep study.

Treatment Group	Group Description	Injected dose (1 ml)
1	oE2	500 µg oE2 plus 1 mg Quil-A
2	oE2/HMSA	500 µg oE2/6.2 mg HMSA
3	Freeze-dried	500 µg oE2/6.2 mg HMSA
4	HMSA only	6.2 mg HMSA

5.2.8 E2-specific ELISA

ELISAs for the detection of oE2-specific antibodies were performed by coating microtitre plates (Nunc Maxisorb, Roskilde, Denmark) with 50 µL oE2 antigen solution (2 ng/µL) in PBS overnight at ambient temperature. The coating solution was removed and the plates were washed once with PBS-T (1x PBS, 0.1% Tween-20, Sigma Aldrich) and then blocked with 1% Bovine Serum Albumin (Sigma Aldrich) and 1% skim milk (Fonterra, Auckland, New Zealand) in 200 µL PBS for 1 hr with gentle shaking at ambient temperature. Plates were washed three times with PBS-T.

Sheep sera samples were diluted from 1:100 to 1:6400 in 50 µL PBS and added to the wells of the blocked plates followed by incubation for 2 hr at ambient temperature. To detect sheep antibodies 100 µL HRP conjugated monoclonal anti-sheep IgG antibodies (Sigma Aldrich) diluted in PBS to 1:40,000 were added to each well and incubated for 1 hr at ambient temperature with gentle shaking. The plates were washed three times in PBS-T and 100 µL TMB substrate (Life Technologies) was added and incubated for 15 min; 100 µL of 1 N HCl was added to the wells to stop the chromogenic reaction. The plates were read at 450 nm on a BioTek microplate reader (Winooski, US).

5.2.9 Isolation of peripheral blood mononucleocytes and interferon-γ (IFN-γ) ELISPOT assay

To 35 mL whole blood in a 50 mL tube (Falcon), 15 mL of D-PBS (Invitrogen) was added. The samples were mixed gently by inverting the tubes. The diluted blood was gently added on top of 15 mL of Ficoll-Paque PLUS (GE Healthcare, Buckinghamshire, United Kingdom). Samples were centrifuged at 1000 *g* for 40 min at ambient temperature in a benchtop swing-out centrifuge (Sigma, settings were "No brake" and medium acceleration). Following centrifugation, the upper plasma layer was drawn off, leaving the lymphocyte layer undistributed at the interface. The lymphocyte layer was transferred and D-PBS up to 50 mL was added and centrifuged at 450 *g* for 10 min at ambient temperature (maximum brake and acceleration). The supernatant was removed leaving 1 mL volume. Red blood cells were lysed by the addition of 9 mL of 0.17 M ammonium chloride pH

7.5 and the cell pellets were resuspended by gentle shaking. The samples were incubated at 4°C for 10 min, then 30 mL of D-PBS was added, followed by centrifugation at 800 *g* (maximum brake and acceleration) for 10 min at ambient temperature. The cells were resuspended in RPMI-40 media and the viable cell number determined by trypan blue (0.2%) staining. Cells from each sheep were seeded at 1.0 - 1.5 x 10^5 cells/well in triplicate into Polyvinylidene fluoride (PVDF) ELISPOT plates coated with interferon- γ (IFN-γ) (Mabtech, Sweden) capture antibody. Cells were incubated in complete DMEM medium at 37°C and 5% CO_2 for 40 h in the presence or absence of 10 μg/mL oE2 antigen or the polyclonal activator concavalin A (Con A, 1 μg/mL, Sigma Aldrich) as a positive control. IFN-γ ELISPOT assays were performed according to the manufacturer's specifications. The ELISPOT plates were read on an ELISPOT reader (Autoimmun Diagnostika, Strassburg, Germany).

5.2.10 Statistical analyses

Statistical analysis of the ELISA data (Fig 5.6) was performed on the average OD values (at 450 nm) of individual animals in each group (serum dilution of 1:200). The ELISA results were analysed by one-way analysis of variance and significant differences between groups were determined using Tukey's HSD test (GraphPad Prism for Windows V5.04).

Statistical analysis of the ELISPOT data (Fig 5.7) was performed on the number of SFU/million cells obtained for individual animals using an unpaired, two-tailed Student's t-test (Microsoft Excel).

5.3 Results and Discussion

5.3.1 Characterisation of HMSA

The HMSA were synthesised as described in our previous study with an E2 nanovaccine in mice.[17] The particles were of a uniform shape and size of 140 to 150 nm (Fig 5.1) as determined by size distribution analysis of transmission electron microscopy (TEM) images (Fig 5.2). These particles were larger than the HMSA used in the previous study (120 nm) although the thickness of the particle shell was the same at 20 nm. The pore structure of HMSA was characterised by nitrogen (N_2) adsorption-desorption isotherms (Fig 5.3). The nanoparticle surface area which was calculated by the Barret-Emmett-Teller (BET) method was 71.04 $m^2 g^{-1}$ and the total pore volume was 0.39 $m^3 g^{-1}$. The elemental analysis showed atomic percentages for nitrogen, carbon and hydrogen were 0.93%, 24.12% and 4.91% respectively.

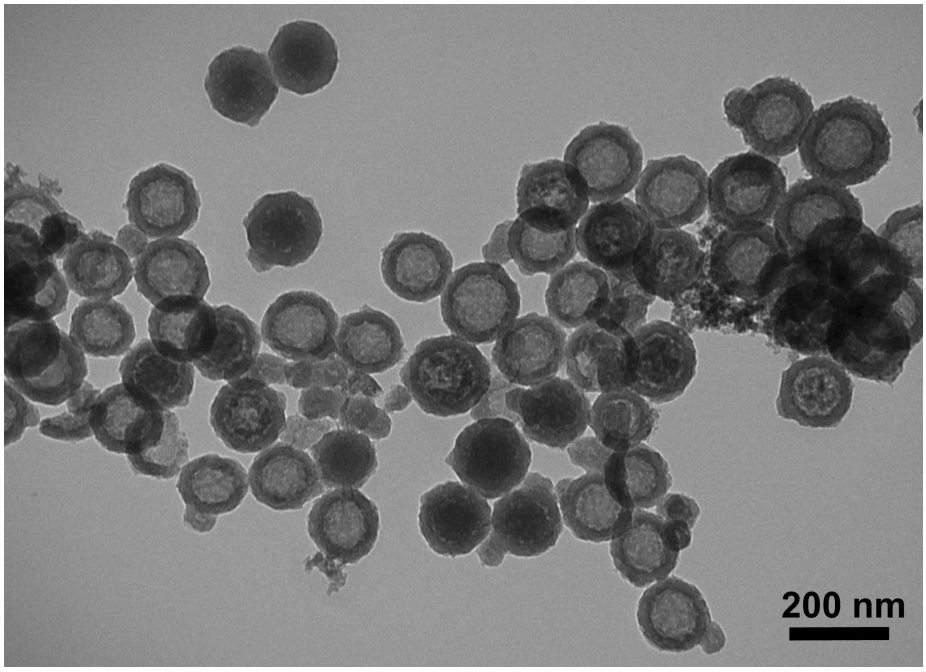

Fig 5.1. The morphology of HMSA observed by transmission electron microscopy.

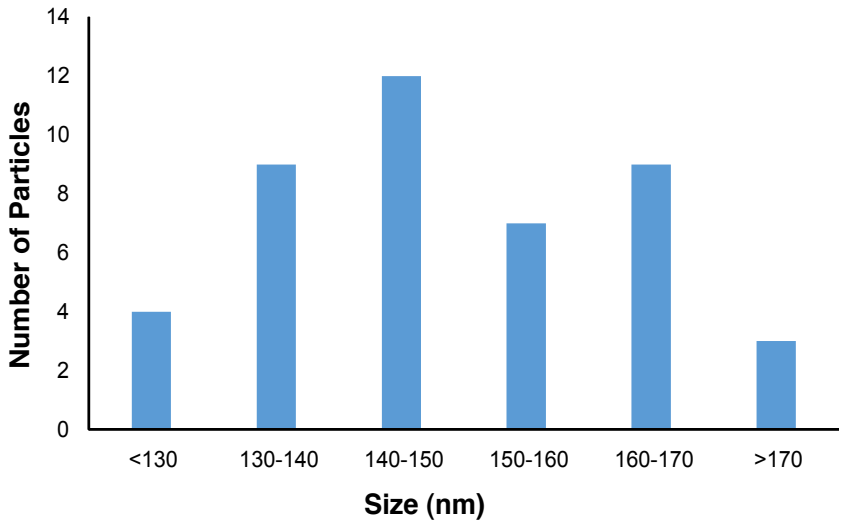

Fig 5.2. Particle size distribution of HMSA determined by TEM imaging

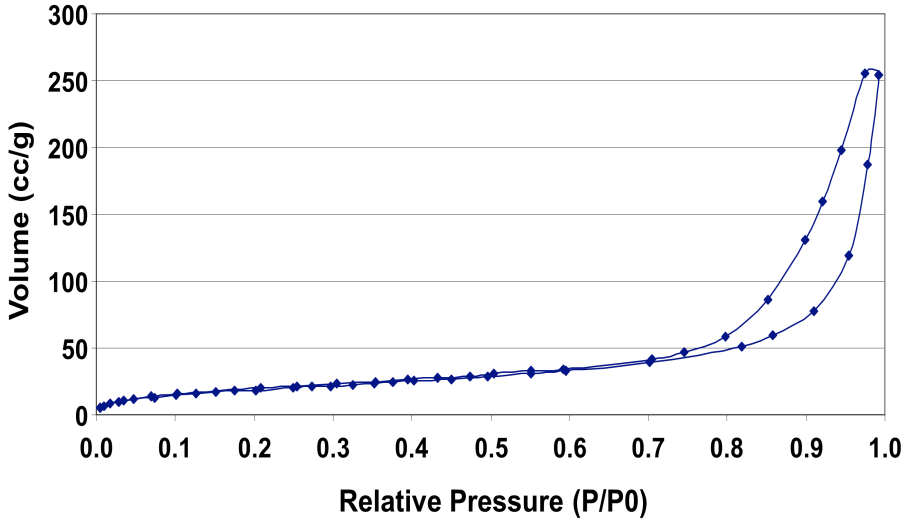

Fig 5.3. N_2 adsorption-desorption isotherms of HMSA.

5.3.2 Freeze Drying of oE2 adsorbed HMSA

The optimal combination of cryoprotectant and lyoprotectant that will preserve both the protein and the nanoparticles during the freeze-drying process needs to be empirically determined for each protein and nanoparticle combination. The oE2 protein was bound to HMSA using isotherm conditions which gives 80 µg oE2/mg HMSA.[17] Following adsorption the excipients were added to the oE2/HMSA and the nanoformulations were rapidly frozen in liquid nitrogen and subsequently freeze-dried.

Previously we have shown successful freeze-drying of ovalbumin adsorbed mesoporous silica nanoparticles using 5% trehalose and 1% PEG8000.[21] Therefore the first combination that was trialed with oE2 bound HMSA was 5% trehalose with either 1%, 0.5% or 0.1% PEG8000. The integrity of the protein after freeze-drying was assessed by SDS-PAGE analysis of the reconstituted samples. The presence of PEG8000 in the samples distorted the electrophoretic migration of protein in SDS-PAGE gels, causing the protein to migrate at an apparently lower molecular weight. In the absence of PEG, the oE2 molecular weight was approximately 42 kDa (Fig 5.4A, Lane 1), while in the presence of PEG8000 the molecular weight was estimated to be 30 kDa (Fig 5.4A, Lane 2). After freeze-drying with the excipients, 5% trehalose and 1% or 0.5% PEG8000, the migration of oE2 was distorted and the protein appeared degraded as the intensity of the band was lower (Fig 5.4A, Lanes 3 and 4) compared to the control oE2 protein (Fig 5.4A, Lane 1). The oE2/HMSA sample freeze-dried with 5% trehalose and 0.1% PEG8000 showed oE2 protein of 42 kDa (Fig 5.4A, Lane 5). This lower concentration of PEG8000 did not affect the electrophoretic migration of oE2. However as with the higher concentrations of PEG8000 the protein was also degraded, as

suggested by the lower intensity of the band compared to the control oE2 protein band (Fig 5.4A). These results suggested that trehalose and PEG8000 were not able to stabilise the oE2 during either the freeze-drying or reconstitution processes and therefore a different lyoprotectant was required.

Glycine was then tested as an alternative lyoprotectant since it has been used successfully for freeze-drying of other proteins such as lactate dehydrogenase and glucose 6-phosphate dehydrogenase in a sucrose-glycine based excipient system.[22] Glycine was used at 1%, 0.5% and 0.1% in combination with 5% trehalose in the freeze-drying formulations. Reconstituted, freeze-dried oE2/HMSA samples were analysed on SDS-PAGE gels and showed that the oE2 protein integrity was maintained at all three concentrations of glycine used (Fig 5.4B). Therefore 1% glycine was selected for freeze-drying of the nanovaccine formulation. The integrity of the nanoparticles following the freeze-drying process with 5% trehalose and 1% glycine was confirmed by TEM analyses. The resulting images showed that the HMSA remain intact and maintained their characteristic round shape and original size of 140-150 nm (Fig 5.5). The freeze-dried nanovaccine reconstituted easily and rapidly in less than 30 seconds. Furthermore, it was found that this excipient combination of 5% trehalose and 1% glycine for freeze-drying of oE2/HMSA maintained the protein integrity after long-term storage (14 months) at ambient temperature, whereas freeze-drying with 5% trehalose and 1% PEG8000 resulted in completely degraded protein.

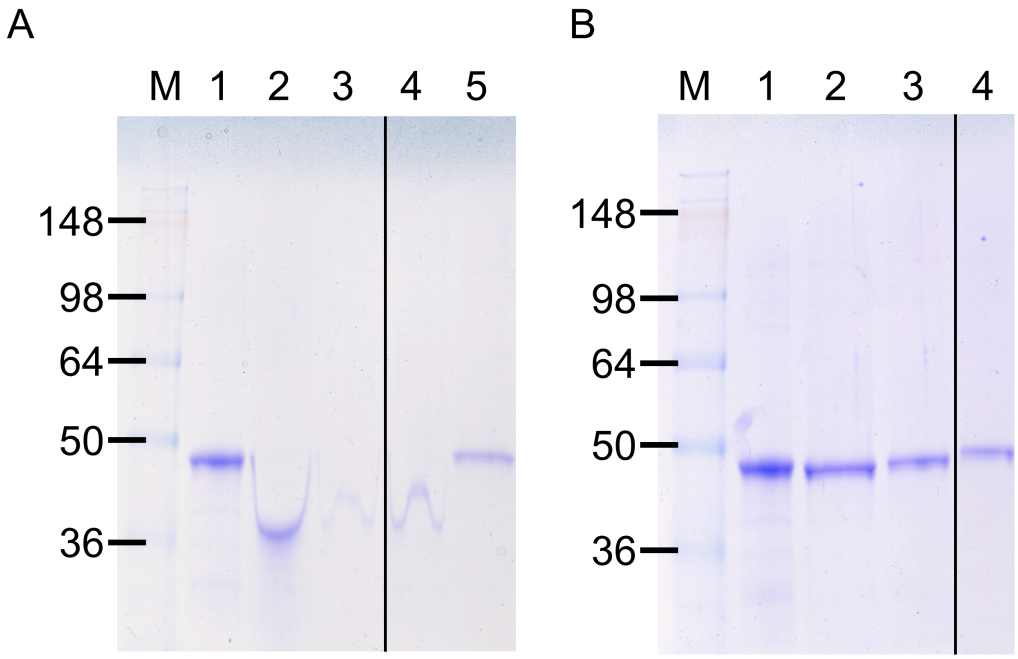

Fig 5.4. (A) Evaluation by SDS-PAGE of oE2/HMSA formulations after freeze-drying with different combinations of trehalose and PEG8000. Lane 1: oE2 control; oE2/HMSA freeze-dried

with Lane 2: 1% PEG8000; lane 3: 5% trehalose and 0.5% PEG8000; lane 4: 5% trehalose and 0.1% PEG8000.

(B) Evaluation by SDS-PAGE of oE2/HMSA formulations after freeze-drying with different combinations of trehalose and glycine. Lane 1: oE2 control; oE2/HMSA freeze-dried with lane 2: 5% trehalose and 1% glycine; lane 3: 5% trehalose and 0.5% glycine; lane 4: 5% trehalose and 0.1% glycine.

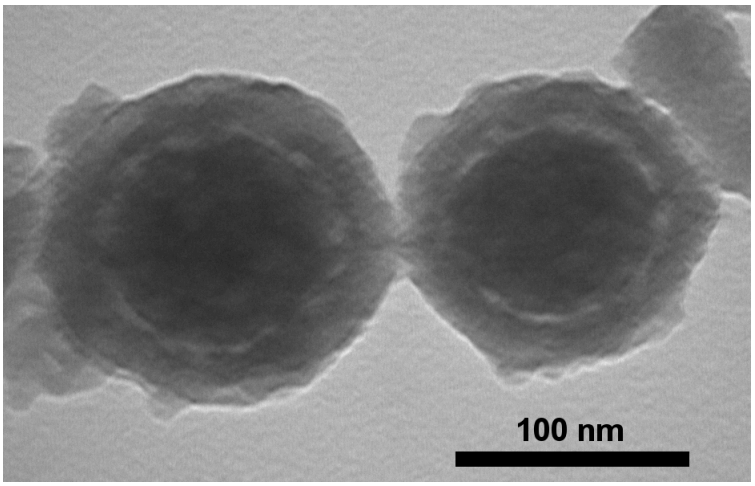

Fig 5.5. The morphology of oE2/HMSA particles visualised by transmission electron microscopy following freeze-drying with 5% trehalose and 1% glycine.

5.3.3 Immunisation of sheep with oE2 nanovaccine formulations

To determine if HMSA can act as a useful delivery vehicle for oE2 protein, in livestock animals, sheep were immunised three times at three week intervals. Freeze-drying is a relatively harsh process but can be used to generate nanoparticle preparations which have long-term stability at ambient temperatures. [23,24] To determine if freeze-drying affected the activity of the oE2 nanoparticle formulation, it was tested in animals both before and after freeze-drying. The sheep trial comprised of 16 BVDV-1 negative animals divided into four groups. Group 1 (sheep 1 to 4) received 500 μg oE2 together with Quil-A, as a conventional adjuvant, Group 2 (sheep 5 to 8) received 500 μg oE2/6.2 mg HMSA which was not freeze-dried, Group 3 (sheep 9 to 12) sheep received 500 μg oE2 per 6.2 mg HMSA which had been freeze-dried with 5% trehalose and 1% glycine. Group 4 (sheep 13 to 16) received 6.2 mg HMSA particles only per dose (Table 5.1). Pre-immune (PI) sera samples were collected prior to immunisation and subsequent sera samples were collected at two week intervals following each immunisation. All of the sheep remained healthy and within the normal weight range throughout the experimental period (data not shown).

Immune responses measured by an E2-specific Enzyme-linked Immunosorbent Assay (ELISA) showed E2-specific antibodies were detectable following two injections (data not shown). The total IgG responses were highest two weeks after the third injection (Fig 5.6). Group 1 animals immunised with oE2 (500 µg) plus Quil-A (1 mg) showed similar antibody responses (average OD value of 1.4) in all four sheep, therefore oE2 protein was immunogenic in a large animal model.
Group 2 animals received three injections of the oE2/HMSA nanoformulation (500 µg oE2 adsorbed to 6.2 mg HMSA). Sheep 6 and sheep 8 showed a similar level of oE2 specific antibody response (average OD value of 1.33, Fig 5.6) to Group 1 animals. Sheep 7, Group 2 showed a low antibody response as a result of not receiving the full booster dose during the second immunisation. All four animals in Group 3 immunised with the freeze-dried oE2/HMSA nanoformulation (500 µg oE2 adsorbed to 6.2 mg HMSA) showed strong antibody responses to oE2/HMSA (OD values from 0.83 to 1.33). This result is important since it has demonstrated that freeze-drying of the oE2 nanoformulation with the excipients 5% trehalose and 1% glycine maintained the immunological integrity of E2 protein. Group 4 sheep immunised with HMSA particles showed no specific antibody response to oE2 protein (Fig 5.6). These results confirmed that nanoformulations can deliver E2 antigen and act as a self-adjuvant in large animals without the need of a conventional adjuvant.

The injections of oE2/HMSA in the sheep at the base of the ear did not result in localised skin redness indicating that subcutaneous route of immunisation of HMSA nanoparticles was well tolerated in sheep (data not shown). The route of immunisation together with adjuvant and the type of antigen itself are important considerations as they can influence the type of immunity generated in response to the vaccine antigen. The subcutaneous route of immunisation was selected based on our previous studies in mice with oE2 adsorbed to HMSA[17] in which this route of immunisation was well tolerated in mice. It has been demonstrated that immunisation of sheep with 50 nm polystyrene beads was most effective at inducing both cellular and humoral immunity when administered through intradermal and subcutaneous routes.[25] The effectiveness of the oE2 nanovaccine formulation using this route of immunisation may result from slower antigen absorption from the subcutaneous injection site creating a depot effect and therefore prolonging the immune response. The BVDV-1 vaccine, Pestigard® used in Australia, is also administered subcutaneously in cattle, therefore subcutaneous delivery of nanovaccine formulations should be a viable immunisation strategy for industry use.

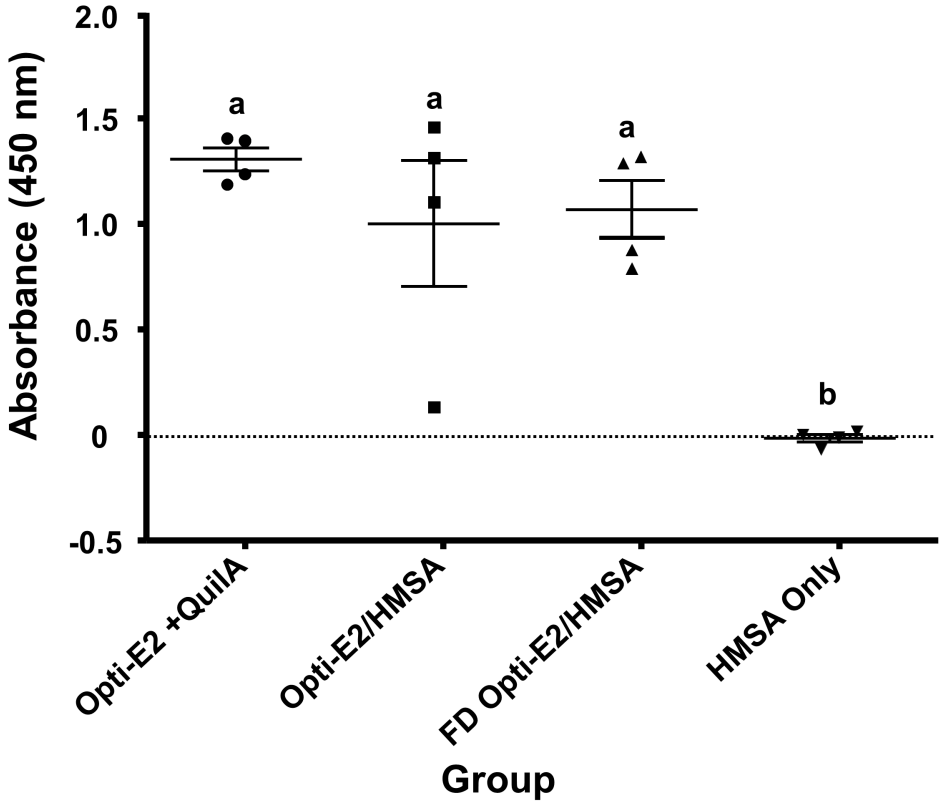

Fig 5.6. oE2-specific ELISA antibody responses in sheep after three subcutaneous immunisations. The individual response for each sheep is shown using a sera dilution of 1:200. Group 1 (sheep 1 to 4) received 500 µg oE2 and 1 mg Quil-A; Group 2 (sheep 5 to 8) received the non-freeze-dried E2 nanovaccine (500 µg oE2 adsorbed to 6.2 mg HMSA), Group 3 (sheep 9 to 12) received the freeze-dried (FD) E2 nanovaccine (500 µg oE2 adsorbed to 6.2 mg HMSA), Group 4 (sheep 13 to 16) received HMSA particles (6.2 mg) only. Groups that do not share a common letter were significantly different ($p<0.001$, unpaired t-test analysis).

5.3.4 Long-term cell-mediated immune responses to oE2/HMSA immunisation by ELISPOT assay

The cell-mediated memory response to an antigen is a vital component of the immune system since it demonstrates uptake of the antigen by professional antigen presenting cells and presentation within the lymphoid organs, an essential process for developing immunity to invading pathogens. To determine if there were long-term cell-mediated immune responses in sheep after immunisation using HMSA, the peripheral blood mononucleocyte cell (PBMC) populations were isolated five months following the third immunisation. Stimulated PBMCs were then used in IFN-γ Enzyme-linked Immunosorbent Spot (ELISPOT) assay to determine if there was T-helper type 1 (Th1)

cell-mediated immune response. Fig 5.7 shows the IFN-γ response of individual sheep as indicated by the number of cells producing Spot Forming Units (SFU). The four animals in Group 1 which received oE2 plus Quil-A showed some variation in the responses. Sheep 1 and 3 showed lower level responses of 244 and 272 SFU/million cells and Sheep 2 and 4 showed high level responses of 1869 and 2032 SFU/million cells in response to oE2 antigen (Fig 5.7, blue bars). One explanation for varied response could be the animal to animal variation of outbred animals. This has been observed in previously immunisation studies with the sheep model. [25-27]

All the animals in Group 2 (sheep 5 to 8) injected with the oE2 nanoformulation showed similar low levels of cell-mediated immunity to oE2 antigen (from 213-500 SFU/million cells). Whereas, interestingly, it was found that Group 3 (sheep 9 to 12) immunised with freeze-dried oE2 nanoformulation showed very high responses (> 2290 SFU/million cells). This result showed there was an excellent long-term Th1 memory response to immunisation with freeze-dried oE2 nanovaccine formulation detectable five months after immunisation. It was also determined that sheep 11 and sheep 12 showed a higher "no antigen" response which we cannot account for. The freeze-dried formulation included the excipients 5% trehalose and 1% glycine which are not known to be immunogenic. We have previously used 5% trehalose and 1% PEG8000 [21] with ovalbumin protein to generate freeze-dried nanovaccine and did not see increased cell-mediated responses for the "no antigen" controls. Once the reconstituted vaccine is injected the excipients should be rapidly adsorbed, metabolised and cleared from the system and have no adjuvant effect on the immune system.

One of the Group 4 sheep (number 3) which received HMSA particles showed 2296 SFU/million cells in the presence of oE2 this could indicate that this animal had become exposed to BVDV-1 as these animals were kept outside for a period of four months after the final immunisation.

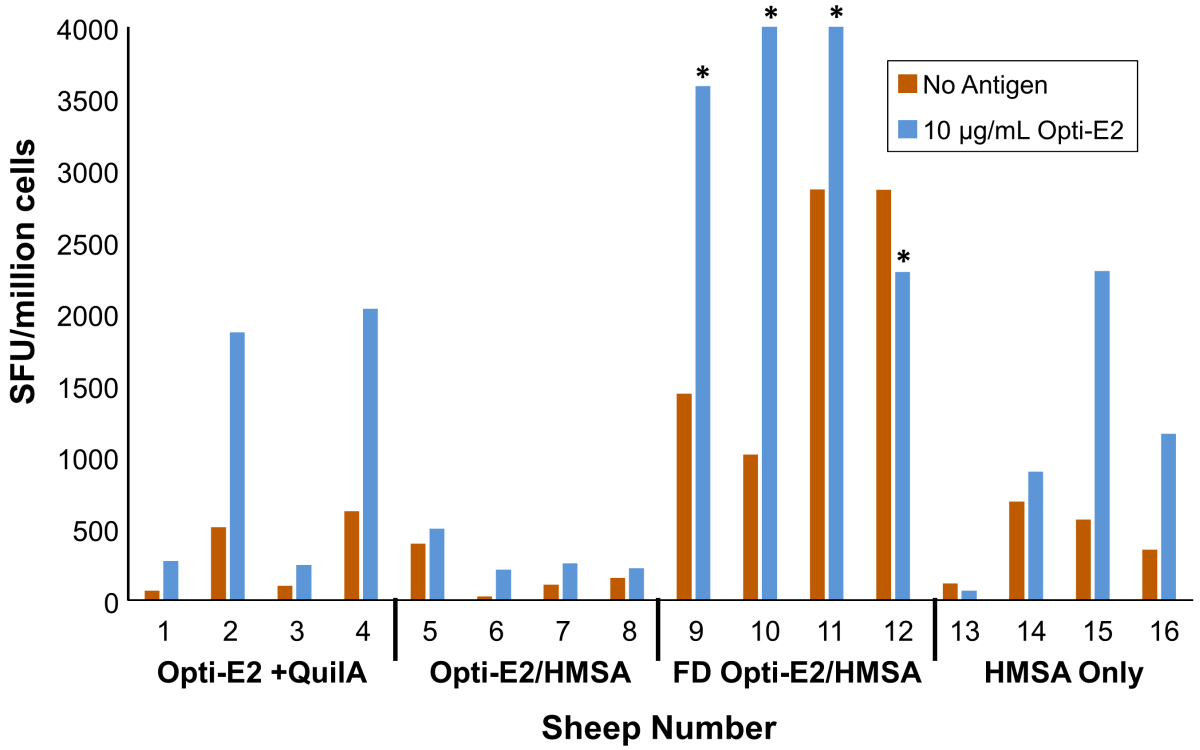

Fig 5.7. The long-term immune memory response of sheep PBMC cells following stimulation to oE2 antigen. IFN-γ secretion of PBMC cells obtained five months after immunisation was assessed by ELISPOT assay in response to oE2 (10 ng/µL, blue bars) and compared to unstimulated cells (red bars). The Mean Spot SFU /million cells is shown for each animal (assayed in triplicate) in the treatment groups. The polyclonal activator, Concavalin A, was used to confirm cell viability and functionality of the assay (data not shown). The asterisk (*) indicates significant responses with $p < 0.001$ (unpaired t-test analysis).

Importantly, this is the first study to the best of our knowledge to investigate the long-term immune responses in a large animal after immunisation with silica nanoparticles as all previous studies have been performed in mice. [16,17,21,28]

The fact that the immune response in animals receiving the E2 nanoformualtion was balanced with both humoral and cellular immunity is an encouraging result. This has also been demonstrated in sheep immunised with ovalbumin covalently conjugated to polystyrene nanobeads of 50 nm in size. In that study both cellular and humoral immunity was induced most effectively when the nanobead formulation was administered through intradermal and subcutaneous routes compared to the intramuscular route. [25]

The freeze-drying process was not detrimental to the nanoformulation and in fact enhanced the levels of the cell-mediated immune responses in the animals receiving the freeze-dried formulation (Fig 5.7). Freeze-drying of cationically modified silica nanoparticles (28 nm in size) for gene delivery in Cos-1 showed that addition of either 5% trehalose or 10% glycerol conserved nanoparticle integrity and subsequent biological activity through DNA-binding and enhanced transfection efficiency. [29]

Here we have demonstrated for the first time that HMSA have the capacity to act as both the antigen delivery vehicle and vaccine adjuvant in a large animal. This is a significant finding since sheep are a natural target species of BVDV-1. In addition, unlike previous studies using an inbred laboratory mice strain,[17] [21] sheep are an outbred animal and although the immune responses can be more variable, demonstration of the feasibility of silica nanovaccine technology in a large animal model is a critical research milestone.

5.4 Conclusion

Hollow mesoporous silica nanoparticles are an attractive new adjuvant which can be precisely tailored to accommodate different antigens. HMSA nanoparticles can have the following advantages; 1) providing stability for the protein antigen through adsorption/encapsulation and therefore improved protection from degradation in the cell environment; 2) are amenable to a freeze-drying process for increased stability at ambient temperatures during storage; 3) providing a mechanism of delivery through efficient uptake due to their size by circulating dendritic cells for subsequent antigen presentation in the lymphoid organs and 4) stimulating a balanced immune response with both humoral and cell-mediated immunity.

The results presented here for a target species of BVDV-1 are a promising step towards establishing the use of silica nanoparticles for an oE2 subunit vaccine for the livestock industry. The effective freeze-drying of the E2 nanoformulation is a significant step towards the development of such a vaccine. The next step in the development of this vaccine delivery system will be to demonstrate the capacity of silica nanoparticle formulations to protect animals from infection in challenge studies.

5.5 Acknowledgements

This work was funded by the Queensland Government through its Department of Employment, Economic Development and Innovation Reinvestment Fund. We thank Andrew Kelly, Beverly Hutchinson and the staff at the Queensland Animal Science Precinct, The University of Queensland for their expert assistance. We thank Rebecca Ambrose for performing the BVDV-1 Real Time PCR assays. We also thank Prof Rajiv Khanna and Dr Corey Smith for the use of the ELISPOT reader system at The Queensland Institute of Medical Research.

5.6 References

1. Thiel HJ, Collett MS, Gould EA, Heinz FX, Houghton M, et al. (2005) Family Flaviviridae. In: Fauquet CM, Mayo MA, Maniloff J, Desselberger U, Ball LA, editors. Virus Taxonomy Eighth Report on the International Committee on the Taxonomy of Viruses. Amsterdam: Academic Press. pp. 981-998.
2. Donis RO, Corapi W, Dubovi EJ (1988) Neutralizing Monoclonal-Antibodies to Bovine Viral Diarrhea Virus Bind to the 56k to 58k Glycoprotein. Journal of General Virology 69: 77-86.
3. van Rijn PA, van Gennip HGP, Leendertse CH, Bruschke CJM, Paton DJ, et al. (1997) Subdivision of the Pestivirus genus based on envelope glycoprotein E2. Virology 237: 337-348.
4. Bruschke CJM, Moormann RJM, van Oirschot JT, van Rijn PA (1997) A subunit vaccine based on glycoprotein E2 of bovine virus diarrhea virus induces fetal protection in sheep against homologous challenge. Vaccine 15: 1940-1945.
5. Thomas C, Young NJ, Heaney J, Collins ME, Brownlie J (2009) Evaluation of efficacy of-mammalian and baculovirus expressed E2 subunit vaccine candidates to bovine viral diarrhoea virus. Vaccine 27: 2387-2393.
6. Nelson G, Marconi P, Periolo O, La Torre J, Alvarez MA (2012) Immunocompetent trucated E2 glycoprotein of bovine viral diarrhea virus (BVDV) expressed in *Nicotiana tabacum* plants: A candidate antigen for new generation of veterinary vaccines. Vaccine: 4499-4504.
7. Aguirreburualde MSP, Fernandez S, Cordoba M (2012) Acrosin Activity Regulation by Protein Kinase C and Tyrosine Kinase in Bovine Sperm Acrosome Exocytosis Induced by Lysophosphatidylcholine. Reproduction in Domestic Animals 47: 915-920.
8. Pecora A, Aguirreburualde MS, Aguirreburualde A, Leunda MR, Odeon A, et al. (2012) Safety and efficacy of an E2 glycoprotein subunit vaccine produced in mammalian cells to prevent experimental infection with bovine viral diarrhoea virus in cattle. Veterinary Research Communications 36: 157-164.
9. Mody KT, Popat A, Mahony D, Cavallaro AS, Yu CZ, et al. (2013) Mesoporous silica nanoparticles as antigen carriers and adjuvants for vaccine delivery. Nanoscale 5: 5167-5179.
10. Popat A, Hartono SB, Stahr F, Liu J, Qiao SZ, et al. (2011) Mesoporous silica nanoparticles for bioadsorption, enzyme immobilisation, and delivery carriers. Nanoscale 3: 2801-2818.
11. Gupta RK, Rost BE, Relyveld E, Siber GR (1995) Adjuvant properties of aluminum and calcium compounds. Pharmaceutical Biotechnology 6: 229-248.

12. Mercuri LP, Carvalho LV, Lima FA, Quayle C, Fantini MCA, et al. (2006) Ordered mesoporous silica SBA-15: A new effective adjuvant to induce antibody response. Small 2: 254-256.

13. Carvalho LV, Ruiz Rde C, Scaramuzzi K, Marengo EB, Matos JR, et al. (2010) Immunological parameters related to the adjuvant effect of the ordered mesoporous silica SBA-15. Vaccine 28: 7829-7836.

14. Wang TY, Jiang HT, Zhao QF, Wang SL, Zou MJ, et al. (2012) Enhanced mucosal and systemic immune responses obtained by porous silica nanoparticles used as an oral vaccine adjuvant: Effect of silica architecture on immunological properties. International Journal of Pharmaceutics 436: 351-358.

15. Guo HC, Feng XM, Sun SQ, Wei YQ, Sun DH, et al. (2012) Immunization of mice by Hollow Mesoporous Silica Nanoparticles as carriers of Porcine Circovirus Type 2 ORF2 Protein. Virology Journal 9: 108.

16. Mahony D, Cavallaro AS, Stahr F, Mahony TJ, Qiao SZ, et al. (2013) Mesoporous Silica Nanoparticles Act as a Self-adjuvant for Ovalbumin Model Antigen in Mice. Small 9: 3138-3146.

17. Mahony D, Cavallaro AS, Mody KT, Xiong L, Mahony TJ, et al. (2014) In vivo delivery of bovine viral diahorrea virus, E2 protein using hollow mesoporous silica nanoparticles. Nanoscale 6: 6617-6626.

18. Mody KT, Mahony D, Zhang J, Cavallaro AS, Zhang B, et al. (2014) Silica vesicles as nanocarriers and adjuvants for generating both antibody and T-cell mediated immune resposes to Bovine Viral Diarrhoea Virus E2 protein. Biomaterials 35: 9972-9983.

19. Cavallaro AS, Mahony D, Commins M, Mahony TJ, Mitter N (2011) Endotoxin-free purification for the isolation of Bovine Viral Diarrhoea Virus E2 protein from insoluble inclusion body aggregates. Microb Cell Fact 10: 57.

20. Horwood PF, Mahony TJ (2011) Multiplex real-time RT-PCR detection of three viruses associated with the bovine respiratory disease complex. Journal of Virological Methods 171: 360-363.

21. Mody KT, Mahony D, Cavallaro AS, Stahr F, Qiao SZ, et al. (2014) Freeze-drying of ovalbumin loaded mesoporous silica nanoparticle vaccine formulation increases antigen stability under ambient conditions. International Journal of Pharmaceutics 465: 325-332.

22. Liu W, Wang DQ, Nail SL (2005) Freeze-drying of proteins from a sucrose-glycine excipient system: Effect of formulation composition on the initial recovery of protein activity. Aaps Pharmscitech 6: E150-E157.

23. Abdelwahed W, Degobert G, Stainmesse S, Fessi H (2006) Freeze-drying of nanoparticles: Formulation, process and storage considerations. Advanced Drug Delivery Reviews 58: 1688-1713.

24. Mody KT, Mahony D, Mahony TJ, Mitter N (2012) Freeze-Drying of Protein-Loaded Nanoparticles for Vaccine Delivery. Drug Delivery Letters 2: 83-91.

25. Scheerlinck JPY, Gloster S, Gamvrellis A, Mottram PL, Plebanski M (2006) Systemic immune responses in sheep, induced by a novel nano-bead adjuvant. Vaccine 24: 1124-1131.

26. Rothel JS, Corner LA, Lightowlers MW, Seow HF, McWaters P, et al. (1998) Antibody and cytokine responses in efferent lymph following vaccination with different adjuvants. Veterinary Immunology and Immunopathology 63: 167-183.

27. De Rose R, Tennent J, McWaters P, Chaplin PJ, Wood PR, et al. (2002) Efficacy of DNA vaccination by different routes of immunisation in sheep. Veterinary Immunology and Immunopathology 90: 55-63.

28. Mody KT, Mahony D, Zhang J, Cavallaro AS, Zhang B, et al. (2014) Silica vesicles as nanocarriers and adjuvants for generating both antibody and T-cell mediated immune resposes to Bovine Viral Diarrhoea Virus E2 protein. Biomaterials 35: 9972-9983.

29. Sameti M, Bohr G, Ravi Kumar MN, Kneuer C, Bakowsky U, et al. (2003) Stabilisation by freeze-drying of cationically modified silica nanoparticles for gene delivery. Int J Pharm 266: 51-60.

6.

Silica Vesicles as Nanocarriers and Adjuvants for generating both Antibody and T-cell mediated Immune Responses to Bovine Viral Diarrhoea Virus E2 protein

---

The Chapter 6 describes a detailed study on *Bovine Viral Diarrhoea Virus-1* (BVDV-1) protein E2 loaded silica vesicles (SV) for the development of efficient vaccine delivery systems. A two-step self-assembly approach have been used to synthesise SV with a uniform 50 nm particle size with precisely controlled entrance size by Zhang *et al.* [1] These SV displayed desirable characteristics like large entrance size and thin shell wall of 6 nm. Our collaborator Prof. Chengzhong (Michael) Yu at Australian Institute for Bioengineering and Nanotechnology (AIBN) provided the four different types of SV (SV-140, SV-140-A, SV-100 and SV-100-A) investigated in this study.

The four SV with different physico-chemical characteristics were evaluated for adsorption of BVDV-1 protein E2 and its sustained release in different types of buffer. After optimising the adsorption and release kinetics, the cellular uptake and in vitro cytotoxicity of the four SV was tested. The unfunctionalised SV-140 was selected as antigen carrier for *in vivo* investigation based on the results from *in vitro* studies and exhibition of the desirable characteristics such as efficient antigen loading, cellular uptake proficiency and non-toxicity. Most importantly, to the best of our knowledge this study was the first to demonstrate induction of excellent immune responses to BVDV-1 E2 protein adsorbed on to the SV-140 vesicles. **Chapter 6 is published in *Biomaterials 2014, 35, 9972-9983.***

6.1 Introduction

Bovine Viral Diarrhoea (BVD) is a prevalent cattle infection of great importance in several countries due to its economical importance to the cattle industries. BVDV causes serious mucosal lesions and clinical disorders such as reproductive loss, congenital defects and persistent infections. [2, 3] An economic analysis in 2009 has shown that yearly losses due to BVDV could reach approximately US$88 per animal. [4] BVDV vaccines are broadly divided in two categories; Modified Live Virus (MLV) and Killed Virus (KV) vaccines. Both of these types of vaccines can have certain drawbacks: MLV vaccines may be deactivated beyond certain temperatures or by some chemicals and revert to virulence while KV vaccines require more antigen per dose compared to the MLV and are more expensive. [5] BVDV commonly known as bovine pestivirus, is a single-stranded RNA virus which infects cattle and sheep. [6] The BVDV genome is a 12.3 kb single stranded RNA molecule, containing a single open reading frame that is translated into a single polyprotein, which is processed into individual viral proteins by viral and cellular proteases. [7] The structural envelope glycoprotein, E2, is the major immunogenic determinant of BVDV virion making it an ideal candidate as a subunit vaccine component. [2, 8-11]

Subunit vaccines comprise of highly purified recombinant antigens such as proteins and peptides and offer advantages such as increased stability and better safety profiles compared to conventional vaccines. [12] However, a limiting factor in the development of subunit vaccines is the need to elicit both the arms of defence, antibody and T- cell mediated immunity. Proteases can degrade the protein or peptide in the biological system, which might limit their bioavailability and subsequent

presentation to the immune system. Hence, adjuvants are often added to in subunit vaccine formulations as helping agents to induce strong antigen specific immune responses. [13]

Quil-A, an extract from the bark of *Quillaja saponaria* is one of the most common adjuvant used in mice trials. The saponin-based adjuvants stimulate Th1 immune responses and production of CD8+ cytotoxic T-lymphocytes against antigens. [14-16] However, disadvantages including pain at the site of injection, severe local reactions and toxicity profile are associated with saponin-based adjuvants. [17, 18] Freund's complete adjuvant (FCA) is one of the most effective adjuvants, nevertheless, FCA is known to induce high toxicity and severe reactions. [19] The drawbacks associated with alum-type adjuvants are that they are not effective for all antigens and often induce local reactions at the site of injection and generally fail to induce CD8+ T-cell immunity. [20] As reviewed recently most conventional vaccines produce either a Th1 or Th2 mediated response, hence there is a need for a robust, non-toxic and effective adjuvant that can induce balanced immune responses (both cellular and humoral) with minimal or no side effects. [21, 22, 29]

In the past few years, silica nanoparticles have been explored as nanocarriers for vaccine delivery. [23-26] In particular, Mesoporous Silica Nanoparticles (MSNs) have desirable properties including ease of synthesis and surface functionalisation, large surface area, and excellent *in vivo* biocompatibility. [27] The controllable pore structures make MSNs excellent candidates to tune the adsorption and release of biomolecules. [28] A few studies on the potential of MSNs as vaccine adjuvants and antigen carriers have been explored, [26, 29, 30] the adjuvant property of MSNs on human-monocyte-derived dendritic cells, showing the capability to tune autologous naïve T cells into different effector cells has been demonstrated. [31] Most of these studies used model proteins such as bovine serum albumin (BSA) [32, 33], cytochrome c [34, 35] and ovalbumin (OVA). [26] Recently, Guo *et al.*[36] used hollow structured MSNs (HMSNs) as delivery vehicles for Porcine CircoVirus type-2 (PCV2) ORF2 protein. However, the antibody response was significantly lower for the group immunised with the protein loaded nanoparticles HMSNs/GST-ORF2-E in comparison to the group treated with GST-ORF2-E protein alone.

Previously, we have described the use of OVA loaded amino functionalised MSNs and BVDV-1 E2 loaded on hollow mesoporous silica nanoparticles (HMSA) to develop vaccine delivery systems. [23-25] Though, we were able to get low levels of detectable antibody and cell mediated responses, the major limitations were very low protein loading efficiency (60-80 μg/mg of particles), small

entrance size (2-3.5nm) and possibly only surface presentation of proteins on these silica nanocarriers. Despite of several studies describing the use of silica nanoparticles as vaccine adjuvants, no previous studies have evaluated structural modification of the particles to increase the antigen adsorption, facilitate sustained release by surface as well as internal cavity loading and improve their adjuvanticity so that no additional adjuvant is required.

We have developed a silica vesicle (SV) nano-carrier delivery system that demonstrates strong self-adjuvant effect, elicits higher antibody and T-cell mediated response and has the potential for reducing dose number, parameters of high significance for an improved vaccine formulation. In this study, for the first time, we have demonstrated the induction of excellent immune responses to a recombinant BVDV-1 E2 protein expressed from a codon-optimised E2 gene (oE2) adsorbed to SV, also termed as 'nanovaccine' treatment group. The carefully tailored SV are sized for effective endocytosis (50 nm), have a total pore volume in the range of (0.49-1.24 cm^3/g) to accommodate high antigen loadings and a thin, porous shell (wall thickness ~ 6 nm) with controllable entrance size (5.7 nm to16 nm) facilitating both surface and internal cavity loading for sustained release of the antigen. Our work may pave the way in the development of state-of-the-art nanotechnology for improved veterinary vaccination.

6.2 Materials & Methods

6.2.1 Chemicals

$EO_{39}BO_{47}EO_{39}$ [commercial name B50-6600, EO is poly(ethylene oxide) and BO is poly(butylene oxide)] was received from Dow Company. Tetraethyl orthosilicate (TEOS), (3-aminopropyl)triethoxysilane (APTES), fluorescein-5-isothiocyanate (FITC), were purchased from Sigma-Aldrich (St. Louis, USA). Analytical reagent grade sodium acetate (NaAc) and acetic acid (HAc) are received from ChemSupply (Port Adelaide, Australia) and Ajax Finechem Pty Ltd (Sydney, Australia), respectively.

6.2.2 Synthesis of hollow silica vesicles

For the synthesis of the silica vesicles (SV), a procedure from the literature was used with some modification [37, 38], 0.5 g of $EO_{39}BO_{47}EO_{39}$ and 0.852 g of Na_2SO_4 were dissolved in 30 g of pH = 4.7 NaAc-HAc buffer solution ([NaAc] = [HAc] = 0.40 M) to form a homogenous solution under stirring at 10 °C, 3.57 mL (3.33 g) of TEOS was added with continuously stirring for 24 h. The reaction mixture was then moved to an autoclave and hydrothermally treated at 100 or 140 °C for

another 24 h, denoted by SV-100 or SV-140, respectively. The as-synthesised samples were collected by filtration and thoroughly washed with deionized water to remove the added salts. The samples were then dried in air. The final products were obtained by calcination at 550 °C for 5 h in air.

6.2.3 Characterisation

Field emission scanning electron microscope (FE-SEM) images were obtained using JEOL JSM 7800 operated at 0.6 kV. Transmission electron microscopy (TEM) images were obtained with JEOL 2100 operated at 200 kV. For TEM measurements, the samples were prepared by dispersing and drying the powder samples-ethanol dispersion on carbon film on a Cu grid. Nitrogen adsorption-desorption isotherms were measured at 77 K by using a Micromeritics Tristar II system, before which the samples were degassed at 453 K overnight on a vacuum line. The total pore volume was calculated from the amount adsorbed at a maximum relative pressure (P/P_0) of 0.99. The Barrett–Joyner–Halanda (BJH) method was utilized to calculate the entrance size from the desorption branches of the isotherms, and the Brunauer–Emmett–Teller (BET) method was utilized to calculate the specific surface areas. Zeta potential measurements were conducted on a Zetasizer Nano ZS analyzer (Malvern Instruments, Worcestershire,UK).

6.2.4 Amino and FITC modification of hollow silica vesicles

In a typical amino-modification process, 1.5 g of calcined SV-100 or SV-140 and 60 mL toluene were added to a flask, and the mixture was stirred for 6 h before adding 1.0 mL APTES. After stirring at 110 °C for 12 h, the mixture was cooled to room temperature (RT), centrifuged, extensively washed with toluene and ethanol, participate was then dried in a fume-hood at RT. The amino- modified sample was denoted by SV-100-A or SV-140-A, respectively.

In FITC modification, 20 mg powdered SV-100-A or SV-140-A was dispersed in 3 mL deionized water, mixed with 5 mL FITC ethanol solution (0.3 mg/mL), and stirred in the dark at RT for 6 h. The products were centrifuged and washed with ethanol extensively until the supernatant was colourless.

6.2.5 oE2 adsorption to SV

Adsorption reactions used 2 mg of SV-140, SV-100, SV-140-A, SV-100-A with 500 μg of oE2 in sterile 50mM Tris buffer (pH7.0) containing 0.2% Igepal CA630, in a 2 mL final volume. This particle-protein slurry was placed on a shaker at RT, 200 rpm. After 24 h a sample of

particle-protein slurry (50 µL) was removed and centrifuged at 16.2 *g* for 1 minute. The amount of unbound oE2 protein was assessed by electrophoresis of the supernatants and the particles on SDS-PAGE gels. Protein assay was conducted on the adsorbed supernatant, using the BioRad DC kit (Hercules, USA), to quantify the amount of the unbound protein; this was done in order to calculate the amount of protein bound to the nanoparticles.

6.2.6 Desorption studies

The oE2 loaded SV-140, SV-100, SV-140-A and SV-100-A vesicle pellets were resuspended in 2 mL of PBS or 2 mL of PBS plus 0.1% sodium lauryl sulfate (SLS). The resuspended samples were left on the shaker at 37 °C for 24 h at 16.2 *g*. 50 µL aliquots were taken at 5 min, 15 min, 30 min, 3 h and 24 h. The oE2 protein released from the SV was assessed by electrophoresis of the supernatants and the particles on SDS-PAGE gels.

6.2.7 Polyacryalamide gel electrophoresis (PAGE)

The pellet samples were resuspended in 15 µL of PBS and 5 µL SRB (SDS Reducing Buffer consisting of 62.5 mM Tris-HCl (pH 6.8), 117 mM DTT, 10% Glycerol, 2% SDS, 0.02% Bromophenol blue), incubated at 85 °C for 2 min then subjected to electrophoresis on 10% Tris-Glycine gels (Life Technologies, Carlsbad, USA). The gels were visualised by staining in 50% methanol, 10% acetic acid, 0.25% Coomassie Blue R250 for 30 min, followed by destaining in 30% methanol, 10% acetic acid for three 30 min washes.

6.2.8 Cell uptake studies using flow cytometry

The cellular uptake was investigated using fluorescence activated cell sorting (FACS) for which the MDBK cells were seeded at 1.0 x 10^6 cells/mL in Earle's Minimum Essential Media (Life Technologies) containing 5% FBS. The MDBK cells were incubated in 5 mL petri dishes and allowed to adhere overnight in a 37 °C, 5% CO_2 incubator. Next day, the cells were treated with SV-140-A-FITC and SV-100-A-FITC at two different concentrations of 0.02 mg/mL and 0.004 mg/mL for 2 h. Media was carefully removed and the dishes were gently washed three times with PBS to remove the nanoparticles. Three millilitres of PBS was added and the cells were collected in a 15 mL falcon tube. The cells were centrifuged at 1000 *g* for 6 min at 5 °C. The supernatant was discarded and the pellet was resuspended in 2% PFA and subsequently transferred into FACS tubes (Becton Dickinson, Franklin Lakes, NJ). BD LSRII analyser was used to determine the cell uptake.

6.2.9 Trypan blue staining for in vitro cytotoxicity assay

MDBK cells (ATCC) were seeded at 80-90% confluency onto glass coverslips in a 24 well plate and allowed to adhere overnight in a 37 °C, 5% CO_2 incubator. To investigate the effect of nanoparticle concentration on the cells a dilution range (0.5 mg/mL, 0.1 mg/mL and 0.01 mg/mL) of SV in Earle's Minimum Essential Media [containing 5% foetal bovine serum (FBS) (Life Technologies)] were prepared and gently added drop wise to the adherent cells. The cells were incubated in the presence of SV-140, SV-100, SV-140-A, SV-100-A vesicles and MCM-41 as synthesised nanoparticles at 37 °C, 5% CO_2 for 20 h. Media was carefully removed and the wells were gently washed three times with PBS to remove the nanoparticles. To determine cell viability 0.2% trypan blue stain (Life Technologies) was added for 2 min. Trypan blue stain was carefully removed and the wells were washed once with PBS. Cells were fixed in 4% paraformaldehyde (PFA) pH 7.4 for 15 min, and then washed three times with PBS. Coverslips were mounted with 5 µL of MOWIOL (Sigma-Aldrich). Cell viability was determined by imaging on a Zeiss HAL100 microscope under bright field.

6.2.10 Cell Viability Assay

The cytotoxicity of the oE2 protein in PBS, oE2/SV-140 and oE2/SV-140 plus traditional adjuvant Quil-A was quantified using the colorimetric assay (MTT based) (Roche cell proliferation Kit I). In a 96 well flat bottom cell culture plate, the MDBK cells were seeded at 5 x 10^4 cells/well in 100 µL of Earle's Minimum Essential Media containing 5% FBS, and incubated overnight in at 37 °C, 5% CO_2. On the following day, different treatments were added to the cells at concentrations of 0.1 mg/mL, 0.02 mg/mL and 0.01 mg/mL, Triton X-100 at a concentration of 0.1 mg/mL was used a positive control for cell death, and the plate was incubated overnight at 37 °C, 5% CO_2. Post overnight incubation, 10 µL of MTT (0.5 mg/mL final concentration) was added to each well and the plate was further incubated for 4 h at 37 °C, 5% CO_2. After 4 h, 100 µL of the solubilising agent was added to all the wells and the plate was incubated overnight at 37 °C, 5% CO_2. Next day, the plate was read at 570 nm using BioTek microplate reader (Winooski, US).

6.2.11 Immunization studies conducted in mice

C57BL/6J mice were purchased from and housed in the Biological Resource Facility, The University of Queensland, Brisbane, Australia under specific pathogen-free conditions. Eight week old female mice were housed in HEPA-filtered cages with 4 animals per group in an environmentally controlled area with a cycle of 12 h of light and 12 h of darkness. Food and water were given *ad libitum*. All procedures were approved by The University of Queensland, Ethics

Committee. Animals were closely monitored throughout the study. All the animals remained in good health for the duration of the study with no visible deleterious health effects.

Pre-immunisation blood samples were collected by retro-orbital bleeds using heparin coated hematocrit tubes (Hirschmann Laborgeräte, Heilbronn, Germany). Pre-immunisation blood samples collected prior to the first immunisation were referred to as the pre-immune (PI) samples. Table 6.1 shows the different treatment groups in the study. Adsorption reactions were prepared aseptically as described above and the adsorbed oE2/SV pellet was washed in 1 mL of saline before preparing the final injectable doses. Quil-A (Superfos Biosector, Vedback, Denmark) was resuspended at 2 mg/mL in sterile injectable water (Pfizer**,** Brooklyn, USA). The injectable doses were administered to investigate the difference between the immune responses produced by the oE2/SV-140 and oE2/SV-140 plus Quil-A. The positive control group of mice received 50 µg oE2 protein and 10 µg Quil-A. The negative control groups received injections of SV-140 (250 µg) plus Quil-A (10 µg). Dose volumes of 100 µL (in 0.9% saline, Pfizer) were administered by subcutaneous injection at the tail base using a sterile 27 gauge needle (Terumo, Tokyo, Japan). Three injections were administered at 2 week intervals to all the treatment groups except for the unimmunised group and mice were sacrificed 14 days after the final immunisation. The animals were weighed and monitored for their health once a week. In addition, they were also observed for clinical signs, any signs of illness were converted to a numerical score as follows: 0 = normal, 1-4 = Moderate changes, animals need to monitored daily, 5-10 = Significant changes: monitor twice daily and the consultant the chief veterinary officer at the animal facility and >10 = Euthanize.

Table 6.1. Immunisation groups in mice trial. All doses were administered at the tail base.

Group	Prototype Vaccine / Injection Dose
1	oE2 (50 µg) + QuilA (10 µg)
2	oE2 (50 µg) / SV-140 (250 µg)
3	oE2 (50 µg) / SV-140 (250 µg) + Quil-A (10 µg)
4	SV-140 (250 µg) + Quil-A (10 µg)
5	Unimmunised

6.2.12 Enzyme-Linked ImmunoSorbent Assay (ELISA) protocol

Detection of oE2-specific antibody responses: ELISA for the detection of oE2-specific antibodies were performed by coating microtitre plates (96 well, Nunc, Maxisorb, Roskilde, Denmark) with oE2 antigen solution (2 ng/µL, 50 µL) in PBS overnight at 4°C. The coating solution was removed

and the plates were washed once with PBS-T (1x PBS, 0.1% Tween-20, Sigma-Aldrich) and blocked with Bovine Serum Albumin (5%, Sigma-Aldrich) and skim milk (5%, Fonterra, Auckland, New Zealand) in 200 µL PBS for 1 h with gentle shaking at RT. Plates were washed three times with PBS-T.

Mouse sera samples were diluted from 1:1000 to 1:2048000 in 50 µL PBS and each dilution was added to the wells of the blocked plates followed by incubation for 2 h at RT. To detect mouse antibodies HRP conjugated polyclonal sheep anti-mouse IgG antibodies (Chemicon Australia, Melbourne, VIC, Australia) diluted in PBS to 1:10000 were added to each well and incubated for 1 h at RT with gentle shaking. Plates were washed three times in PBS-T. TMB substrate (100 µL, Life Technologies) was added to each well and incubated for 15 min at RT; 100 µL of 1N HCl was added to the wells to stop the chromogenic reaction. The plates were read at 450 nm on the BioTek microplate reader (Winooski, US).

6.2.13 Isolation of murine splenocytes and enzyme-linked immunosorbent spot (ELISPOT) Assay

Spleens were aseptically removed following euthanasia and placed into 5 mL ice cold DMEM media (Life Technologies) supplemented with 10% foetal bovine serum (FBS, Life Technologies), 20 mM Hepes (pH 7.3), 1 M sodium pyruvate, 1 M Glutamax, 100 units/mL penicillin G, 100 µg/mL streptomycin, 0.25 µg/mL Fungizone. Spleens were gently disrupted and passed through a 100 µm nylon mesh (Becton Dickinson) using a syringe plunger. Cells were washed with 5 mL DMEM and centrifuged at 800 g for 5 min at 4°C and then resuspended in 1 mL lysis buffer (0.15 M NH_4Cl, 10 mM $KHCO_3$, 0.1 mM Na_2-EDTA) for 5 min at RT. Repeat wash steps twice with DMEM (9 mL and 5 mL) each time. Cell pellets were resuspended in 2 mL DMEM and cell numbers determined by staining with 0.2 % trypan blue. Cells from each mouse spleen were seeded at 1.0 - 1.5 x 10^5 cells/well in triplicate into Polyvinylidene fluoride (PVDF) ELISPOT plates precoated with monoclonal interferon- γ (IFN-γ) (Mabtech, Sweden) capture antibody. Cells were incubated in complete DMEM medium at 37°C and 5% CO_2 for 40 h in the presence or absence of 1 µg/mL oE2 antigen or the polyclonal activator concavalin A (Con A, 1 µg/mL, Sigma Aldrich) as a positive control. IFN-γ ELISPOT assays were performed according to the manufacturer's specifications. The ELISPOT plates were read on an ELISPOT reader (Autoimmun Diagnostika, Strassburg, Germany).

6.3 Results

We initially characterised SV-100 and SV-140 with and without amino modification as potential nano-carriers for BVDV-1 oE2 vaccine formulation. The SEM images (Fig 6.1, a and c) of SV show that both SV-100 and SV-140 have spherical morphology with a uniform particle size of 50 nm, while some openings can be observed on the surface of SV-140. Both SV show a hollow nature with wall thickness of ~ 6 nm and cavity size of ~ 40 nm (Fig 6.1, b and d). Small openings (also called entrance) on the siliceous walls can be directly observed in TEM images (indicated by white arrows) and the entrance size can be measured to be about 6 and >10 nm for SV-100 and SV-140, respectively. The pore structure of SV is further investigated by N_2 sorption analysis. Both SV-100 and SV-140 show type IV isotherms and type H_3 hysteresis loop (Fig 6.2a) with the adsorption branch showing major capillary condensation at relative pressure (P/P_0) of ~ 0.9. The desorption branch of SV-140 shifts to higher relative pressure compared to that of SV-100, indicating a larger entrance size. The entrance size of SV was calculated by the BJH method from the desorption branch (Fig 6.2b).

The entrance sizes of SV-100 and SV-140 were found to be 5.9 and 16 nm, respectively. The other structrual information of SV are listed in Table 6.2. The total pore volume and BET surface area of SV-100 were 1.24 cm^3/g and 450 m^2/g, respectively. SV-140 has a smaller total pore volume and BET surface area (0.78 cm^3/g and 273 m^2/g) because the spherical integrity of SV-140 decreased with larger entrance on the wall. After surface functionalization with amino-groups, the zeta potential of SV becomes positive (33.9 and 23.8 mV for SV-100-A and SV-140-A, respectively). The SV-A (where A denotes amino modification) showed similar N_2 sorption isotherms as unmodified SV (Fig 6.2a). As a result, SV-100-A and SV-140-A maitain the same entrance sizes (5.7 and 16 nm, respectively) from BJH pore size distribution calculated from the desorption branches (Fig 6.2b). However, the total pore volume and BET surface area of SV-A decreased after amino-modification (0.67 cm3/g and 219 m^2/g for SV-100-A, 0.49 cm^3/g and 153 m^2/g for SV-140-A) as mentioned in Table 6.2.

Table 6.2. Structural information from N2 sorption results of SV.

Sample Name	Entrance Size (nm)	V_p(cm^3/g)	S_{BET} (m^2/g)	Zeta Potential (mV)
SV-100	5.9	1.24	450	-16.7±1.0
SV-100-A	5.7	0.67	219	33.9±2.0
SV-140	16	0.78	273	-15.9±0.4
SV-140-A	16	0.49	153	23.8±0.8

Note: V_p: total pore colume; S_{BET}: BET surface area

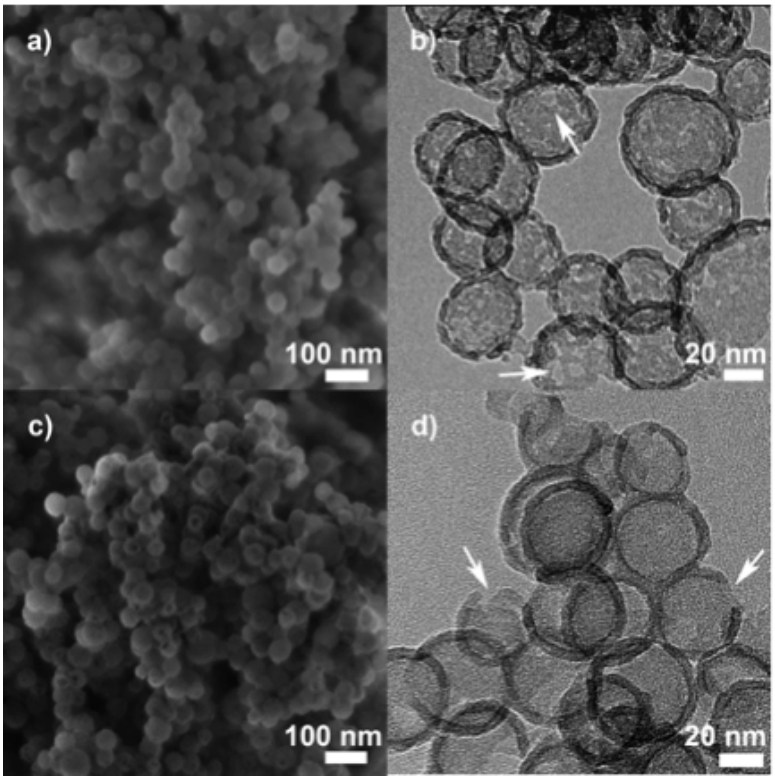

Fig 6.1. Field-emission scanning electron microscope (FE-SEM) image (a) transmission electron microscopy (TEM) image (b) SV-100 after calcination; (c) FE-SEM and TEM image of (d) SV-140 after calcination.

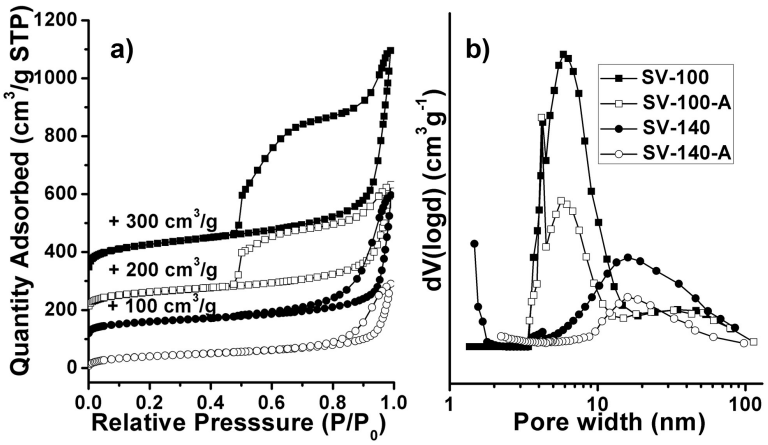

Fig 6.2. Nitrogen sorption isotherm plot (a) Barrett-Joyner-Halanda pore size distribution curve calculated from desorption branches (b) of SV.

6.3.1 Adsorption

Adsorption tests were conducted to determine the ability of SV-140, SV-100, SV-140-A and SV-100-A to bind to the oE2 protein by incubating 500 μg of oE2 with 2 mg of each SV for 24 h. The molecular weight of the expressed oE2 is 42 kDa. The samples of the protein and particle slurry were collected and separated into supernatant and particle samples and analysed by SDS-PAGE to determine the protein loading on the vesicles. The gel analysis indicates that after 24 h of binding with all the four SV, no protein could be was detected in the supernatants (Fig 6.3).

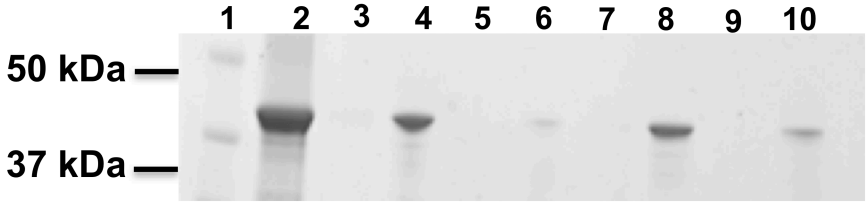

Fig 6.3. Adsorption of the oE2 protein on SV on SDS-PAGE. Lane 1: Marker; lane 2: oE2 protein; lane 3: oE2/SV-140 supernatant; lane 4: oE2/SV-140 pellet; lane 5: oE2/SV-140-A supernatant; lane 6: oE2/SV-140-A pellet; lane 7: oE2/SV-100 supernatant; lane 8: oE2/SV-100 pellet; lane 9: oE2/SV-100-A supernatant; lane 10: oE2/SV-100-A pellet.

The amount of protein loaded onto the nanoparticles was quantified by performing protein assays on the supernatants. The oE2 protein adsorbed was found to be 216, 249, 248 and 236 μg to per mg of SV-100, SV-100-A, SV-140 and SV-140-A respectively (Fig 6.4).

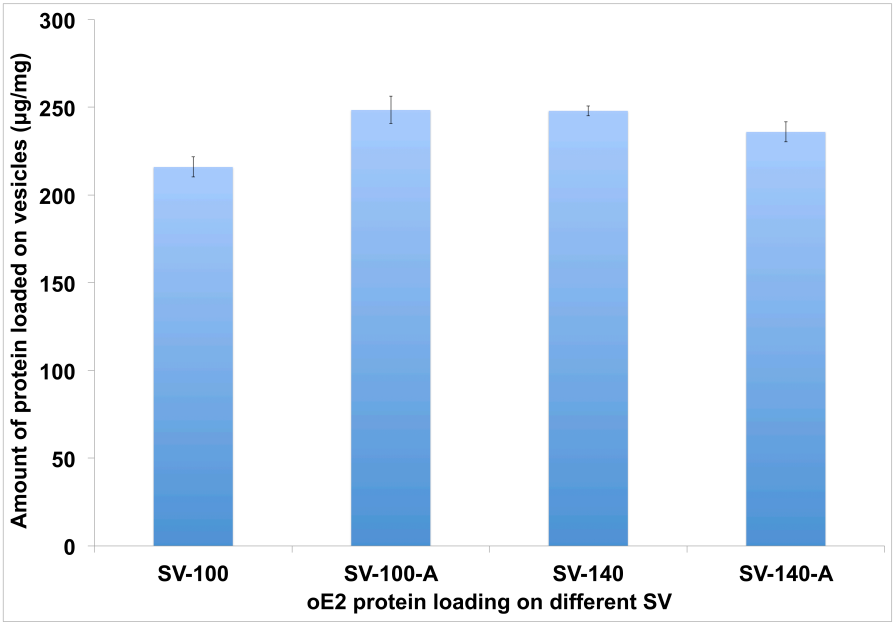

Fig 6.4. Adsorption amount of oE2 protein on the different SV. The amonut of protein bound to the nanoparticles was calculated using protein assay. (The average of two repeat adsorptions was used to calculate the oE2 protein loading).

6.3.2 Desorption studies

Desorption studies were conducted on protein loaded SV to investigate the release of protein. To determine the desorption profiles, sample slurry of the protein and particles were collected at five different time points ranging from 5 min to 24 h, separated into desorbed supernatant and particles samples and analysed by SDS-PAGE. The gel analysis following desorption in PBS showed that the protein remained strongly bound to the vesicles, indicating no oE2 protein desorbed from the SV-140, SV-140-A, SV-100 or SV-100-A vesicles, after 24 h incubation (Fig 6.5).

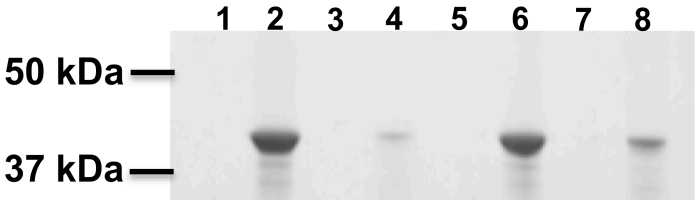

Fig 6.5. SDS-PAGE analysis – Desorption of the oE2 protein on SV in PBS after 24 h. Lane 1: oE2/SV-140 supernatant; lane 2: oE2/SV-140 pellet; lane 2: oE2/SV-140-A supernatant; lane 4: oE2/SV-140-A pellet; lane 5: oE2/SV-100 supernatant; lane 6: oE2/SV-100 pellet; lane 7: oE2/SV-100-A supernatant; lane 8: oE2/SV-100-A pellet.

A second release study conducted using PBS plus 0.1% SLS buffer, showed rapid (after 5 min) release of the oE2 protein into the supernatants from the particle pellets (Fig 6.6, lane 1) and no protein band was observed in the pellet after 24 h (Fig 6.6, lane 10). All the four vesicles exhibited similar desorption profiles, hence the gel analysis of the protein desorption for only one vesicle, SV-140, has been shown in Fig 6.6. The exact amount of protein released in the supernatant could not be quantified due to the presence of SLS, which inhibited the protein assay. However, the SDS-PAGE results indicate that about >95% of the oE2 protein was released in the supernant after 24 h.

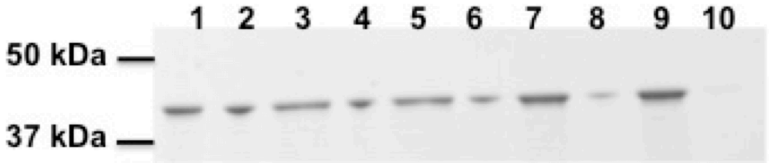

Fig 6.6. SDS-PAGE analysis – Desorption studies of oE2/SV-140 in PBS plus 0.1% SLS at different time points. Lane 1: Supernatant 5 min; lane 2: Pellet 5 min; lane 3: Supernatant 15 min; lane 4: Pellet 15 min; lane 5: Supernatant 30 min; lane 6: Pellet 30 min; lane 7: Supernatant 3 h; lane 8: Pellet 3 h; lane 9: Supernatant 24 h; lane 10: Pellet 24 h.

6.3.3 Cell uptake studies using FITC labelled silica vesicles

Cellular uptake is usually a prerequisite when developing a vaccine using nanoparticles. Cellular uptake of FITC labeled SV was studied in MDBK cells at two different concentrations of 0.02 mg/mL and 0.004 mg/mL and was compared to the untreated cells. At 0.02 mg/mL the SV-140-A-FITC were taken up by 86.4% of the total cell population and the SV-100-A-FITC by 97.3%. Furthermore, the Mean Fluorescence Intensity (MFI) values, which is proportional to the amount of FITC labelled vesicles taken up by the cells, followed the order SV-100-A-FITC 0.02 mg/mL > SV-140-A-FITC 0.02 mg/mL > SV-100-A-FITC 0.004 mg/mL > SV-140-FITC 0.004 mg/mL > MDBK cells alone (non-treated cells). The amino functionalised SV-100-A-FITC at the 0.02 mg/mL concentration showed the highest cellular uptake, which might be due the specific characteristics of SV-100-A, a large surface area and the high charge interaction with cell membranes. The cellular uptake was found to be dose dependant, however, the difference between the SV-140-A-FITC and SV-100-A-FITC at both 0.02 mg/mL and 0.004 mg/mL was found to be less than ~10% (Fig 6.7).

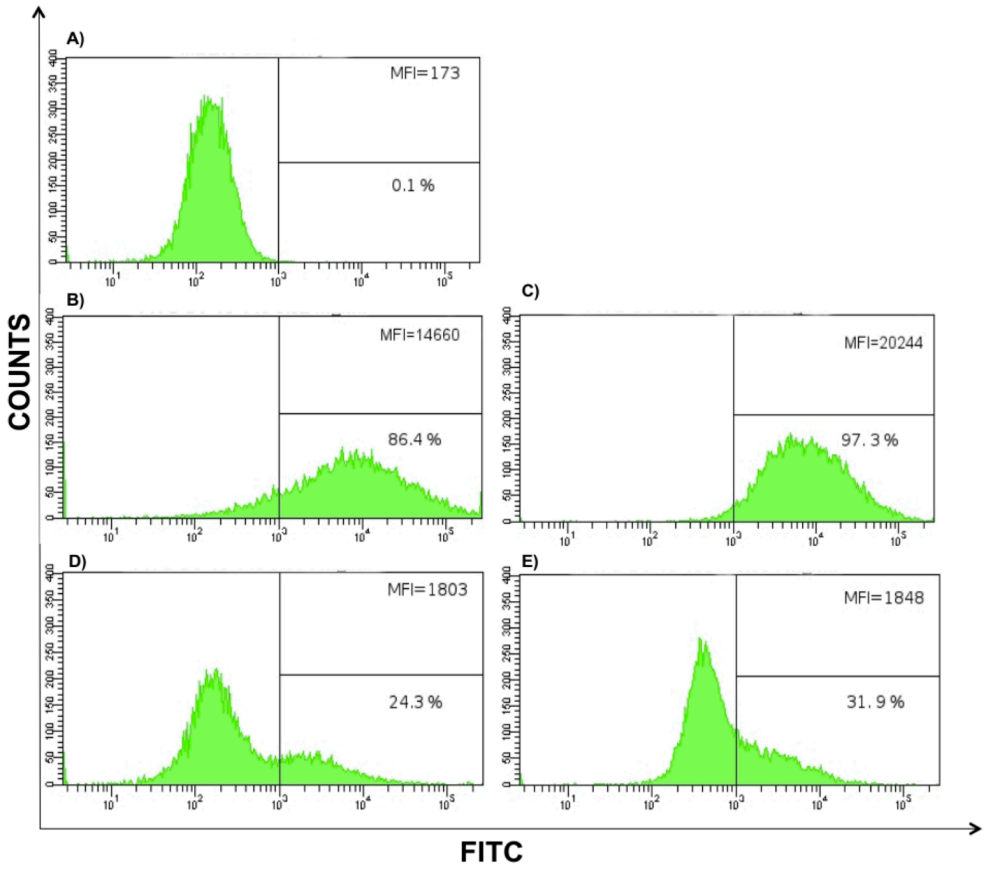

Fig 6.7. Flow cytometry histogram. Uptake of SV-140-A-FITC and SV-100-A-FITC nanoparticles were analysed by flow cytometry. The FITC labelled and SV-140-A and SV-100-A vesicles were added to the MDBK cells at different concentrations of 0.02 mg/mL and 0.04 mg/mL and incubated for 2 h. The cells were harvested and analysed by flow cytometry. Cell counts versus the FITC fluorescence are shown; (A) MDBK cells only (control), (B) SV-140-A-FITC 0.02 mg/mL, (C) SV-100-A-FITC 0.02 mg/mL, (D) SV-140-A-FITC 0.004 mg/mL, (E) SV-100-A-FITC 0.004 mg/mL. The number of cells taking up FITC is represented in percentage of total counting cells. Mean fluorescence intensity (MFI) is indicated in the panel.

6.3.4 In vitro cytotoxicity studies

The *in vitro* cytotoxicity of all the four SV was determined by trypan blue dye exclusion staining of MDBK cells. The cells were treated with three different concentrations (0.5 mg/mL, 0.1 mg/mL and 0.01 mg/mL) of SV for 20 h. As synthesised MCM-41 nanoparticles were used as a positive control for cell death and untreated cells as negative control. The cell membrane of the viable cells remains intact, hence they do not take up the trypan blue stain, whereas, the dead cells exhibit a blue colour due to the uptake of the dye via permeabilised cell membranes. The cells incubated with lower concentrations (0.1 mg/mL and 0.01 mg/mL) of all four SV

appeared comparable to the non-treated cells (Fig 6.8, b, c, e, f, h, I, k and l). However, the amino functionalised SV-140-A and SV-100-A at 0.5 mg/mL were found to have a toxic effect on the MDBK cells (Fig 6.8, g and j) in comparison to their unfunctionalised counter parts SV-140 and SV-100 (Fig 6.8, a and d).

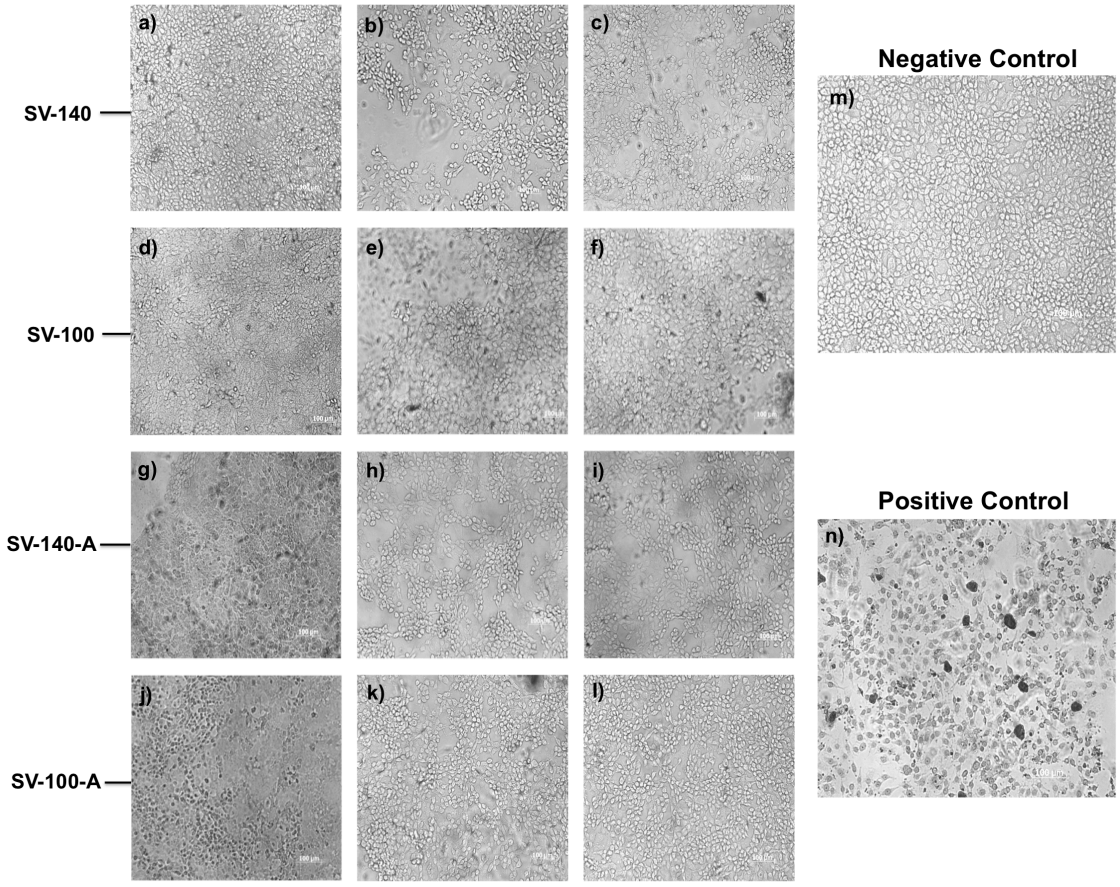

Fig 6.8. Semi-quantitative assay to determine the cytotoxicity of nanoparticles using trypan blue Staining (0.2%) of MDBK cells; (a) 0.5 mg/mL SV-140; (b) 0.1 mg/mL SV-140; (c) 0.01 mg/mL SV-140; (d) 0.5 mg/mL SV-100; (e) 0.1 mg/mL SV-100; (f) 0.01 mg/mL SV-100; (g) 0.5 mg/mL SV-140-A; (h) 0.1 mg/mL SV-140-A; (i) 0.01 mg/mL SV-140-A; (j) 0.5 mg/mL SV-100-A; (k) 0.1 mg/mL SV-100-A; (l) 0.01 mg/mL SV-100-A; (m) cells alone without nanoparticles; (n) 0.5mg/mL MCM-41 as synthesised particles. All images were taken at × 20 magnification.

The four vesicles SV-100, SV-100-A, SV-140 and SV-140-A demonstrated similar adsorption and desorption characteristics. However, SV-100-A, SV-140 and SV-140-A were found to have a marginally better adsorption capacity of the oE2 protein in comparison to SV-100 (Fig 6.4). The cellular uptake difference between the SV-140-A-FITC and SV-100-A-FITC vesicles was found to be less than 10%. Nevertheless, both amino functionalised SV-100-A and SV-140-A

were found to be toxic on the MDBK cells at a higher concentration.

Hence, based on the results from *in vitro* studies described above and exhibition of the desirable characteristics such as efficient antigen loading, cellular uptake proficiency, non-toxicity on MDBK cells at all the three concentrations, the unfunctionalised SV-140 was selected as antigen carrier for *in vivo* investigation.

6.3.5 Cell Viability

Before commencing with the animal trial with selected SV-140 as vesicle of choice, the cytotoxicity of the vaccine formulations oE2, oE2/SV-140 and oE2/SV-140 plus Quil-A, was quantified using MTT assay. Quantitative cytotoxicity analyses were conducted at three different concentrations of 0.1 mg/mL, 0.2 mg/mL and 0.01 mg/mL in MDBK cell lines. The treatment formulations were prepared similar to the injectable samples as described in the methods section. The MDBK cells were incubated with the treatment formulations for 24 h. At the higher concentration of 0.1 mg/mL the oE2, oE2/SV-140 and oE2/SV-140 plus Quil-A, the cells exhibited cell viability of >70%. However, at lower concentrations of 0.02 and 0.01 mg/mL the oE2 protein, oE2/SV-140 and oE2/SV-140 plus Quil-A the MBDK cells exhibited cell viability of >85% cell (Fig 6.9). Addition of two adjuvants Quil-A plus SV did not have a detrimental affect on the cell viability of the MDBK cells, suggesting that the nanovaccine formulations were suitable for use in animal studies.

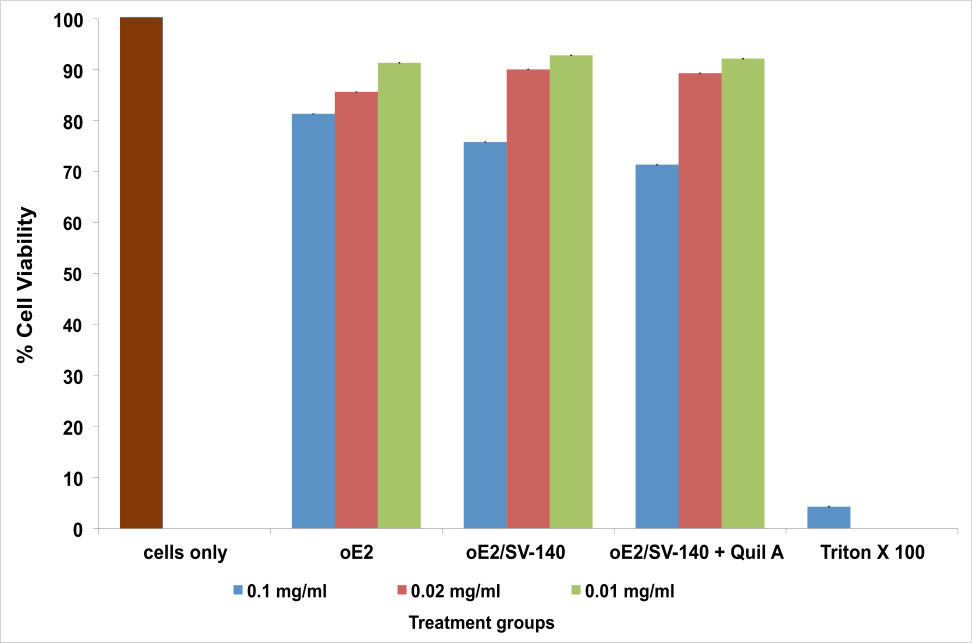

Fig 6.9. Cytotoxicity of the oE2 in PBS, SV-140, oE2 loaded SV-140 and oE2 loaded SV-140 plus Quil-A was evaluated using the MTT assay. Different concentrations of both the nanoparticles and oE2 protein were tested.

6.3.6 ELISA data

The mice were immunised with vaccine formulations comprising of unfunctionalised SV-140 vesicle as described above. The total IgG responses of the immunised mice were analysed by anti-oE2-specific ELISA, following three subcutaneous vaccine injections. The vaccine formulations were freshly prepared on the day of the injection. PI sera samples from mice were collected at the start of the trial, and subsequent sera samples were collected at two-week intervals following each injection over a 6 week period. All the mice remained healthy and in the normal weight range throughout the experiment (Fig 6.10).

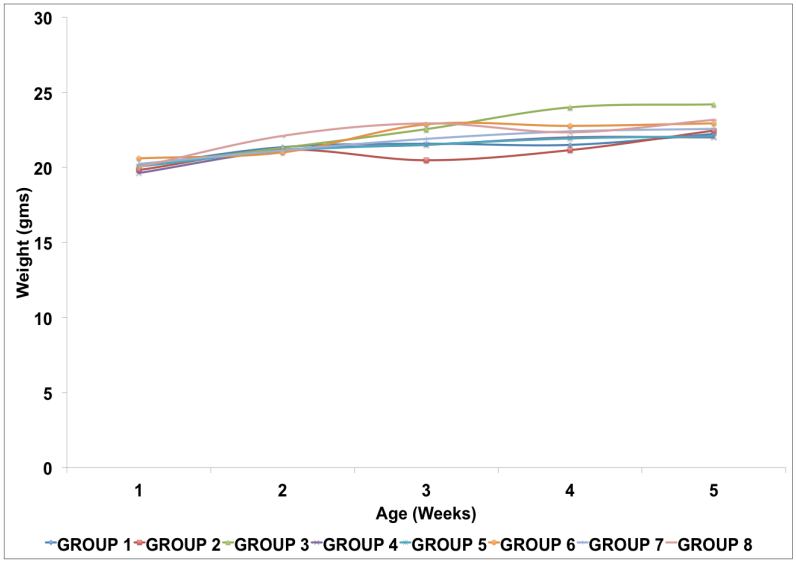

Fig 6.10. Mice weight chart, individual lines represent average of four animals per group.

The nanovaccine treatment group immunised with oE2/SV-140, without any traditional adjuvant elicited strong antibody responses end-point titres of 2.56 x 10^5 (1:256000) (Fig 6.11 B). The antibody response generated by the group injected with oE2/SV-140 was found to be stronger than the response obtained from the positive control oE2 plus Quil-A, which showed detectable oE2 specific antibody responses at an end-point titre of 3.2 x 10^4 (1:32000). Interestingly, the co-administration of two adjuvants, SV along with traditional adjuvant Quil-A, did not result in a more robust immune response, as the antibody responses generated by this group was of 6.4 x 10^4 (1:64000) (Fig 6.11 C). The IgG response elicited by oE2/SV-140 plus Quil-A appeared to be almost similar to the positive control group oE2 plus Quil-A, (Fig 6.11 A & C) however, they were both lower than that of oE2/SV-140 (Fig 6.11 B). The ELISA result from the terminal bleeds, suggest that the negative control groups receiving SV-140 vesicles plus Quil-A (Fig 6.11 D) and the unimmunised group (Fig 6.11), showed no oE2-specific antibody responses.

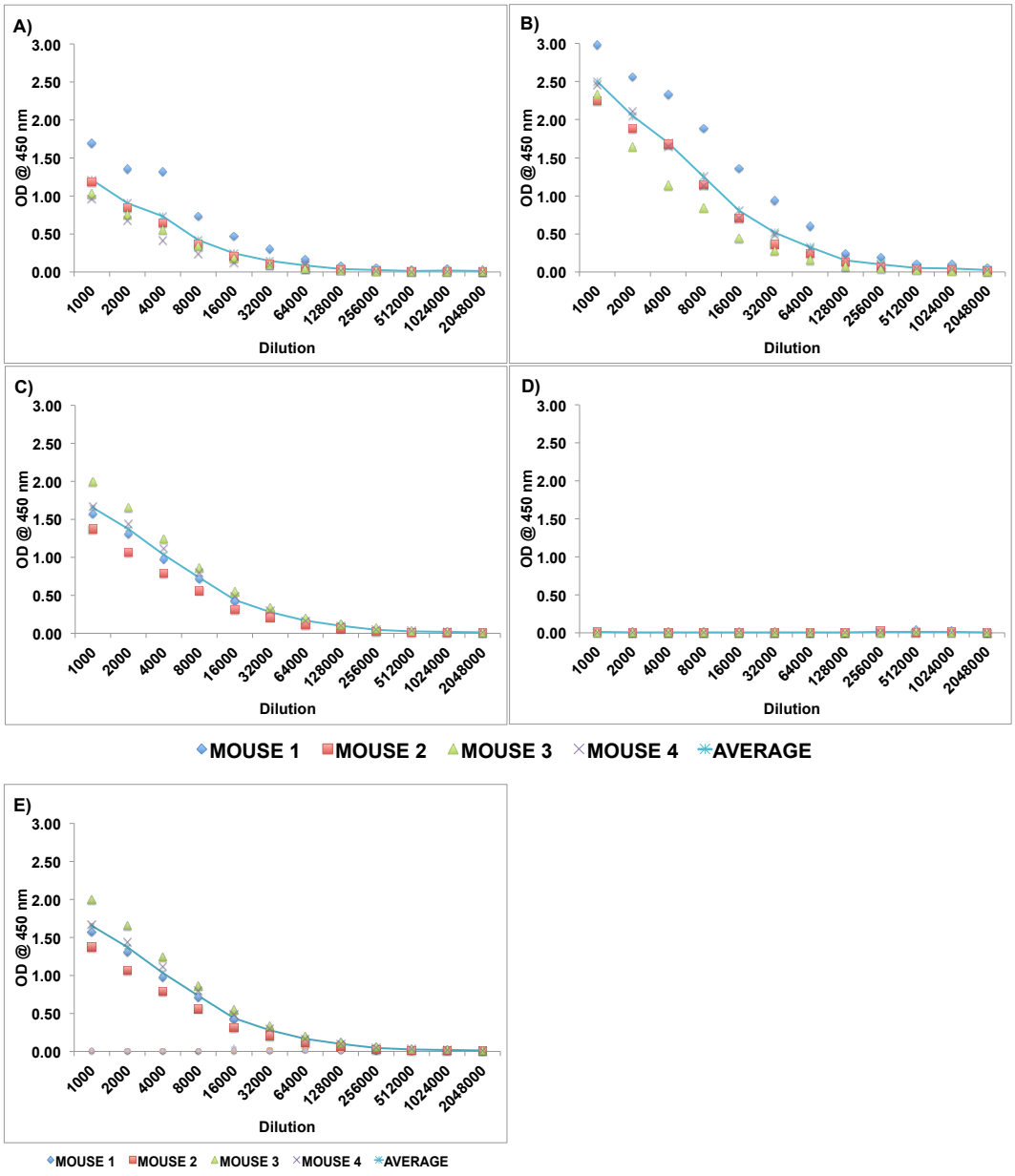

Fig 6.11. End point titer data of terminal sera bleeds (average of all 4 individual mice in each group). All the mice were administered 100 µL dose at 2 week intervals to the tail base. **A)** oE2 (50 µg) + Quil-A (10 µg); **B)** oE2 (50 µg) loaded SV-140 (250 µg); **C)** oE2 (50 µg) loaded SV-140 (250 µg) plus Quil-A (10 µg); **D)** SV-140 plus Quil-A; **E)** Unimmunised group. Sera of individual animals were diluted from 1:1000 to 1:2048000.

6.3.7 ELISPOT Assay

ELISPOT assays were used to determine the T-helper type 1 (Th1) cell mediated interferon- γ (IFN-γ) responses to oE2 antigen. Two weeks post the final immunisation; spleens from sacrificed mice were collected and harvested to obtain splenocyte cell populations. The mice receiving nanovaccine formulations oE2/SV-140 showed an excellent cell-mediated immune response to oE2

antigen as indicated by the number of cells producing Spot Forming Units (SFU). The bars in the Fig 6.12 indicate the responses to oE2 antigen. All the animals in the oE2 plus traditional adjuvant Quil-A showed a low cell-mediated immune response ranging from 499-755 SFU/million cells, in comparison to animals in oE2/SV-140 group, which produced strong responses in the range of 1954-2628 SFU/million cells. The three out of four mice vaccinated with the oE2/SV-140 plus Quil-A nanovaccine formulation, showed a low cell mediated response (512-1369 SFU/million cells) and only one animal induced a high oE2-specific response >3000 SFU/million cells. The oE2-specific response elicited by all the individual animals in the oE2/SV-140 was much stronger in comparison to the positive control group oE2 plus Quil-A as well as the oE2/SV-140 plus Quil-A group. The excellent IFN-γ response generated by oE2/SV-140 highlights the potential of SV as exceptional adjuvants and their ability to induce memory responses. The animals in the negative control groups, SV-140 plus Quil-A and the unimmunised group did not produce IFN-γ response specific to the oE2 antigen, expect for only one animal in the unimmunised group, which produced some background Th1 response (Fig 6.12).

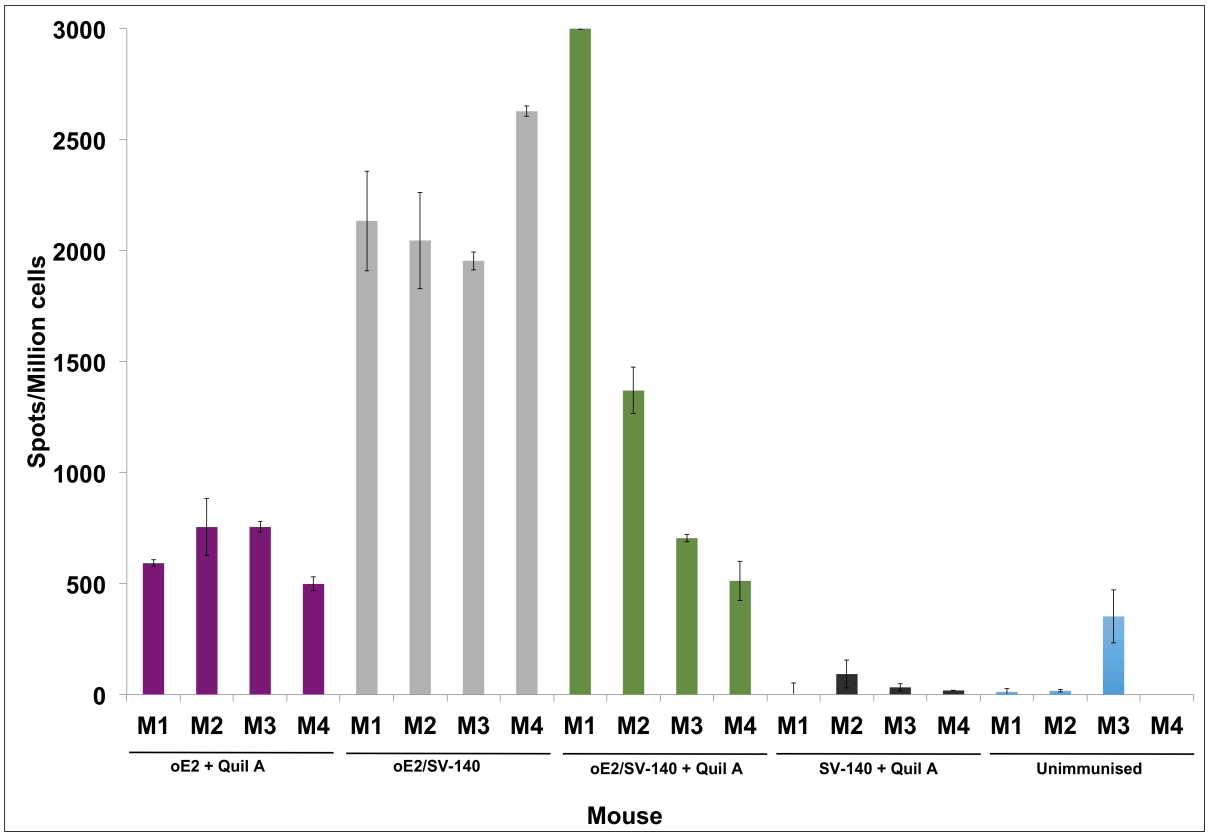

Fig 6.12. Detection of antigen specific IFN-γ secretion by ELISPOT assay of murine splenocytes from immunised mice. M1 to M4 are the individual mice in each group. The bars in the figure indicate the number of cells producing IFN-γ in response to the oE2 antigen.

6.4 Discussion

The current research was aimed at addressing the issues in delivery of subunit vaccines in terms of eliciting sustained humoral and cell-mediated response as well as overcoming the limitations of available adjuvants by improving the particle design. The rationale behind the design of SV was to minimise the use of silica to be administered as a positive step towards regulatory framework. In this paper, we report the use of SV synthesised using the two-step self-assembly approach with a uniform 50 nm particle size and precisely controlled large entrance size as well as internal cavity and thin porous shell as optimal carriers for vaccine delivery. The SV were able to maintain the integrity of vesicular structure even in the presence of entrance pores as big as 15 nm and shell wall thickness of only 6 nm. These characteristics of the SV improved the protein loading and extended release of the antigen, allowing a sustained immune response.

To demonstrate that this new generation of SV can efficiently deliver a real virus antigen, we chose the BVDV-1 oE2 protein due to the economic significance associated with the disease throughout the world. Pestigard® (Zoetis) is the only BVDV vaccine approved for use in Australia. This vaccine is an inactivated viral vaccine with a shelf-life of one month after opening and needs to be refrigerated. It also has to be administered as two initial doses, 4-6 weeks apart and then an annual booster dose thereafter. BVDV vaccine Bovilis BVD by Merck is available in the UK; this inactivated vaccine contains BVDV strain C86, which also requires an annual booster dose. The shelf-life of this vaccine is 18 months when stored at +2 to +8 °C; however, the shelf-life is reduced to 10 h once the vaccine bottle is opened. [39] The neutralising antibodies produced by E2 protein after natural infection or vaccination is considered as the most important protective mediator against subsequent BVDV infection. [40-42] In our laboratory, generation of soluble and endotoxin-free oE2 using an *E. coli* expression system has been well established. [43, 44]

The adsorption capacity of proteins to the nanoparticles is greatly dependant on the physicochemical characteristics of the proteins as well as the nanoparticles. Proteins with the hydrodynamic diameter that is smaller than the pore diameter can easily enter the mesopores and show higher loading capacity, while the ones with larger diameter adsorb on the outer surface of the nanoparticles. [45] Previously, we reported the use of HMSA surface functionalised with amino groups for the development of BVDV-1 E2 nanovaccine. [24] However, the amount of protein that could be loaded on the HMSA, which was only 80 μg of the oE2 protein per mg of HMSA (particle size 120 nm). Additionally, most of the protein was possibly presented on the outer surface on

HMSA due to small entrance size of 2 nm to 3 nm. The four SV (particle size 50 nm) used in the current study, with different entrance sizes (5.7/5.9 and 16 nm) enhanced the oE2 protein loading efficiency by three times. The oE2 protein loading on SV-140, SV-140-A, SV-100 and SV-100-A vesicles was approximately in the range of 216 to 249 μg protein/mg of vesicles after overnight adsorption (Fig 6.4). As determined by DLS the hydrodynamic size of oE2 is 7.1 nm. [44] Utilising the iTasser protein structure prediction software [46, 47] and the recent publication on E2 crystal structure, 2YQ2[48] as a structural template, oE2 is hypothesised to be an elongated protein with an estimated physical size length of 12-13 nm and a width of 3-4 nm. [24] Since the entrance size of the SV is in the range of 5.7 nm to 16 nm (Table 6.2), which is larger than the estimated width size of the oE2, which supports our hypothesis that the protein gets adsorbed on the internal as well as external wall of the vesicles leading to higher loading capacity.

The *in vitro* release studies on the oE2 loaded SV at 37 °C in PBS buffer indicated that protein once bound to the vesicles does not dissociate easily. SLS is the most commonly used surfactant in dissolution media for poorly water-soluble drugs to facilitate the significant release of drugs. [49] The release profile of the drugs/vaccines can be adjusted by changing the concentration of the surfactant in the medium. We observed release of the oE2 protein in the presence of surfactant 0.1% (w/v) SLS in the PBS buffer (Fig 6.6) after only 5 minutes. oE2 protein was not observed in the pellet of the four SV after 24 h of desorption 0.1% (w/v) SLS buffer therefore indicating that >95% of the oE2 protein got released from the vesicles. This confirms the usefulness of SV as both an adjuvant and delivery vehicles, with the ability of sustained release of the bound protein. Different researchers observed similar findings as they found that the *in vitro* dissolution rate of curcumin formulations improved in the presence of 0.5% w/v SLS as a surfactant. [50, 51]

Cytotoxicity of nanoparticles is an important parameter to consider while developing vaccines. Since, the thiocyanate group of FITC is highly aminoreactive, the amino functionalised SV were labelled with the fluorescence dye FITC. The cellular uptake by the MDBK cells was noticeably higher with SV-100-A-FITC compared to SV-140-A-FITC (Fig 6.7). The higher MFI values of the FITC SV-100-A can be attributed partly due to the difference in the surface characteristics confirming that the surface, particle characteristics along with the net charge of the carrier play a significant role in cellular uptake. In previous reports, MSNs functionalised by aminofluorescein [52] and FITC tagged HMSNs [53] were efficiently taken up into the cell cytoplasm after intracellular uptake in HeLa cell lines. A study, demonstrated that the cellular uptake was found to be two times higher for 50 nm sized MSNs compared to 30 nm MSNs, while for larger sized

MSNs (110 nm, 280 nm and 170 nm) the cellular uptake was found to be proportionally lower. [54] The 50 nm SV used in the current study were of optimal size for cellular uptake. The pore structure of MSNs is also known to have a great influence on biocompatibility and biological response. [55] The *in vitro* cytotoxic effects of MSNs in various cell lines have been established [56-59]; at lower concentrations MSNs have been found to be non-toxic, but at higher concentrations, they can have a toxic effect on the cells. [60-62] We tested the cytotoxicity of all the four SV and observed similar results, as the amino functionalised SV-140-A and SV-100-A at the higher concentration of 0.5 mg/mL were found to have a toxic effect on the cells compared to its unfunctionalised counter parts SV-140 and SV-100 (Fig 6.8). Even though, the cellular uptake was higher with the SV-100-A-FITC, the cytotoxicity results indicate that both the amino functionalised vesicles SV-140-A and SV-100-A were found to be more toxic on the MDBK cells. Hence, to demonstrate that the SV can efficiently deliver the real viral antigen and act as excellent adjuvants and based on the results from the adsorption, release, cellular uptake and cytotoxicity studies, the unfunctionalised SV-140 vesicle was selected for mice immunisations. However, before proceeding with the animal trial, quantitative toxicity analyses were conducted on the nanovaccine formulations to be used in the animal trial. At lower concentrations of 0.02 mg/mL and 0.01 mg/mL the nanovaccine treatment groups were found to have the least toxic effect on the MDBK cells viability (Fig 6.9). This also reiterates the importance of high loading, which reduces the dose of SV keeping it well within its toxicity limits.

The process of generating an immune response to a vaccine greatly depends on the efficient uptake of the antigen by dendritic cells and subsequent presentation of the antigen within the major lymphoid organs. Silica nanoparticles can protect the antigen and also slowly release the antigen *in vivo*. [63] To date there are very few studies that have reported the use of silica nanoparticles for *in vivo* delivery of proteins. In a study, BSA adsorbed/encapsulated in SBA-15 (a silica cylinder mesostructure of 2 μm in length) particles were administered via intramuscular and oral routes in high and low antibody responder mice lines; the SBA-15 particles proved to efficient adjuvants as well as delivery vehicles as the protein loaded nanoparticles both humoral and cell-mediated immunity in mice. [33]

In the past, we have reported the induction of humoral and cell mediated immune responses by amino functionalised MSNs as well as HMSAs [24, 26], however due to the low loading of proteins obtained on the nanoparticles, a direct comparison between the positive control group comprising of conventional adjuvant and the nanovaccine treatment could not be performed. In the

current research study, the improvement in the particle design enabled us to directly compare the immune responses generated by the conventional adjuvant used in the positive control group (oE2 plus Quil-A) and the nanovaccine treatment group. Moreover, variation in one parameter such as the antigen or silica nanoparticles may change the generation of the overall immune response. [29]

Hence, to clearly understand the efficacy of SV as adjuvants on the induction of immune responses as well as the significance of using two adjuvants in one vaccine formulation, three treatment groups oE2 plus Quil-A, oE2/SV-140 and oE2/SV-140 plus Quil-A were tested (Table 6.1). All the animals remained healthy throughout the duration of the trial and none of the nanovaccine formulations caused localised skin redness or reaction at the site of the injection, indicating that the SV were very well tolerated in mice. The treatment groups injected with oE2/SV-140 (50 μg/250 μg) induced excellent antibody response at 10^5 titre, which was higher than the positive control group oE2 (50 μg) plus Quil-A (10 μg) (10^4 titre) as well as the responses generated by the mice treated with oE2/HMSA (10^3 titre) [24] . In addition to elicitation of the humoral response, the oE2/SV-140 induced a stronger and higher memory response (1954-2628 SFU/million cells) compared to the group treated with Quil-A (512-1369 SFU/million cells). For the first time, we have shown that the BVDV oE2 loaded SV induced stronger Th1 as well as Th2 responses compared to the traditional adjuvant. This is a significant finding, as it shows that SV synthesised with a large entrance size can act as efficient delivery vehicles plus strong adjuvants, with a potential to remove the use of conventional adjuvants in a vaccine formulation.

Adjuvants act as immunostimulators or antigen delivery vehicles, Quil-A is known to initiate T-cell mediated immune response and from our previous experiments we know that silica nanoparticles have the ability to induce both antibody and T-cell mediated responses. [24-26] Immunisation of rats with the combination of tetanus toxoid antigen with biodegradable nanoparticles and alum induced a rapid induction of antibody response. However, administration of single injection of tetanus toxoid antigen with nanoparticles alone or tetanus toxoid antigen with Alum did not induce a stronger systemic IgG response. [64]

Few reports have highlighted the synergistic effect of vaccine adjuvants when they are used in combinations. Adjuvants like liposomes and microspheres when mixed with mineral oil have shown to have a synergistic effect. [65] Therefore, we hypothesised that co-administration of Quil-A and SV would induce robust immune responses. The mechanism of action of saponins is to interact with APCs to induce production of cytokines such as interleukins and interferons to

facilitate immunostimulant effects. [66, 67] Secondly, the small sized (50 nm) SV would create a 'slow release' effect at the site of injection and provide sufficient time for the antigen to interact with the macrophages and APCs. However, this was not the case, as the total antibody responses as well as the cell-mediated responses generated by the co-administration of Quil-A and SV were lower than oE2/SV-140. This suggests that Quil-A and SV may have failed to show a synergistic effect on the induction of strong immune responses. The presence of two strong adjuvants such as Quil-A and SV in one formulation may have resulted in too high responses and the immune system didn't cope well. Further studies are required to elucidate this finding.

6.5 Conclusion

In conclusion, the rationally designed SV with thin shell wall, large cavity and entrance size, improved the protein adsorption and release. The oE2/SV-140 formulation induced higher anti-oE2 IgG as well as IFN-γ responses compared to the positive control group oE2 plus Quil-A, demonstrating the potential of SV as both efficient vaccine delivery vehicles and potent adjuvants. The large internal cavity acts as a high capacity reservoir for biologics such as proteins, which are easily loaded through the large entrance in the vesicle walls. The slow release of vaccine means that larger than normal amounts can be delivered in a single dose as not all vaccine is bioavailable on administration. The size of the vesicle pores can be tailored for a specific release rate and specific molecules. The work identifies the use of SV towards the development of a new platform technology for safer and more effective subunit vaccines.

6.6 Acknowledgements

The work was facilitated by Queensland Government Research Partnerships grant. The PhD support scholarship of Karishma T. Mody from Queensland Alliance of Agriculture and Food Innovation, The University of Queensland is gratefully acknowledged. We thank Prof. Rajiv Khanna and Dr. Corey Smith for the use of the ELISPOT reader system at The Queensland Institute of Medical Research.

6.7 References

1. Zhang J, Karmakar S, Yu M, Mitter N, Zou J, et al. (2014) Synthesis of silica vesicles with controlled entrance size for high loading, sustained release, and cellular delivery of therapeutical proteins. Small 10: 5068-5076.
2. Nelson G, Marconi P, Periolo O, La Torre J, Alvarez MaA (2012) Immunocompetent truncated E2 glycoprotein of bovine viral diarrhea virus (BVDV) expressed in Nicotiana tabacum plants: A candidate antigen for new generation of veterinary vaccines. Vaccine 30: 4499-4504.
3. Houe H (1999) Epidemiological features and economical importance of bovine virus diarrhoea virus (BVDV) infections. Veterinary Microbiology 64: 89-107.
4. Hessman BE, Fulton RW, Sjeklocha DB, Murphy TA, Ridpath JF, et al. (2009) Evaluation of economic effects and the health and performance of the general cattle population after exposure to cattle persistently infected with bovine viral diarrhea virus in a starter feedlot. American Journal of Veterinary Research 70: 73-85.
5. Services V (December 2007) Bovine Viral Diarrhea Virus In: health CfEaA, editor. Safeguarding American Agriculture. Colorado: United States Department of Agriculture.
6. Gard JA, Givens MD, Stringfellow DA (2007) Bovine viral diarrhea virus (BVDV): Epidemiologic concerns relative to semen and embryos. Theriogenology 68: 434-442.
7. Donis RO, Corapi W, Dubovi EJ (1988) Neutralizing monoclonal antibodies to bovine viral diarrhoea virus bind to the 56K to 58K glycoprotein. Journal of General Virology 69 (Pt 1): 77-86.
8. Patterson R, Nerren J, Kogut M, Court P, Villarreal-Ramos B, et al. (2012) Yeast-surface expressed BVDV E2 protein induces a Th1/Th2 response in naive T cells. Developmental & Comparative Immunology 37: 107-114.
9. Pecora A, Aguirreburualde MS, Aguirreburualde A, Leunda MR, Odeon A, et al. (2012) Safety and efficacy of an E2 glycoprotein subunit vaccine produced in mammalian cells to prevent experimental infection with bovine viral diarrhoea virus in cattle. Veterinary Research Communications.
10. Ciulli S, Galletti E, Battilani M, Galligioni V, Prosperi S (2009) Analysis of variability and antigenic peptide prediction of E2 BVDV glycoprotein in a mucosal-disease affected animal. Veterinary Research Communications 33 Suppl 1: 125-127.

11. Bolin SR, Ridpath JF (1996) Glycoprotein E2 of bovine viral diarrhea virus expressed in insect cells provides calves limited protection from systemic infection and disease. Archives of Virology 141: 1463-1477.
12. Skwarczynski. M, Toth. I (2011) Peptide-Based Subunit Nanovaccines. Curr Drug Deliv 8: 282-289.
13. Foged C (2011) Subunit vaccines of the future: the need for safe, customized and optimized particulate delivery systems. Ther Deliv 2: 1057-1077.
14. Wen ZS, Xu YL, Zou XT, Xu ZR (2011) Chitosan nanoparticles act as an adjuvant to promote both Th1 and Th2 immune responses induced by ovalbumin in mice. Mar Drugs 9: 1038-1055.
15. Kensil CR, Kammer R (1998) QS-21: a water-soluble triterpene glycoside adjuvant. Expert Opinion on Investigational Drugs 7: 1475-1482.
16. Skene CD, Sutton P (2006) Saponin-adjuvanted particulate vaccines for clinical use. Methods 40: 53-59.
17. Reed SG, Bertholet S, Coler RN, Friede M (2009) New horizons in adjuvants for vaccine development. Trends in Immunology 30: 23-32.
18. Chwalek M, Lalun N, Bobichon H, Ple K, Voutquenne-Nazabadioko L (2006) Structure-acitivity relationships of some hederagenin diglycosides: Haemolysis, cytotoxicity and apoptosis induction. Biochim Biophys Acta 1760: 1418-1427.
19. Freund J, Casals J, Hosmer E (1937) Sensitization and antibody formation after injection of tubercle bacili and paraffin oil. Proc Soc Exp Biol Med 37: 509-513.
20. HogenEsch H (2002) Mechanisms of stimulation of the immune response by aluminum adjuvants. Vaccine 20, Supplement 3: S34-S39.
21. Bomford R, Stapleton M, Winsor S, McKnight A, Andronova T (1992) The control of the antibody isotype response to recombinant human immunodeficiency virus gp120 antigen by adjuvants. AIDS Research and Human Retroviruses 8: 1765-1771.
22. Comoy EE, Capron A, Thyphronitis G (1997) In vivo induction of type 1 and 2 immune responses against protein antigens. International Immunology 9: 523-531.
23. Popat A, Jambhrunkar S, Zhang J, Yang J, Zhang H, et al. (2014) Programmable drug release using bioresponsive mesoporous silica nanoparticles for site-specific oral drug delivery. Chemical Communications 50: 5547-5550.
24. Mahony D, Cavallaro AS, Mody KT, Xiong L, Mahony TJ, et al. (2014) In vivo delivery of bovine viral diahorrea virus, E2 protein using hollow mesoporous silica nanoparticles. Nanoscale 6: 6617-6626.

25. Mody KT, Mahony D, Cavallaro AS, Stahr F, Qiao SZ, et al. (2014) Freeze-drying of ovalbumin loaded mesoporous silica nanoparticle vaccine formulation increases antigen stability under ambient conditions. International Journal of Pharmaceutics 465: 325-332.
26. Mahony D, Cavallaro AS, Stahr F, Mahony TJ, Qiao SZ, et al. (2013) Mesoporous Silica Nanoparticles Act as a Self-Adjuvant for Ovalbumin Model Antigen in Mice. Small 9: 3138-3146.
27. Popat A, Hartono SB, Stahr F, Liu J, Qiao SZ, et al. (2011) Mesoporous silica nanoparticles for bioadsorption, enzyme immobilisation, and delivery carriers. Nanoscale 3: 2801-2818.
28. Popat A, Liu J, Hu Q, Kennedy M, Peters B, et al. (2012) Adsorption and release of biocides with mesoporous silica nanoparticles. Nanoscale 4: 970-975.
29. Mody KT, Popat A, Mahony D, Cavallaro AS, Yu C, et al. (2013) Mesoporous silica nanoparticles as antigen carriers and adjuvants for vaccine delivery. Nanoscale: 5167-5179.
30. Liu T, Liu H, Fu C, Li L, Chen D, et al. (2013) Silica nanorattle with enhanced protein loading: A potential vaccine adjuvant. Journal of Colloid and Interface Science 400: 168-174.
31. Vallhov H, Kupferschmidt N, Gabrielsson S, Paulie S, Stromme M, et al. (2012) Adjuvant properties of mesoporous silica particles tune the development of effector T cells. Small 8: 2116-2124.
32. Yague C, Moros M, Grazu V, Arruebo M, Santamaria J (2008) Synthesis and stealthing study of bare and PEGylated silica micro- and nanoparticles as potential drug-delivery vectors. Chemical Engineering Journal 137: 45-53.
33. Carvalho LV, Ruiz Rde C, Scaramuzzi K, Marengo EB, Matos JR, et al. (2010) Immunological parameters related to the adjuvant effect of the ordered mesoporous silica SBA-15. Vaccine 28: 7829-7836.
34. Slowing II, Trewyn BG, Lin VSY (2007) Mesoporous Silica Nanoparticles for Intracellular Delivery of Membrane-Impermeable Proteins. Journal of the American Chemical Society 129: 8845-8849.
35. Park HS, Kim CW, Lee HJ, Choi JH, Lee SG, et al. (2010) A mesoporous silica nanoparticle with charge-convertible pore walls for efficient intracellular protein delivery. Nanotechnology 21: 225101.
36. Guo HC, Feng XM, Sun SQ, Wei YQ, Sun DH, et al. (2012) Immunization of mice by Hollow Mesoporous Silica Nanoparticles as carriers of Porcine Circovirus Type 2 ORF2 Protein. Virology Journal 9: 108.
37. Yu MH, Zhang J, Yuan P, Wang HN, Liu N, et al. (2009) Preparation of Siliceous Vesicles with Adjustable Sizes, Wall Thickness, and Shapes. Chemistry Letters 38: 442-443.

38. Zhang J, Yu MH, Yuan P, Lu GQ, Yu CZ (2011) Controlled release of volatile (-)-menthol in nanoporous silica materials. Journal of Inclusion Phenomena and Macrocyclic Chemistry 71: 593-602.

39. Bovilis BVD. [cited 16.04.12]. Merck.

40. Ridpath JE, Neill JD, Endsley J, Roth JA (2003) Effect of passive immunity on the development of a protective immune response against bovine viral diarrhea virus in calves. American Journal of Veterinary Research 64: 65-69.

41. Howard CJ, Clarke MC, Brownlie J (1989) Protection against respiratory infection with bovine virus diarrhoea virus by passively acquired antibody. Veterinary Microbiology 19: 195-203.

42. Howard CJ, Clarke MC, Sopp P, Brownlie J (1994) Systemic vaccination with inactivated bovine virus diarrhoea virus protects against respiratory challenge. Veterinary Microbiology 42: 171-179.

43. Cavallaro AS, Mahony D, Commins M, Mahony TJ, Mitter N (2011) Endotoxin-free purification for the isolation of Bovine Viral Diarrhoea Virus E2 protein from insoluble inclusion body aggregates. Microb Cell Fact 10: 57.

44. Cavallaro A, Mahony D, Mody K, Mahony T, Mitter N (2013) Lots of Bovine Viral Diarrhoea Virus E2 protein – A Subunit Vaccine.; Ltd iP, editor: iConcept Press.

45. Katiyar A, Ji L, Smirniotis P, Pinto NG (2005) Protein adsorption on the mesoporous molecular sieve silicate SBA-15: effects of pH and pore size. Journal of Chromatography A 1069: 119-126.

46. Roy A, Kucukural A, Zhang Y (2010) I-TASSER: a unified platform for automated protein structure and function prediction. Nature Protocols 5: 725-738.

47. Zhang Y (2008) I-TASSER server for protein 3D structure prediction. BMC Bioinformatics 9: 40.

48. El Omari K, Iourin O, Harlos K, Grimes JM, Stuart DI (2013) Structure of a pestivirus envelope glycoprotein E2 clarifies its role in cell entry. Cell Rep 3: 30-35.

49. Zhao F, Malayev V, Rao V, Hussain M (2004) Effect of sodium lauryl sulfate in dissolution media on dissolution of hard gelatin capsule shells. Pharmaceutical Research 21: 144-148.

50. Jambhrunkar S, Karmakar S, Popat A, Yu M, Yu C (2014) Mesoporous silica nanoparticles enhance the cytotoxicity of curcumin. RSC Advances 4: 709-712.

51. Rahman SM, Telny TC, Ravi TK, Kuppusamy S (2009) Role of Surfactant and pH in Dissolution of Curcumin. Indian Journal of Pharmaceutical Sciences 71: 139-142.

52. Fisichella M, Dabboue H, Bhattacharyya S, Lelong G, Saboungi ML, et al. (2010) Uptake of functionalized mesoporous silica nanoparticles by human cancer cells. Journal of Nanoscience and Nanotechnology 10: 2314-2324.

53. Guo H, Qian H, Sun S, Sun D, Yin H, et al. (2011) Hollow mesoporous silica nanoparticles for intracellular delivery of fluorescent dye. Chemistry Central Journal 5: 1.

54. Lu F, Wu S-H, Hung Y, Mou C-Y (2009) Size Effect on Cell Uptake in Well-Suspended, Uniform Mesoporous Silica Nanoparticles. Small 5: 1408-1413.

55. Lee S, Yun H-S, Kim S-H (2011) The comparative effects of mesoporous silica nanoparticles and colloidal silica on inflammation and apoptosis. Biomaterials 32: 9434-9443.

56. Fisichella M, Dabboue H, Bhattacharyya S, Saboungi M-L, Salvetat J-P, et al. (2009) Mesoporous silica nanoparticles enhance MTT formazan exocytosis in HeLa cells and astrocytes. Toxicology In Vitro 23: 697-703.

57. Huang D-M, Chung T-H, Hung Y, Lu F, Wu S-H, et al. (2008) Internalization of mesoporous silica nanoparticles induces transient but not sufficient osteogenic signals in human mesenchymal stem cells. Toxicology and Applied Pharmacology 231: 208-215.

58. Heikkila T, Santos HlA, Kumar N, Murzin DY, Salonen J, et al. (2010) Cytotoxicity study of ordered mesoporous silica MCM-41 and SBA-15 microparticles on Caco-2 cells. European Journal of Pharmaceutics and Biopharmaceutics 74: 483-494.

59. Hudson SP, Padera RF, Langer R, Kohane DS (2008) The biocompatibility of mesoporous silicates. Biomaterials 29: 4045-4055.

60. Lu J, Liong M, Li Z, Zink JI, Tamanoi F (2010) Biocompatibility, Biodistribution, and Drug-Delivery Efficiency of Mesoporous Silica Nanoparticles for Cancer Therapy in Animals. Small 6: 1794-1805.

61. Slowing I, Trewyn BG, Lin VSY (2006) Effect of Surface Functionalization of MCM-41-Type Mesoporous Silica Nanoparticles on the Endocytosis by Human Cancer Cells. Journal of the American Chemical Society 128: 14792-14793.

62. Lu J, Liong M, Zink JI, Tamanoi F (2007) Mesoporous Silica Nanoparticles as a Delivery System for Hydrophobic Anticancer Drugs. Small 3: 1341-1346.

63. Slowing, II, Vivero-Escoto JL, Wu CW, Lin VS (2008) Mesoporous silica nanoparticles as controlled release drug delivery and gene transfection carriers. Adv Drug Deliv Rev 60: 1278-1288.

64. J. Raghuvanshi AM, G. P. Talwar, R. J. Levy, V. Labhasetwar, R. (2001) Enhanced immune response with a combination of alum and biodegradable nanoparticles containing tetanus toxoid. Journal of Microencapsulation 18: 723-732.

65. Esparza I, Kissel T (1992) Parameters affecting the immunogenicity of microencapsulated tetanus toxoid. Vaccine 10: 714-720.

66. Rajput ZI, Hu SH, Xiao CW, Arijo AG (2007) Adjuvant effects of saponins on animal immune responses. Journal of Zhejiang University Science B 8: 153-161.

67. Barr IG, Sjölander A, Cox JC (1998) ISCOMs and other saponin based adjuvants. Advanced Drug Delivery Reviews 32: 247-271.

7.

Silica Vesicle Nanovaccine Formulations Stimulate Long-term Immune Responses to the Bovine Viral Diarrhoea Virus E2 Protein

---

The SV-140 vesicles (particle size 50 nm, wall thickness 6 nm, perforated by pores of entrance size 16 nm and total pore volume of 0.934 cm^3g^{-1}) proved to be ideal candidates to load BVDV-1 *Escherichia coli*-expressed optimised E2 (oE2) antigen and generate immune responses. In this chapter the ability of freeze-dried (FD) as well as non-FD oE2/SV140 nanovaccine formulation to induce long-term balanced antibody and cell mediated memory responses with a shortened dosing regimen of two doses in small animal model was determined. This study was the first to show that

both non-FD and FD oE2/SV-140 induced oE2 specific antibody and cell-mediated immune responses in mice for at least six months post the final immunisation. The manuscript is submitted to PLoS ONE.

7.1 Introduction

Development of veterinary vaccines comes with a spectrum of challenges, as the storage, shipping and administration of the vaccine should be easy and also the cost of veterinary vaccine production needs to be kept low. [1] Subunit vaccines often need to be refrigerated, require addition of adjuvants and also need to be administered multiple times in order to induce long-term immunity. Therefore, to reduce the need for booster immunisations, a system needs to be developed that delivers the antigen and is also efficient as an adjuvant. Adjuvants are biomolecules that are added to vaccines to stimulate immune responses, however, only a few adjuvants have been approved for human as well as veterinary use. [2] Another issue that needs to be taken into account is transport and storage of subunit vaccines requiring cold chain storage, which can be challenging and expensive, especially in remote areas. The storage stability of the subunit vaccines can be improved by freeze-drying the vaccine formulations. Excipients such as sugars, surfactants, amino acids and polymers are typically added to the vaccine formulations to prevent degradation in the freeze-drying process and aide in the reconstitution of vaccines prior to use. [3,4]

Bovine viral diarrhoea virus 1 (BVDV-1) is a single-stranded RNA virus that is a major contributor to the bovine respiratory disease complex and other disease of cattle. BVDV-1 infection of cattle has been highly investigated in several countries as it causes tremendous economic losses to the cattle industry. [5] The major source of new BVDV-1 infection in herds is transmission from susceptible animals coming contact with secretions or body fluids of persistent infected or acutely infected animals. [6] Immunosuppression caused by BVDV-1 infection can lead to a secondary infection, which is a major cause of death in BVDV-1 infected cattle. [7] The current BVDV-1 vaccine approved for use in Australia needs to be refrigerated at 2°C to 8°C.

The structural protein, E2, from BVDV is a major immunogenic determinant and is an ideal candidate as a subunit vaccine as it can elicit neutralising antibodies. [8] In a recent study, a plant expressed truncated version of BVDV E2 fused to molecule that targets antigen presenting cells

(APCH-tE2) induced neutralising antibodies in bovines. [1] Further, BVDV E2 formulated with a combination adjuvant poly[di(sodium carboxylatoethylphenoxy)]-phosphazene, a toll-like receptor agonist and an innate defence regulator peptide (designated as TriAdj) induced antibody and cell-mediated immune responses and provided protection in animals from BVDV-2 infection. [9]

The role of mesoporous silica nanoparticles (MSNs), as antigen carriers and self-adjuvant vaccines has been investigated to develop successful vaccine delivery systems targeting BVDV-1. [10,11,12,13] In addition, we have also been focusing on developing freeze-dried (FD) silica nanoparticle based vaccine delivery systems and have demonstrated that the model protein ovalbumin (OVA) adsorbed mesoporous silica nanoparticles can be freeze-dried using 5% (w/v) trehalose and 1% PEG8000 (w/v) as excipients. [10] The FD 10 μg OVA/150 μg AM-41 formulation was tested in mice and has shown to stimulate both antibody and cell-mediated immune responses. [10,13]

Amino functionalised hollow mesoporous silica nanoparticles (HMSAs) with small pore entrance size 2 to 3.5 nm [12] were trialled for BVDV codon optimised E2 expressed in *E. coli* (oE2) adsorption (80 μg oE2 bound to per 1 mg of HMSA). Although this formulation elicited antibody as well as cell mediated responses after three injections, the constraint here was also the low antigen binding capacity of the HMSA particles. [12] To address this issue and in order to move towards our goal of generating enhanced immune response in comparison to conventional adjuvant Quil-A, we designed novel silica vesicles (SV) of 50 nm with a thin shell wall of 6 nm and controlled entrance size varying between 5.7 nm to 16 nm. These SV exhibited higher loading to Ribonuclease A with sustained release behaviour. [14] The SV-140 with an entrance size of 16 nm significantly improved the oE2 adsorption as ~250 μg oE2 bound to per mg SV. The oE2 (50 μg)/SV-140 (250 μg) induced anti-oE2 IgG (10^5) and interferon-γ (IFN-γ) responses stronger than the conventional adjuvant Quil-A (anti-oE2 IgG response of 10^4) after three subcutaneous injections. [11]

To further develop SVs as vaccine nanocarriers, which are self-adjuvanting, the first goal of the current study was to determine if the oE2/SV140 formulation previously shown to be effective in generating antibody and cell mediated responses could also stimulate long-term immune responses with reduced number of injections. The second goal was to develop FD oE2/SV140 formulation and

compare it with oE2/SV140 for addressing the issue of storability. In this work for the first time we have demonstrated that vaccination with oE2 (100 μg)/SV-140 (500 μg) elicited balanced T-helper type 2 (Th2) antibody and T-helper type 1 (Th1) cell-mediated responses not only after three weeks of two subcutaneous injections but also showed strong cell-mediated responses for at least six months after the second immunisation. In addition, we have also shown that FD oE2/SV-140 nano-formulation also induced both antibody and cell-mediated immune responses. This work for the first time clearly demonstrates the potential of silica vesicles for developing a nanovaccine with reduced number of injections, induction of long-term immune responses and improved storage.

7.2 Materials and Methods

7.2.1 Preparation of SV-140 and Adsorption of oE2 on SV-140

The SV-140 were prepared and adsorption reactions were set up as previously described and the amount of unbound oE2 protein was assessed by electrophoresis of the supernatants and the particles on SDS-PAGE gels. [11]

7.2.2 Freeze-drying process

The oE2 adsorbed SV-140 samples were centrifuged at 16.2 *g* for 5 min and the supernatants were removed. Prior to freeze-drying, oE2/SV-140 pellets were resuspended in different combinations and concentrations of excipients (Table 7.1). Samples were frozen in liquid nitrogen then placed in a freeze-dryer (Martin Christ Model LPC-32, Osterode AM Harz, Germany) at 24°C, 0.11 mbar for 22 h for drying. Freeze-dried samples were stored in a vacuum desiccator at ambient temperature (25°C). The optimal excipients trehalose (5% final concentration) and glycine (0.1% final concentration) were added to the oE2 bound vesicles and the final volume adjusted to 1 ml. The oE2 (500 μg) plus Quil-A (2mg/mL) sample was prepared in sterile injectable water without any excipients and the SV-140 alone with excipients 5% trehalose and 0.1% glycine. All the samples were freeze-dried as described in this section.

Table 7.1. Different concentrations of Trehalose and Glycine tested to freeze-dry oE2/SV-140.

Excipients added	0.1% Glycine	0.5% Glycine	1% Glycine
5% Trehalose	*	*	*
10% Trehalose	*	*	*
20% Trehalose	*	*	*

7.2.3 Western hybridisation

Following SDS-PAGE electrophoresis the oE2 protein in the nanovaccine formulations was detected using Western blot hybridisation as previously described. [12]

7.2.4 Reconstitution and transmission electron microscope (TEM) and scanning electron microscope (SEM) of lyophilised samples

Samples were reconstituted in 1 mL water. The physical characteristics of the freeze-dried vesicles in solution were observed using transmission electron microscopy (TEM) and scanning electron microscopy (SEM) before and after reconstitution the freeze-drying preparations.

7.2.5 Ethics Statement

All procedures were approved by The University of Queensland, Ethics Committee, (Approval No: 2012001137) as required by the Animal Care and Protection Act (2001) and The Australian Code for the Care and Use of Animals for Scientific Purposes (8th Edition). [21]

7.2.6 Immunisation studies conducted in mice

C57BL/6J mice were purchased from and housed in the Biological Resource Facility, The University of Queensland, Brisbane, Australia under specific pathogen-free conditions. Eight week old female mice were housed in HEPA-filtered cages with eight animals per group in an environmentally controlled area with a cycle of 12 h of light and 12 h of darkness. Food and water were given *ad libitum*.

Pre-immunisation (PI) blood samples were collected and processed; immunisations were prepared and administrated as detailed in [11]. The conventional adjuvant Quil-A (Superfos Biosector, Vedback, Denmark) was resuspended at 2 mg/mL in sterile injectable water (Pfizer**,** Brooklyn, USA). The injectable doses were administered to investigate the induction of immune responses and the treatment groups received injections as mentioned in Table 7.2. Two injections were administered at 3 week intervals to all the treatment groups except for the unimmunised group. Four mice from each group were sacrificed 21 days after the final immunisation. Blood samples from the remaining four mice were collected every four weeks via tail bleeds for up to six months and at the end of the trial period animals were sacrificed. The animals were weighed and monitored for general health once a week. All the animals were assessed weekly and they remained in good health throughout the duration of the study.

Table 7.2. Immunisation groups in mice trial. All doses were administered subcutaneously at the tail base.

Group	Prototype vaccine/Injection Dose
1	oE2 (100 μg) + Quil-A (10 μg)
2	FD oE2 (100 μg) + Quil-A (10 μg)
3	oE2 (100 μg) / SV-140 (500 μg)
4	FD oE2 (100 μg) / SV-140 (500 μg)
5	FD SV-140 (500 μg)
6	Unimmunised

7.2.7 Enzyme-Linked ImmunoSorbent Assay (ELISA) protocol

The detection of oE2-specific antibodies were performed by coating microtitre plates (96 well, Nunc, Maxisorb, Roskilde, Denmark) with oE2 antigen solution (2 ng/μL, 50 μL) in PBS overnight at 4°C. The coating solution was removed and the plates were washed once with PBS-T (1x PBS, 0.1% Tween-20, Sigma-Aldrich) and blocked with Bovine Serum Albumin (5%, Sigma-Aldrich) and skim milk (5%, Fonterra, Auckland, New Zealand) in 200 μL PBS for 1 h with gentle shaking at RT. Plates were washed three times with PBS-T.

Mouse sera samples were diluted from 1:100 to 1:6400 in 50 μL PBS and each dilution was added to the wells of the blocked plates followed by incubation for 2 h at RT. To detect mouse antibodies HRP conjugated polyclonal sheep anti-mouse IgG antibodies (Chemicon Australia, Melbourne, VIC, Australia) diluted in PBS to 1:50,000 were added to each well and incubated for 1 h at RT with gentle shaking. Plates were washed three times in PBS-T. TMB substrate (100 μL, Life Technologies) was added to each well and incubated for 15 min at RT; 100 μL of 1N HCl was added to the wells to stop the chromogenic reaction. The plates were read at 450 nm on the BioTek microplate reader (Winooski, US).

7.2.8 Isolation of murine splenocytes and enzyme-linked immunosorbent spot (ELISPOT) Assay

Spleens were aseptically removed following euthanasia from the four animals sacrificed at three weeks and the other four at six months after the final immunisation; the collected spleens were processed as previously described. [11]

7.2.9 Immunohistochemistry (IHC)

Spleen sections were collected from the sacrificed mice at both the time points three weeks and six months. A part of the spleen was dissected and frozen in OCT embedding medium and 5 µm sections were cut using Hyrax C60 cryostat. The slides with cryosections were fixed in cold ethanol on ice for 8 min and then dried at RT for 20 min. The slides were then washed 3 x 5 min in PBS, left to dry at RT for 20 min and using a Dako pen circles were marked around the sections. The sections were then incubated overnight with the blocking buffer (PBS containing 1% BSA and 5% FBS) at 4°C. Next day, to remove the block the slides were washed for 5 min in PBS three times. The sections were then incubated with Alexa Fluor 488 Goat Anti-Mouse IgG at 1:500 for 1 h at RT in dark, the slides were then washed as previously described in PBS. To stain the nuclei of cells the sections were then incubated with DAPI for 5 min and quickly washed in PBS. The sections were mounted with ProLong® Gold Antifade mounting medium and examined under the microscope.

7.2.10 Histopathology

Heart, kidney, liver and injection sites from the sacrificed mice were collected and fixed in 10% formalin for 48 h. The organs were further processed and embedded in paraffin and 8 µm sections were cut using the Leica RM 2245 Rotary Microtome. The sections were then stained using the following haematoxylin and eosin staining procedure. Sections were first Dewaxed in xylene (3 changes of 2 min each), and then rehydrated in absolute alcohol (2 changes of 2 min each), in 90% for 2 min, in 70% for 2 min. Then washed in running tap water for 2 min and stained in haematoxylin for 3 min and again washed in running tap water for 2 min. Sections were then washed in 70% alcohol for 2 min and stained in eosin for 3 min. Sections were then washed in 95% alcohol for 2 min, then in absolute alcohol (3 changes of 2 min each). Finally, the sections were rapidly dehydrated and fixed in xylene (3 changes of 2 min each) and mounted in DePeX. The sections were then observed under the Zeiss LSM 510 META confocal microscope.

7.3 Results

7.3.1 Physicochemical properties of FD oE2 SV-140

The SV-140 particles investigated in this study have been characterised previously [11,14] and have been shown to load ~250 µg of oE2 protein adsorbed to per mg of the SV-140 vesicles. [11] Different concentrations of 5%, 10% and 20% (w/v) trehalose in combination with 0.1%, 0.5% or 1% (w/v) glycine as excipients were tested to develop FD oE2/SV-140 nanovaccine following adsorption. The samples freeze-dried with different concentrations of trehalose and glycine looked voluminous and snow-like (Fig 7.1a), as opposed to samples freeze-dried without excipients, which failed to form a freeze-dried cake (Fig 7.1b) The FD oE2/SV-140 developed with combination of 5% trehalose and 0.1% glycine as excipients reconstituted within 10 seconds on addition of 1 mL of water. However, the samples containing 10% and 20% trehalose required additional measure like shaking to obtain complete resuspension.

The SDS-PAGE analyses on the reconstituted sample freeze-dried with 5% trehalose and 0.1% glycine showed that the integrity of oE2 protein was preserved post freeze-drying (Fig 7.1c, lane 4). Furthermore, Western blot recognised the oE2 protein in the non-FD and the FD vaccine formulations (Fig 7.1d, lane 3 and 4).

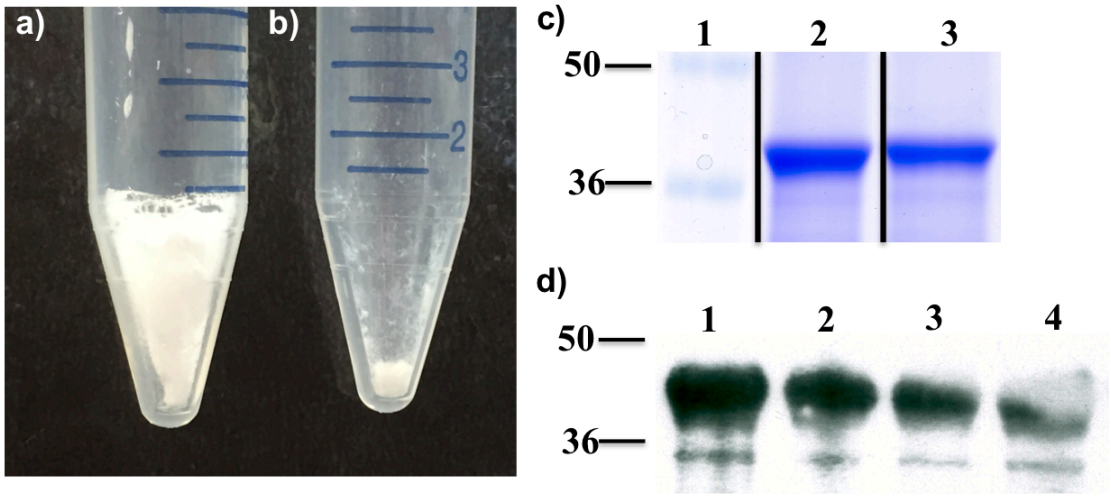

Fig 7.1: Photograph of FD oE2/SV-140 **a)** with 5% trehalose and 0.1% glycine; **b)** without excipients; **c)** SDS PAGE - adsorption of oE2 on SV-140, lane 1 – marker, lane 2 – oE2/SV-140 pellet, lane 3 – FD oE2/SV-140 pellet; **d)** Western hybridisation analysis of oE2 in the vaccine formulations, lane 1 – oE2 protein, lane 2 – oE2 plus Quil-A, lane 3 – oE2/SV-140, lane 4 – FD oE2/SV-140.

The integrity of the vesicles following freeze-drying with 5% trehalose and 0.1% glycine was further confirmed by TEM and SEM analyses. The TEM results show that the silica vesicles remained intact and maintained their characteristic round shape and size of 50 nm post freeze-drying. Furthermore, the SEM also data indicated that the FD SV-140 and FD oE2/SV-140 samples did not suffer structural collapse (Fig 7.2 c and d). The *in vivo* efficacy of the oE2/SV140 freeze-dried with 5% trehalose and 0.1% glycine and the oE2/SV-140 was investigated in a mice trial.

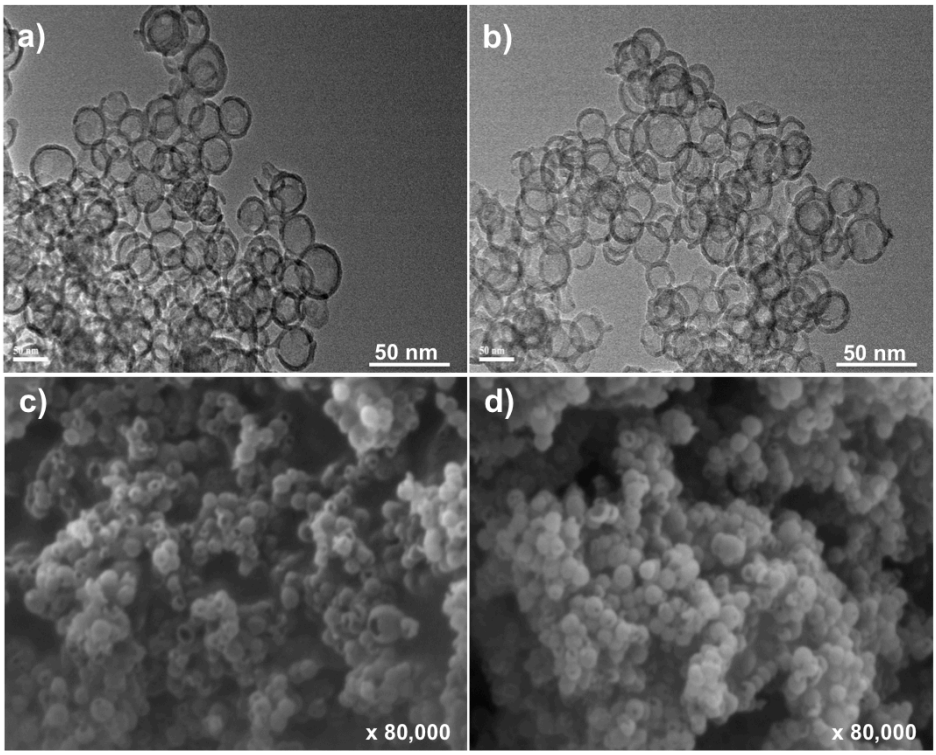

Fig 7.2: The morphology of FD SV-140 vesicles visualized by transmission electron microscope (TEM), **(a)** SV-140 and **(b)** oE2/SV-140 after lyophilisation in the presence of 5% trehalose and 0.1% glycine. The appearance of FD SV-140 by scanning electron microscope (SEM), **(c)** SV-140 **(d)** oE2/SV-140 after lyophilisation in the presence of 5% trehalose and 0.1% glycine.

7.3.2 Generation of antibody and cell-mediated immune responses three weeks post immunisation

To evaluate the efficacy of the oE2/SV-140 and FD oE2/SV-140 nanovaccine formulations, animals were immunised with two subcutaneous vaccinations at a three-week interval. The mice trial comprised of 48 animals divided into six groups and were immunised as described in Table 7.1. PI sera samples were collected prior to immunisation. Three weeks after the second vaccination sera samples were collected from all eight mice in each group and four randomly selected mice from

each group were sacrificed for the analyses of Th1 response. The total IgG responses of the immunised mice were analysed by anti-oE2-specific ELISA assays. The animals in all the treatment groups remained healthy and in the normal weight range throughout the trial period. The non-FD and FD oE2 plus Quil-A and the FD oE2/SV-140 showed a similar trend of reduction in the level of the antibody responses and were not found to be significantly different at 1:1600 dilution (Fig 7.3). The FD oE2/SV-140 induced strong responses (average OD value of 1.42). Less animal-to-animal variation was observed in the mice treated with the oE2/SV-140 nanovaccine (average OD value of 1.18) (Fig 7.3). The average OD values for oE2 plus Quil-A and FD oE2 plus Quil-A were 2.07 and 1.34 respectively. The mice receiving the FD SV-140 only and the unimmunised group showed no oE2 specific antibody responses.

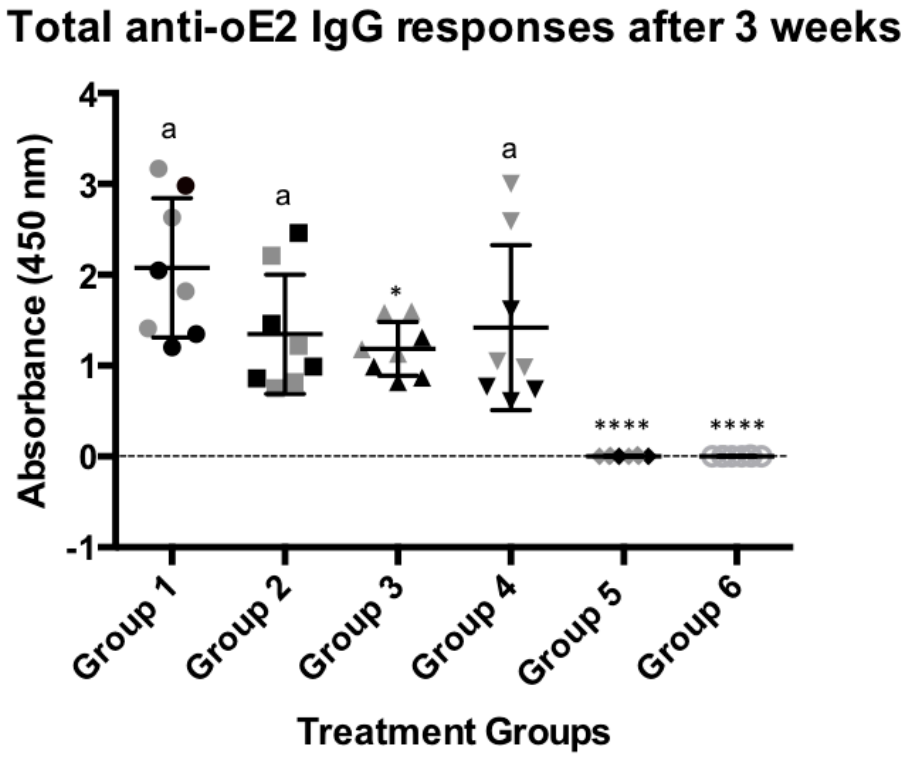

Fig 7.3: oE2-specific ELISA antibody responses in 8 mice after two subcutaneous immunisations. The individual response for each mouse is shown using a sera dilution of 1:1600. Group 1 (mouse 1 to 8) received 100 µg oE2 plus 10 µg Quil-A; Group 2 (mouse 1 to 8) received the 100 µg FD oE2 plus 10 µg Quil-A, Group 3 (mouse 1 to 8) received the oE2/SV-140 nanovaccine (100 µg oE2 adsorbed to 500 µg SV-140), Group 4 (mouse 1 to 8) received the FD oE2/SV-140 nanovaccine (100 µg oE2 adsorbed to 500 µg SV-140), Group 5 (mouse 1 to 8) received the 500 µg FD SV-140 only, Group 6 (mouse 1 to 8) was the unimmunised group and did not receive any vaccination. The

black symbols in each group represent the 4 mice that were monitored for six months. The letter 'a' denotes that the groups were not significantly different. Groups that do not share a common letter were significantly different (* low and **** high) (p<0.001, unpaired t-test analysis).

ELISPOT assays were used to determine the Th1 cell-mediated IFN-γ responses. Three weeks post the final immunisation spleens were collected from the four mice of the eight mice (mice shown as grey in Fig 7.3). The remaining four mice were retained for investigating the long-term immune responses. The number of cells producing Spot Forming Units (SFU) indicates cell-mediated immune responses to oE2 epitope. The four individual mice in oE2 plus Quil-A (551-1500 SFU/million cells) and the FD oE2 plus Quil-A (766-1500 SFU/million cells) induced strong cell-mediated responses. The oE2 specific memory responses generated by oE2/SV-140 (599-1500 SFU/million cells; average of four mice 1095 SFU/million cells) were similar to oE2 plus Quil-A (average of four mice 1094 SFU/million cells). The FD oE2/SV-140 elicited responses in the range of 222-1500 SFU/million cells; the difference in the Th1 response might be attributed to the mice-to-mice variation with 1-2 mice in each group showing a low response (Fig 7.4). As expected, the negative controls SV-140 freeze-dried with 5% trehalose and 0.1% glycine and unimmunised treatment groups did not generate oE2 specific responses (Fig 7.4).

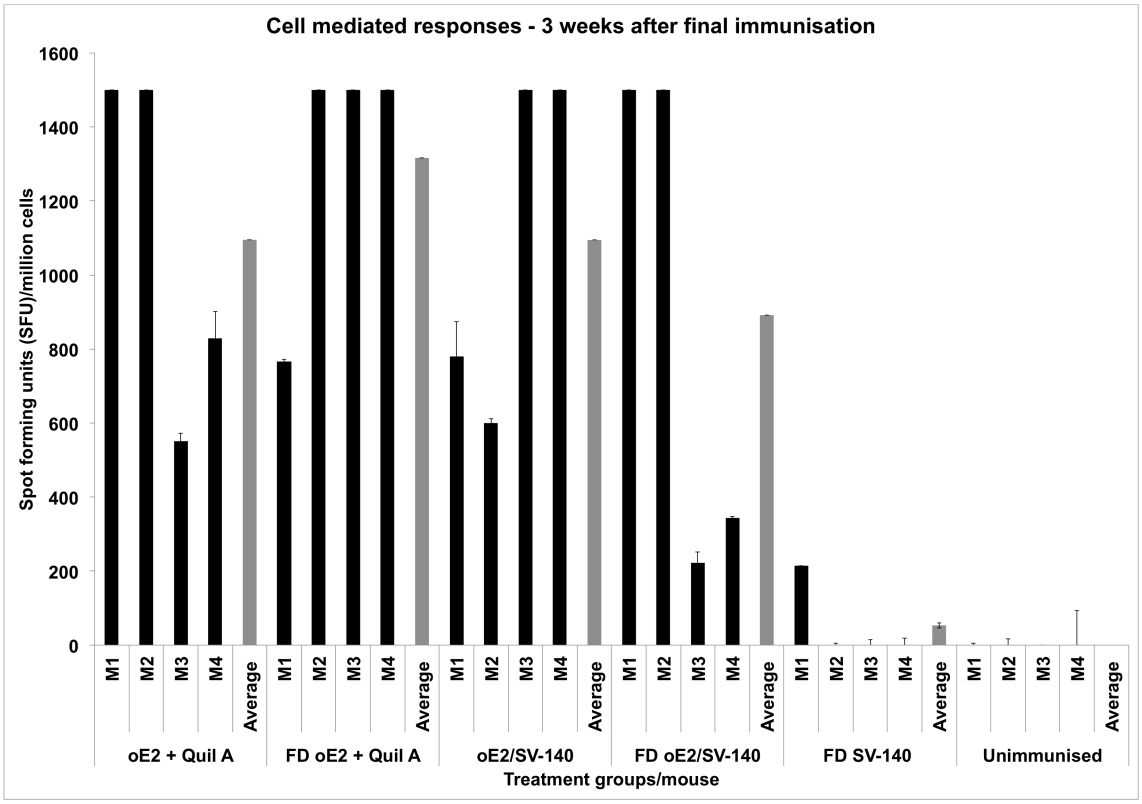

Fig 7.4: Detection of antigen specific IFN-γ secretion by ELISPOT assay of murine splenocytes from immunised mice. The black bars represent the number of cells producing IFN-γ in response to

the oE2 antigen 3 weeks after the final immunisation. The grey bars show the average for each group and M1 to M4 represent the four individual mice in each group.

7.3.3 Generation of long-term antibody and cell-mediated immune responses six months post immunisation

To monitor the long-term responses sera samples were collected once every four weeks for up to six months after the final second immunisation. oE2-specific humoral immune responses were measured by ELISA at the different time points. A gradual trend of reduction in the antibody responses generated by the oE2 injected with conventional adjuvant Quil-A as well as SV-140 was observed at 7 weeks, 11 weeks, 15 weeks and 19 weeks (Fig 7.5). Antibody responses to the oE2 epitope generated by the oE2 plus Quil-A, FD oE2 plus Quil-A, oE2/SV-140 as well as FD oE2/SV-140 reduced significantly by the end of six months, however, detectable level of antibody responses were still generated at 1:1600 dilution by both oE2/SV-140 (average OD value of 0.19) and FD oE2/SV-140 (average OD value of 0.13, Fig 7.6) at the six month time point. The oE2 plus Quil-A induced strong antibody responses (average OD value of 0.68), which could be due to the two mice in this group showing higher response. The FD oE2 plus Quil-A also showed high antibody responses (average OD values of 0.43). The FD SV-140 alone and the unimmunised treatments did not generate oE2 specific antibody responses. This is an important finding as for the first time we have demonstrated that the oE2 adsorbed SV-140 induced long-term antibody responses in mice and also that freeze-drying the oE2/SV-140 nanovaccine with 5% trehalose and 0.1% glycine maintained the immunological integrity of oE2 protein.

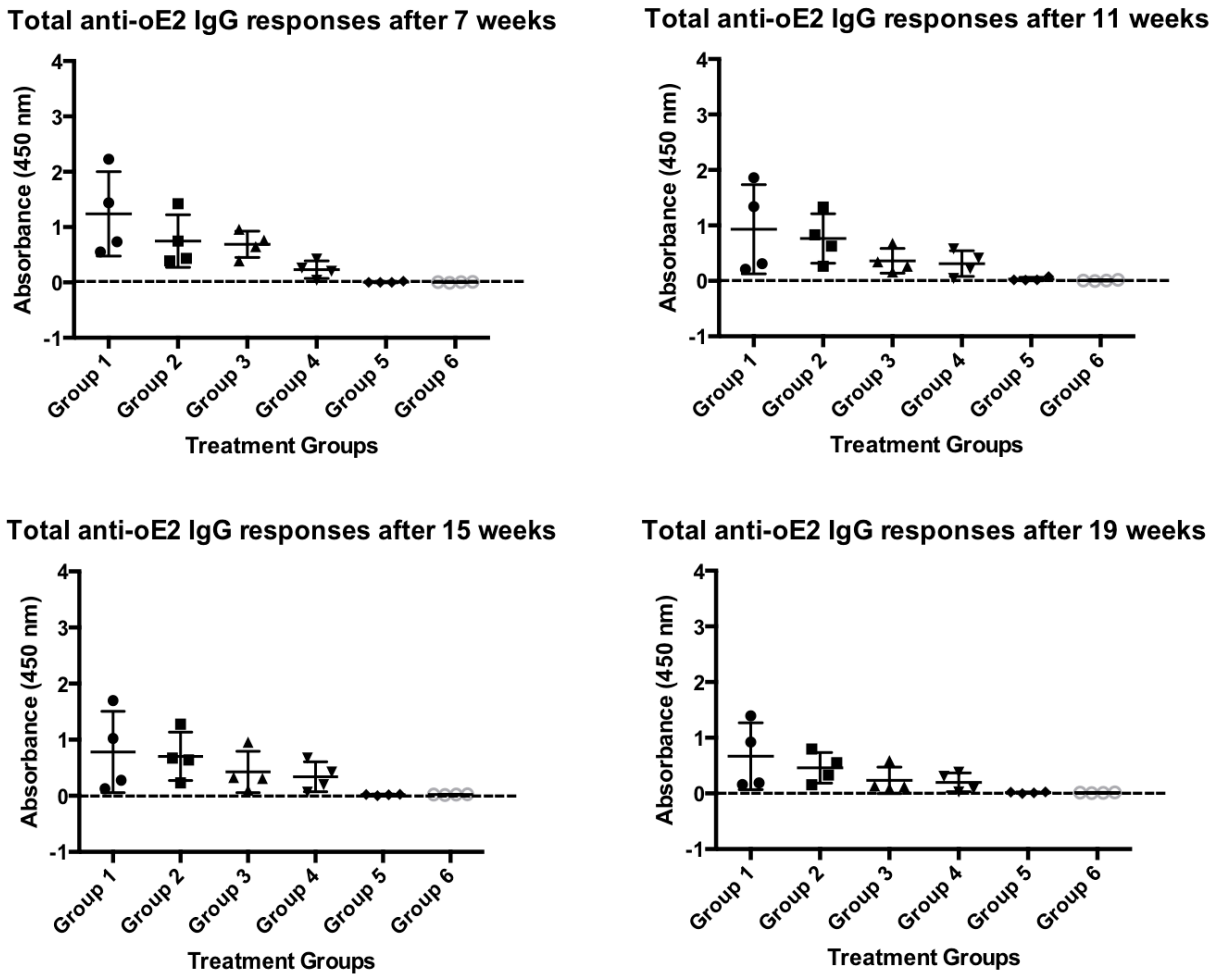

Fig 7.5: oE2-specific ELISA antibody responses in mice after two subcutaneous immunisations. The individual response for each mouse is shown using a sera dilution of 1:1600. Group 1 (mouse 5 to 8) received 100 µg oE2 plus 10 µg Quil-A; Group 2 (mouse 5 to 8) received the FD 100 µg oE2 plus 10 µg Quil-A, Group 3 (mouse 5 to 8) received the oE2 nanovaccine (100 µg oE2 adsorbed to 500 µg SV-140), Group 4 (mouse 5 to 8) received the FD oE2 nanovaccine (100 µg oE2 adsorbed to 500 µg SV-140), Group 5 (mouse 5 to 8) received the FD 500 µg SV-140, Group 6 (mouse 5 to 8) was the unimmunised group and did not receive any vaccination.

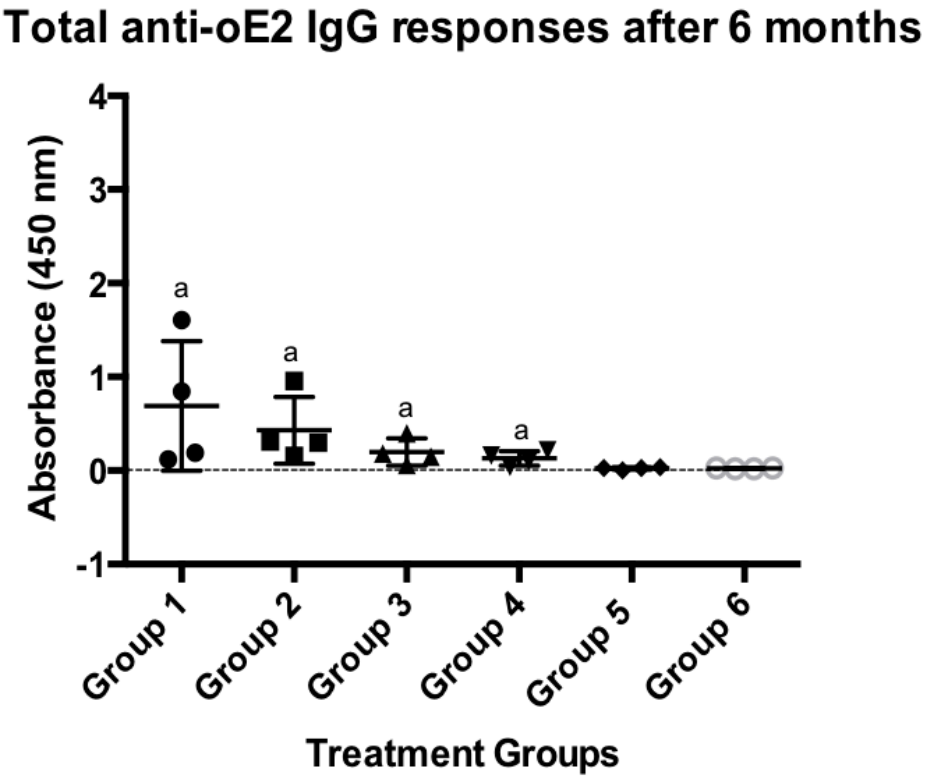

Fig 7.6: oE2-specific ELISA antibody responses in mice after two subcutaneous immunisations. The individual response for each mouse is shown using a sera dilution of 1:1600. Group 1 (mouse 5 to 8) received 100 µg oE2 plus 10 µg Quil-A; Group 2 (mouse 5 to 8) received the FD 100 µg oE2 plus 10 µg Quil-A, Group 3 (mouse 5 to 8) received the oE2 nanovaccine (100 µg oE2 adsorbed to 500 µg SV-140), Group 4 (mouse 5 to 8) received the FD oE2 nanovaccine (100 µg oE2 adsorbed to 500 µg SV-140), Group 5 (mouse 5 to 8) received the FD 500 µg SV-140, Group 6 (mouse 5 to 8) was the unimmunised group and did not receive any vaccination. The letter 'a' denotes that the groups were not significantly different. Groups that do not share a common letter were significantly different ($p<0.001$, unpaired t-test analysis).

Generation of long-term cell-mediated immune response is crucial as it shows uptake of the antigen by the antigen presenting cells, which is an essential process for developing immunity to invading pathogens. To determine the long-term cell-mediated immune responses spleens were collected from the four sacrificed mice at the end of the trial at six months following the second immunisation. The negative controls FD SV-140 alone and unimmunised did not generate oE2 specific cell-mediated responses (Fig 7.7). The oE2/SV-140 generated very strong long-term Th1 responses, the average value was found to be significantly higher (1500 SFU/million cells) than all the treatment groups. The FD oE2/SV-140 treatment group showed some variation in Th1 cell-

mediated immune responses to oE2 antigen as two mice generated low level responses of 340-1049 SFU/million cells while the other two mice generated high level responses of 1500 SFU/million cells. Similarly, two mice in the oE2 plus Quil-A group induced low level of responses (473-690 SFU/million cells) whereas the other two mice generated high level of responses (1406-1500 SFU/million cells), this varied response can be attributed to mouse-to-mouse variation. All the four mice in the FD oE2 plus Quil-A group induced low level responses of 206-583 SFU/million cells.

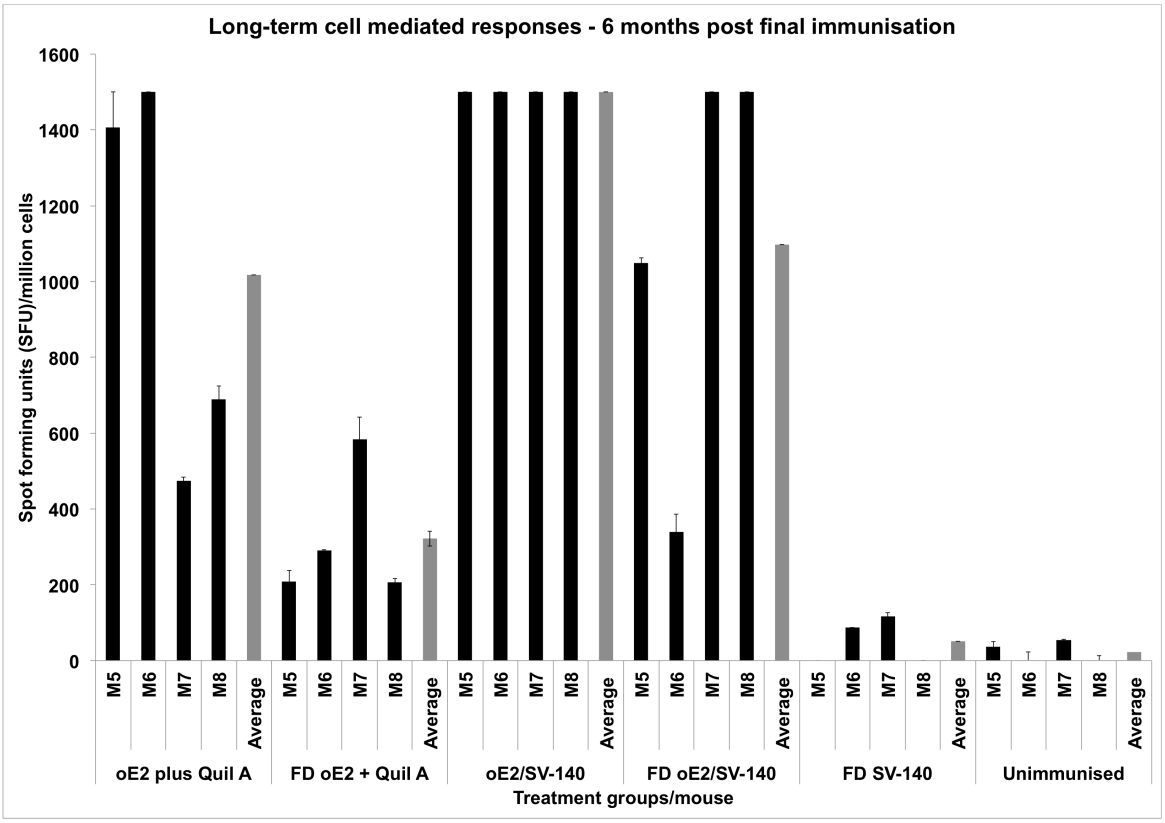

Fig 7.7: Detection of antigen specific IFN-γ secretion by ELISPOT assay of murine splenocytes from immunised mice. The bars represent the number of cells producing IFN-γ in response to the oE2 antigen six months after the final immunisation. The grey bars show the average for each group and M5 to M8 represent the four individual mice in each group.

ELISA and ELISpot assay results showed good oE2-specific antibody and cell-mediated immune responses at three week and six month time points and this further confirmed the effectiveness of the non-FD and the FD SV-140 as self-adjuvants and efficient nanocarriers. This is a significant finding as for the first time we have shown that the SV can induce long-term balanced immune responses.

7.3.4 IHC analyses

Immunohistochemistry analyses of mice spleen sections were conducted to determine semi quantitative IgG responses and the representative results are shown in Fig 7.8. The fluorescent FITC staining in the spleen section represents the presence of total IgG response; spleen section from one mouse in each group was investigated. The IgG responses appeared stronger at both the time points (three weeks and six months) with oE2/SV-140 (Fig 7.8 e and f) compared to the positive control oE2 plus Quil-A (Fig 7.8 a and b). Similarly, even the FD oE2/SV-140 showed good antibody responses after three weeks (Fig 7.8 g) and six months (Fig 7.8 h) compared to the FD oE2 plus Quil-A (Fig 7.8 c and d). The absence of the green color in the sections of the FD SV-140 and the unimmunised treatment group confirms that the mice in the negative control group did not generate specific antibody responses [Fig 7.8 (i and j) and (k and l)].

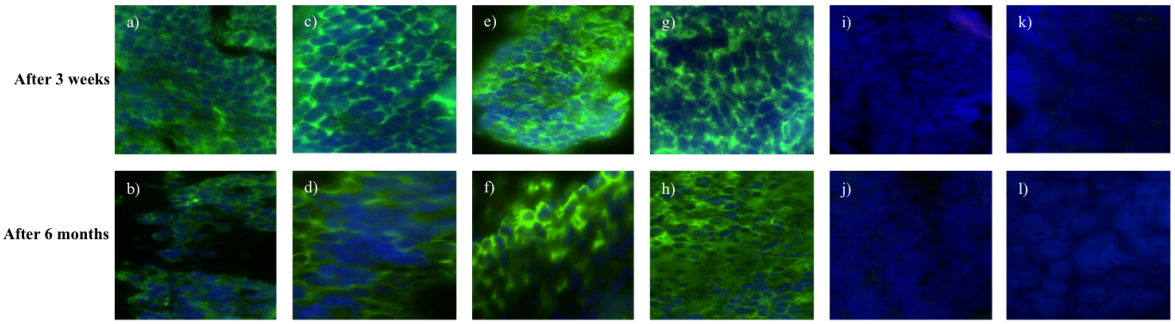

Fig 7.8: Representative immunohistochemistry analyses to determine the induction of total IgG in the spleen sections of the vaccinated animals after three weeks and six months post the final immunisation, oE2 plus Quil-A **(a)** and **(b)**; FD oE2 plus Quil-A **(c)** and **(d)**; oE2/SV-140 **(e)** and **(f)**; FD oE2/SV-140 **(g)** and **(h)**; FD SV-140 **(i)** and **(j)**; unimmnised **(k)** and **(l)**.

7.3.5 Histopathology data

To determine if there were deleterious side effects associated with the administration of 500 µg SV-140 vesicles, tissue from the injection sites and different organs were harvested from two mice in each group. The sections were then stained with hematoxylin and eosin stain to examine the effect of nano-vaccination. No morphological changes could were observed in the tissue at the site of injection and in the organs of the mice vaccinated with 500 µg of 50 nm SV-140. The histopathology results demonstrate that administration of the oE2/SV-140, FD oE2/SV-140 and FD SV-140 alone did not have a detrimental effect on the mouse organs at three weeks as well as six months as the sections of mice injected with the nanoformulations looked similar to the unimmunised treatment group (Fig 7.9 A & B).

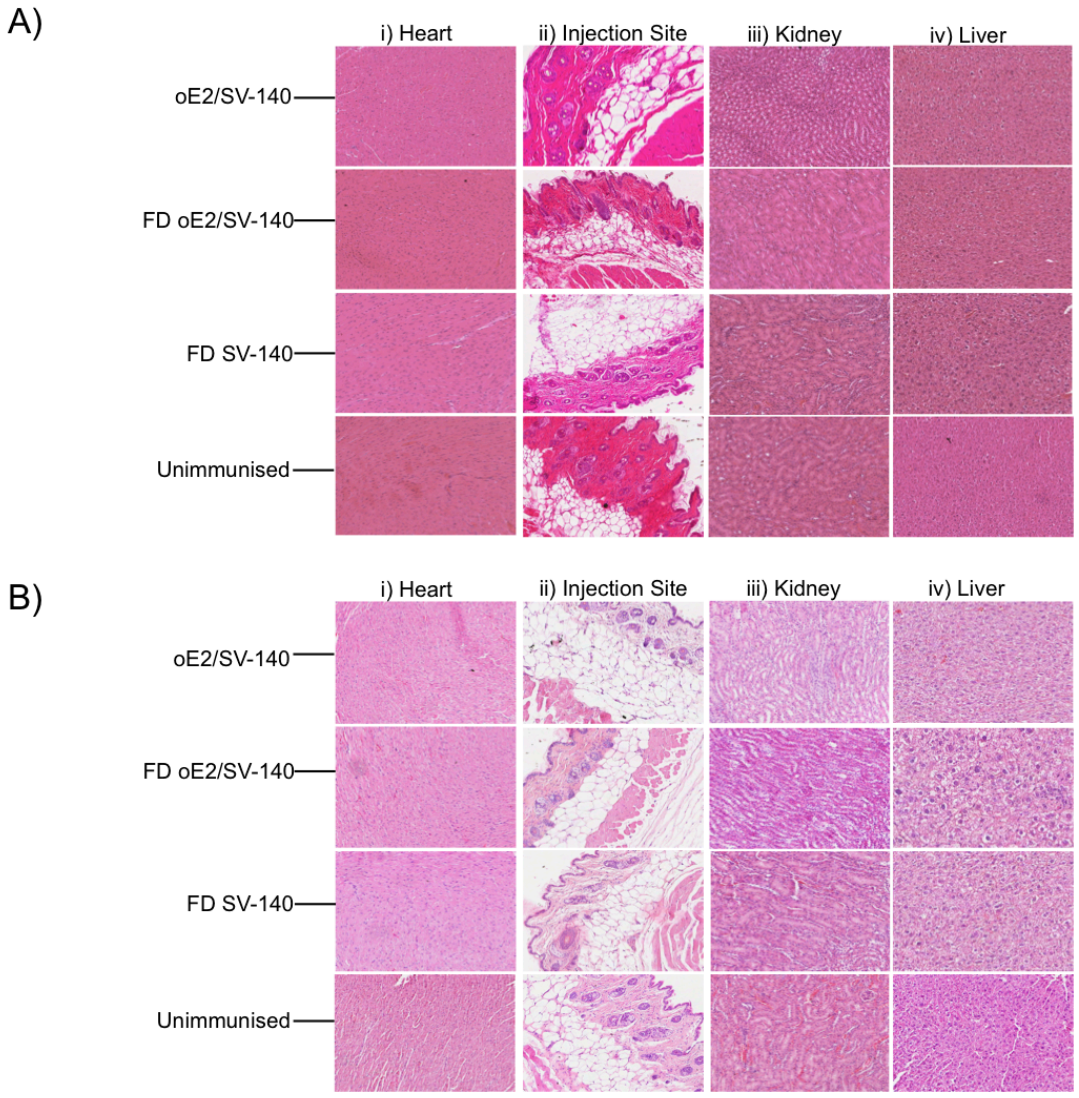

Fig 7.9: Histopathology studies of tissue organs from a mouse injected with nanovaccine immunisations; **A)** Three weeks post the final immunisation, organs fixed in formalin were harvested from two mice for each treatment group and embedded in paraffin, sections were stained with hematoxylin and eosin stain. i) Heart, ii) Injection sites, iii) Kidney, iv) Liver.
B) Six months post the final immunisation, organs fixed in formalin were harvested from two mice for each treatment group and embedded in paraffin, sections were stained with hematoxylin and eosin stain. i) Heart, ii) Injection sites, iii) Kidney, iv) Liver.

7.4 Discussion

For subunit vaccines to be commercial success it is important that they induce balanced antibody and cell-mediated responses as well as sustain long-term immunogenicity. This research work aims on developing a freeze-dried and non freeze-dried veterinary subunit vaccine delivery system, using

SV-140 as adjuvants and delivery vehicles for BVDV-1 oE2 antigen, with the potential to initiate long-term immunity. Here, for the first time we have shown that the oE2/SV-140 formulation induced humoral and cell-mediated immune responses for up to six months in mice after two subcutaneous immunisations. In addition, FD of the oE2/SV-140 formulation also generated balanced long-term antibody and cell-mediated immune responses for up to six months.

In a recent study, we reported the capacity of SV-140 as nanocarriers for efficient adsorption of oE2; SV-140 materials displayed excellent cellular uptake proficiency and were found to be non-toxic on MDBK cells. The oE2/SV-140 formulation was then tested in mice and the animals were vaccinated with three vaccinations at two week intervals subcutaneously with 50 μg oE2/250 μg SV-140 and 50 μg oE2 plus 10 μg Quil-A as positive control. The oE2/SV-140 induced higher anti-oE2 IgG as well as IFN-γ responses compared to traditional adjuvant Quil-A, demonstrating the potential of SV-140 as both efficient vaccine delivery vehicles and potent adjuvants. [11] These results encouraged us to test the long-term efficacy of the oE2/SV-140 nanovaccine, as generation of long-term immunity is a requisite for the development of a successful subunit vaccine. We also developed and tested the ability of the FD oE2/SV-140 nanovaccine to generate immunity in mice to address the issue of cold chain storage often associated to subunit vaccines.

Freeze-drying is considered an excellent technique to improve the long-term stability of the nanoformulations but it is a very complex process. Post freeze-drying the integrity of the nanoparticles and protein needs to be investigated. Various studies have reported the use of trehalose in combination to preserve the immunogenicity of proteins such as lactose dehydrogenase, hepatitis B surface antigen (HBsAg) and human serum albumin. [15,16,17] Likewise, glycine also has been used successfully for freeze-drying of model proteins lactate dehydrogenase and glucose 6-phosphate dehydrogenase in a sucrose-glycine based excipient system. [18] In the past, we have observed that 5% trehalose along with either 1% PEG8000 helped preserve silica nanoparticles and immunogenicity of OVA protein. [10]

For freeze-drying, oE2 adsorbed SV-140 the combination of 5% trehalose and 0.1% glycine was found to be suitable as it preserved the structural integrity of the vesicles as well as the integrity of the oE2 protein. As determined by western analyses the antigenicity of the FD BVDV oE2 adsorbed on SV-140 was preserved (Fig 7.1d lane 4). Sameti *et al.* demonstrated that the activity of cationic silica nanoparticles was preserved when freeze-dried with either trehalose or glycerol. [19] The

freeze-drying process did not have an adverse affect on the ability of the dried formulations the oE2/SV-140 and SV-140 to spontaneously go into the solution upon hydration. Furthermore, as observed by TEM and SEM the structural integrity of the SV-140 adsorbed with oE2 and SV-140 before and after freeze-drying was well preserved. In addition, previous work from our laboratory has demonstrated that the FD silica nanovaccine formulations (OVA/AM-41 and oE2/HMSA) induced both antibody and cell-mediated immune responses in mice [10] and sheep (personal communication).

In the current study, mice were administered with two vaccinations of the non-FD and the FD 100 µg oE2/500 µg SV-140 formulations at three week intervals. The animals were maintained for up to six months post the final immunisation and mice in all the groups remaining healthy throughout the trial period. Quantitative toxicity analyses on SV-140 nanovaccine formulations conducted at 0.02 mg/mL and 0.01 mg/mL showed that >85% of the MDBK cells remained viable. [11] Both oE2/SV-140 and the FD oE2/SV-140 induced oE2 specific antibody responses (1:1600) at three weeks (average OD range of 1.18 vs. 1.42) and six months (average OD range of 0.19 vs. 0.13) after the final second immunisation (Fig 7.3 and 7.6). As expected, with time the oE2/SV-140, oE2 plus Quil-A, the FD oE2/SV-140 and FD oE2 plus Quil-A showed a gradual trend of reduction in the antibody response. Hollow mesoporous silica nanoparticles used to deliver Porcine Circovirus Type 2 ORF2 protein in mice showed significant reduction in the antibody titres at the six week time point post immunisation. [20]

The cell-mediated response, which is very important part of the anti-viral response, was found to be strong with oE2/SV-140 and FD oE2/SV-140 at the three week as well as six month time points (222-1500 SFU/million cells) (Fig 7.4 & 7.7). The uniformly strong high cell-mediated response induced by the four mice (1500 SFU/million cells) in the oE2/SV-140 could be due to the sustained release of the antigen from the vesicles. Even though, the oE2 specific cell-mediated immune responses with the oE2/SV-140 were higher than the FD oE2/SV-140 at 3 weeks as well as six months, this study confirms the ability of FD oE2/SV-140 to induce long-term Th1 and Th2 immune responses. Tonnis *et al.* [15] demonstrated similar finding as they found that the freeze-dried aluminum hydroxide adjuvanted HBsAg formulation did not induce high immune responses but was able to induce both Th1 and Th2 responses. [15]

The elicitation of total IgG response was further confirmed by fluorescent FITC staining of the spleen sections, which showed that both oE2/SV-140 as well as FD oE2/SV-140 generated strong antibody responses at three week and six month time points. Previously, we have demonstrated that administration of 150 μg AM-41 silica nanoparticles did not cause any morphological changes in the mice organs. [13] Similarly, the histopathology studies on different organs of mice immunised with the oE2/SV-140, FD oE2/SV-140 and FD SV-140 nanovaccine treatments groups confirmed that the 50 nm SV are biocompatible materials and that administration of 500 μg SV-140 vesicles did not have deleterious side effects (Fig 7.9).

In conclusion, the elicitation of balanced Th1 and Th2 responses by the non-FD and FD oE2 adsorbed to SV-140 for up to six months after the final second vaccination, further proves the potential of silica vesicles as a promising new generation adjuvant and delivery vehicle for the development of BVDV subunit vaccine. The efficacy of this adjuvant platform suggests that it can be applied to produce cost effective veterinary subunit vaccines with improved shelf-life.

7.5 Acknowledgements

We thank Kevin Wathen-Dunn, Barbara Arnts and the staff at the Australian Institute for Bioengineering and Nanotechnology Animal Facility, University of Queensland Biological Resources for their expert assistance. The expert assistance of Darryl Whitehead and Erica Mu at the School of Biomedical Science Histology Facility, The University of Queensland was greatly appreciated. We thank Prof. Rajiv Khanna and Dr. Corey Smith for the use of the ELISPOT reader system at The Queensland Institute of Medical Research. Karishma Mody's PhD was supported by Queensland Alliance for Agriculture and Food Innovation, The University of Queensland.

7.6 References

1. Aguirreburualde MSP, Gomez MC, Ostachuk A, Wolman F, Albanesi G, et al. (2013) Efficacy of a BVDV subunit vaccine produced in alfalfa transgenic plants. Veterinary Immunology and Immunopathology 151: 315-324.
2. Mody KT, Popat A, Mahony D, Cavallaro AS, Yu C, et al. (2013) Mesoporous silica nanoparticles as antigen carriers and adjuvants for vaccine delivery. Nanoscale: 5167-5179.
3. Baheti A, Kumar L, Bansal AK (2010) Excipients used in lyophilization of small molecules. J Excipients and Food Chem 1.
4. Mody K, Mahony D, Mahony TJ, Mitter N (2012) Freeze-drying of protein loaded nanoparticles for vaccine delivery. Drug Deliv Lett 2: 83-91.
5. Gard JA, Givens MD, Stringfellow DA (2007) Bovine viral diarrhea virus (BVDV): Epidemiologic concerns relative to semen and embryos. Theriogenology 68: 434-442.
6. McGowan M, Kirkland P, Howard R, Morton J, Younis P, et al. (2008) Guidelines for hte investigation and control of BVDV (bovine viral diarrhea virus of bovine pestivirus) in beef and dairy herds and feedlots.
7. Divers TJ, Peek SF (2008) Rebuhn's Diseases of Dairy Cattle. St Louis,USA: Saunders Elsevier.
8. Cavallaro AS, Mahony D, Commins M, Mahony TJ, Mitter N (2011) Endotoxin-free purification for the isolation of Bovine Viral Diarrhoea Virus E2 protein from insoluble inclusion body aggregates. Microb Cell Fact 10: 57.
9. Snider M, Garg R, Brownlie R, van den Hurk JV, Hurk SvDL-vd (2014) The bovine viral diarrhea virus E2 protein formulated with a novel adjuvant induces strong, balanced immune responses and provides protection from viral challenge in cattle. Vaccine 32: 6758-6764.
10. Mody KT, Mahony D, Cavallaro AS, Stahr F, Qiao SZ, et al. (2014) Freeze-drying of ovalbumin loaded mesoporous silica nanoparticle vaccine formulation increases antigen stability under ambient conditions. International Journal of Pharmaceutics 465: 325-332.
11. Mody KT, Mahony D, Zhang J, Cavallaro AS, Zhang B, et al. (2014) Silica vesicles as nanocarriers and adjuvants for generating both antibody and T-cell mediated immune resposes to Bovine Viral Diarrhoea Virus E2 protein. Biomaterials 35: 9972-9983.
12. Mahony D, Cavallaro AS, Mody KT, Xiong L, Mahony TJ, et al. (2014) In vivo delivery of bovine viral diahorrea virus, E2 protein using hollow mesoporous silica nanoparticles. Nanoscale 6: 6617-6626.

13. Mahony D, Cavallaro AS, Stahr F, Mahony TJ, Qiao SZ, et al. (2013) Mesoporous Silica Nanoparticles Act as a Self-Adjuvant for Ovalbumin Model Antigen in Mice. Small 9: 3138-3146.
14. Zhang J, Karmakar S, Yu M, Mitter N, Zou J, et al. (2014) Synthesis of silica vesicles with controlled entrance size for high loading, sustained release, and cellular delivery of therapeutical proteins. Small 10: 5068-5076.
15. Tonnis WF, Amorij JP, Vreeman MA, Frijlink HW, Kersten GF, et al. (2014) Improved storage stability and immunogenicity of hepatitis B vaccine after spray-freeze drying in presence of sugars. European Journal of Pharmaceutical Sciences 55: 36-45.
16. Anhorn MG, Mahler HC, Langer K (2008) Freeze drying of human serum albumin (HSA) nanoparticles with different excipients. Int J Pharm 363: 162-169.
17. Miller DP, Anderson RE, de Pablo JJ (1998) Stabilization of lactate dehydrogenase following freeze thawing and vacuum-drying in the presence of trehalose and borate. Pharmaceutical Research 15: 1215-1221.
18. Liu W, Wang DQ, Nail SL (2005) Freeze-drying of proteins from a sucrose-glycine excipient system: effect of formulation composition on the initial recovery of protein activity. AAPS PharmSciTech 6: E150-157.
19. Sameti M, Bohr G, Ravi Kumar MN, Kneuer C, Bakowsky U, et al. (2003) Stabilisation by freeze-drying of cationically modified silica nanoparticles for gene delivery. Int J Pharm 266: 51-60.
20. Guo HC, Feng XM, Sun SQ, Wei YQ, Sun DH, et al. (2012) Immunization of mice by Hollow Mesoporous Silica Nanoparticles as carriers of Porcine Circovirus Type 2 ORF2 Protein. Virology Journal 9: 108.
21. National Health and Medical Research Council (2013) Australian code for the care and use of animals for scientific purposes, 8th edition. In: National Health and Medical Research Council.

8.

Conclusions and Recommendations

The research that was carried out within the scope of this project has advanced the application of silica nanoparticles as a highly effective vaccine delivery system. A thorough review of the literature identified two fundamental issues which have been a bottleneck in the field of subunit vaccine development. These are the lack of efficient adjuvants that can induce both humoral and cell-mediated immune responses and the cold storage restrictions of current vaccines.

Previous work established that OVA protein bound to the AM-41 nanoparticles at a capacity of 72 μg OVA/mg AM-41. The adsorption was due to the strong electrostatic interactions between the

positive amino groups on the particles and the negative carboxyl groups present on the protein. The first major finding of this study was that the freeze-dried silica nanoparticles could elicit immune responses. As demonstrated in Chapter 4, the OVA adsorbed AM-41 freeze-dried with 5% trehalose and 1% PEG8000 induced total anti-OVA-specific IgG responses and the anti-OVA-specific IFN-γ responses after four immunisations in mice. This study established that the immunogenicity of the protein adsorbed silica nanoparticles was preserved post freeze-drying.

The second advancement that was made as a result of this study was the investigation of using amino functionalised hollow mesoporous silica nanoparticles (HMSA) with shell thickness of 20 nm and entrance size of 2 to 3.5 nm for the delivery of BVDV-1 codon optimised E2 (oE2) protein. As described in Chapter 5, this study was the first to demonstrate that humoral and cell-mediated immune responses were generated by freeze-dried silica mesoporous nanovaccine formulation in a production in sheep. However, the major constraint of AM-41 and HMSA nanoparticles was the low protein loading efficiency as discussed in Chapter 6. In both the cases, due to the pore size of the nanoparticles being limited to 1 to 2 nm, the presentation of antigen may have been only on the surface of the particles.

The results obtained with OVA and BVDV oE2 delivery using AM-41 and HMSA resulted in further work to improve the nanoparticle design to accommodate more protein and possible sustained release to reduce the number of injections. The novel 50 nm silica vesicles (SV) with a thin shell wall of 6 nm, entrance size ranging from 5.7 nm to 16 nm were found to greatly improve the oE2 adsorption (~250 µg to per mg of SV). The SV improved the BVDV-1 adsorption by ~3 fold compared to the HMSAs. Since the entrance size of the SV is in the range of 5.7 nm to 16 nm, which is larger than the estimated width size of the oE2 (3 to 4 nm), it is highly probable that the protein was adsorbed in the internal cavity as well as external surface of the vesicles leading to higher loading of the BVDV-1 E2 protein. The oE2/ SV-140 induced oE2 specific antibody and cell-mediated responses higher than the oE2 plus Quil-A after three subcutaneous injections as described in Chapter 6.

The next step was to investigate whether the number of subcutaneous injections could be reduced to two in addition to generating long term (up to 6 months) immune responses upon the delivery of oE2 protein bound to SVs. The ability of non-FD and FD oE2/SV-140 to induce long-term immunogenicity was further evaluated as discussed in Chapter 7. This was the first study that

demonstrated that silica nanoformulations induced long-term balanced Th1 and Th2 immune responses for at least six month post the final second immunisation in mice. The long-term immune responses by silica nanovaccines might have been due to the sustained release of the antigen from the vesicles resulting in its efficient uptake by antigen presenting cells, efficient processing and continuous presentation to T-helper cells. Furthermore, the FD oE2/SV-140 nanoformulation was developed by using 5% trehalose and 0.1% glycine as excipients. The FD oE2/SV-140 nanoformulation injected in mice also yielded humoral and cell-mediated immune responses for six months, which showed the potential to eliminate cold chain storage for vaccine delivery. Quantitative cytotoxicity assays on the oE2 adsorbed SV-140 and SV-140 alone, showed that the Madin-Darby bovine kidney cells exhibited cell viability of >90% at lower concentrations. The histopathology analyses on the organs of the mouse treated with 500 μg SV-140 showed that the silica vesicles did not have a toxic effect. The SV-140 were found to be biocompatible material as it elicited immune responses in animals without producing any adverse effects.

8.1 Contribution to knowledge

The findings presented here offer a significant contribution to research in development of novel vaccine delivery systems using silica nanoparticles by: 1) investigating a variety of novel MSNs to accommodate high antigen loadings and sustained release of the antigen, 2) developing stable protein adsorbed nanovaccine formulations using the freeze-drying process for increased stability at ambient temperatures during storage, and 3) validating the efficacy of the developed nanovaccines in animal trials.

This thesis has successfully delivered a platform using silica nanoparticles for the development of vaccine delivery systems. The developed nanovaccines generated balanced immune responses in animal trials. The silica materials were designed for effective endocytosis and displayed a strong adjuvant effect, with a potential to remove the requirement for dedicated adjuvants in the vaccine formulation. Development of this novel delivery platform aims to reduce the administration costs of vaccines, which will offer significant advantages for immunisation regimes especially in remote areas. In addition, freeze-drying the vaccine formulation can reduce the volume for storage as the end product is in a powder form and this would enable easy handling and transport of the vaccine. The highly stable nanoformulations will allow stockpiling of vaccines to be distributed in case of

epidemics, a major breakthrough for Queensland with its tropical/subtropical environment and biosecurity issues.

8.2 Recommendations for future work

This thesis has provided a pathway towards developing efficient silica nanoparticle based vaccine delivery systems by providing a proof-of-concept that the novel silica nanoparticles can be the new generation 'self-adjuvants' and 'nanocarriers'.

A.) Determining the location of protein adsorption on the nanoparticles

Whether the protein adsorbs on the outside or inside of the nanoparticles has been debated for years. This is a critical issue in the challenging field of developing delivery systems using nanoparticles. In Prof. Yu's laboratory, attempts were made to determine how much protein is adsorbed on the surface of particles by using solid silica spheres without any entrance pores and extrapolate the difference with protein bound to the SV. However, the exact location of the protein on SV could not be determined using UV measurements due to the buffer in which the adsorption reaction was performed. Future work will need to focus on the development of an experimental methodology that will allow the quantification of surface vs internal protein adsorbed to nanoparticles. The capacity to measure this ratio may influence the type and duration of the immune response elicited. For example, if the majority of the protein is absorbed on the surface of the nanoparticles the duration of exposure to the immune system might be shorter, however if the protein is adsorbed on the inside of the nanoparticles the protein might get released overtime thus prolonging immune stimulation. Thus, the ratio of internal to external adsorption could be an important immunological determinant, which requires further investigation.

B.) Biocompatibility and Bio-distribution of the nanoparticles

Understanding the *in vivo* fate of nanoparticles and breakdown products is an essential in preclinical investigations. In spite of the ability of the silica nanoparticles to induce immunogenicity, the knowledge of their *in vivo* biocompatibility and bio-distribution remains limited. Urine and faeces samples were collected from the animals administered with 500 μg of SV-140, to investigate the amount of silica excreted in the samples using inductively coupled plasma mass spectrometry. However, the collected data could not be analysed, as the amount of silica injected was below detection limits following excretion. Further investigations would therefore need to either tag the

nanoparticles or deliver a higher dose of the nanovaccine to examine the fate of the silica nanoparticles. A variety of fluorescent probes have been developed for *in vitro/in vivo* sensing and imaging applications. Fluorescence imaging techniques could be used to better understand the fate of the particles *in vivo*. For example, the bio-distribution of the nanoparticles could be understood by administering animals with fluorescence tagged nanoparticles and screening the site of injection and organs from these animals for the presence of fluorescence signals. Once the fate of the nanoparticles is determined research maybe required to determine the fate of any breakdown products from the nanoparticles, particularly if used in food producing animals where chemical residues are tightly regulated. Attempts were made to address this issue in the current study; however, no products could be detected which suggests if breakdown was occurring it was below the level of detection. Future studies should continue similar monitoring as a failure to detect any products will provide some of the critical information required to satisfy the authorities who would regulate nanoparticle vaccine usage.

C.) Testing the applicability of the developed platform technology

The final area of the future research required on the silica nanoparticle platform is translating the capacity of the developed nanovaccines to induce strong immunological responses in small animal to production and companion animals. The SV platform also opens up the possibility of translation to human vaccine applications. This concept is strongly supported by the animal trials conducted, as the initial histopathology studies indicate no adverse effect on all organs tested even with a dose of 500 μg of SV in mice. For an average mouse weighing 20 g, this dose equates to 0.0025% of body weight; direct translation of this dose to a bovine weighing 500 kg would result a 12.5 g SV dose, which may not be feasible. However, similar arguments were made when DNA vaccines were first introduced and it has since been demonstrated that linear determination of dose is always applicable when moving to larger animals. It is anticipated a similar scenario will eventuate with the SV platform, as described here when a dose of 6.2 mg HMSA nanoparticles was effective in sheep (weighing 49 kg) equating to 0.000012% of body weight. The enhanced loading capacity of SV particles and dose titration experiments may allow further reductions in the amount of nanoparticles administered.

Further development of the SV platform will also require the loading capacity of antigens from pathogens to be determined. It is possible that the systems for adsorption can be optimised by varying the binding conditions to match the properties of the antigen in question. The final stage in

the development of the SV nanovaccine platform would be the testing of the immunological responses in a pathogen challenge model whereby the effectiveness of the stimulated immunological responses can be interpreted in the context of protection from infection and/or disease.

These areas of future research were beyond the scope of the studies presented here. However, these studies provide an excellent framework for the future development and application of SV nanovaccine formulations that will lead to improve disease management by addressing the limitations of many existing vaccine technologies.